Report Title

"Improved Oil Recovery from Upper Jurassic Smackover Carbonates through the Application of Advanced Technologies at Womack Hill Oil Field, Choctaw and Clarke Counties, Eastern Gulf Coastal Plain"

Type of Report

Final Report, Phase I

Reporting Period Start Date

May 1, 2000

Reporting Period End Date

December 31, 2003

Principal Author

Ernest A. Mancini (205/348-4319)
Department of Geological Sciences
Box 870338
202 Bevill Building
University of Alabama
Tuscaloosa, AL 35487-0338

Date Report was Issued

January 15, 2004

DOE Award Number

DE-FC26-00BC15129

Name and Address of Contacts for Participants

Ernest A. Mancini Dept. of Geological Sciences Box 870338 Tuscaloosa, AL 35487-0338	David Cate Pruet Production Co. 217 West Capitol St., Suite 201 Jackson, MS 39201	Thomas Blasingame Dept. of Petroleum Engineering Texas A&M University College Station, TX 77843-3116
R. P. Major Dept. of Geology & Geological Engr. University of Mississippi University, MS 38677	Lewis Brown Dept. of Biology Mississippi State University Mississippi State, MS 39762	Wayne Stafford 558 Highway 468 Brandon, MS 39042

Disclaimer

IMPROVED OIL RECOVERY FROM UPPER JURASSIC SMACKOVER CARBONATES THROUGH THE APPLICATION OF ADVANCED TECHNOLOGIES AT WOMACK HILL OIL FIELD, CHOCTAW AND CLARKE COUNTIES, EASTERN GULF COASTAL PLAIN

Final Report, Phase I
January 15, 2004

By:
Ernest A. Mancini
Charles Haynes
Joe Benson
Eric Carlson
Hannah Chen
David Hilton
David Cate
Thomas Blasingame
Wayne Ahr
Rosalind Archer
R. P. Major
Lewis Brown
Alex Vadie
Wayne Stafford
Brian Panetta
William Tedesco
Tiffany Hopkins
Aaron Adams
Juan Avila
Ekene Chijuka
Ammi Tan
Leo Lynch
Todd French
Karen Thompson
Magan Green
John Sorrell

Work Performed Under Contract No. DE-FC26-00BC15129

University of Alabama
Tuscaloosa, Alabama

National Energy Technology Laboratory
National Petroleum Technology Office
U.S. DEPARTMENT OF ENERGY
Tulsa, Oklahoma

ABSTRACT

Pruet Production Co. and the Center for Sedimentary Basin Studies at the University of Alabama, in cooperation with Texas A&M University, Mississippi State University, University of Mississippi, and Wayne Stafford and Associates proposed a three-phase, focused, comprehensive, integrated and multidisciplinary study of Upper Jurassic Smackover carbonates (Class II Reservoir), involving reservoir characterization and 3-D modeling (Phase I) and a field demonstration project (Phases II and III) at Womack Hill Field Unit, Choctaw and Clarke Counties, Alabama, eastern Gulf Coastal Plain. Phase I of the project has been completed.

The principal objectives of the project are: increasing the productivity and profitability of the Womack Hill Field Unit, thereby extending the economic life of this Class II Reservoir and transferring effectively and in a timely manner the knowledge gained and technology developed from this project to producers who are operating other domestic fields with Class II Reservoirs.

The major tasks of the project included reservoir characterization, recovery technology analysis, recovery technology evaluation, and the decision to implement a demonstration project. Reservoir characterization consisted of geoscientific reservoir characterization, petrophysical and engineering property characterization, microbial characterization, and integration of the characterization data. Recovery technology analysis included 3-D geologic modeling, reservoir simulation, and microbial core experiments. Recovery technology evaluation consisted of acquiring and evaluating new high quality 2-D seismic data, evaluating the existing pressure maintenance project in the Womack Hill Field Unit, and evaluating the concept of an immobilized enzyme technology project for the Womack Hill Field Unit. The decision to implement a demonstration project essentially resulted in the decision on whether to conduct an infill drilling project in Womack Hill Field. Reservoir performance, multiwell productivity

analysis, and reservoir simulation studies indicate that water injection continues to provide stable support to maintain production from wells in the western unitized area of the field and that the strong water drive present in the eastern area of the field is adequate to sustain production from this part of the field. Although the results from the microbial characterization and microbial core experiments are very promising, it is recommended that an immobilized enzyme technology project not be implemented in the Womack Hill Field Unit until live (freshly taken and properly preserved) cores from the Smackover reservoir in the field are acquired to confirm the microbial core experiments to date.

From 3-D geologic modeling, reservoir performance analysis, and reservoir simulation, four areas in the Womack Hill Field were identified as prospective infill drilling sites to recover undrained oil from the field. It was determined that the two areas in the unit area probably can be effectively drained by perforating higher zones in the Smackover reservoir in currently producing wells. The two areas in the eastern (non-unitized) part of the field require the drilling of new wells. The successful drilling and testing of a well in 2003 by J. R. Pounds, Inc. has proven the oil potential of the easternmost site in the non-unitized part of the field.

Pruet Production Co. acquired new 2-D seismic data to evaluate the oil potential of the westernmost site. Because of the effects of a fault shadow from the major fault bounding the southern border of the Womack Hill Field, it is difficult to evaluate conclusively this potential drill site. Pruet Production Co. has decided not to drill this new well at this time and to further evaluate the new 2-D seismic profiles after these data have been processed using a pre-stack migration technique.

Pruet Production Co. has elected not to continue into Phase II of this project because they are not prepared to make a proposal to the other mineral interest owners regarding the drilling of

new wells as part of an infill drilling program at this time. Pruet is integrating the reservoir characterization, 3-D geologic modeling, reservoir performance analysis, and reservoir simulation results of the project into their field-scale reservoir management strategy for the Womack Hill Field to improve field operations.

TABLE OF CONTENTS

INTRODUCTION

Pruet Production Co. and the Center for Sedimentary Basin Studies at the University of Alabama, in cooperation with Texas A&M University, Mississippi State University, University of Mississippi, and Wayne Stafford and Associates proposed a three-phase, focused, comprehensive, integrated and multidisciplinary study of Upper Jurassic Smackover carbonates (Class II Reservoir), involving reservoir characterization and 3-D modeling (Phase I) and a field demonstration project (Phases II and III) at Womack Hill Field Unit, Choctaw and Clarke Counties, Alabama, eastern Gulf Coastal Plain (Fig. 1). This report presents the results from Phase I of the project and the decision on whether to implement a new demonstration project (Phases II and III) at Womack Hill Field.

Estimated reserves for Womack Hill Field are 87 million barrels of oil and 46 million barrels for the unitized area of the field. During the production history of the field, which began in 1970, 31.1 million barrels of oil have been produced from the field and 16.4 million barrels from the Unit area. The implementation of a water injection program for pressure maintenance in the western (unitized) part of the field was estimated to result in the production of 17 million barrels of oil from the Unit area. An additional 8.7 million barrels of oil (10 percent of the estimated reserves) have been estimated to remain to be recovered through the application of advanced technologies in optimizing field management and production. The reservoir drive in the western portion of the field is principally solution gas, and the reservoir drive in the eastern portion of the field is water. Womack Hill Field is one of some 60 Smackover fields in the regional peripheral fault trend play of the eastern Gulf Coastal Plain. To date, some 700 million barrels of oil have been produced from these fields. The fields in this play have a common petroleum trapping mechanism (faulted salt anticlines), petroleum reservoir (ooid grainstone and

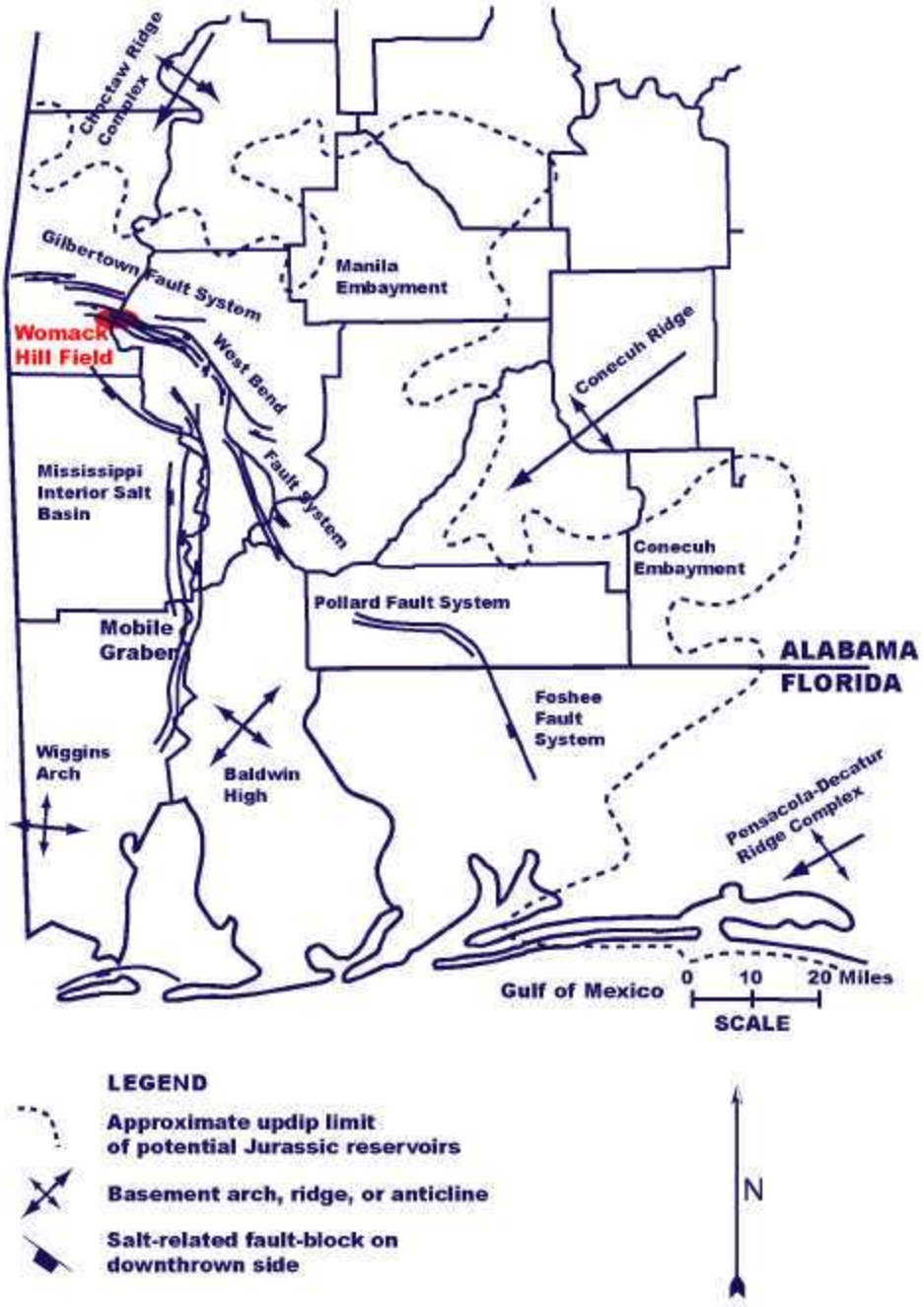

Figure 1. Regional setting and location of Womack Hill Oil Field

dolograinstone shoal deposits), petroleum seal (anhydrite), petroleum source (microbial carbonate mudstone, overburden section, and timing of trap formation and oil migration. Therefore, this work at Womack Hill Field is directly applicable to other Smackover fields in the eastern Gulf Coastal Plain and can be transferred to Smackover fields located along this fault trend from Florida to Texas.

The objective of the project is to increase the productivity and profitability of the Womack Hill Field Unit, thereby extending the economic life of this Class II Reservoir and enhancing National economic and energy security.

The specific objectives of Phase I of the project are to:

1. Demonstrate to producers in the Eastern Gulf Region the significance and procedures for developing an integrated reservoir approach based on geological, geophysical, petrophysical, and reservoir performance data, and which highlights reservoir characterization activities and utilizes 3-D geologic modeling, reservoir performance analysis, and reservoir simulation as mechanisms for making decisions regarding field operations, such as selecting well locations for strategic infill drilling as well as identifying wells for recompletion (and/or simulation).
2. Demonstrate to producers in the Eastern Gulf Region the value of reservoir simulation in the design, implementation, and maximizing of a pressure maintenance program, including optimization of injection wells and well locations.
3. Transfer the knowledge gained, technology developed and successes and failures of this project to producers who are operating other fields with Class II Reservoirs through technology workshops, presentations at professional meetings, and publications in scientific and/or trade journals.

4. Contribute to the knowledge base on carbonate sequence stratigraphy, depositional systems, lithofacies analysis, diagenesis, and pore systems and to the understanding of carbonate reservoir architecture, heterogeneity and producibility, carbonate petroleum systems, fluid-rock interactions, petrophysical properties of carbonates, reservoir pressure communication in carbonates, immobilized enzyme recovery process, and dynamics of effective and balanced pressure maintenance in heterogeneous grainstone and dolograinstone reservoirs.

The principal problem at Womack Hill Field is productivity and profitability. With time, there has been a decrease in oil production from the field, while operating costs in the field continue to increase. In order to maintain pressure in the reservoir, increasing amounts of water must be injected annually. These problems are related to cost-effective, field-scale reservoir management, to reservoir connectivity due to carbonate rock architecture and heterogeneity, to pressure communication due to carbonate petrophysical and engineering properties, and to cost-effective operations associated with the oil recovery process.

Improved reservoir producibility will lead to an increase in productivity and profitability. To increase reservoir producibility, a field-scale reservoir management strategy based on a better understanding of reservoir architecture and heterogeneity, of reservoir communication and of the geological, geophysical, petrophysical and engineering properties of the reservoir is required. Also, an increased understanding of these reservoir properties provides insight into operational problems, such as how the multiple pay zones in the field are vertically and laterally connected and the nature of the communication within a pay zone.

The project has built on the experiences and lessons learned from the previous Class II Reservoir studies. Techniques, methods and technologies utilized in previous studies have been

applied and modified accordingly for application to the Womack Hill Field reservoir. These technologies and techniques include reservoir characterization and modeling, reservoir simulation, seismic imaging, and waterflood design for Class II Reservoirs. The particular advanced technologies applied have included developing an integrated geoscientific and engineering digital database for Womack Hill Field, characterizing the Smackover reservoir and modeling (in 3-dimensions) these heterogeneous carbonates for cost-effective management of the reservoir on a field-wide scale and for making decisions regarding field operations. These data and this modeling will be integrated with petrophysical properties of the reservoir, production data, and other engineering information and used in reservoir simulation to evaluate the effectiveness of the existing pressure maintenance program. These data and 3-D geologic modeling will be utilized in developing an infill drilling strategy for this heterogeneous reservoir.

EXECUTIVE SUMMARY

Pruet Production Co. and the Center for Sedimentary Basin Studies at the University of Alabama, in cooperation with Texas A&M University, Mississippi State University, University of Mississippi, and Wayne Stafford and Associates proposed a three-phase, focused, comprehensive, integrated and multidisciplinary study of Upper Jurassic Smackover carbonates (Class II Reservoir), involving reservoir characterization and 3-D modeling (Phase I) and a field demonstration project (Phases II and III) at Womack Hill Oil Field Unit, Choctaw and Clarke Counties, Alabama, eastern Gulf Coastal Plain.

The principal problem at Womack Hill Field is productivity and profitability. With time, there has been a decrease in oil production from the field, while operating costs in the field continue to increase. In order to maintain pressure in the reservoir, increasing amounts of water

must be injected annually. These problems are related to cost-effective, field-scale reservoir management, to reservoir connectivity due to carbonate rock architecture and heterogeneity, to pressure communication due to carbonate petrophysical and engineering properties, and to cost-effective operations associated with the oil recovery process.

Improved reservoir producibility will lead to an increase in productivity and profitability. To increase reservoir producibility, a field-scale reservoir management strategy based on a better understanding of reservoir architecture and heterogeneity, of reservoir communication and of the geological, geophysical, petrophysical and engineering properties of the reservoir is required. Also, an increased understanding of these reservoir properties should provide insight into operational problems, such as how the multiple pay zones in the field are vertically and laterally connected and the nature of the communication within a pay zone.

The objective of the project is to increase the producibility and profitability of the Womack Hill Field Unit, thereby extending the economic life of this Class II Reservoir. The specific objectives of Phase I of the project are to: demonstrate the significance and procedures for developing an integrated reservoir approach for making decisions regarding field operations, demonstrate the value of reservoir simulation to a pressure maintenance program, transfer the knowledge gained from the project to operators of fields with Class II Reservoirs, and contribute to knowledge about Class II Reservoirs.

Reservoir Characterization tasks of Phase I of the project included geoscientific reservoir characterization, petrophysical and engineering property characterization, microbial characterization, and integration of the characterization data.

Geoscientific Reservoir Characterization has shown the following. The upper part of the Smackover Formation is productive from carbonate shoal complex reservoirs that occur in

vertically stacked heterogeneous porosity cycles (A, B, and C). The cycles typically consist of lime mudstone/wackestone at the base and ooid and oncoidal grainstone at the top. The lime mudstone/wackestone lithofacies has been interpreted as restricted bay and lagoon sediments, and the grainstone lithofacies has been described as beach shoreface and shoal deposits. Porosity has been enhanced through dissolution and dolomitization. The grainstone associated with Cycle A is dolomitized (upper dolomitized zone) in much of the field area. Although Cycle A is present across the field, its reservoir quality varies laterally. Dolomitization (lower dolomitized zone) can be pervasive in Cycle B, Cycle C and the interval immediately below Cycle C. Cycle B and Cycle C occur across the field, but they are heterogeneous in depositional texture and diagenetic fabric laterally. Porosity consists chiefly of depositional interparticle, intraparticle, solution-enlarged interparticle, grain moldic, dolomite intercrystalline and vuggy pores. Dolostone pore systems and flow units dominated by intercrystalline and vuggy pores have the highest reservoir potential. Pore systems and flow units dominated by depositional interparticle and solution-enlarged pores have higher reservoir potential than pore systems and flow units dominated by intercrystalline and grain moldic pores. Dolostone flow units have a higher percentage of large-sized pores with larger pore throats, and dolomitized and leached grainstone flow units have a lower percentage of large-sized pores with narrow pore throats. Median pore throat aperture tends to increase with increasing porosity. Probe permeability strongly correlates with median pore throat aperture, and tortuosity increases with increasing median pore throat aperture. Larger tortuosity and median pore throat aperture values are associated with pore systems dominated by intercrystalline and vuggy pores.

Petrophysical and Engineering Characterization have shown the following. Reservoir permeability has been correlated with core porosity, gamma ray well log response, and resistivity

well log response. The petrophysical data have been segregated into flow units prescribed by the geological data, and for the data in these flow units a histogram of core porosity and the logarithm of core permeability were prepared. These histograms yield statistical measures, such as the mean and median values, which were used to develop spatial distributions and to provide data for the numerical simulation model. Evaluation of production, injection and shut-in bottomhole pressure data for the field have been interpreted and analyzed using appropriate mechanisms, such as decline type curve analysis and estimated ultimate recovery analysis. The volumetric results are relevant as virtually every well yielded an appropriate signature for decline type curve analysis. Reservoir performance studies have shown that 10% of the recoverable 34.6 million barrels of oil remains to be produced from the field. The undrained oil is concentrated in the vicinity of the structural high in the south-central part of the field (unitized area) and along an elongated west-east high in the eastern part of the field (non-unitized area). New pressure transient test data support the interpretations that the Womack Hill Field reservoir is compartmentalized and that a fault bounds the field reservoir to the south.

Microbial Characterization has shown the following. Initially water samples and core samples taken from wells in the Womack Hill Field yielded no micro-organisms capable of growing at 90°C. This result was due to a combination of factors, including the fact that the core samples were exposed to air for decades and the equipment necessary to maintain an anaerobic environment was inadequate. Well cuttings from the Smackover Formation acquired from a field near Womack Hill Field were analyzed for micro-organisms. Growth of micro-organisms was evident in the samples prepared from these well cuttings in association with oil from the Womack Hill Field. These organisms consumed ethanol and produced carbon dioxide. This gas is presumed to have come from the reaction of acetic acid with carbonate or other organic acids

produced directly from the oil reacting with carbonate. These findings suggest that micro-organisms capable of producing acetic acid from ethanol have a high probability of being present in Womack Hill Field and of being induced to grow and be metabolically active at the subsurface temperature in the reservoir.

Data for Womack Hill Field have been entered into a comprehensive digital database to facilitate integration into a field-scale reservoir management strategy to improve field operations.

Recovery Technology Analysis tasks included 3-D geologic modeling, reservoir simulation, and microbial core experiments.

A 3-D Geologic Model has been constructed for the Womack Hill Field structure and reservoirs. The 3-D geologic modeling shows that the petroleum trap is more complex than originally interpreted. The geologic modeling indicates that the trap in the western part of the field is a fault trap with closure to the south against the fault, and that the trap in the central and eastern parts of the field is a faulted anticline trap with four-way dip closure. The pressure difference between wells in the western and central parts of the field and wells in the eastern part of the field may be attributed to a flow barrier due to the presence of a north-south trending fault in the field area. The presence of a north-south trending fault is indicated from old 2-D seismic data and by using a correlation algorithm employing heuristic methods for correlation of logs for wells located in the central part of the field. The geologic modeling shows that the Smackover reservoirs are heterogeneous. Four reservoir intervals are identified in the field area: Cycle A, Cycle B, Cycle C, and the interval immediately below Cycle C. A permeability barrier to flow is present potentially between the western and eastern parts of the field.

Reservoir Characterization and Geologic Modeling have shown that four areas in the Womack Hill Field have potential for the recovery of undrained/attic oil. Two areas are located

in the western (unitized) part of the field. These include the northern part of the northeast quarter of Section 16, south of well Permit #2109 (only perforated in reservoir zone C), and the area around well Permit #4575B (only perforated below reservoir zone C) in the west-central part of Section 14. Two areas are located in the eastern (non-unitized) part of the field. These include the northern part of Section 14 and part of the northwest quarter of Section 13, north of well Permits #1804, #1826, #1825 and #1760, and the center of Section 13, around well Permits #1781 and #1847, and north of well Permit #1811, southwest of well Permit #1713, east of well Permit #1760, and west of well Permit #2327.

Reservoir Simulation has produced a model for the Womack Hill Field reservoir based on the 3-D geologic model, and this simulation model has been used for history matching. The history match of the performance of the field is satisfactory and indicates that oil remains to be recovered in the eastern (non-unitized) part of the field. The simulation model showed that a well capable of producing 664 to 825 MSTB could be drilled successfully in the northwestern portion of the eastern part of the field. The western unitized part of the field appears to have little oil remaining to be recovered except in the south-central portion of the Unit area.

Microbial Core Experiments have resulted in the construction of a core plug testing system that is operative at 90°C. Tests conducted in the system with dilute acetic acid demonstrated the effectiveness of a weak acid concentration in dissolving portions of the Smackover core carbonate. Other tests conducted indicate that a sodium nitrate concentration and a sodium dihydrogen phosphate concentration appear to be satisfactory to stimulate the growth of indigenous bacteria. Test results suggest that a dilute ethanol concentration appears to be effective for the production of acetic acid by bacteria, and that supplemental sodium nitrate for

cell maintenance will not be required for at least two months. The dissolution and flow tests were more favorable for limestone samples than dolostone samples.

Recovery Technology Evaluation Tasks included acquiring and evaluating new 2-D seismic data, evaluating the existing pressure maintenance project in the Womack Hill Field Unit, and evaluating the concept of an immobilized enzyme technology project for the Womack Hill Field Unit.

Pruet Production Co. decided to acquire new 2-D seismic data, rather than 3-D seismic data, for the northeastern portion of the eastern part of Womack Hill Field. They focused on this part of the field because reservoir simulation indicated little oil remained to be recovered in the Unit area except in the south-central portion of the Unit area where Pruet believes they can recover the undrained oil in this area by perforating higher zones in the Smackover reservoir in a currently producing well. Also, in 2003 J. R. Pounds, Inc. drilled and tested a successful well in the northwestern portion of the eastern part of the field proving that uncontacted oil remains in this part of the field to be recovered. Pruet's experience and the recent experiences of other operators have shown that the fault shadow associated with the major fault, with significant stratal displacement, bounding the southern border of the field causes seismic imaging problems which could result in increasing the risks of drilling a dry hole. The new 2-D seismic lines are of high quality, but the fault shadow effect from the major fault persists. Pruet is pursuing a pre-stack depth migration processing technique to minimize the effect of the fault shadow.

Multiwell Productivity Analysis has shown that the wells located in the unitized part of the Womack Hill Field continue to receive stable water support to maintain production and that the wells located in the eastern part of the field, where a strong bottom-up water drive exists, continue to experience natural water support to sustain production. This analysis indicates that

the pressure maintenance project utilizing water injection continues to be effective in the Unit area and that the natural water influx in the western part of the field continues to facilitate production. Water injection should be conducted down-dip and focused towards structurally low areas of the field.

The Immobilized Enzyme Technology (IET) project concept appears promising for the Womack Hill Field Unit. Dissolution and flow experiments utilizing carbonate core samples from other Smackover fields in Alabama and other carbonate samples have been effective. An IET project should not be implemented in the Unit, however, until live (freshly taken and properly preserved) core is available to confirm the experiments conducted on other carbonates.

Pruet Production Co. is integrating the information and results from Phase I of this project into their field-scale reservoir management strategy in order to improve operations at the Womack Hill Field. They will consider perforating well Permits #4575B and #2109 in higher zones in the Smackover reservoir to recover undrained/attic oil in the Unit area at the appropriate time. Pruet is using the new pressure transient test data to assess the effectiveness of the pressure maintenance project involving water injection in the Unit area. Pruet continues to evaluate the cost-effectiveness and risks associated with instituting an infill drilling program to recover undrained oil in the eastern (non-unitized) area of the Womack Hill Field. They do not plan to drill a new well in Womack Hill Field at this time.

The results of Phase I of this project have contributed to the further understanding of the Class II Reservoirs, and these results have been and will continue to be transferred through technology workshops, technical presentations, and technical publications.

Pruet Production Co. has elected not to continue into Phase II of this project because they are not prepared to make a proposal to other mineral interest owners regarding the drilling of

new wells as part of an infill drilling program in the Womack Hill Field at this time. This project, therefore, is concluded.

EXPERIMENTAL

Reservoir Characterization

Task RC-1. Geoscientific Reservoir Characterization

Description of Work.--This task is designed to characterize reservoir architecture, pore systems and heterogeneity based on geological and geophysical properties. Landmark Graphics software used in this task includes OpenWorks (data integration), Stratworks (cross section construction), Zmap (subsurface map preparation), ProMax (seismic processing), and SeisWorks (seismic interpretation). Platte River software, BasinMod, was used for construction of burial history and thermal maturation profiles. KINGDOM suite (Seismic Micro-Technology 2d/3d PAK) seismic software and GeoSec software were also utilized.

Rationale.--Reservoir characterization is fundamental to determining reservoir architecture, pore systems, and heterogeneity. It is critical in the design of a cost-effective field-wide reservoir management strategy and for making sound operational decisions. Deformational (structural), depositional, and diagenetic processes exert the major influences on reservoir quality and evolution and produce heterogeneities at various scales. To predict accurately changes in reservoir quality, heterogeneity, and producibility in interwell areas, it is crucial to characterize and understand the processes that produce carbonate rock textures and the diagenetic fluid-rock interactions that have altered the primary rock fabric and pore system.

Core Description.--Reservoir characterization began with core description and analysis. Six slabbed cores from Womack Hill Field were described following the methodology of Bebout and Loucks (1984). Graphic logs were constructed for each of the cores (Figs. 2 through 7). One

Well: Counselman 18-12

Logged By: W. A. Tedesco

Stratigraphic Interval: Smackover Formation 11460 - 11540

Date: January 10, 2001

Depth (ft.)	Pore Type	Mineral Composition (Incl. Porosity) 0% 50% 100%	Structures	Texture	Fabric	Grain Size (mm)	Color	Cement	Comments
11460	BC			Peloidal	WS	004 - 25	B	D	
	WP BP M V			Oolitic	GS	004 - 4 0	G	C	Anhydnte laths Very fossiliferous algae, pelecypods,gastropods, echinoids, cinoids
	WP BP M V			Oolitic Peloidal	GS	004 - 4 0	B	C	Anhydnte healed pores Echinoids and pelecypods
11470		No Recovery							
	WP BP M V M BP			Oolitic Peloidal	PS WS	004 - 1 0	B	C	Interbedded Packstone and Wackestone Wackestone lamina seem more dolomitized
11480	M BP			Oolitic Peloidal	WS	004 - 5	DG	C	Pelecypod shell frags
	M BP BP BP		Shale Partings	Peloidal	WS	004 - 125	DG	C	Anhydnte along shale partings
		No Recovery							
11490	M BP			Peloidal	WS	004 - 25	G	C	Anhydnte filled molds
	M BP M BP			Oolitic Peloidal	PS	004 - 1 0	LB	C	Algae and Pelecypods common
11500	BC BC BC BC		Shale Partings	Peloidal	MS	004 062 004 - 1 0	B LB	C	Silty Large anhydnte healed molds of oncoids & pelecypods
11510		No Recovery							
	V M BP			Peloidal	MS	004 062	LB	C	Anhydnte laths common
11520	V M BP		Vague Bedding	Oncoidal Peloidal	WS	004 - 1 0	LB	C	Algae & Pelecypods
		No Recovery							
	BC BC			Micritic	MS	004 - 125	LG	C	Anhydnitic
11530	BC M BC M BC M		Shale Partings	Oncolitic	WS	004 - 1 0	LG	C	Numerous oncoids
		No Recovery							
	BC BC		Shale Partings	Peloidal	MS	004 - 1 0	LG	C	Anhydnte vugs and pelecypod shell frags Selective dolomitization of rare grains
11540									

Figure 2 Graph of the core for the 18-12 well

KEY

Mineral Composition


Porosity


Calcite


Dolomite


Anhydrite

Pore Types

BP - Interparticle
WP - Intraparticle
BC - Intercrystalline
M - Moldic
F - Fenestral
FR - Fracture
V - Vuggy

Carbonate Fabrics

MS - Micrite
WS - Wackestone
PS - Packstone
GS - Grainstone

Structures

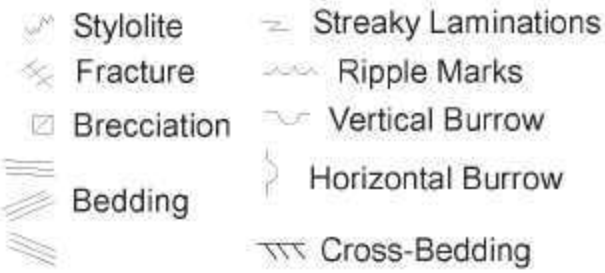

Cements

C - Calcite
D - Dolomite
A - Anhydrite

Colors

G - Gray
B - Brown
W - White

Color Modifiers

L - Light
D - Dark
M - Mottled
VD - Very Dark

Well: Scruggs, Parker, Norton 9-14 Logged By: W. A. Tedesco

Stratigraphic Interval: Smackover Formation, 11402 - 11555 Date: August 15, 2000

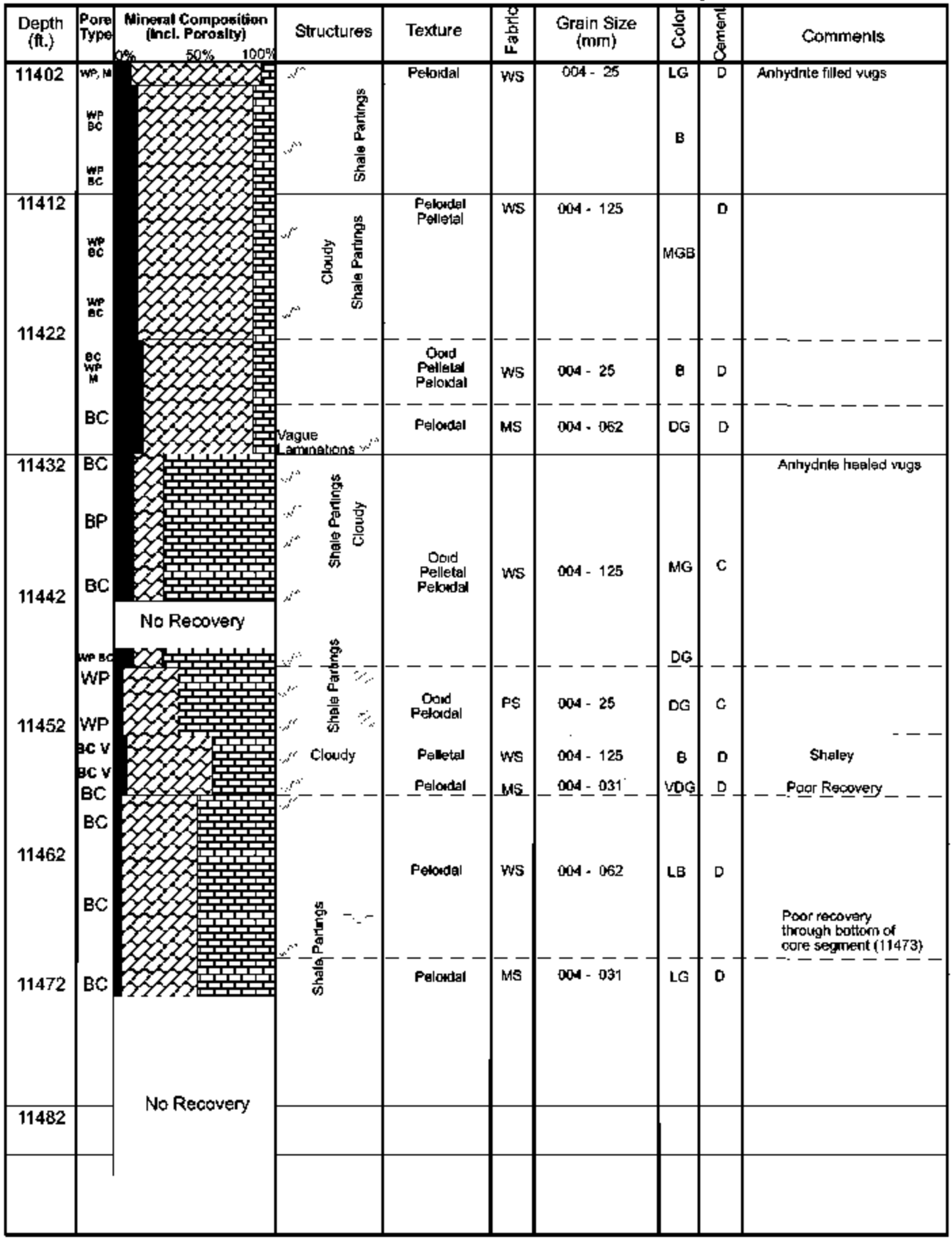

Figure 3 Graph of the core for the 9-14 well

Well: Scruggs. Parker. Norton 9-14 Logged By: W. A. Tedesco

Stratigraphic Interval: Smackover Formation 11402 - 11555 Date: August 15, 2000

Depth (ft.)	Pore Type	Mineral Composition (Incl. Porosity) 0% 50% 100%	Structures	Texture	Fabric	Grain Size (mm)	Color	Cement	Comments
11492		No Recovery							
	BC		Shale Partings	Peloidal	WS	.004 - .062	DG	C	Very Shaley Increasing Organics
	BC, F								
11502	BP			Ooid Peloidal Pelletal	WS	.004 - .062	DG	C	Crumbly till top of cored segment (11495)
	BC		Shale Partings Vague Laminations	Pelletal	WS	.004 - .062	LB	D	
11512	BC						DB		
				Pelletal	WS	.004 - .125		D	Significant Oil Stain
	BC								
11522	BC		Vague Laminations	Pelletal	WS	.004 - .125	DB	D	Interbedded brown/gray laminations
	BC			Peloidal	MS	.004 - .031	LG	D	
11532	BC		Shale Partings Vague Laminations	Peloidal	WS	.004 - .125	LB	D	Shaley, vague laminations
	BC		Shale Partings Vague Laminations	Peloidal Pelletal	WS	.004 - .062	DG	D	Shaley, vague laminations
11542						.004 - .125	G		
	BC			Peloidal Pelletal	WS	.004 - .062	G	D	Shaley, vague laminations
11552									
11555									

Figure 3 (continued) Graph of the core for the 9-14 well

Well: Turner 13-25 Logged By: W. A. Tedesco

Stratigraphic Interval: Buckner Anhydrite / Smackover Formation 11421 - 11451 Date: August 16, 2000

Depth (ft.)	Pore Type	Mineral Composition (Incl. Porosity) 0% 50% 100%	Structures	Texture	Fabric	Grain Size (mm)	Color	Cement	Comments
11421			Shale Partings	Chickenwire Anhydrite	--	--	W	A	Buckner Anhydrite Sabkha
11431				Sucrosic	MS	.004 - .125	G	D	Pyrite Common
	M BC		Cloudy						
	M BC		Shale Partings	Peloidal Oolitic	WS	.004 - .5	B	D	Oomoldic Porosity
11441	M BC								
	M BC								
				Micrite	MS	.004 - .031	DG	D	Silty
	WP M			Oolitic Peloidal	PS	.004 - .5	G	C	
	WP M								
	WP M			Algal Oolitic	BS/GS	.004 - .5	G	C	Top Patch Reef?
11451									

Figure 4 Graph of the core for the 13-25 well

Well: Turner 13-5

Stratigraphic Interval: Smackover Formation 11318 - 11500

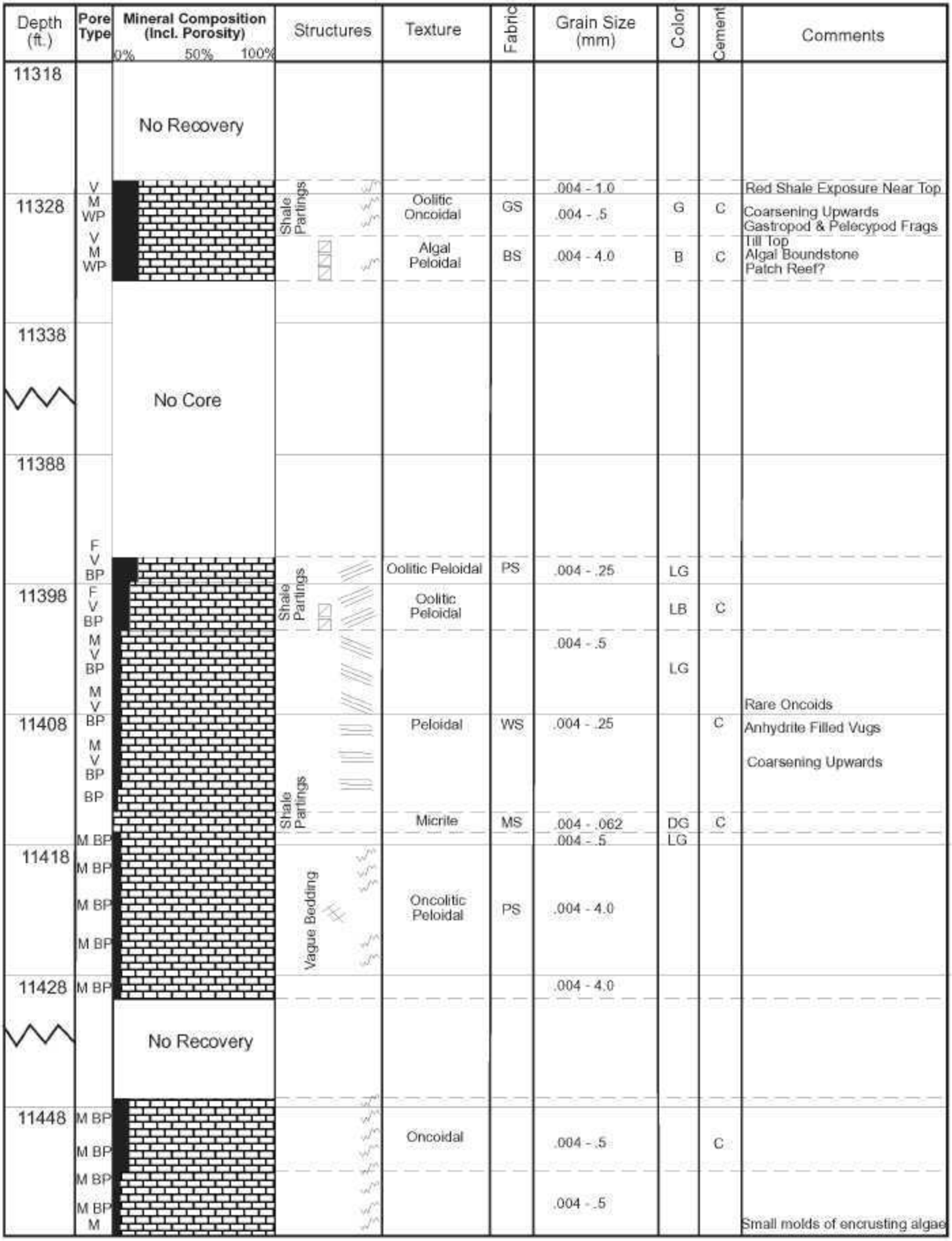

Figure 5. Graph of the core for the 13-5 well.

Well: Turner 13-5

Logged By: W. A. Tedesco

Stratigraphic Interval: Smackover 11318 - 11500

Date: August 16, 2000

Depth (ft.)	Pore Type	Mineral Composition (Incl. Porosity) 0% 50% 100%	Structures	Texture	Fabric	Grain Size (mm)	Color	Cement	Comments
11458	M M WP M WP			Peloidal	WS	.004 - .25	LG	C	Many small molds of round colonial algae
11468		No Recovery							
11478	M M M			Oncolitic Peloidal	WS	.004 - 4.0	G	C	Abundant large oncoids and rounded colonial algae
				Peloidal	MS	.004 - .062	DG	C	
	M			Anhydritic Peloidal	WS	.004 - .5	DG	C	Abundant Anhydrite Vugs
11488				Peloidal	MS	.004 - .062	DG	C	Anhydrite laths along laminations
11498									Vague laminations
11508									

Figure 5 (continued) Graph of the core for the 13-5 well

Well: Turner 13-6

Logged By: W. A. Tedesco

Stratigraphic Interval: Smackover Formation 11400 - 11525

Date: August 15, 2000

Depth (ft.)	Pore Type	Mineral Composition (Incl. Porosity) 0% 50% 100%	Structures	Texture	Fabric	Grain Size (mm)	Color	Cement	Comments
11400	V			Oolitic	GS	031 - 1.0	G	C	cross-bedded
	WP M			Oolitic Peloidal	PS	031 - 25	LB	C	
	V WP M			Peloidal	WS	004 - 062	LB	C	
	V WP			Oolitic Peloidal	PS	031 - 5	LB	C	
11410	M			Oolitic Peloidal	WS	031 - 25	LB	C	
	V WP M			Oolitic Peloidal	GS	031 - 5	LB	C	
11420	V WP BP			Oolitic Peloidal	PS	004 - 25	LB	C	Some oods dolomitized
		No Recovery	Shale Parting						
11430	V WP BP			Oolitic Peloidal	PS	004 - 25	LB	C	Some oods dolomitized
	BP BP BP			Oolitic Peloidal	WS	004 - 25	LG	C	Some ooids dolomitized
11440		No Recovery							
11450	M WP V M WP V M WP V			Oolitic Peloidal Skeletal	WS	004 - 5	G	C	Pelecypod shell fragments common
11460	M WP M WP M WP			Oolitic Peloidal	WS	004 - 5	MG	C	Oncoids and pelecypods Bioturbated
	WP M BP			Oolitic Peloidal	PS	004 - 5	LB	C	Oncoids
11470	WP WP			Peloidal	WS	004 - 5	LB	C	Oncoids
	WP FR			Peloidal	GS	004 - 5	LB	C	Oncoids
	WP WP WP F			Peloidal	WS	004 - 5	LB	C	
11480	WP WP			Oolitic Peloidal	WS	004 - 25	LG	C	Oncoids and pelecypods
		No Recovery							

Figure 6 Graph of the core for the 13-6 well

Well: Turner 13-6

Logged By: W. A. Tedesco

Stratigraphic Interval: Smackover Formation 11400 - 11525

Date: August 15, 2000

Depth (ft.)	Pore Type	Mineral Composition (Incl. Porosity) 0% 50% 100%	Structures	Texture	Fabric	Grain Size (mm)	Color	Cement	Comments
11490		No Recovery							
	WP			Peloidal	WS	004 - 25	LB	C	
	WP								
11500	WP		Shale Partings	Peloidal	PS	031 - 5	G	C	Healed fractures off of stylolite Pelecypods and oncoids
	WP								
	WP								
	WP BP			Oolitic Peloidal	WS	031 - 5	DG	C	
11510	WP BP			Peloidal	WS	004 - 125	LG	C	
		No Recovery							
	WP BP V					004 - 25			
11520	WP BP V		Shale Partings	Oolitic Peloidal	WS	004 - 125	LG	C	Oncoids
11530									

Figure 6 (continued) Graph of the core for the 13-6 well

Well: Womack Hill Field Unit 14-5 #2 — Logged By: W. A. Tedesco

Stratigraphic Interval: Smackover Formation 11115 - 11206 — Date: August 14 - 15, 2000

Depth (ft.)	Pore Type	Mineral Composition (Incl. Porosity) 0% 50% 100%	Structures	Texture	Fabric	Grain Size (mm)	Color	Cement	Comments
11115			Shale Partings	Oolitic Intraclasts	WS	.004 - 4.0	LG	C	Red Shale - Exposure Surface Dense Limestone
	M WP V			Oolitic Peloidal Oncoidal	PS	.062 - .5	LB	D	Anhydrite Laths Pelecypods, Gastropods, Oncoids, and Forams Finger Stromatolite
11125	M WP V		Cloudy	Oolitic	GS	.031 - .5	MGB	C	Dissolution Surface? Large Anhydrite Nodules
	M WP V								Bitumen healed fracture
11135	WP M		Shale Partings Cloudy	Oolitic Peloidal	WS	.004 - .5	LB	D	Shaley Resembles Lagoonal Depositional Environment
	WP M								
	WP M								Shaley
11145	WP M					.004 - 1.0 .004 - .5	LB	D	Vague cross-laminations
	WP M								pelecypods
11155	WP M			Oolitic Peloidal	PS	.031 - .25	G	C	
	M Wp V			Oolitic	GS	.125 - 1.0	G	C	Numerous Pelecypods
11165	WP M								Small Nautiloid Fossil
	WP M			Oolitic Peloidal	PS	.004 - 1.0	LB	D	
	WP M			Peloidal	WS	.004 - 1.0	LB	D	
11175	M WP V								Pelecypods and Gastropods
	WP BC V			Peloidal	MS	.004 - .25	DB	D	
11185	BC		Faint Laminations						Pelecypods, Gastropods, Oncoids Chert Nodules
	BC			Peloidal	WS	.004 - .5	DB	D	
	BC								Bioturbation, Oncoids Fabric probably destroyed
11195	BC		Faint Laminations			.004 - .25			
	BC V		Shale Partings	Peloidal	MS	.004 - .5	LB	D	Oncoids
11206	BP V								Finely Laminated

Figure 7 Graph of the core for the 14-5 #2 well

hundred eighteen thin sections were cut from the cores, with care taken to sample all diagenetic and stratigraphic changes. In addition, 66 thin sections were available from the Alabama State Oil and Gas Board. Thin section petrography was conducted using standard-sized, polished thin sections, with one half of each section stained with Alizarin Red-S and Potassium ferricyanide. Thin sections were described using a Nikon microscope and Swift Model F point counter. Stable carbon and oxygen isotopic analyses were conducted at the Stable Isotope Laboratory of the University of Miami Resensteil School of Marine and Atmospheric Science following standard procedures and are reported relative to the Peedee Belemnite standard (PDB). Reproducibility for isotope data is better than 0.05 ‰ for oxygen and better than 0.1 ‰ for carbon. Cathodoluminescence petrography was conducted on polished thin sections using a Technosyn Cold Cathode Luminescence Model 8200 MK II with a 450 – 550 nA current, 15-20 kw KV, and a 0.05 torr vacuum. Detailed component microsampling was done using a JEOL 733 Superprobe. Probing was completed with an accelerator voltage of 15 kV, 12 nA sample current and a 10 μ spot. Pore systems from the Smackover facies with reservoir potential were studied using a JEOL 8600 automated electron probe microanalyzer. A scanning electron microscope (SEM) was used in studying the effects of dissolution of carbonate rock during microbial core experiments. Mineralogical analyses were accomplished using a Rigaku D/Max-B X-ray diffractometer with a Copper Kα radiation source.

Well Log Study.--Electrical and geophysical well logs were obtained and analyzed for 42 wells within and immediately adjacent to Womack Hill Field (Fig. 8) and core analysis for 24 cores in the field area were studied. Log types studied include resistivity, compensated neutron, bulk density, gamma ray, SP, and acoustic. Compensated neutron, bulk density and resistivity logs were used to pick and distinguish the Smackover, Buckner, and Norphlet units. Three

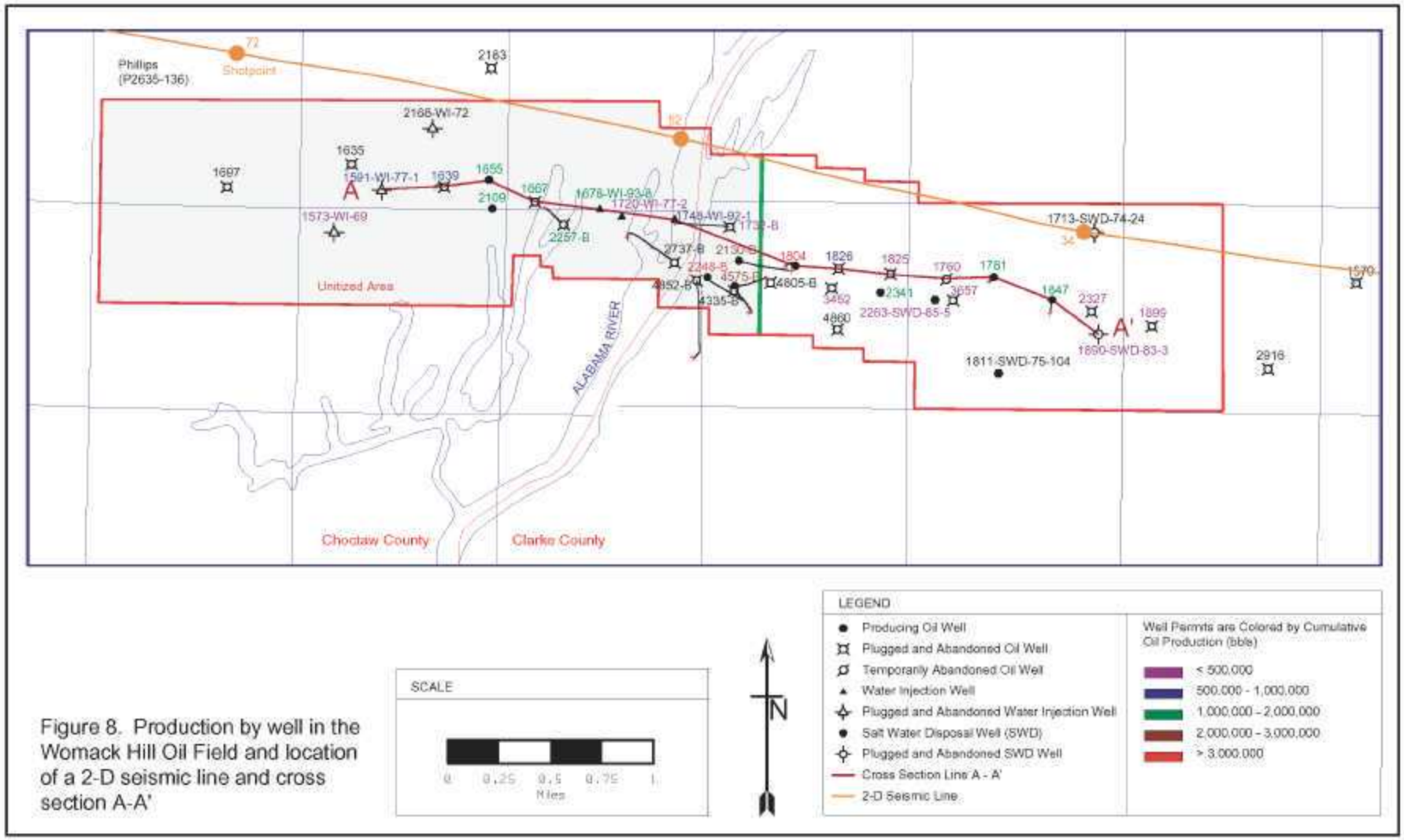

Figure 8. Production by well in the Womack Hill Oil Field and location of a 2-D seismic line and cross section A-A'

shallowing-upward cycles in the upper Smackover Formation (labeled A, B, and C) were also determined and picked on all logs (Fig. 9). These picks were correlated across the field and used to create cross-sections (Fig. 10). Well log picks (cycles) and correlation were checked using heuristic methods. Core descriptions were also added to the logs, allowing correlation of rock types, facies, and reservoir units across the field. The core data were calibrated to the well log patterns to establish electrofacies for correlation, mapping and modeling.

The three shallowing-upward cycles (A, B, and C) (Fig. 11) are generally composed of a basal peloidal lime mudstone, overlain by peloidal wackestone. The tops of each cycle are comprised of peloidal to ooid packstone and are capped by ooid and oncoidal grainstone. The cycles suggest a gradual regression of sea level. There are general increases in porosity, permeability, and dolomite toward the tops of each cycle suggesting some stratigraphic control on reservoir development at Womack Hill Field.

Two completely dolomitized zones (Fig. 12) were identified and named the upper and lower dolomitized zones. These zones consist of completely dolomitized carbonate rock and are the best reservoir zones at Womack Hill Field. The upper dolomitized zone is found in the upper 10-15 feet of the Smackover Formation, just beneath the Buckner Anhydrite Member. The lower dolomitized zone cuts across depositional lithofacies in the field. This zone is commonly 40 to 50 feet thick and is stratigraphically lower in the structurally higher parts of the field.

Subsurface Mapping.--Several different subsurface maps of the Womack Hill Field have been constructed to assist with analysis of production controls in the field. Structure maps of the top of the Smackover Formation (Fig. 13) and Buckner Anhydrite Member of the Haynesville Formation (Fig. 14) have been made using depths determined from the geophysical logs. Isopach

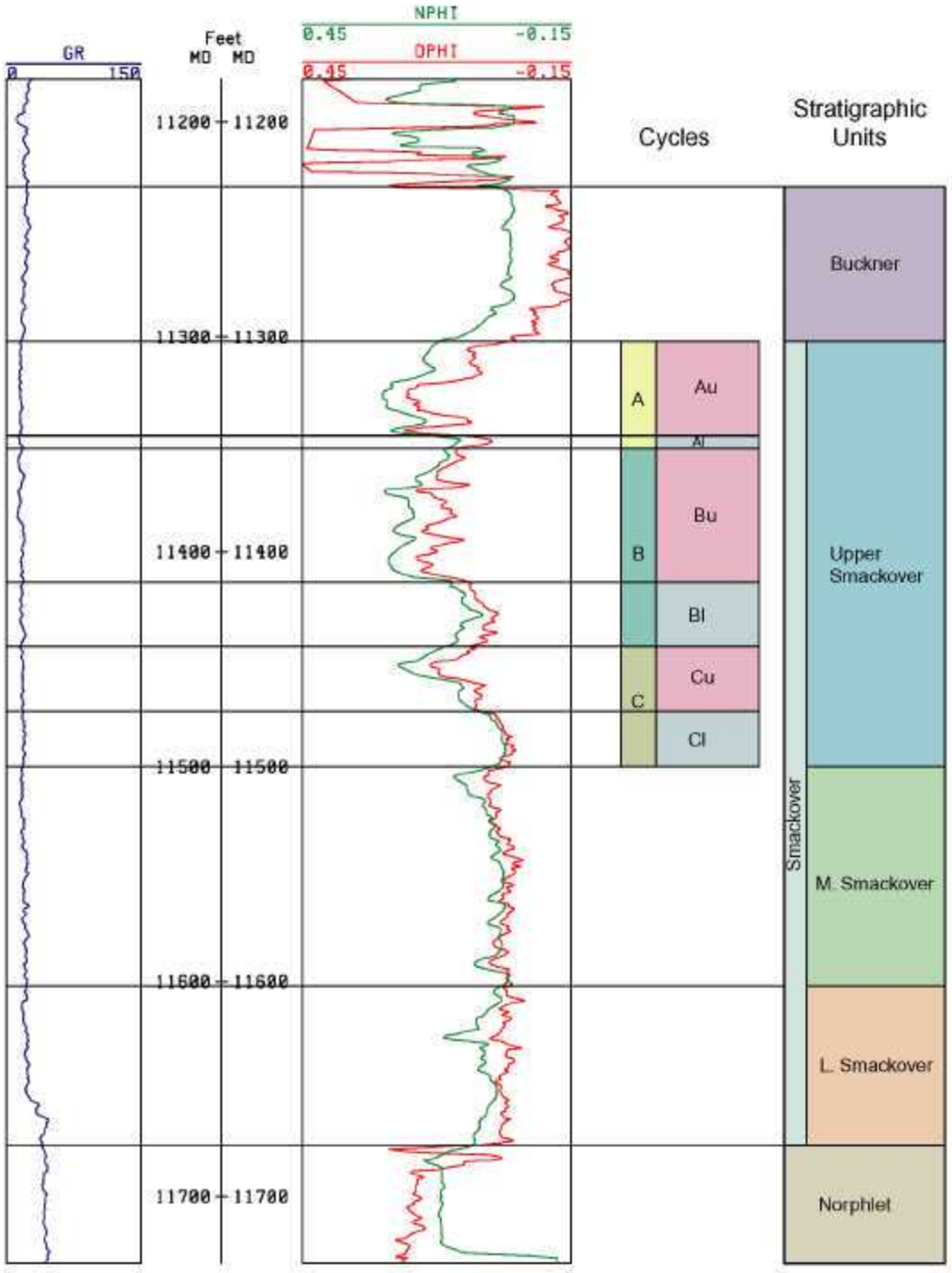

Figure 9. Well log patterns of the Louise Locke 10-14 well (Permit #1667) illustrating Smackover stratigraphic units and upper Smackover cycles at Womack Hill Oil Field. GR=gamma ray log, NPHI=neutron porosity log, DPHI=density porosity log; Au=upper Cycle A, Al=lower Cycle A, Bu=upper Cycle B, Bl=lower Cycle B, Cu=upper Cycle C, Cl=lower Cycle C. See Figure 8 for location of well.

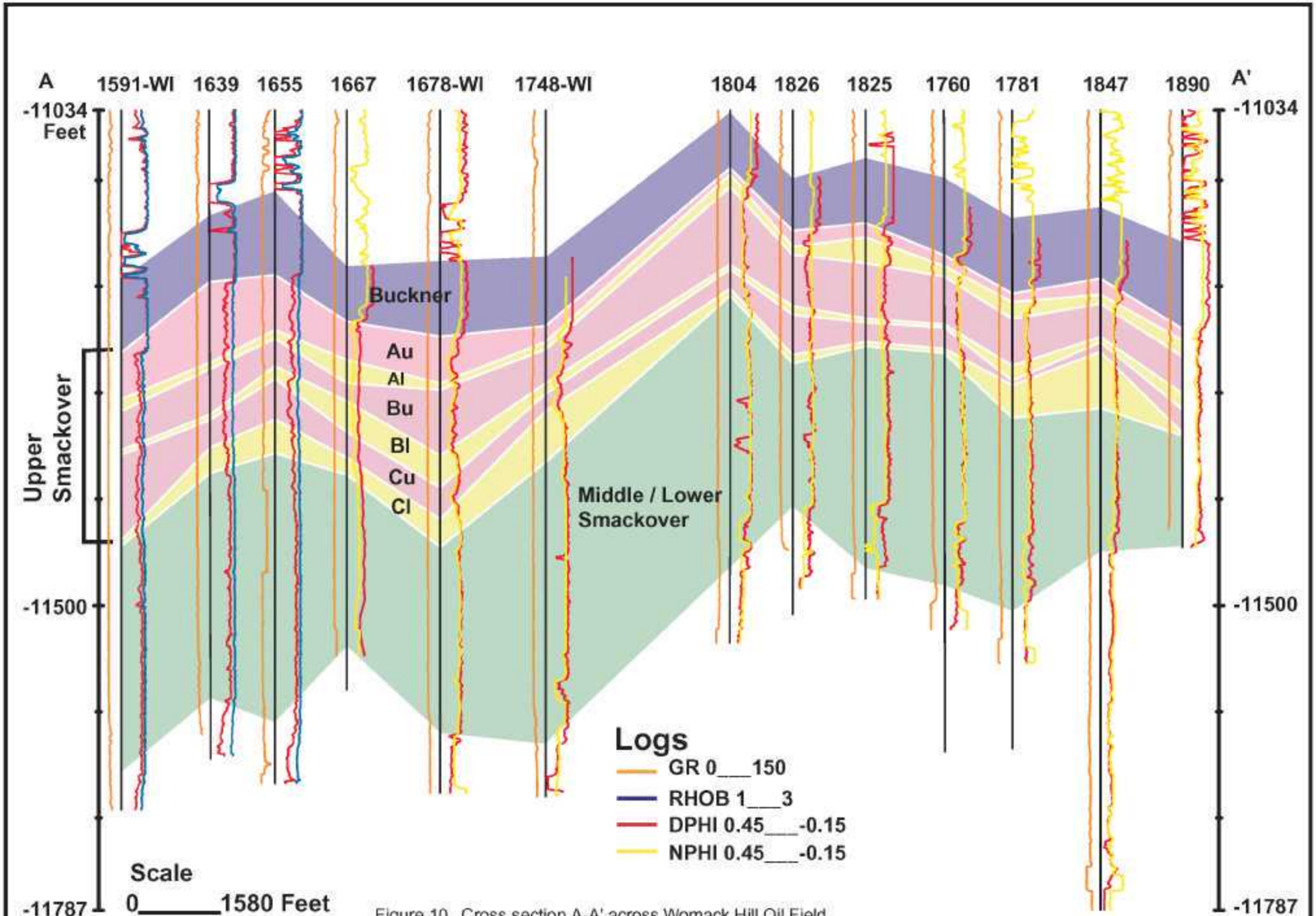

Figure 10. Cross section A-A' across Womack Hill Oil Field.
Au=upper Cycle A, Al=lower Cycle A, Bu=upper Cycle B, Bl=lower Cycle B, Cu=upper Cycle C, Cl=lower Cycle C, See Figure 8 for location of wells.

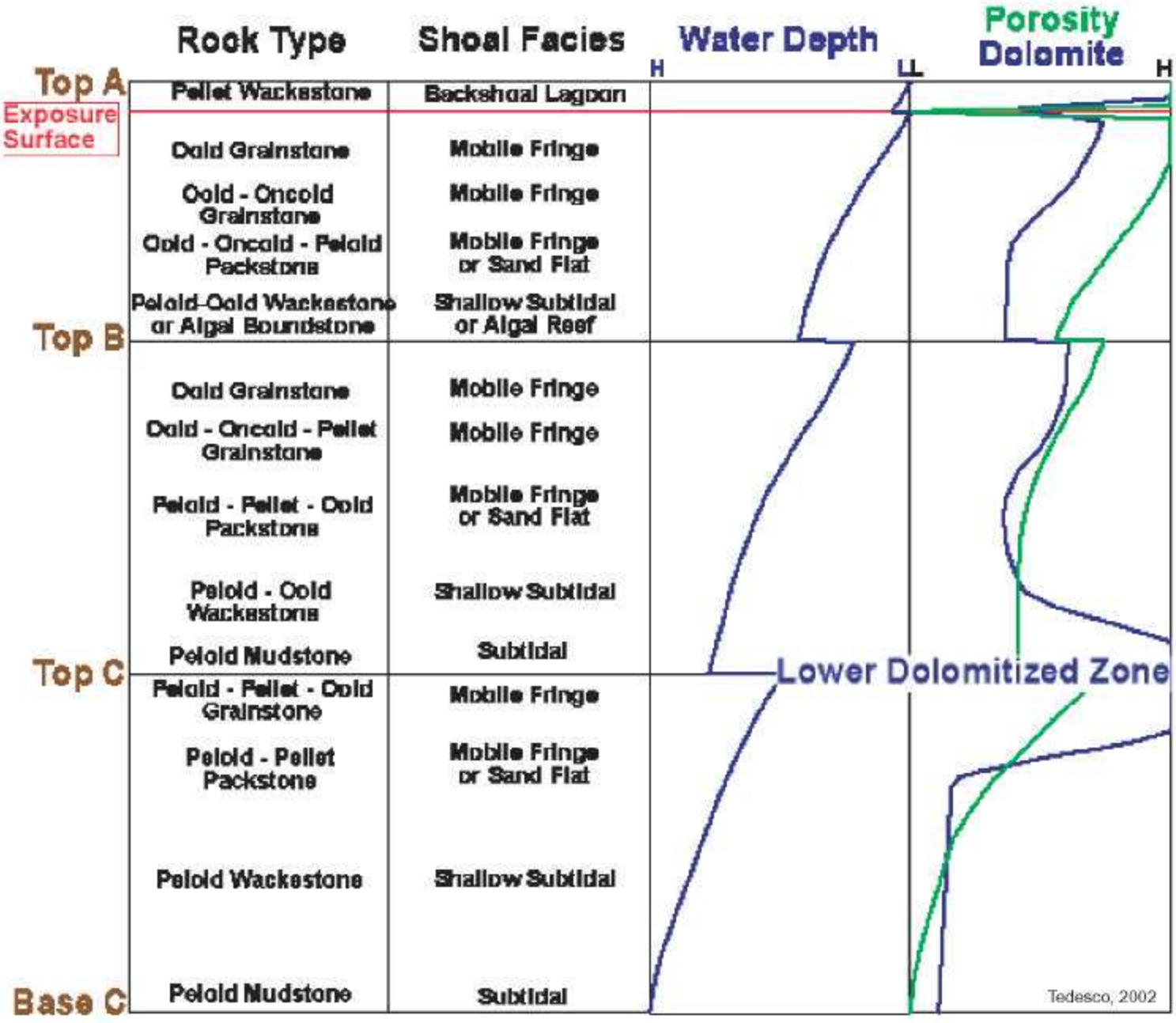

Figure 11. Idealized cycle facies in Upper Smackover at Womack Hill Field. Each cycle comprised of an upward-shallowing sequence of facies on an oold shoal. Porosity, permeability and dolomite percents generally increase towards the top of each cycle. Location of lower dolomitized zone idealized for a well near the crest of the field structure. Upper dolomitized zone at top of Cycle A.

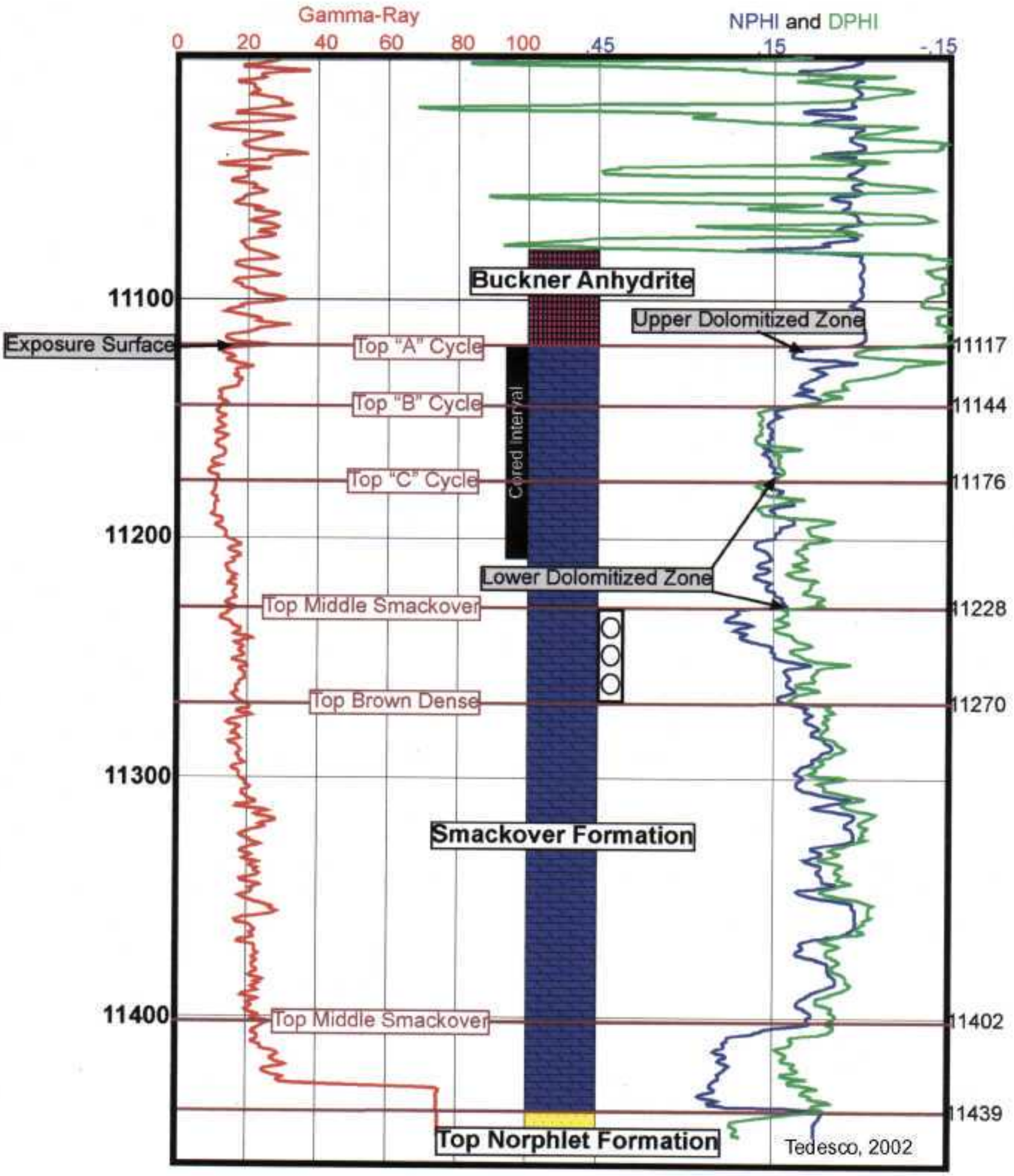

Figure 12. Porosity and gamma-ray logs for Womack Hill Field Unit 14-5 No. 2 well. Formation boundaries and cycles denoted by brown lines. Exposure surface identified at top of Smackover Formation from core data correlates with gamma-ray spike near Buckner-Smackover contact. "Type 1" dolomitizated zone just below exposure. Lower dolomitized zone comprised of "Types 2 & 3" dolomite.

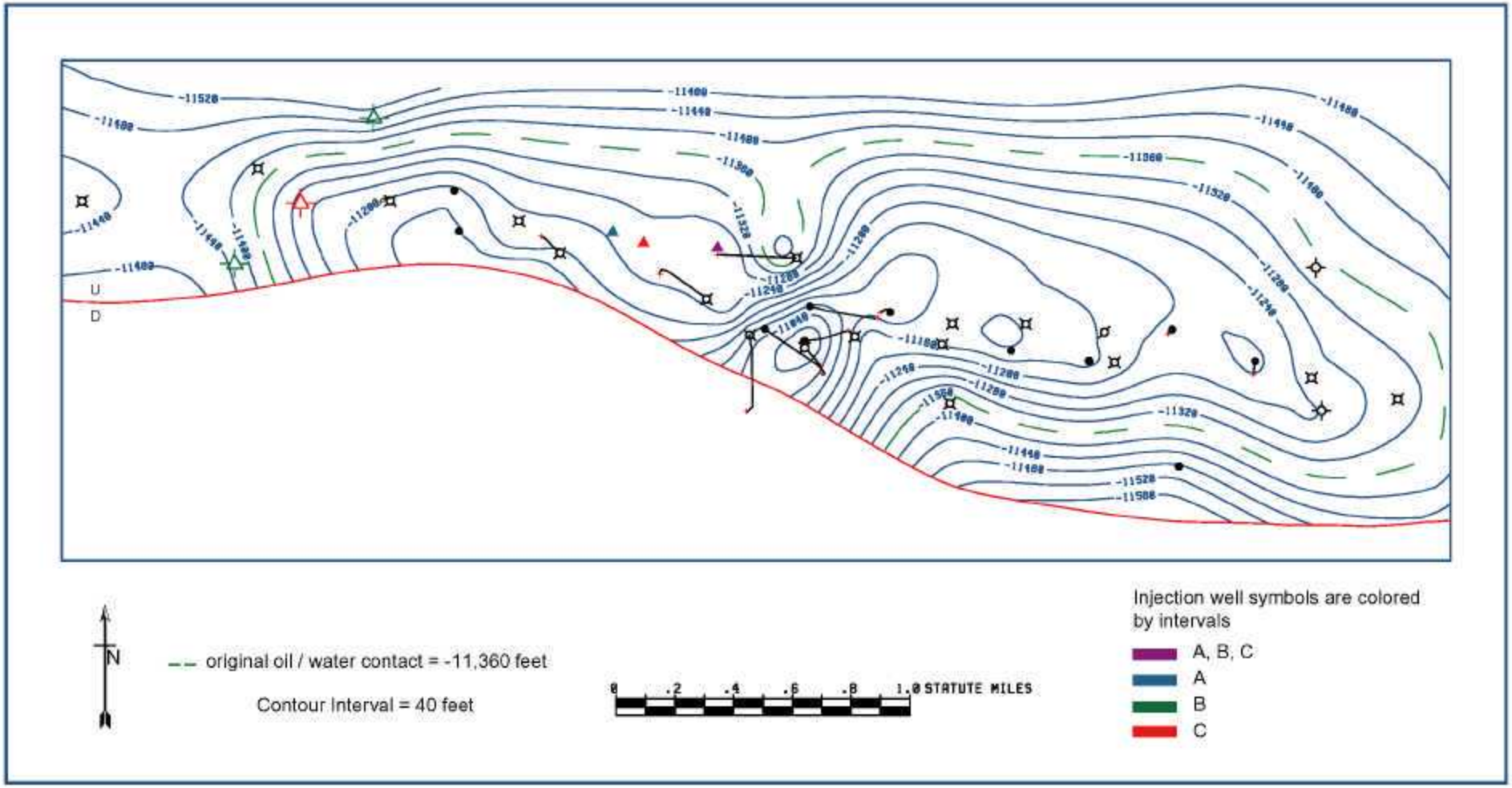

Figure 13. Structure map on top of the Smackover Formation at Womack Hill Oil Field. See Figure 8 for well symbols.

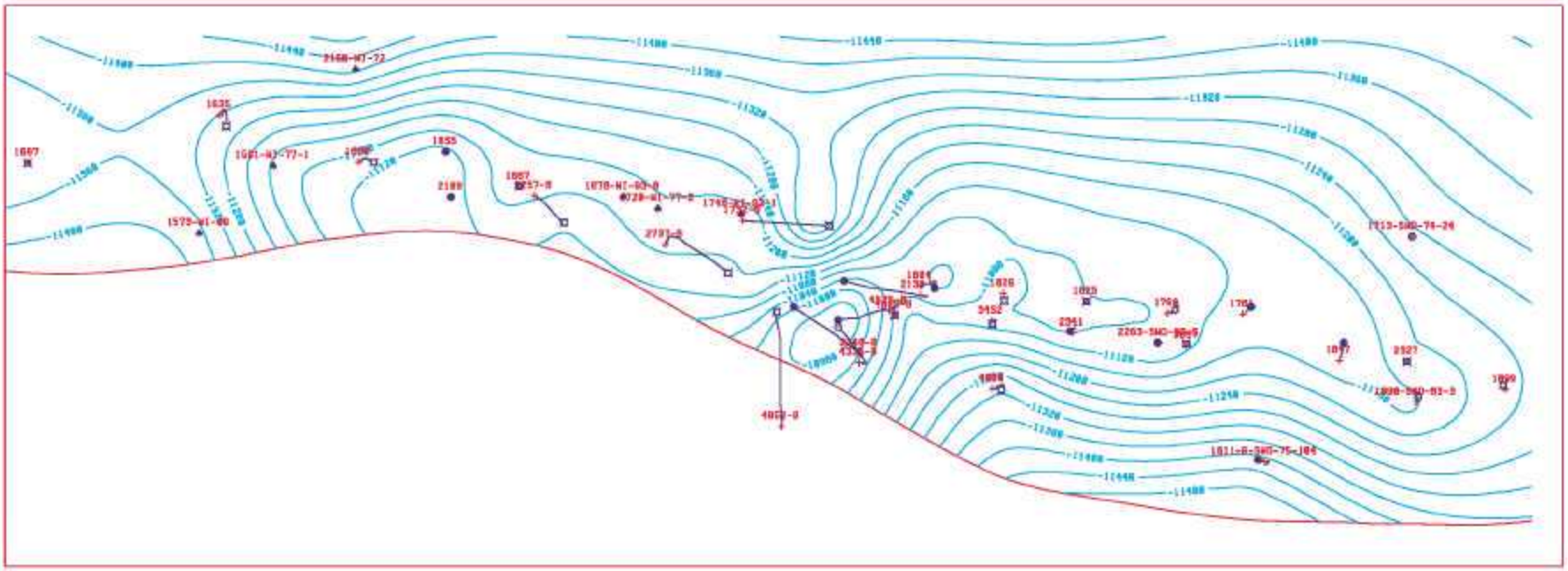

STATUTE MILES 0 .2 .4 .6 .8 1.0 STATUTE MILES

FEET 0 2000 4000 6000 8000 10000 FEET

Figure 14. Structure map on top of the Buckner Formation.

Contour Interval = 40 feet

maps of the Smackover (Fig. 15), upper Smackover (Fig. 16), Cycle A (Fig. 17), Cycle B (Fig. 18), and Cycle C (Fig. 19) have been made using log derived thicknesses.

Seismic Interpretation.--Seismic reflection data (2-D) have been acquired from Seismic Exchange, Inc. These data (Fig. 20) were reprocessed by Geo-Seis Processing and interpreted. Figure 8 shows the location of the seismic data acquired.

Petrographic Analysis.--Thin section petrographic analysis was performed. All 184 thin sections available at Womack Hill Field have been described. A clasticity index was determined for all thin sections and then compared to porosity and permeability data. Clasticity index is a measure of the largest coated grain present in each sample (Carozzi, 1958; Erwin *et al.*, 1979; Humphrey *et al.*, 1986). In general, a direct relationship with permeability and porosity was found with the clasticity index. With increasing clasticity there is a corresponding increase in porosity and permeability. The only zones not following this trend are zones with complete or near complete fabric-destructive dolomitization. In these zones, clasticity index drops to zero, whereas porosity and permeability increase. At the top of Cycle A, a low clasticity index also correlates well with an exposure surface identified and mapped across the field.

One hundred twenty-two (122) powders for isotope analysis were prepared from thin section butts and core pieces for stable carbon and oxygen isotopic analysis. Sampling ensured that all rock types present in each of the cores were analyzed. Data from isotopic analysis (Fig. 21) show clear separation of the upper and lower dolomitized zones. Dolomite in the upper dolomitized zone has isotopically enriched δO^{18} values compared to the lower dolomitized zone. This suggests that the dolomitizing fluid for the upper zone was supersaturated brine at relatively low temperature. The upper zone of dolomitization is fabric destructive and is the result of an early stage diagenetic event that involves downward moving, evaporitically concentrated brine, and

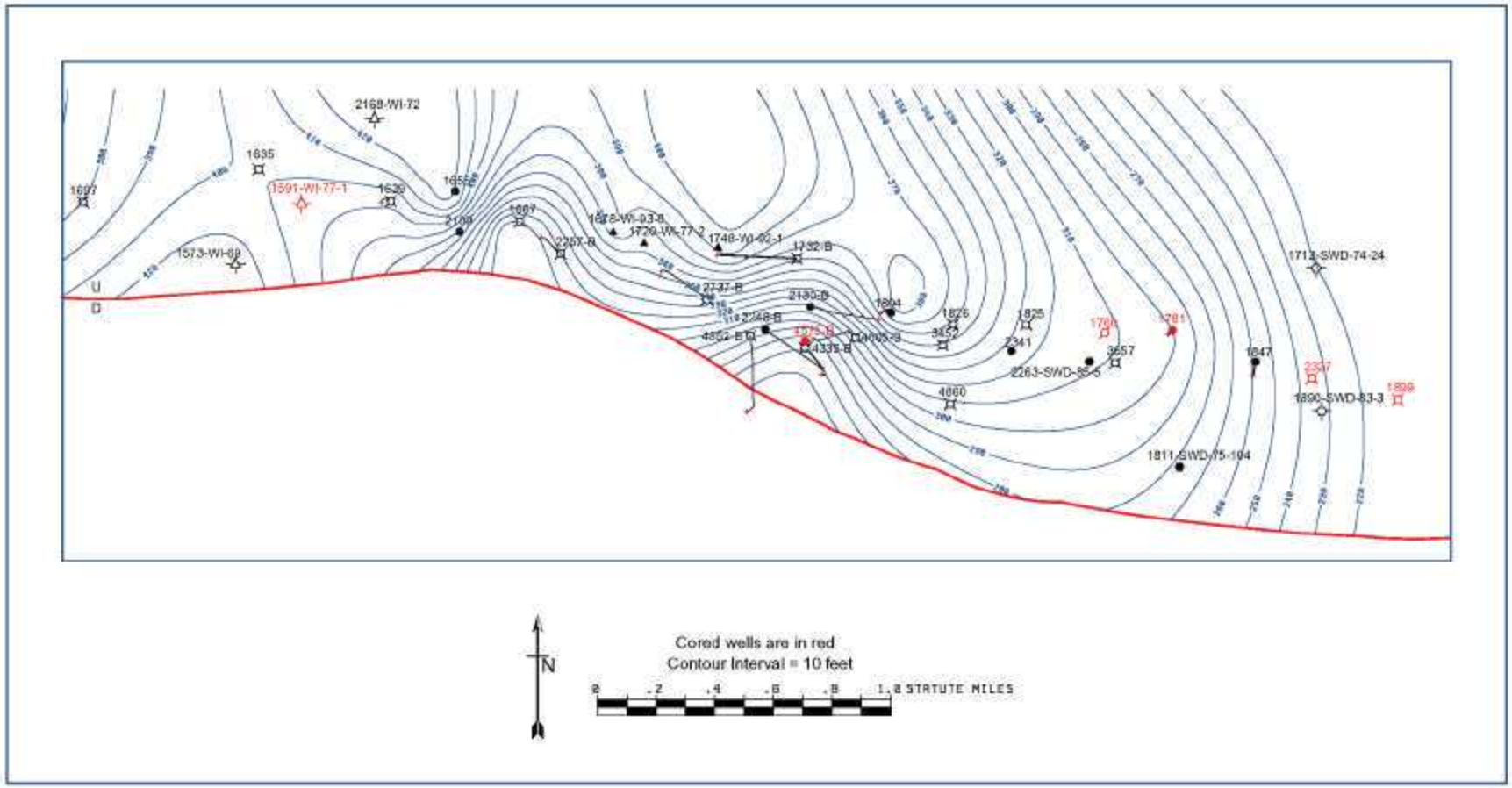

Figure 15. Isopach map of the Smackover Formation at Womack Hill Oil Field. See Figure 8 for well symbols.

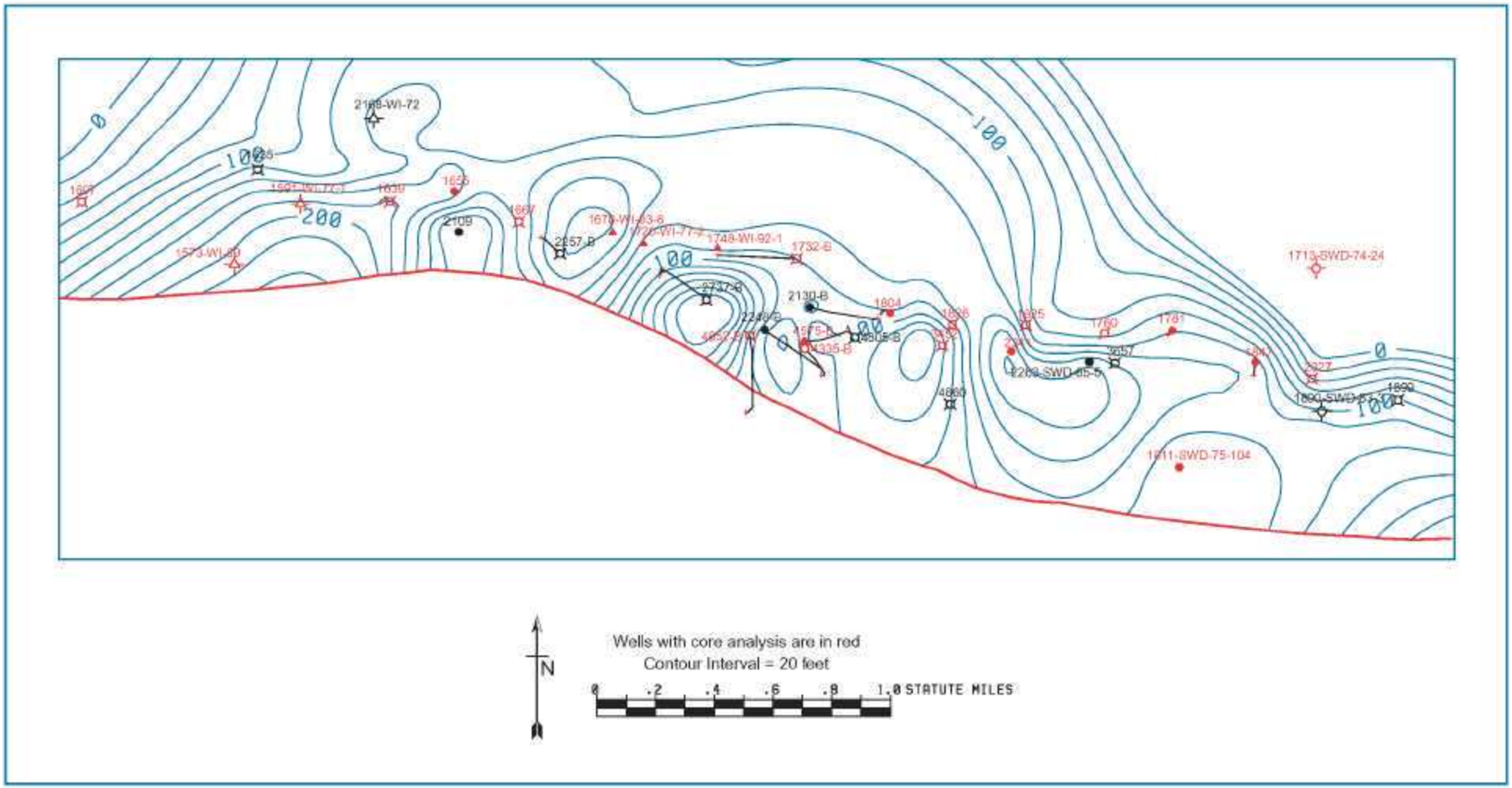

Figure 16. Isopach map of the upper part of the Smackover Formation at Womack Hill Oil Field and location of wells with core analysis data. See Figure 8 for well symbols.

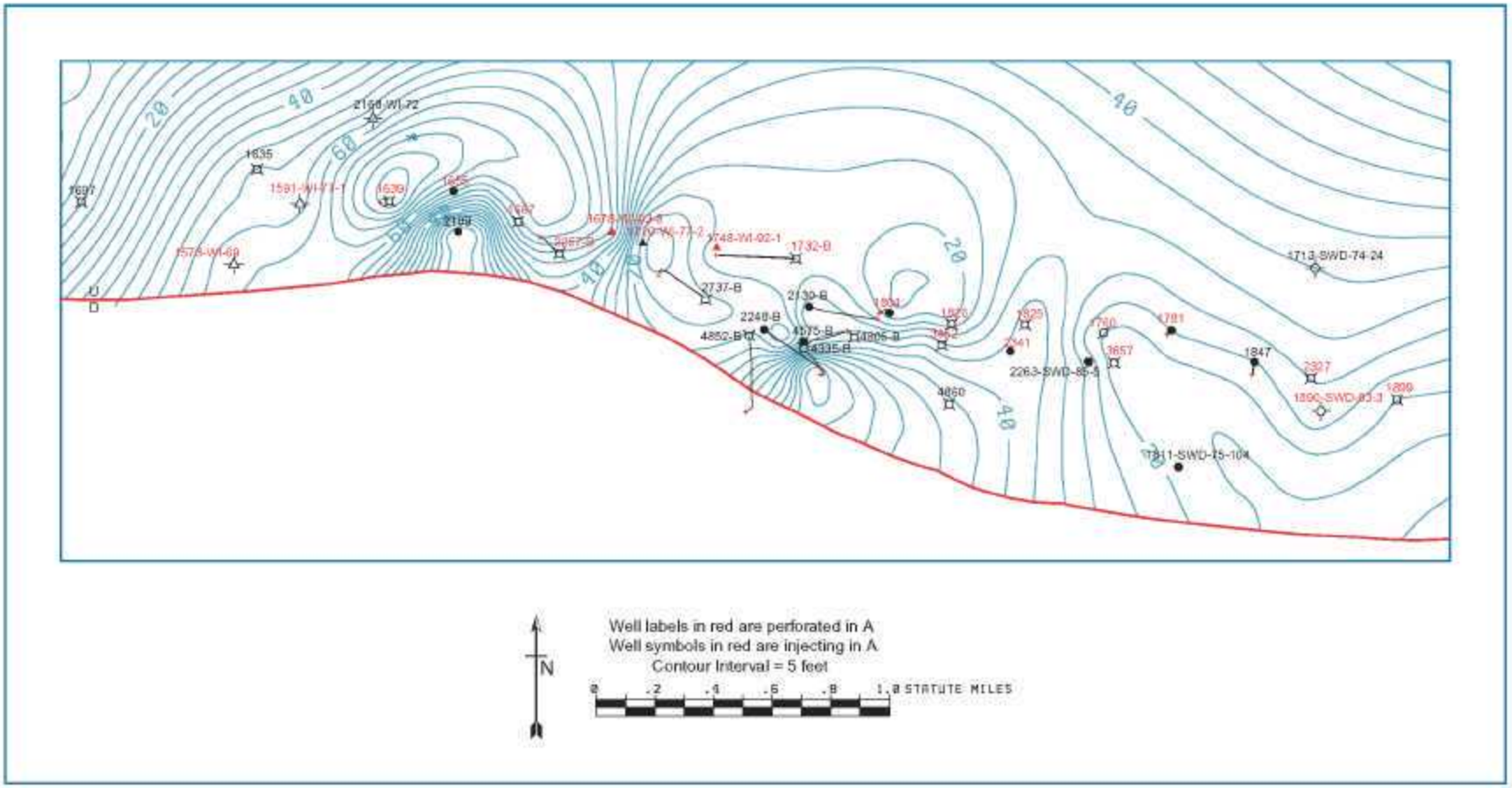

Figure 17. Isopach map of Cycle A and locations of wells perforated in Cycle A and wells injecting water into Cycle A. See Figure 6 for well symbols.

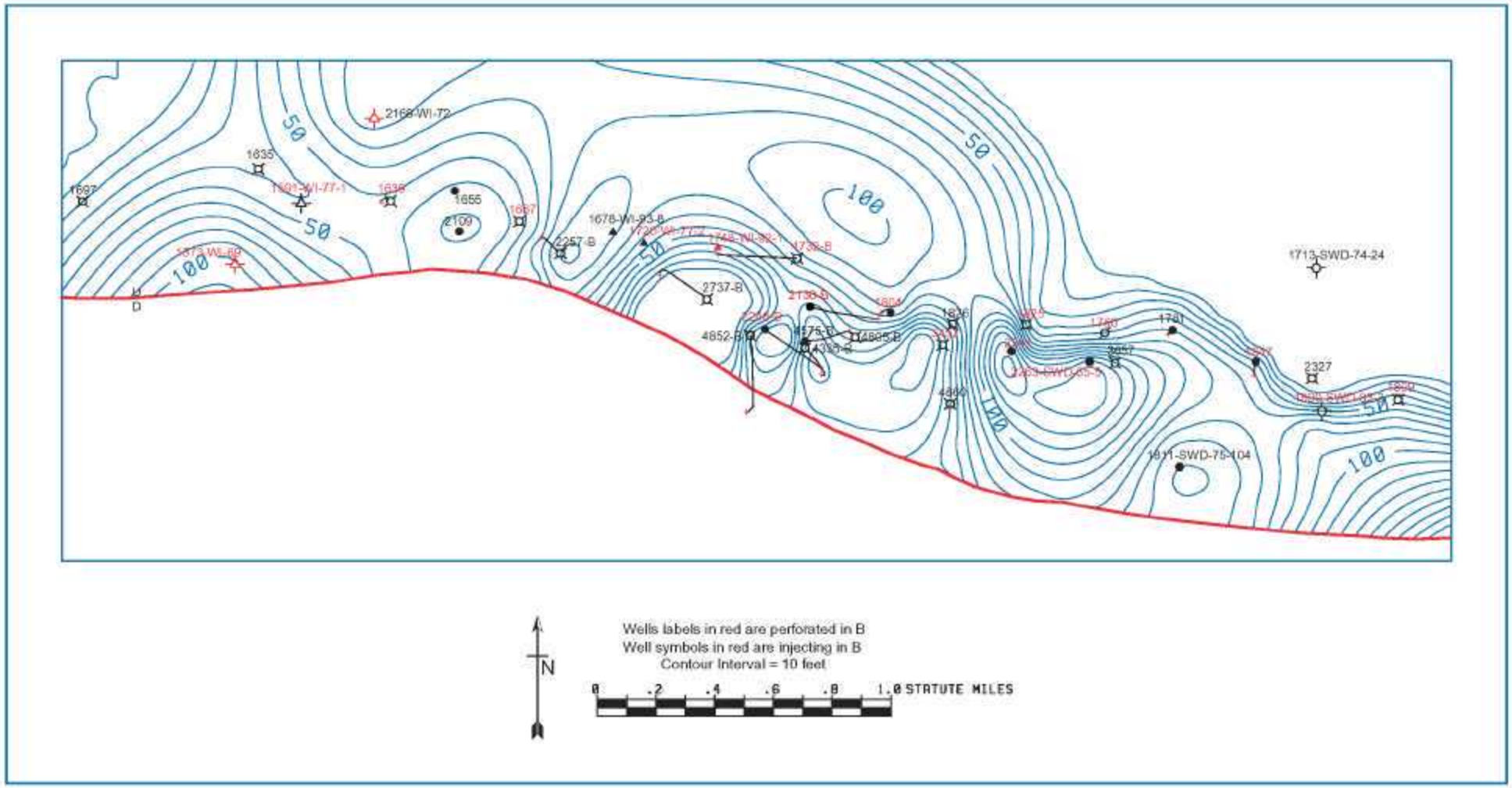

Figure 18. Isopach map of Cycle B and locations of wells perforated in Cycle B and wells injecting water into Cycle B. See Figure 8 for well symbols.

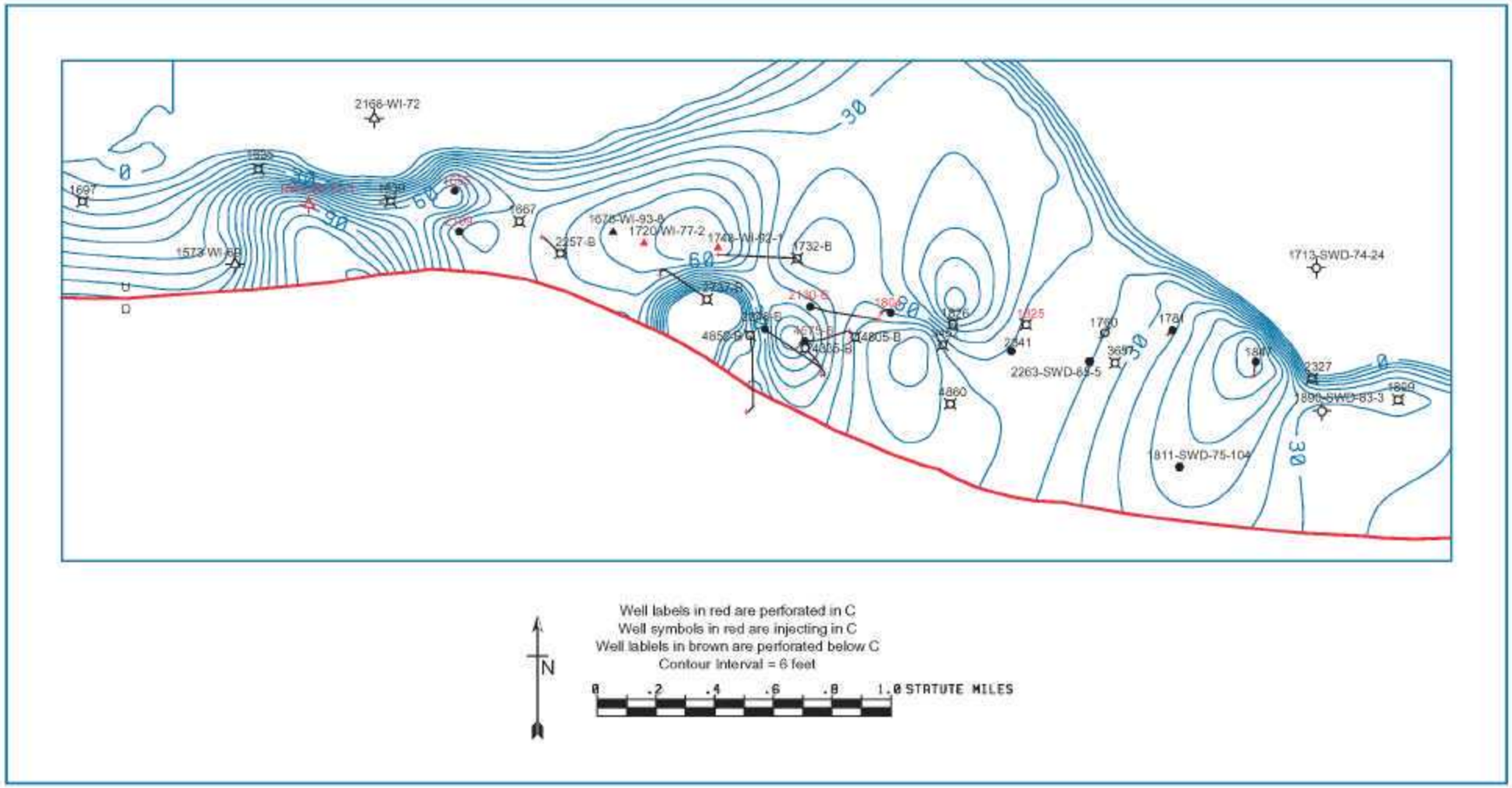

Figure 19. Isopach map of Cycle C and locations of wells perforated in Cycle C, wells perforated immediately below Cycle C, and wells injecting water into Cycle C. See Figure 8 for well symbols.

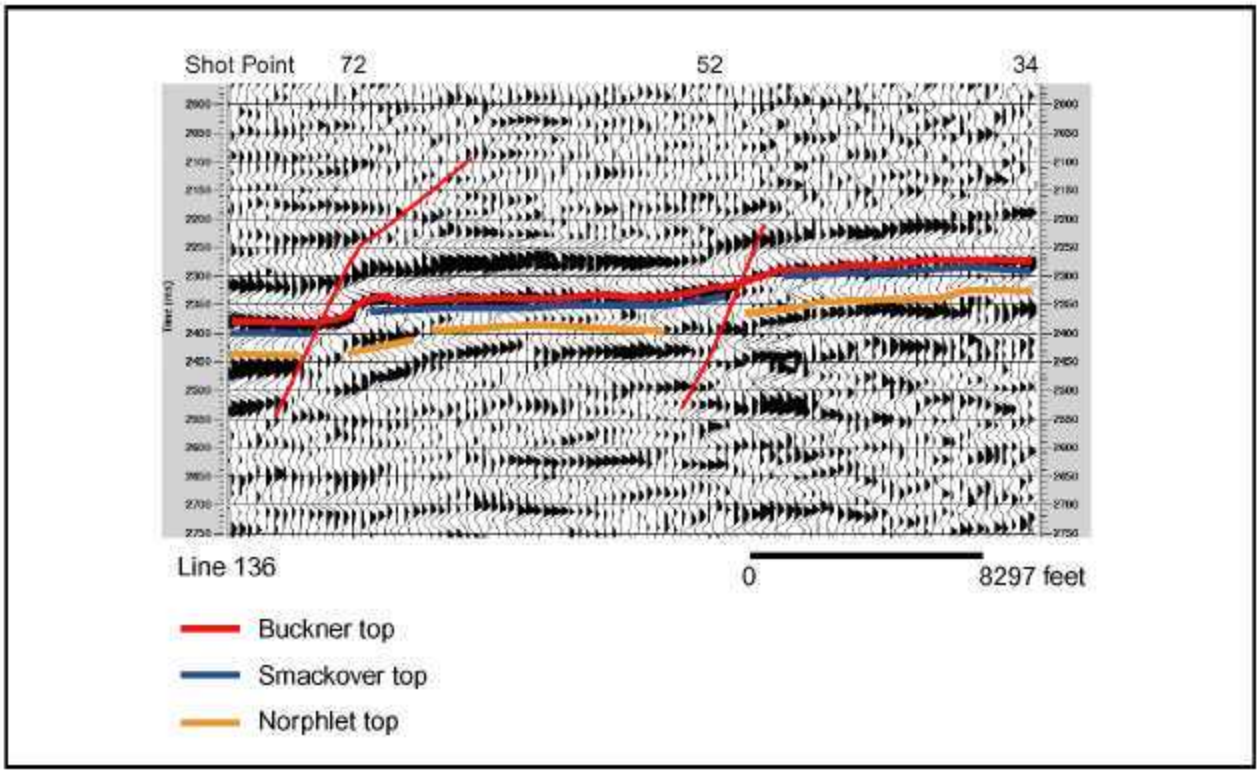

Figure 20. 2-D reflection profile, west-east line, Phillips P2635-136. See Figure 8 for location of seismic line.

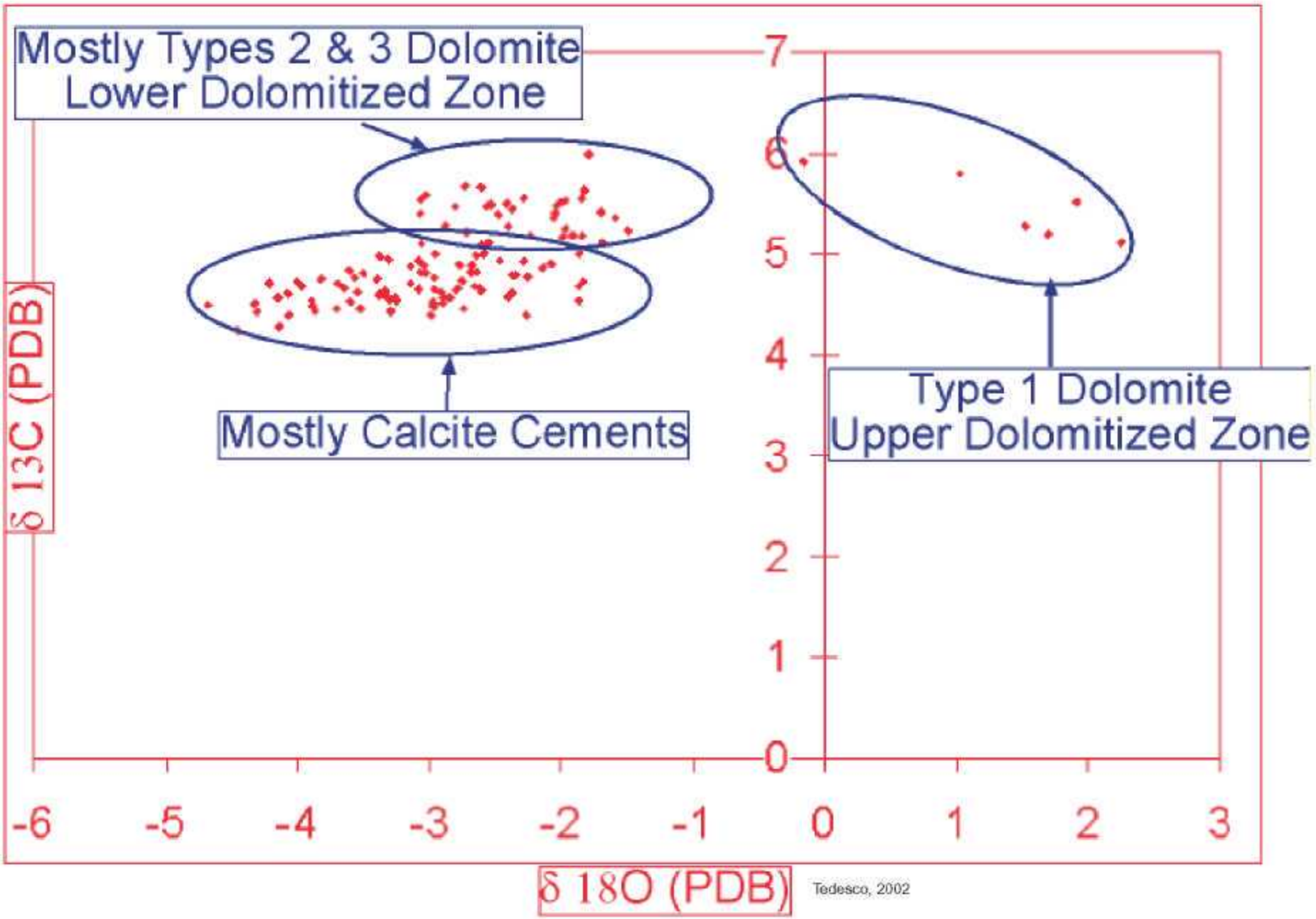

Figure 21. Stable isotope geochemistry. Upper dolomitized zone enriched relative to lower dolomitized zone suggesting two seperate dolotimizing fluids. Upper dolotimized zone isotropic signiture suggests dolotimization by hypersaline brine at near-surface tempeartures.

the lower zone of dolomitization is, in part, fabric destructive and is the result of mixing zone processes (Tedesco, 2002). Calcite cements form a linear trend probably reflecting a transition from earlier precipitated cement at cooler temperature through later burial calcite cements.

Cathodoluminescence (CL) petrography was conducted on all petrographically identified dolomite and calcite cements and grains. Zoned cements and bimineralic ooid grains were recognized during petrography. In addition, changing CL intensities in some dolomite crystals suggests changing fluid chemistry during precipitation. Detailed CL mapping was used to determine traverse and sampling locations for microprobe study. Results of CL study will be discussed in the diagenesis section below.

Strontium, calcium, magnesium, iron, and manganese concentrations have been determined through detailed component microsampling using a JEOL 733 Superprobe. We collected 98 data points, which include data from each dolomite type identified during transmitted light and cathodoluminescence petrography. Calcite and dolomite percentages were determined using an X-ray diffractometer.

Diagenetic Study.--Core descriptions, well log analysis, thin section petrography, and stable isotope geochemistry have been used to create a model of Smackover diagenesis at Womack Hill Field. Smackover diagenesis began with early marine cementation of grains by fibrous aragonite and development of micrite envelopes through algal borings. Partially preserved fabrics in ooids suggest these grains had three different original compositions: aragonite, Mg-calcite, and bimineralic. These unstable sediments were highly altered in the meteoric diagenetic realm, creating large amounts of moldic porosity. Isopachous rim and equigranular drusy spar cements precipitated in intergranular and moldic pores. Both cements

precipitated contemporaneously with dissolution and can be found in intergranular and moldic pores. Meteoric cementation was followed by at least four major phases of dolomitization.

The first event was a fabric-destructive dolomitization in the uppermost Smackover (Cycle A; upper dolomitized zone) (Fig. 22). This event likely occurred soon after deposition by penecontemporaneous, downward-moving, evaporitically-concentrated brine. The dolomite phase is associated with an exposure event identified from core and petrographic analysis (Fig. 23). At wells located on the structural high area of the field, the exposure is located above the phase 1 dolomitized zone near the Buckner-Smackover contact. In wells off the structural high, the exposure is located at or near the base of the dolomitized zone. A gamma-ray spike commonly occurs at the exposure surface, allowing for recognition and correlation of this surface. The dolomite is composed of inclusion-rich, euhedral to subhedral dolomite crystals, is completely fabric destructive, and exhibits a dull red luminescence (Fig. 22). The dolomitized zone is commonly 4 to 15 feet thick, has high porosity (15-30%) and high permeability (5-45 md). This first dolomitization event can be recognized on logs across the entire field.

The second phase of dolomitization likely occurred during or immediately following meteoric leaching of unstable aragonite grains, occluding much of the moldic porosity. The dolomite is characterized by inclusion-rich, xenotopic, fine-crystalline to microcrystalline (commonly less than 50 microns), anhedral crystals selectively replacing ooids and peloids (Fig. 24). The dolomite has a slightly brighter red luminescence than other dolomite phases. This event occluded moldic porosity and is a porosity destructive event.

The third dolomitizing event was fabric-destructive, creating large amounts of intercrystalline porosity and increasing permeability. This dolomite event is the most common throughout the wells, except where dolomite type 1 is present. Reservoir zones in the lower part

A.

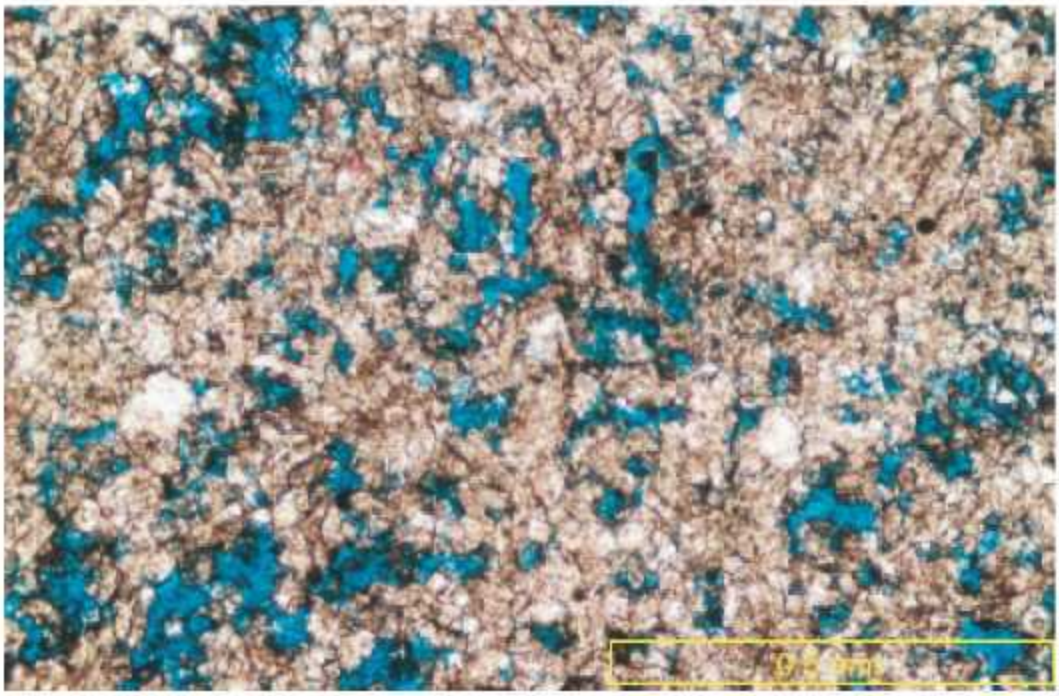

B.

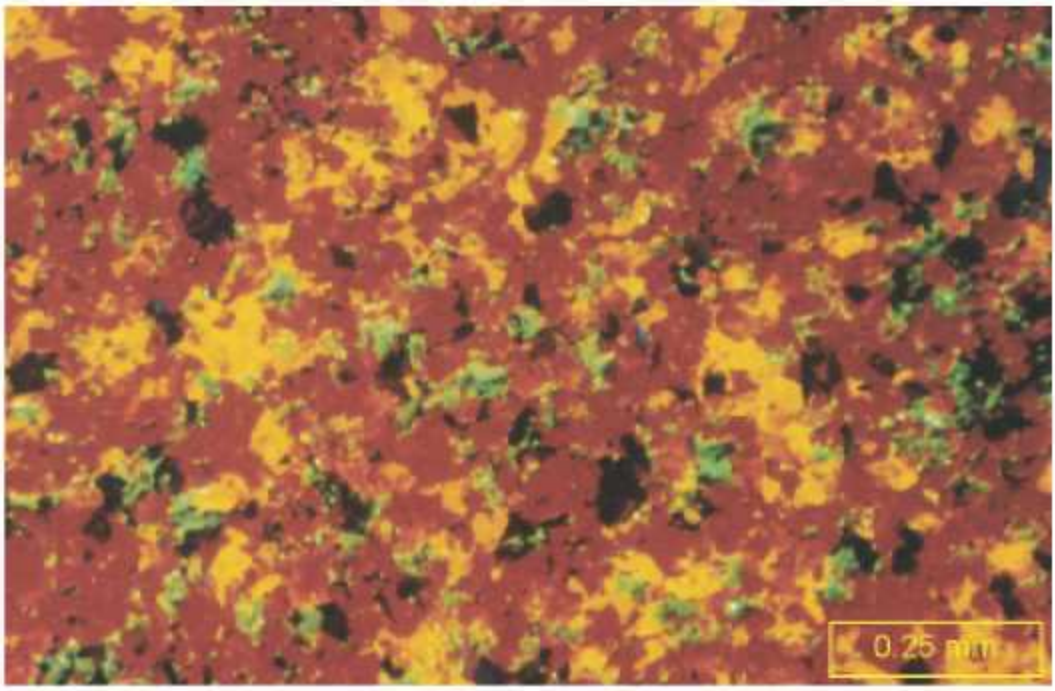

Figure 22. "Type 1" dolomite from near the top of the Smackover Formation.
A. Note inclusion-rich sucrosic dolomite crystals and large amount of intercrystalline porosity, Turner 13-25 well (11,434.4 ft).
B. Cathodoluminescence in Type 1 dolomite. Dolomite has red luminescence, burial calcite cement exhibits yellow luminescence, and bitumen exhibits green luminescence, Counselman 18-12 well (11,462 ft.).
(photographs by Tedesco).

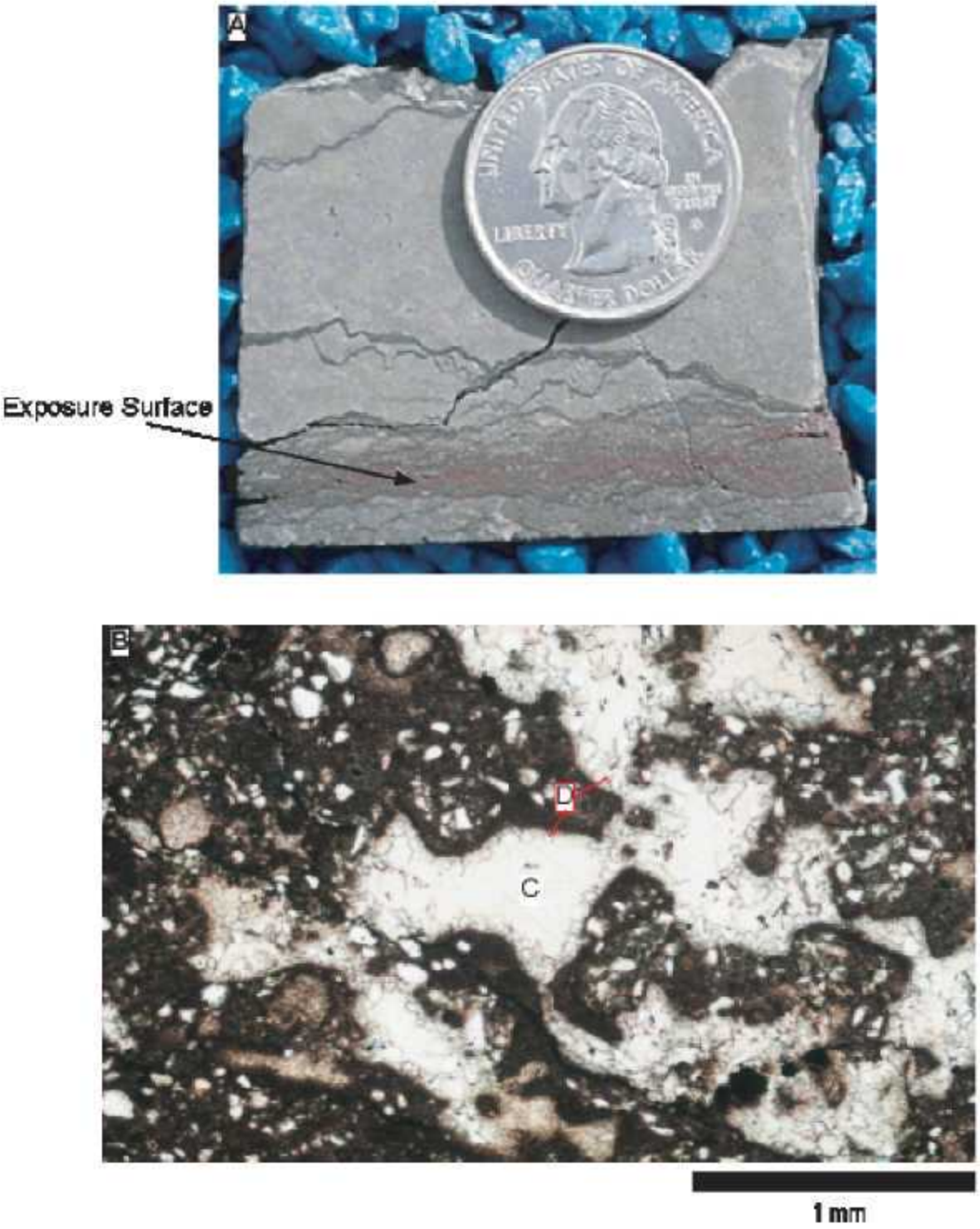

Figure 23. Upper "A" cycle exposure surface. Turner 13-5 well (11,326 ft.).
A. Red shale lamina at exposure surface.
B. Phtomicrograph at exposure surface. Dark brown groundmass composed of microcrystalline dolomite. Note alveolar texture. Pore lined idiotopic-C dolomite cement (D) followed by blocky calcite (C) cements that completely occlude porosity. Note high clastic content which is responsible for gamma ray spike characteristic of exposure surface.
(photographs by Tedesco).

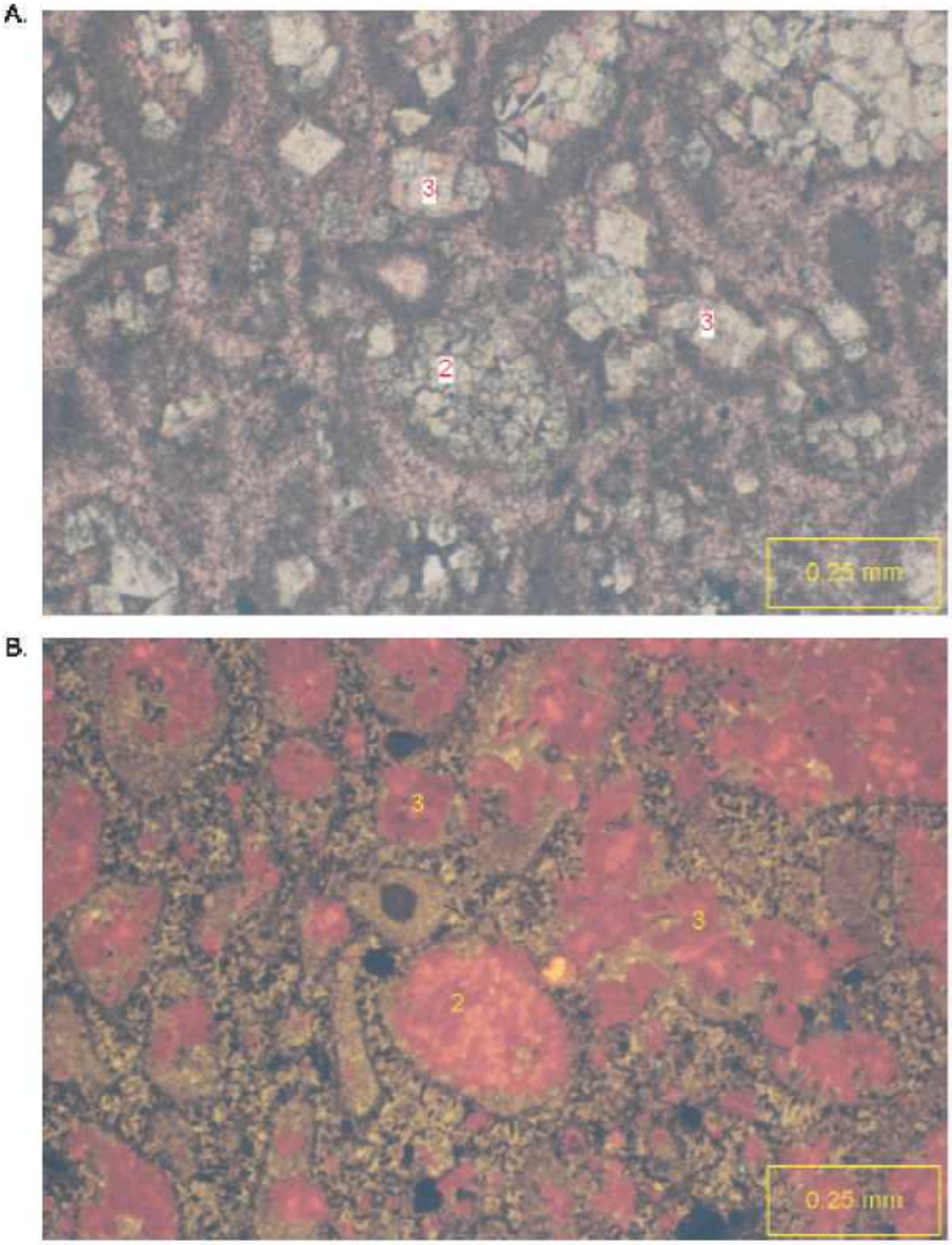

Figure 24. "Types 2 and 3" dolomite. Womack Hill Field Unit 14-5 well (11,116.5 ft.).
A. Note Type 2 (2) fabric selective replacement of grains by anhedral fine-crystalline dolomite and Type 3 (3) fabric destructive dolotimization by euhedral rhombs.
B. Cathodoluminescence view of A. Note brighter luminescence by Type 2 (2) dolomite.
(photographs by Tedesco).

of Cycle A, Cycle B, and Cycle C are commonly associated with dolomite phase 3. The lower dolomitized reservoir zone, which is primarily composed of type 3 dolomite, climbs stratigraphically higher from north to south in the field area. Two distinct dolomite crystal morphologies are recognized in this phase. The two morphologies may represent two separate phases of dolomitization from different brines or may represent a continuum of dolomitization with changing water chemistry. The first dolomite morphology is characterized by subhedral hypidiotopic to idiotopic, relatively inclusion-free crystals 50 to 100 microns in diameter (Figs. 24 and 25). The second morphology is comprised of euhedral, ideotopic, inclusion-free crystals 50 to 150 microns in diameter. Larger crystals commonly have an inclusion-rich core and more inclusion-free outer zone (Fig. 25). Both morphologies are commonly associated with stylolites and fractures throughout the cores, suggesting stylolites may have been fluid migration pathways.

The fourth dolomitization phase is comprised of idiotopic-c (Gregg and Sibley, 1984) dolomite cement lining vuggy pores in the Cycle A (Fig. 26). The cement commonly follows an early phreatic isopachous calcite cement and is followed by syntaxial blocky calcite spar cement. This cement is found in Cycle A near the identified exposure surface. The dolomite commonly has a bright red luminescence with quenched crystal terminations, suggesting changing fluid chemistry during precipitation. Microprobe data indicate a decrease in Mn concentration across the crystals, explaining the change in luminescence.

A minor dolomitization phase occurred in the deep burial environment and is characterized by precipitation of large saddle dolomite rhombs in fractures and vuggy pores. Other late burial cements include syntaxial and poikilotopic calcite spar cements, potassium feldspar overgrowths, blocky and poikilotopic anhydrite and celestite cement, and rare gypsum and sulfur cements.

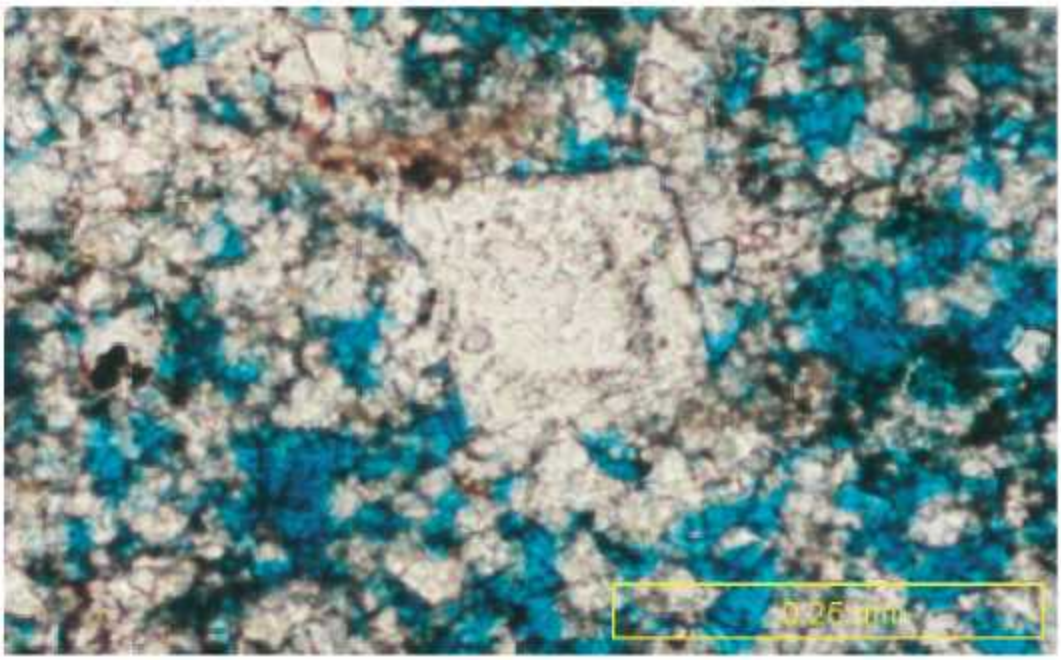

Figure 25. Close-up of "Type 3" dolomite crystal. Zones of inclusions toward center of crystal is a common observation across the field. Scruggs, Parker, Norton 9-14 well (11,413 ft.). (photograph by Tedesco).

A.

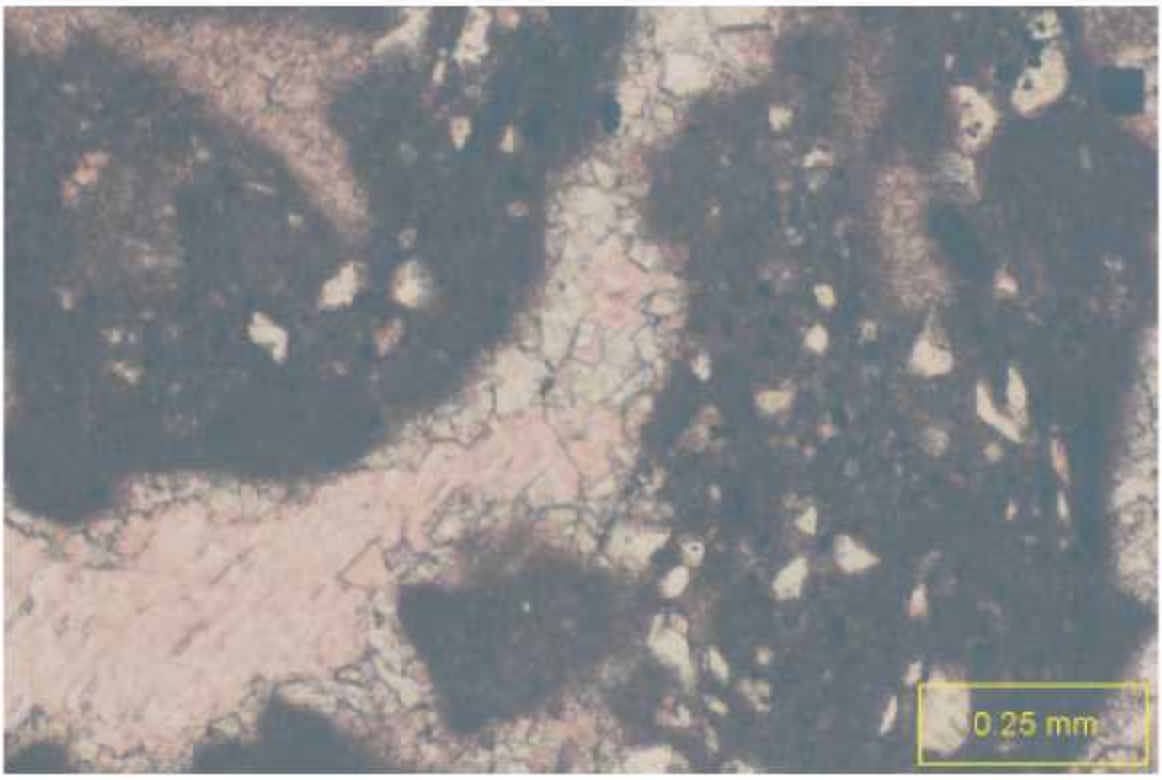

B.

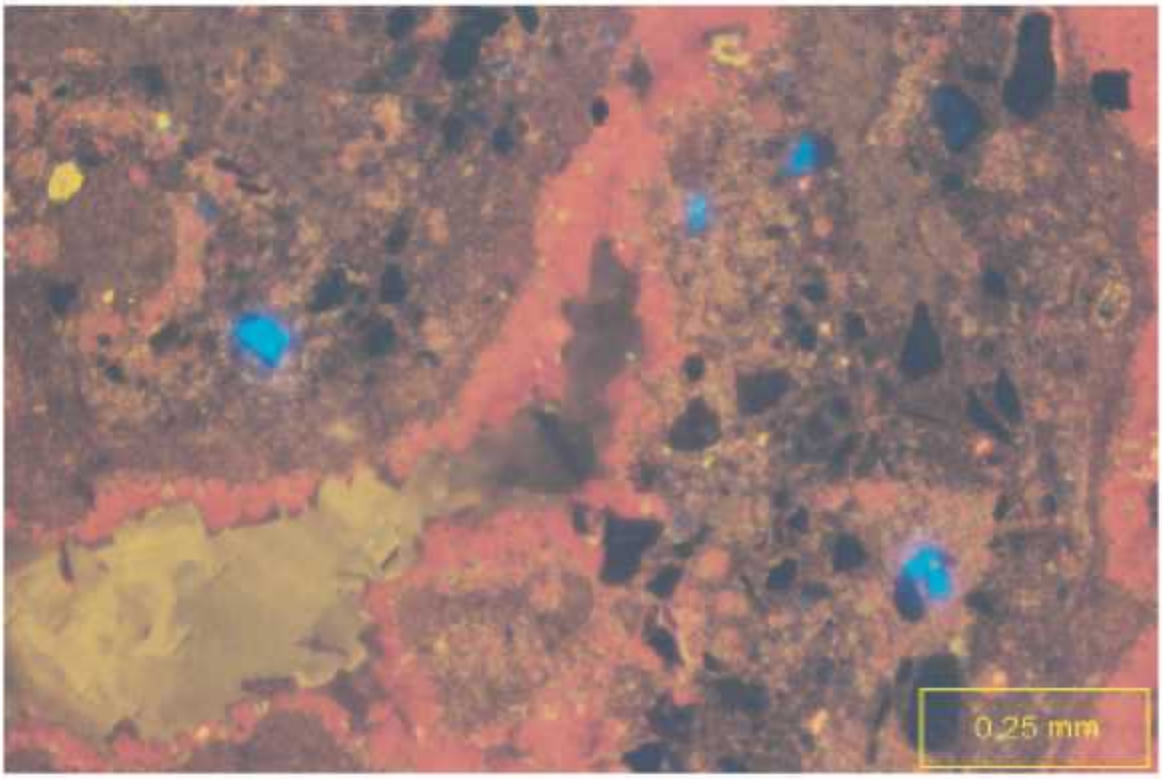

Figure 26. Idiotopic-C dolomite cement. Turner 13-5 well (11,327 ft.).
A. Note dolomite cement lining pore walls and following isopachous calcite cement. Dolomite followed by coarse syntaxial calcite cement which completely occludes porosity.
B. Cathodoluminescence of same view as in A. Note red luminescence and quenched crystal edges in dolomite cement.
(phtographs by Tedesco).

Burial effects include both physical and chemical compaction (Fig. 27). These have led to significant reductions of porosity and permeability in sediments not already dolomitized or altered to stable calcite. Burial features include crushed and deformed or broken grains, spalled oolites, stylolites and microstylolites, stylolitic grain contacts, interpenetrating grains, and fractures.

Pore System and Petrophysical Study.--The pore systems in the Smackover reservoir at Womack Hill Field have been studied and classified using the classification of Choquette and Pray (1970). Pore types consist of interparticle (includes solution-enlarged), intraparticle, vuggy, dolomite intercrystalline and grain moldic (Table 1). The probe permeameter (mini-permeameter) was used to determine horizontal and vertical permeabilities from the 118 billets cut from the cores for thin sections. Average log vertical permeabilities were plotted with average log horizontal permeabilities, and no significant difference was observed between vertical and horizontal permeabilities (Figs. 28 and 29). High pressure mercury injection capillary pressure (MICP) analysis was performed on 11 core plugs representative of the pore systems (Table 2). See Figures 30 through 42 for results of the MICP testing.

Porosity and permeability data representative of the pore systems and acquired from the plugs were combined with mercury derived data to compare porosities and permeabilities (Table 3). Helium derived porosity values were found to average 2% higher than the mercury derived values (Figs. 43 and 44). Probe permeability values closely approximate the mercury derived permeabilities, except where the permeability value is below 1 md (Figs. 45 and 46). Capillary pressure permeability correlates with measured probe permeabilities (Fig. 47). Capillary pressure porosity has a high correlation with helium derived porosity values (Fig. 48); however, porosity from core analysis correlates poorly with the mercury and helium derived porosities (Figs. 48

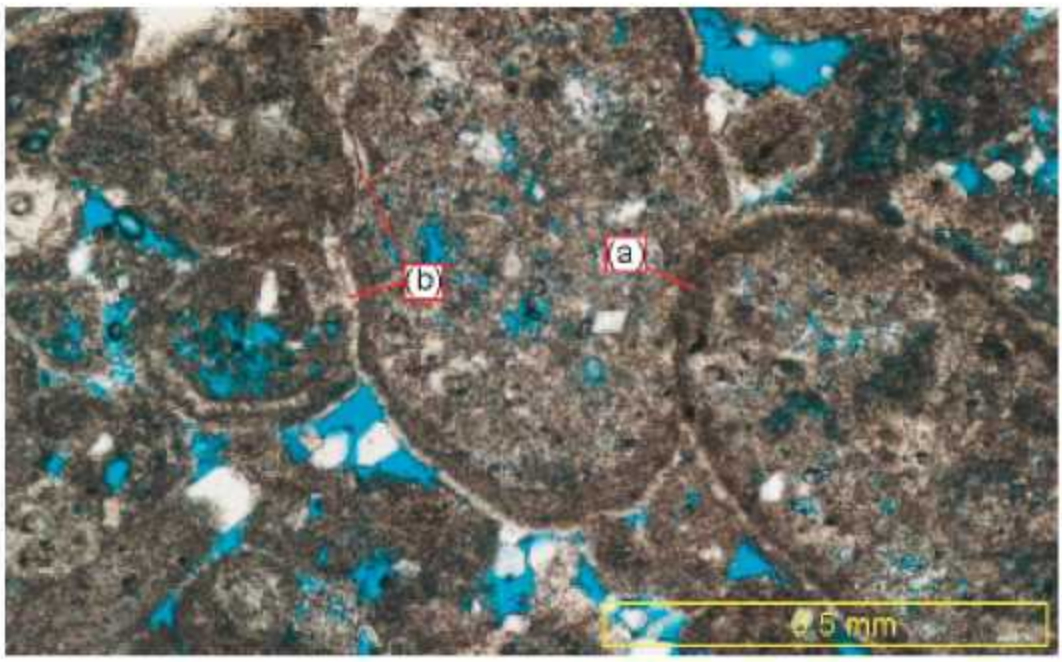

Figure 27. Deformation features in calcite-dominated zones. Note interpenetration and deformation of grains. These features can significantly reduce porosity. Deformation occurred both before (a) and following (b) early marine cementation. Rare "Type 3" dolomite rhombs scattered in interparticle pores. Turner 13-6 well (11,412 ft.). (photograph by Tedesco).

Table 1. Data on plugs chosen for capillary pressure testing (from Hopkins, 2002).

Well Permit #	Cycle	Core Depth	Lithology	*Est* % Dolomite	Pore Types	(Cleaned) He % Porosity	Cleaned Pr Permeability (md)
1591	A	11,405.0	pel, oo ws	*90*	ic 21.	52	35.07
1591	A	11,411.0	ms	*80*	ip, vg	12.10	5.60
1591	A	11,413.0	oo, pel ws	*80*	ic 17.	15	8.19
1591	C	11,515.0	pel ws	*88*	ic 18.	33	41.83
1591	C	11,528.0	pel ms	*90*	ic 16.	39	9.04
4575b	A	11,120.0	oo, pel ps	*20*	vg 8.	56	19.90
4575b	A	11,129.0	oo, pel ps	*10*	ip, ap, vg	20.73	22.40
4575b	B	11,146.0	onc, pel, oo gs	*15*	ip, ap	17.68	6.87
4575b	B	11,156.0	onc, oo gs	*15*	ip, ap, vg	18.22	7.46
4575b	B	11,174.0	onc, pel, oo gs	*20*	ip, ap, vg	15.25	2.27
4575b	C	11,192.0	pel ws	*87*	ic 17.	27	42.67

ms=mudstone
ws=wackestone
ps=packstone
gs=grainstone

ip=interparticle
ap=intraparticle
vg=vuggy
ic=intercrystalline
mo=moldic

Est - Visually Estimated
He - Helium Porosimeter
Pr - Probe Permeameter

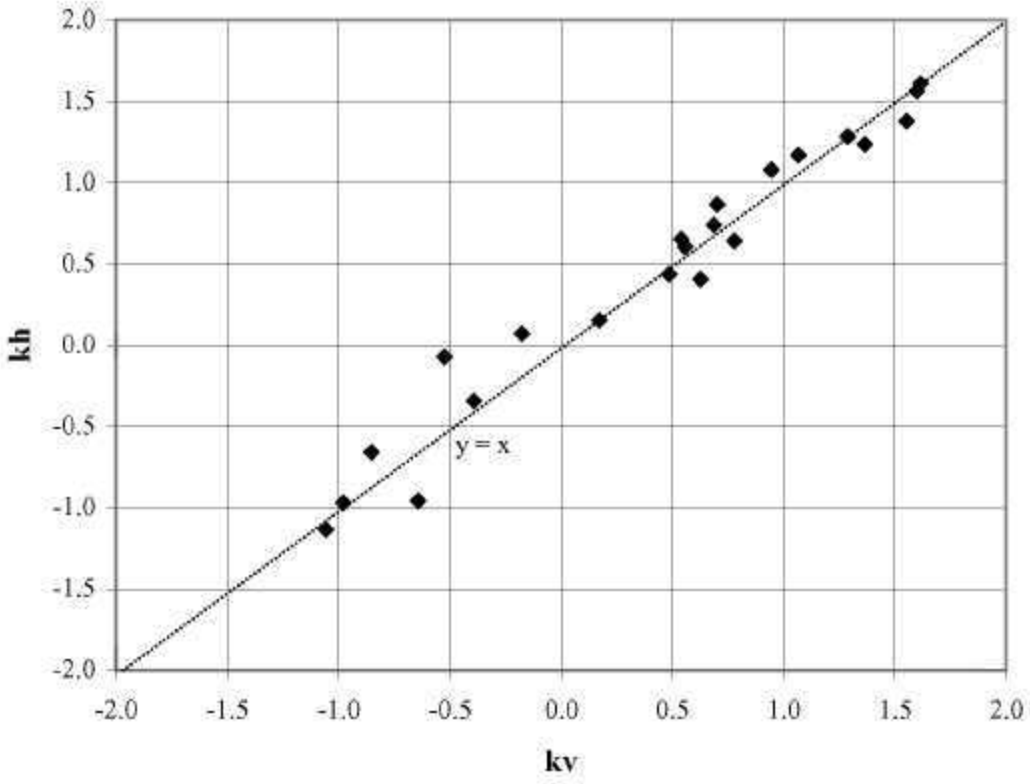

Figure 28. Average log vertical permeability (kv) vs. average log horizontal permeability (kh) measured from the probe pemeameter for Well Permit 1591 (from Hopkins, 2002).

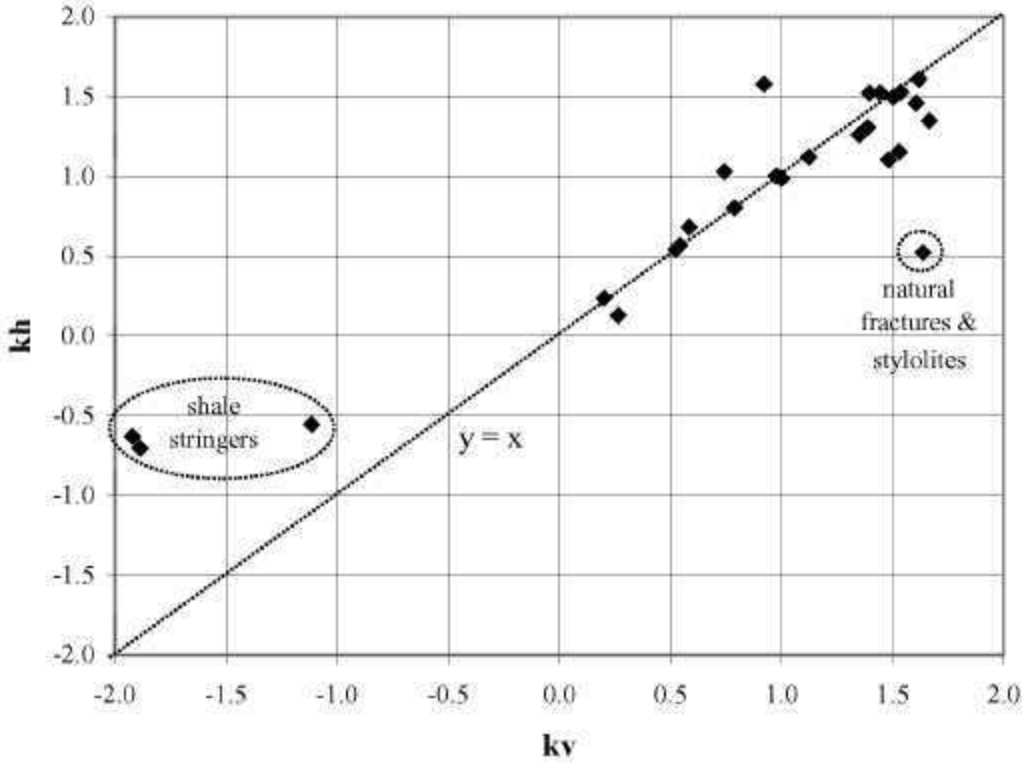

Figure 29. Average log vertical permeability (kv) vs. average log horizontal permeability (kh) measured from the probe permeameter for Well Permit 4575-B (from Hopkins, 2002).

Table 2. List of mercury injection capillary pressure plugs and associated data (from Hopkins, 2002).

Permit #	Sample Depth (ft)	Plug #	Core Analysis		Mercury Derived		Median Pore Aperture (m)	Saturation At End of Initial		Pore Structure
			phi (%)	k (md)	phi (%)	k (md)		Drainage Cycle	Imbibition Cycle	
1591	11,405.0	1	21.52	35.1	19.6	35.3	4.62	3	34	unimodal sharp
	11,411.0	2	12.10	5.6	9.02	0.982	1.07	12	25	unimodal broad
	11,413.0	3	17.15	8.19	15.3	8.83	2.59	7	29	unimodal sharp
	11,515.0	4	18.33	41.8	16.4	34.7	5.20	4	24	unimodal sharp
	11,528.0	5	16.39	9.04	15.0	8.95	2.33	2	52	unimodal sharp
4575b	11,120.0	11	8.56	19.9	2.27	0.021	0.262	44	46	poorly defined
	11,129.0	12	20.73	22.4	18.7	17.8	3.33	3	44	unimodal broad
	11,146.0	14	17.68	6.87	16.6	8.67	2.36	2	37	unimodal sharp
	11,156.0	15	18.22	7.46	15.9	7.19	2.22	4	44	unimodal broad
	11,174.0	16	15.25	2.27	12.9	2.07	1.28	8	40	unimodal broad
	11,192.0	18	17.27	42.3	16.0	49.5	6.75	3	23	unimodal sharp

Table 3. Plug data: measured values versus mercury (Hg) derived values (from Hopkins, 2002).

Plug Number	Well Permit #	Core Depth	Pore Types	Hg Median Pore Aperture (μm)	He % Porosity	Hg % Porosity	Pr Permeability (md)	Hg Permeability (md)
1	1591	11,405.0	ic	4.62	21.52	19.6	35.07	35.3
2	1591	11,411.0	ip, vg	1.07	12.10	9.02	5.60	0.98
3	1591	11,413.0	ic	2.59	17.15	15.3	8.19	8.83
4	1591	11,515.0	ic	5.20	18.33	16.4	41.83	34.7
5	1591	11,528.0	ic	2.33	16.39	15.0	9.04	8.95
11	4575b	11,120.0	vg	0.26	8.56	2.27	19.90	0.02
12	4575b	11,129.0	ip, ap, vg	3.33	20.73	18.7	22.40	17.8
14	4575b	11,146.0	ip, ap	2.36	17.68	16.6	6.87	8.67
15	4575b	11,156.0	ip, ap, vg	2.22	18.22	15.9	7.46	7.19
16	4575b	11,174.0	ip, ap, vg	1.28	15.25	12.9	2.27	2.07
18	4575b	11,192.0	ic	6.75	17.27	16.0	42.67	49.5

ic=intercrystalline
ip=interparticle
vg=vuggy
ap=intraparticle

Hg - Mercury Derived
He - Helium Porosimeter
Pr - Probe Permeameter

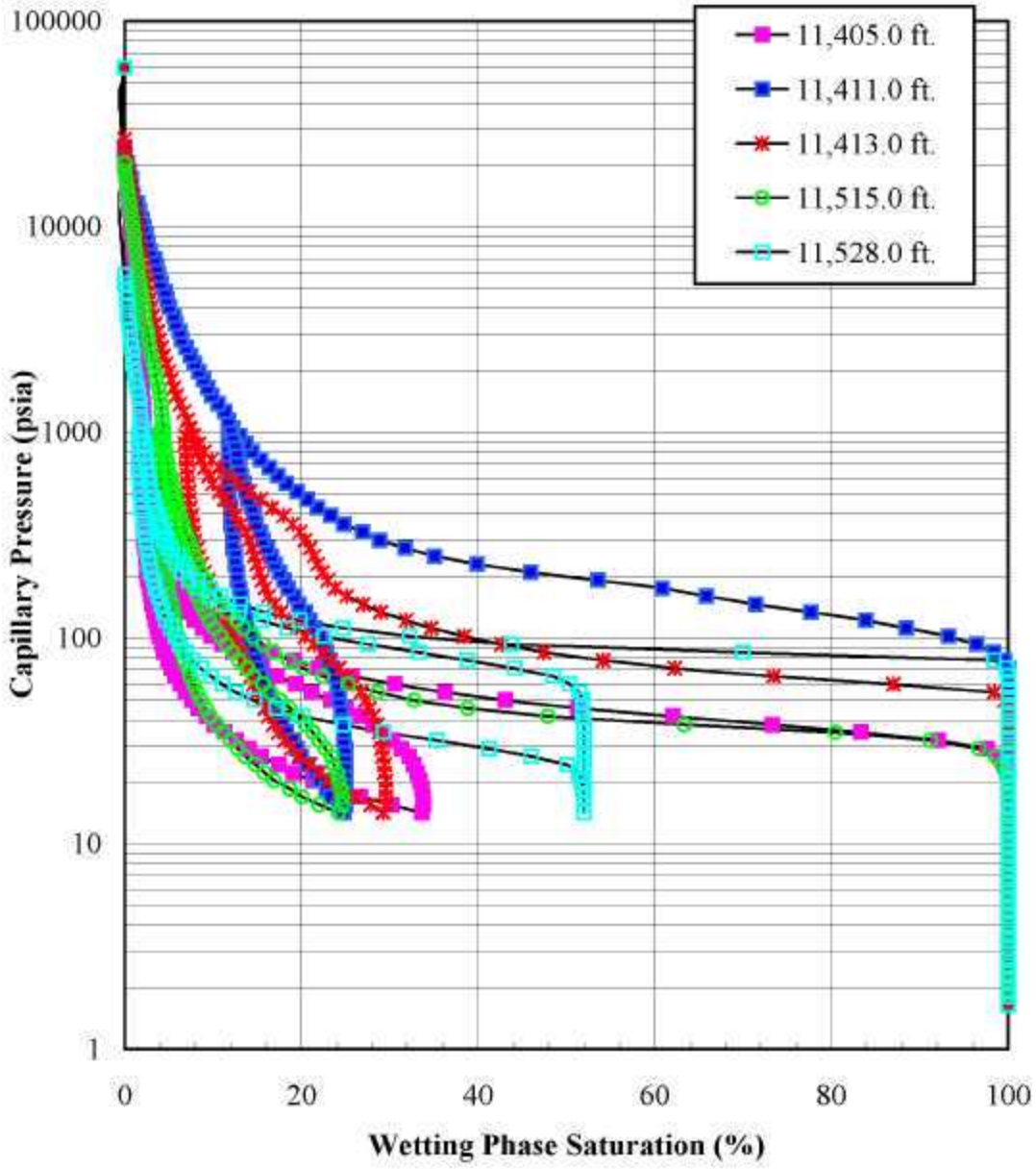

Figure 30. Mercury injection capillary pressure (pore volume) for Well Permit 1591 (from Hopkins, 2002).

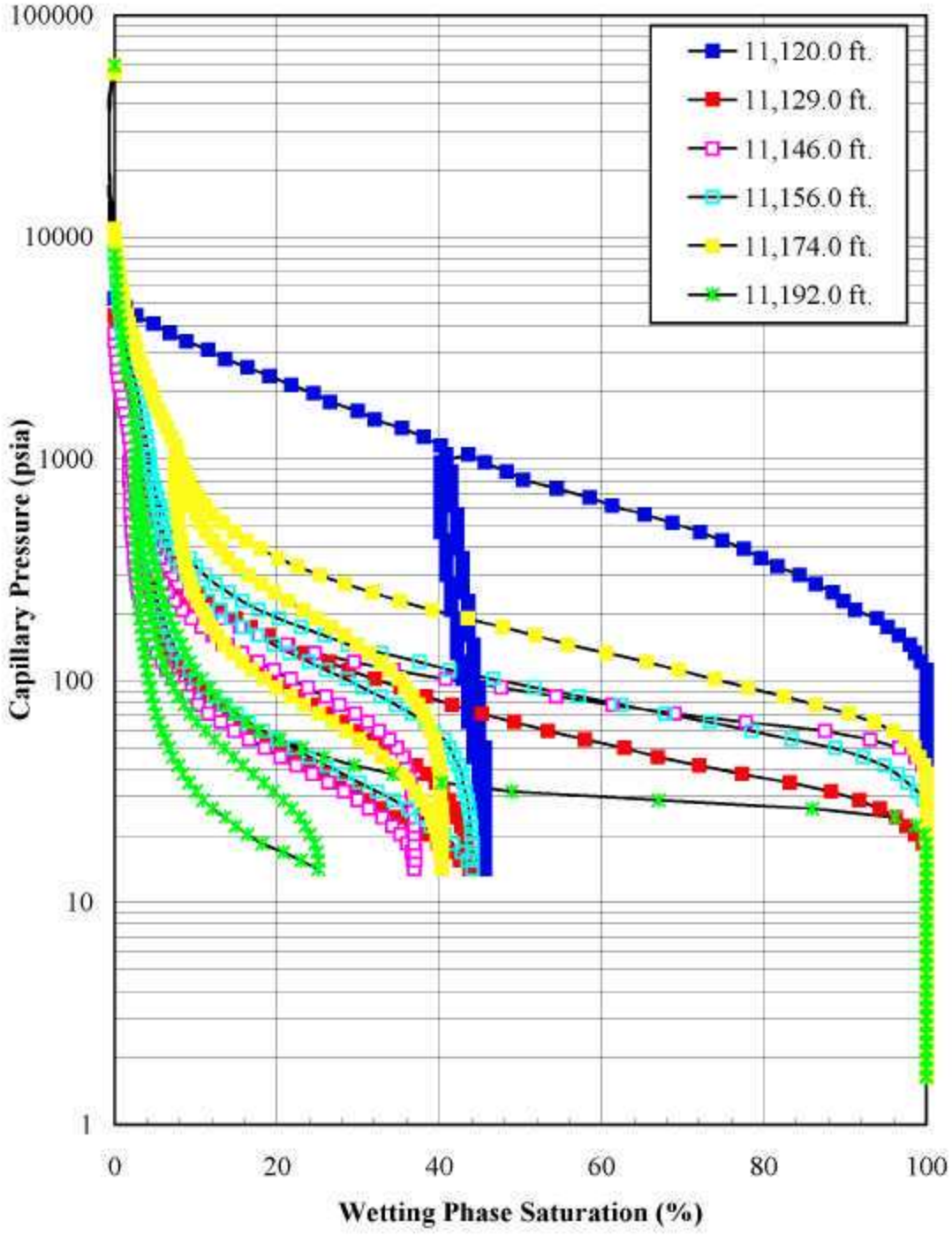

Figure 31. Mercury injection capillary pressure (pore volume) for Well Permit 4575-B (from Hopkins, 2002).

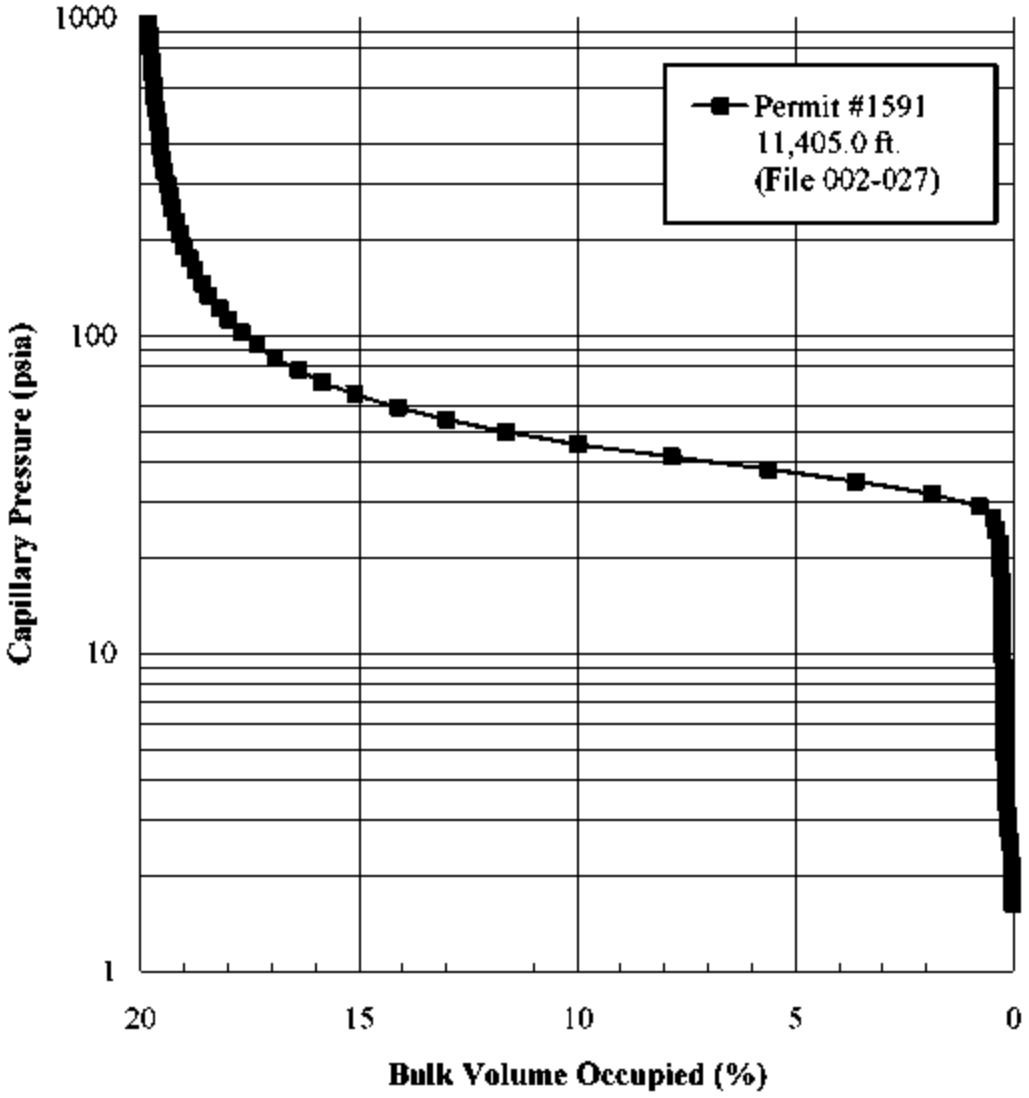

Figure 32. Mercury injection capillary pressure (pore volume) for Well Permit 1591 at 11,405 ft (from Hopkins, 2002).

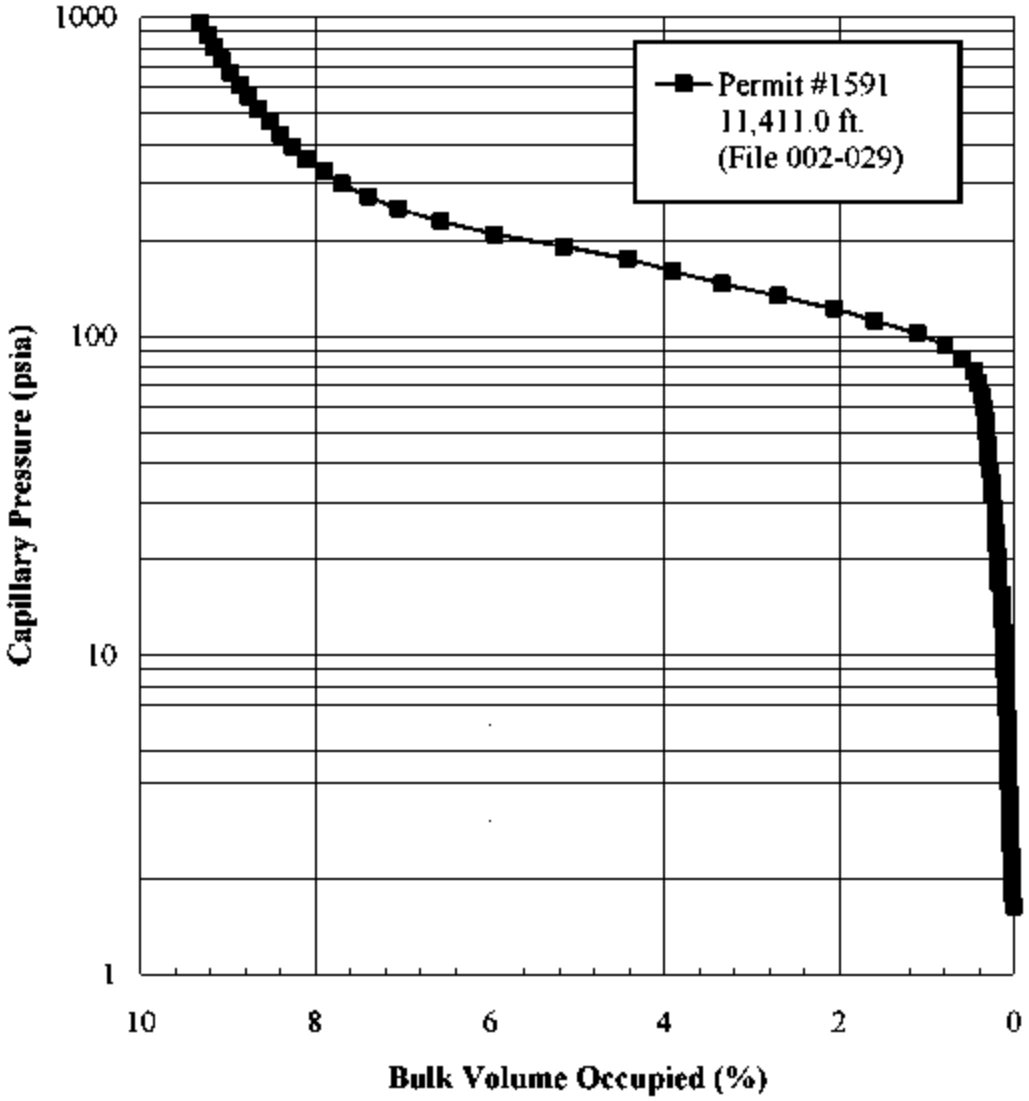

Figure 33. Mercury injection capillary pressure (pore volume) for Well Permit 1591 at 11,411 ft (from Hopkins, 2002).

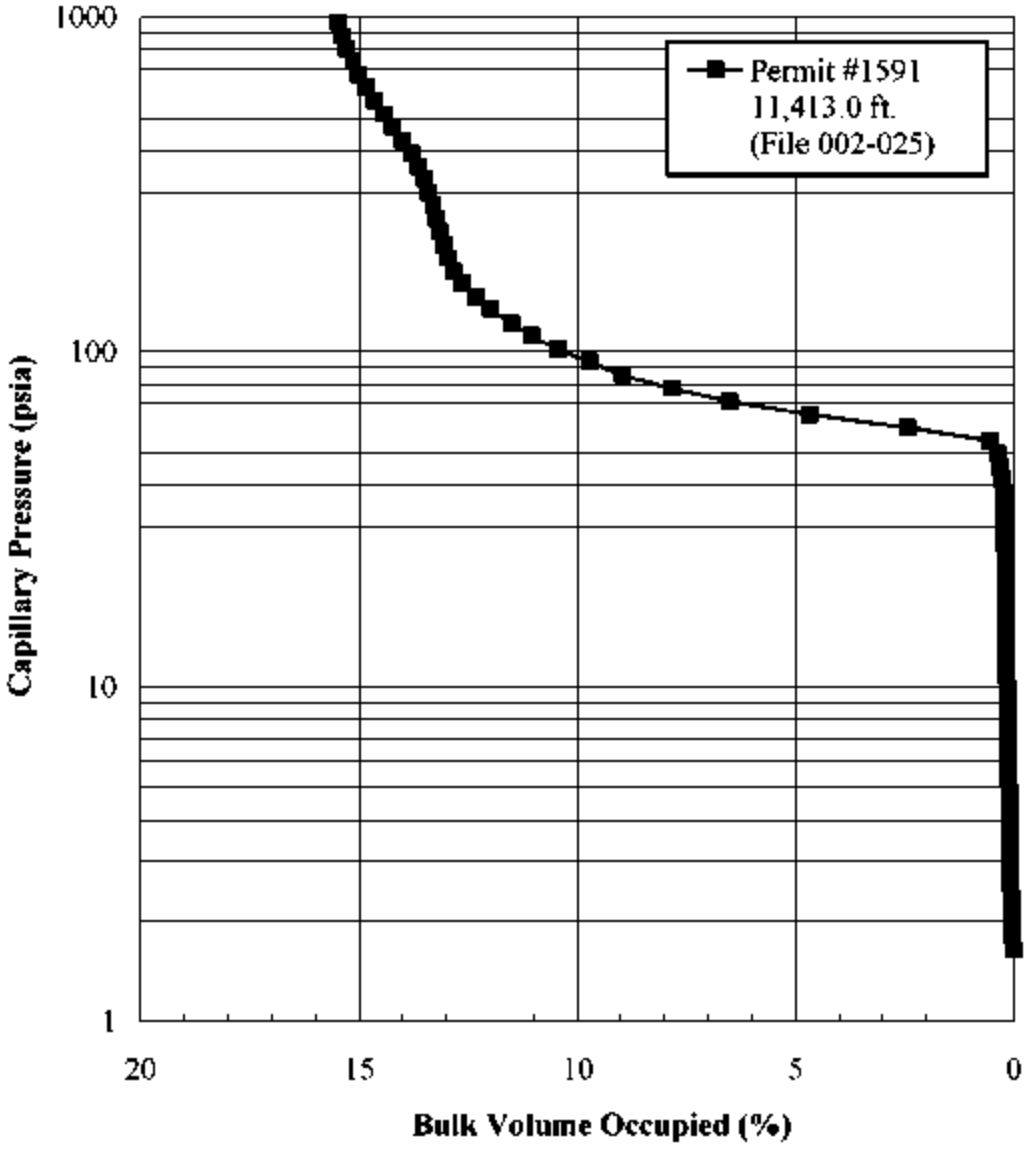

Figure 34. Mercury injection capillary pressure (pore volume) for Well Permit 1591 at 11,413 ft (from Hopkins, 2002).

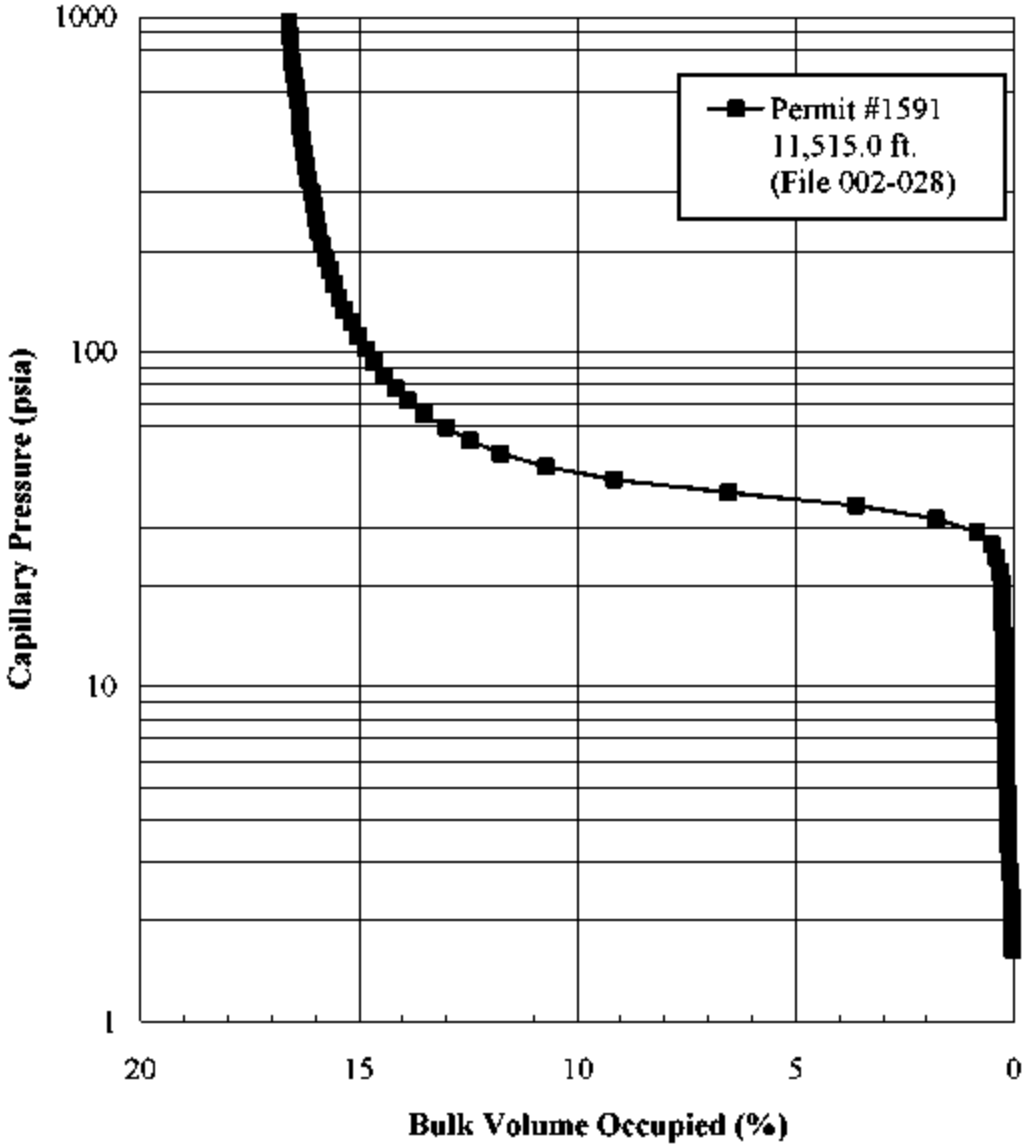

Figure 35. Mercury injection capillary pressure (pore volume) for Well Permit 1591 at 11,515 ft (from Hopkins, 2002).

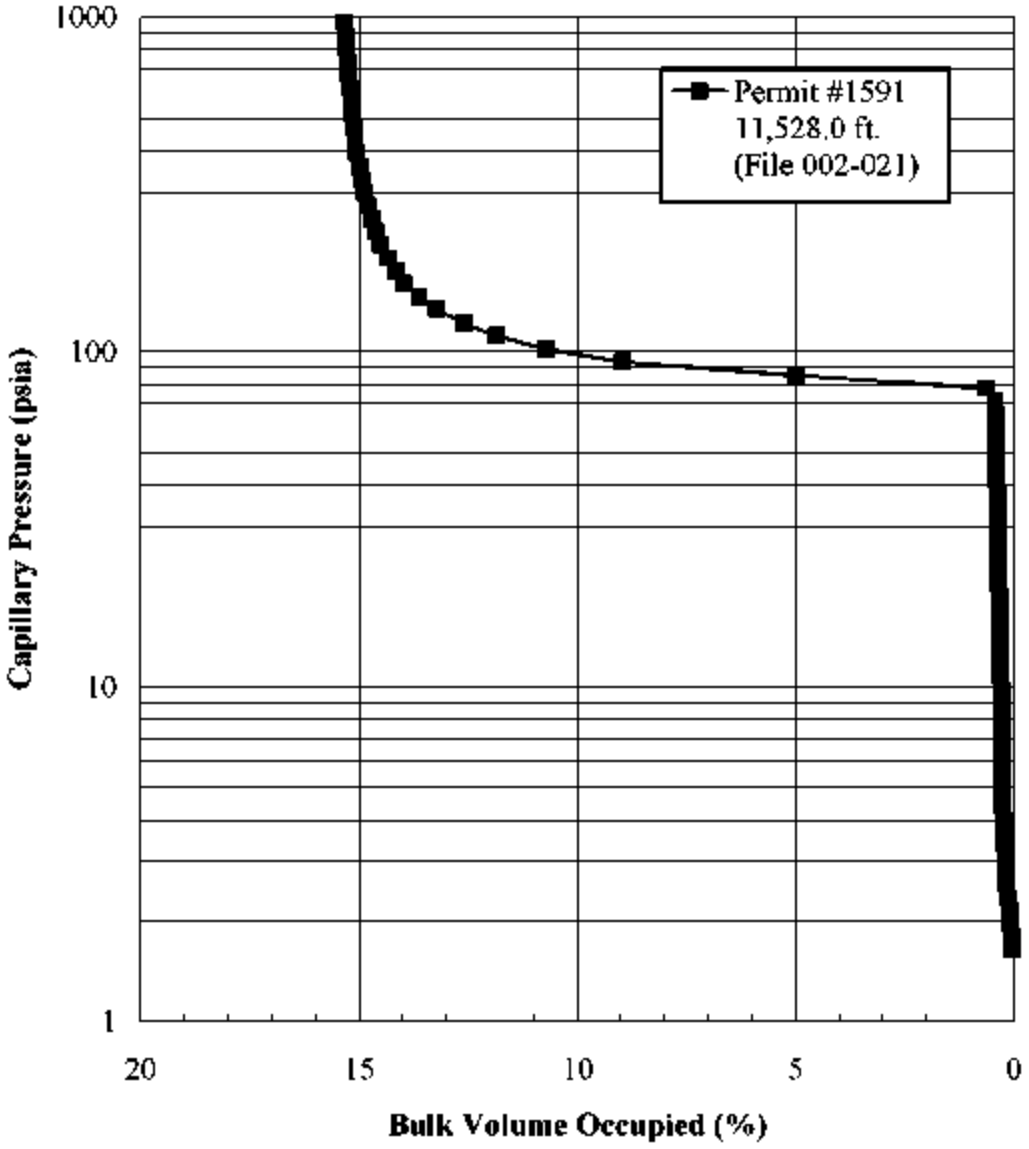

Figure 36. Mercury injection capillary pressure (pore volume) for Well Permit 1591 at 11,528 ft (from Hopkins, 2002).

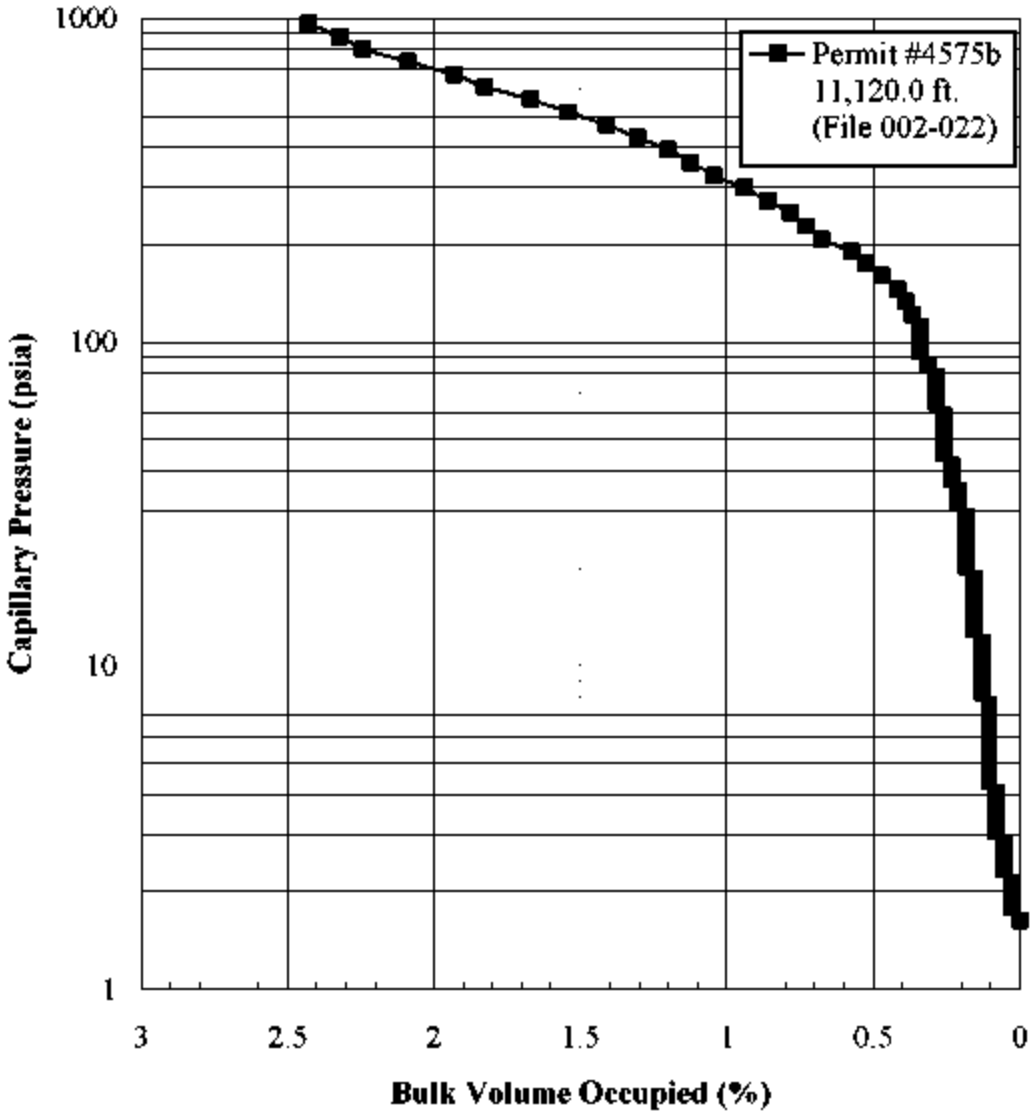

Figure 37. Mercury injection capillary pressure (pore volume) for Well Permit 4575B at 11,120 ft (from Hopkins, 2002).

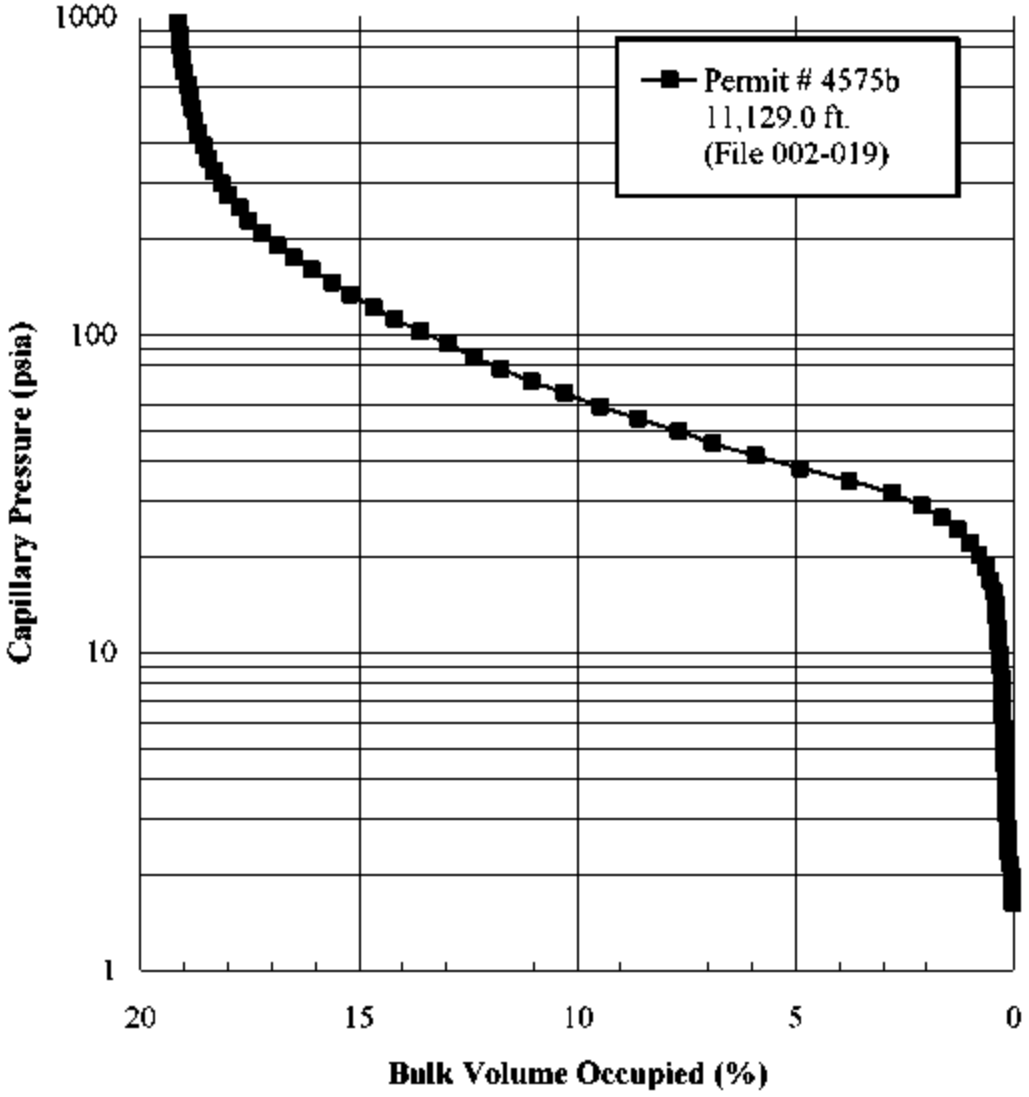

Figure 38. Mercury injection capillary pressure (pore volume) for Well Permit 4575B at 11,129 ft (from Hopkins, 2002).

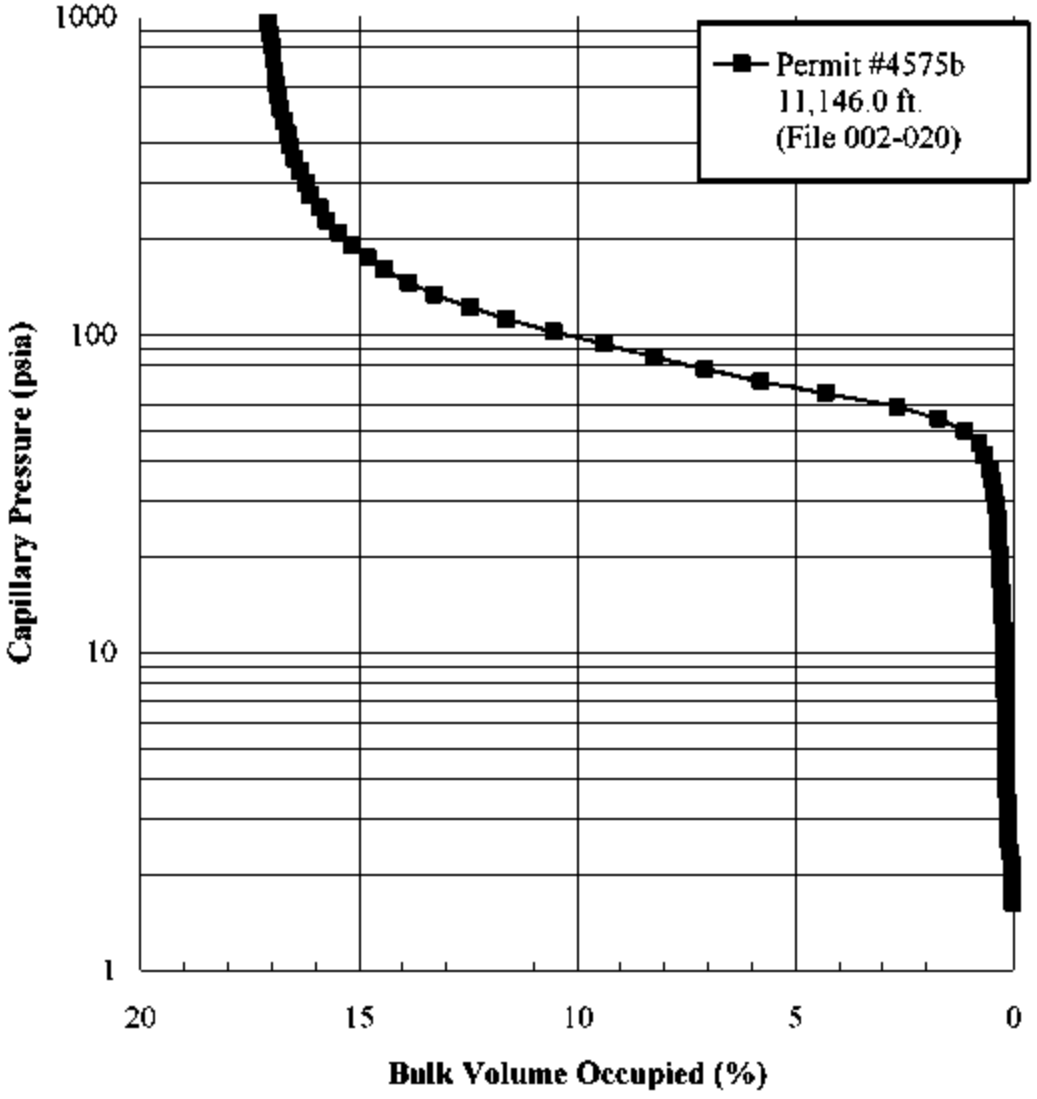

Figure 39. Mercury injection capillary pressure (pore volume) for Well Permit 4575B at 11,146 ft (from Hopkins, 2002).

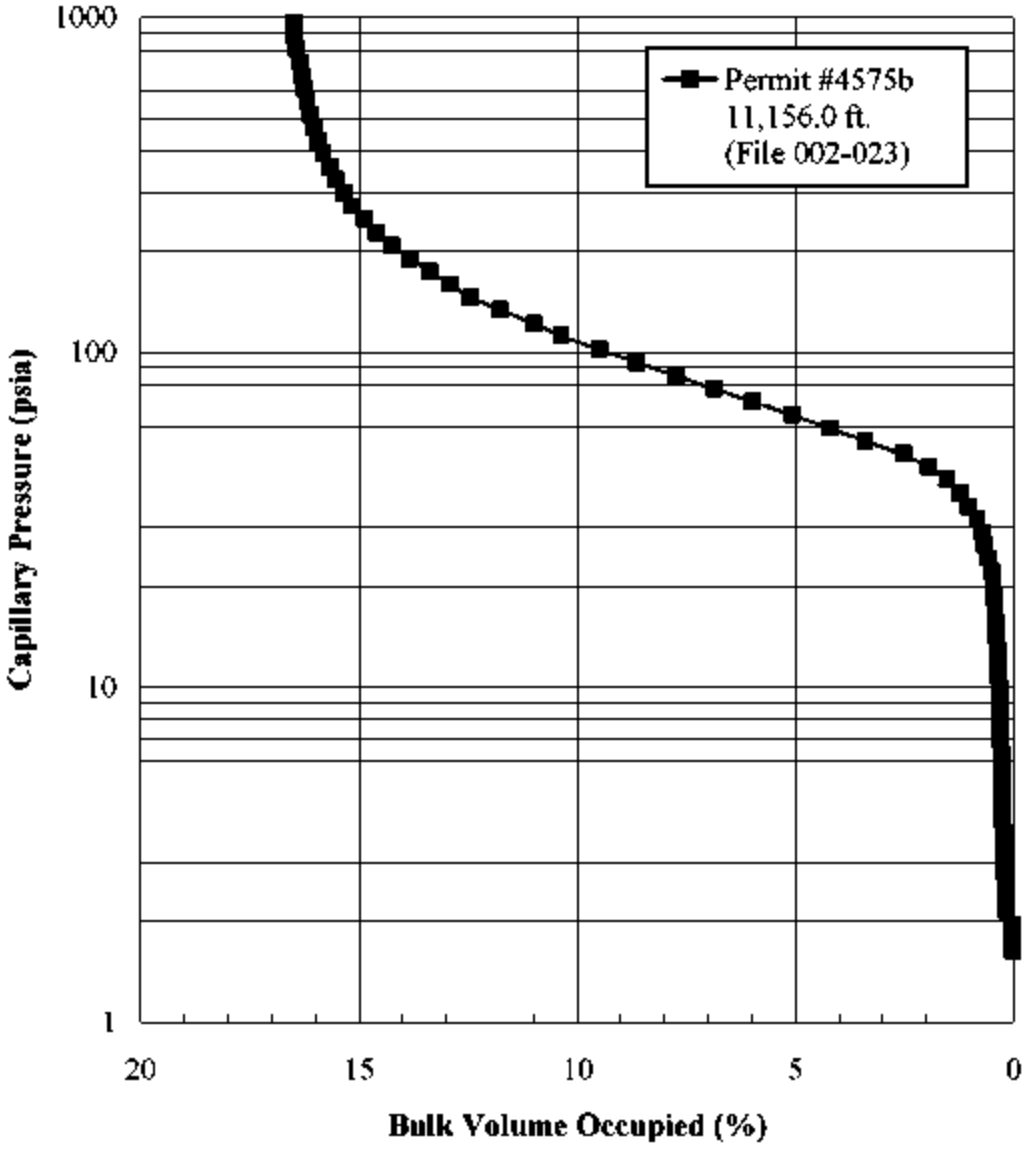

Figure 40. Mercury injection capillary pressure (pore volume) for Well Permit 4575B at 11,156 ft (from Hopkins, 2002).

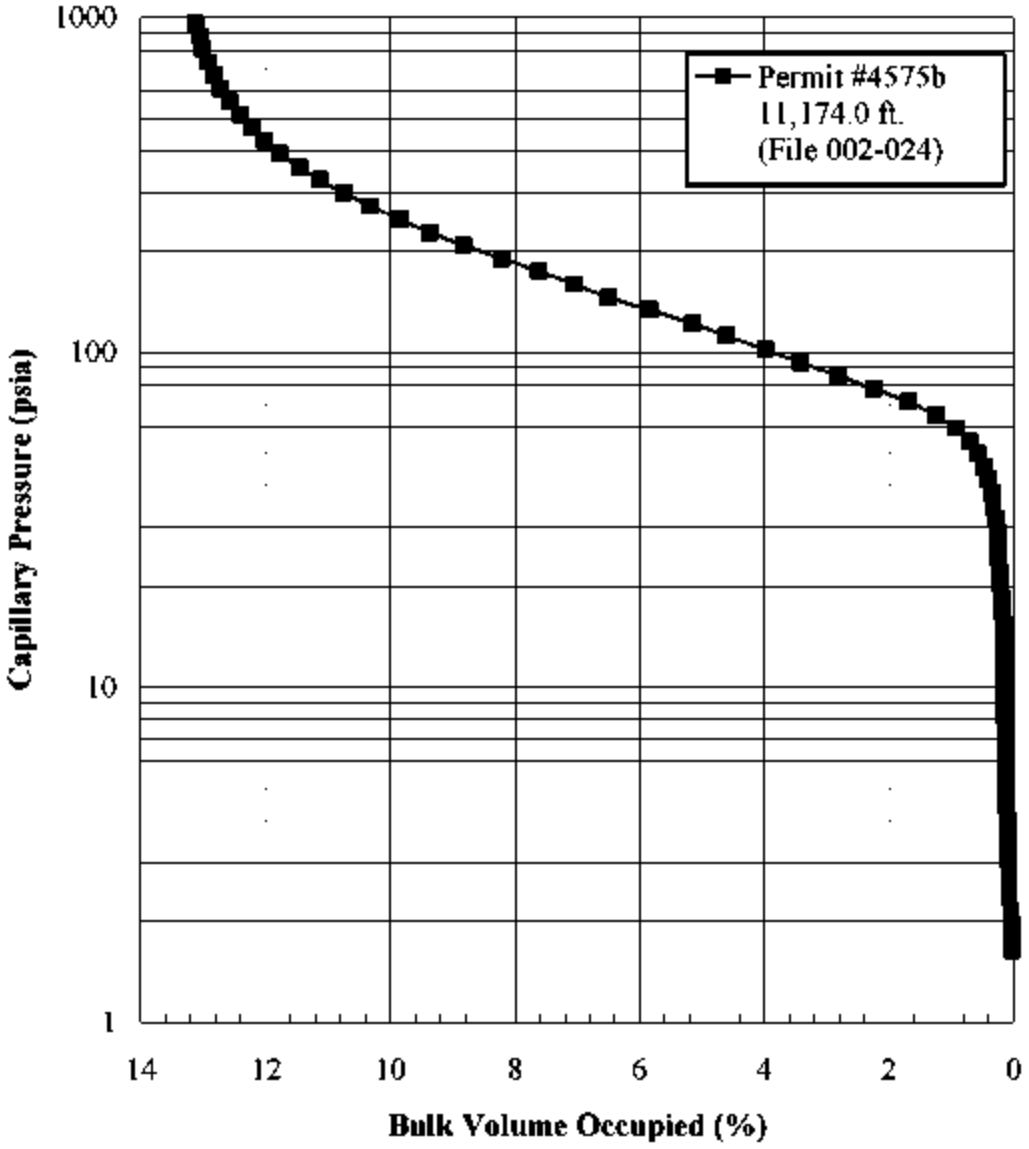

Figure 41. Mercury injection capillary pressure (pore volume) for Well Permit 4575B at 11,174 ft (from Hopkins, 2002).

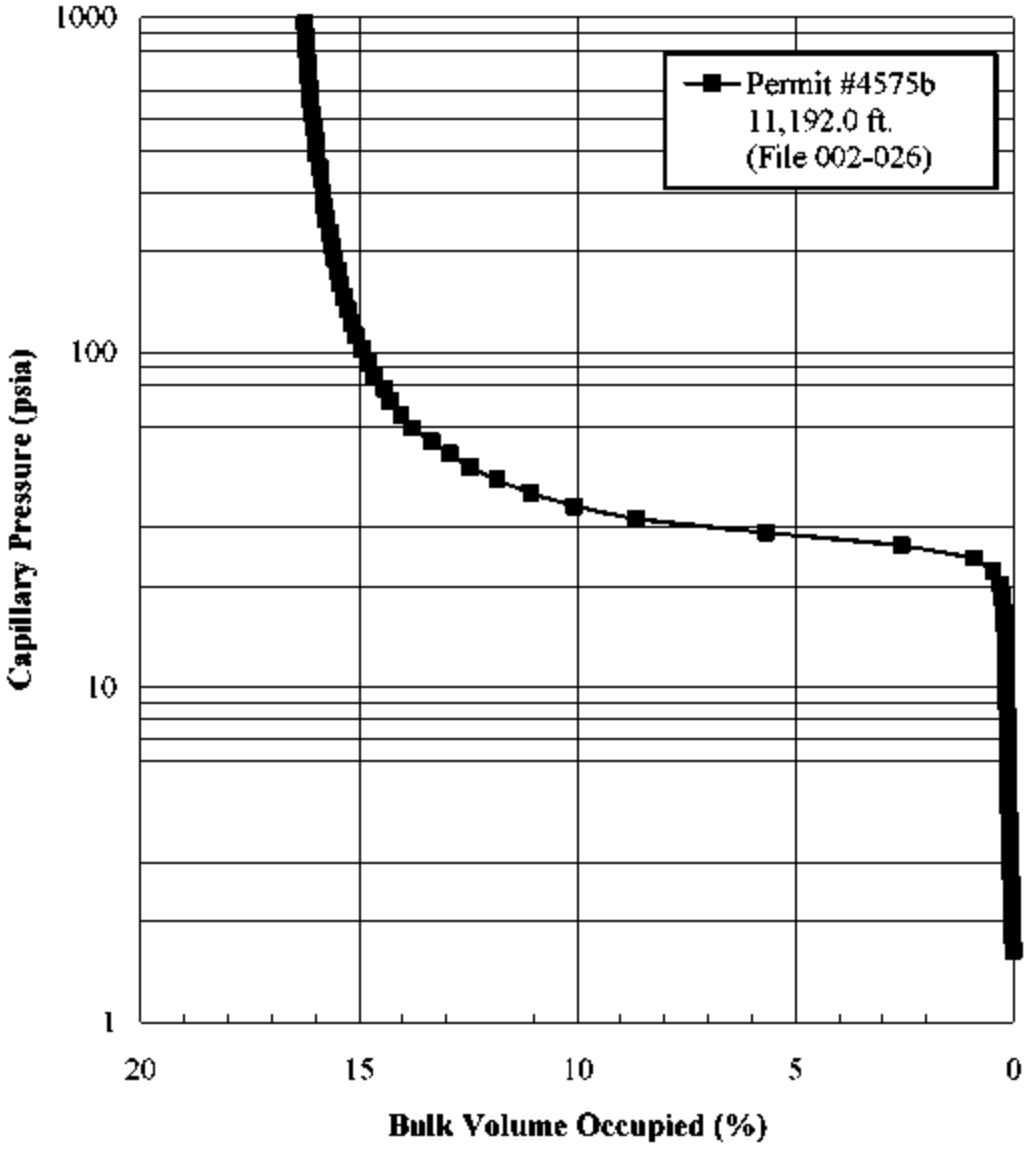

Figure 42. Mercury injection capillary pressure (pore volume) for Well Permit 4575B at 11,192 ft (from Hopkins, 2002).

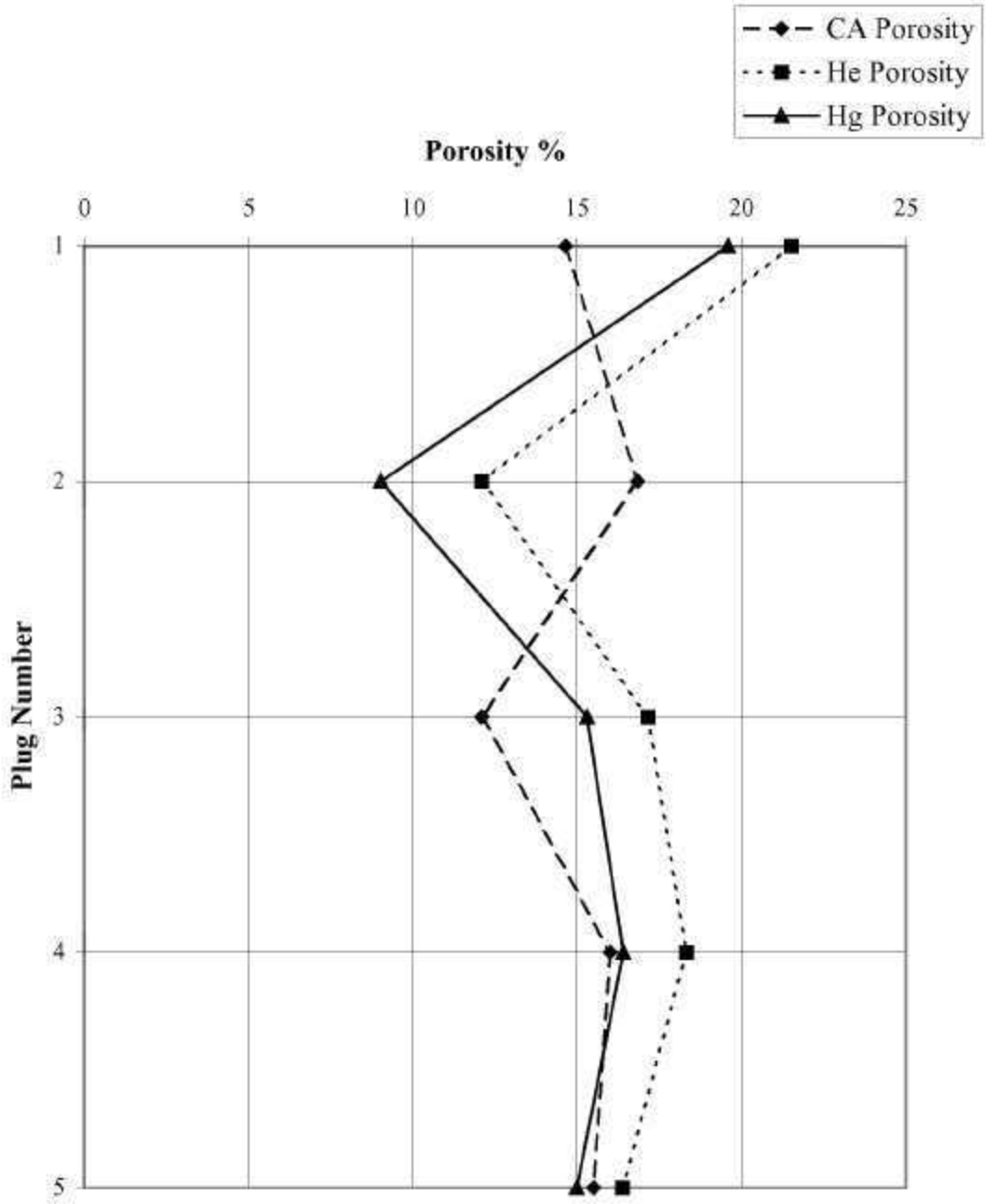

Figure 43. Comparison of porosities derived from various tests for Well Permit 1591. CA=core analysis, He=helium derived, Hg=mercury derived (from Hopkins, 2002).

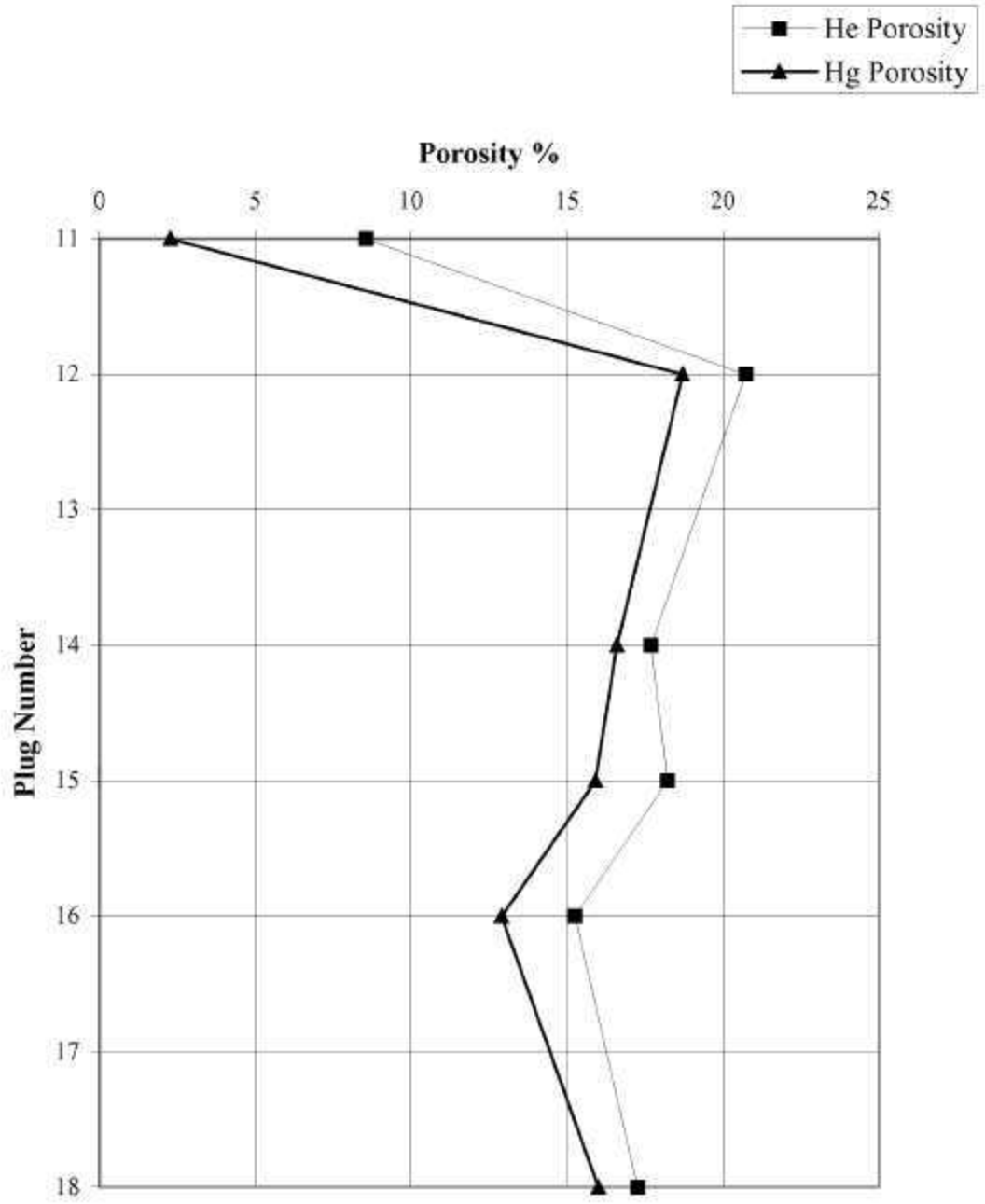

Figure 44. Comparison of porosities derived from various tests for Well Permit 4547B. CA=core analysis, He=helium derived, Hg=mercury derived (from Hopkins, 2002).

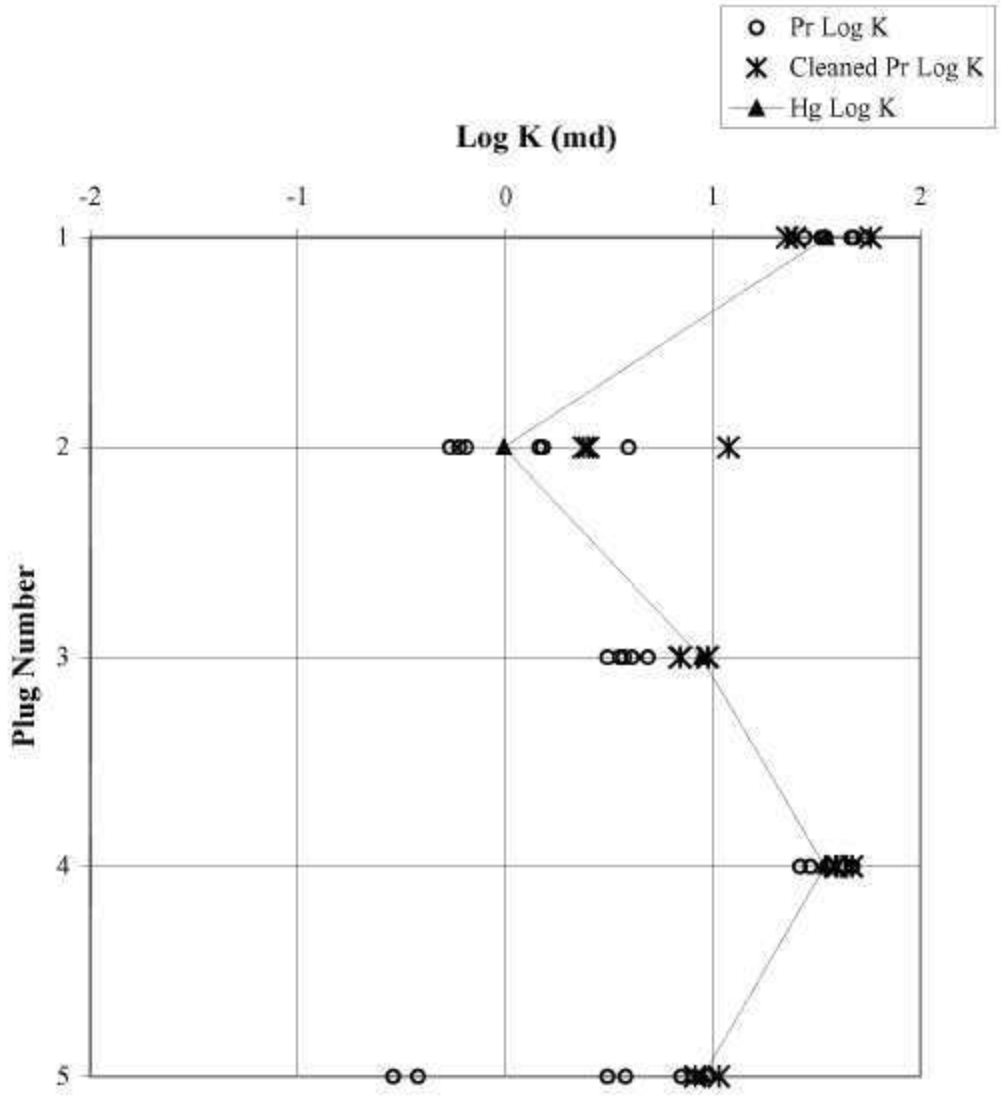

Figure 45. Comparison of log permeabilities derived from various tests for Well Permit 1591 (from Hopkins, 2002).

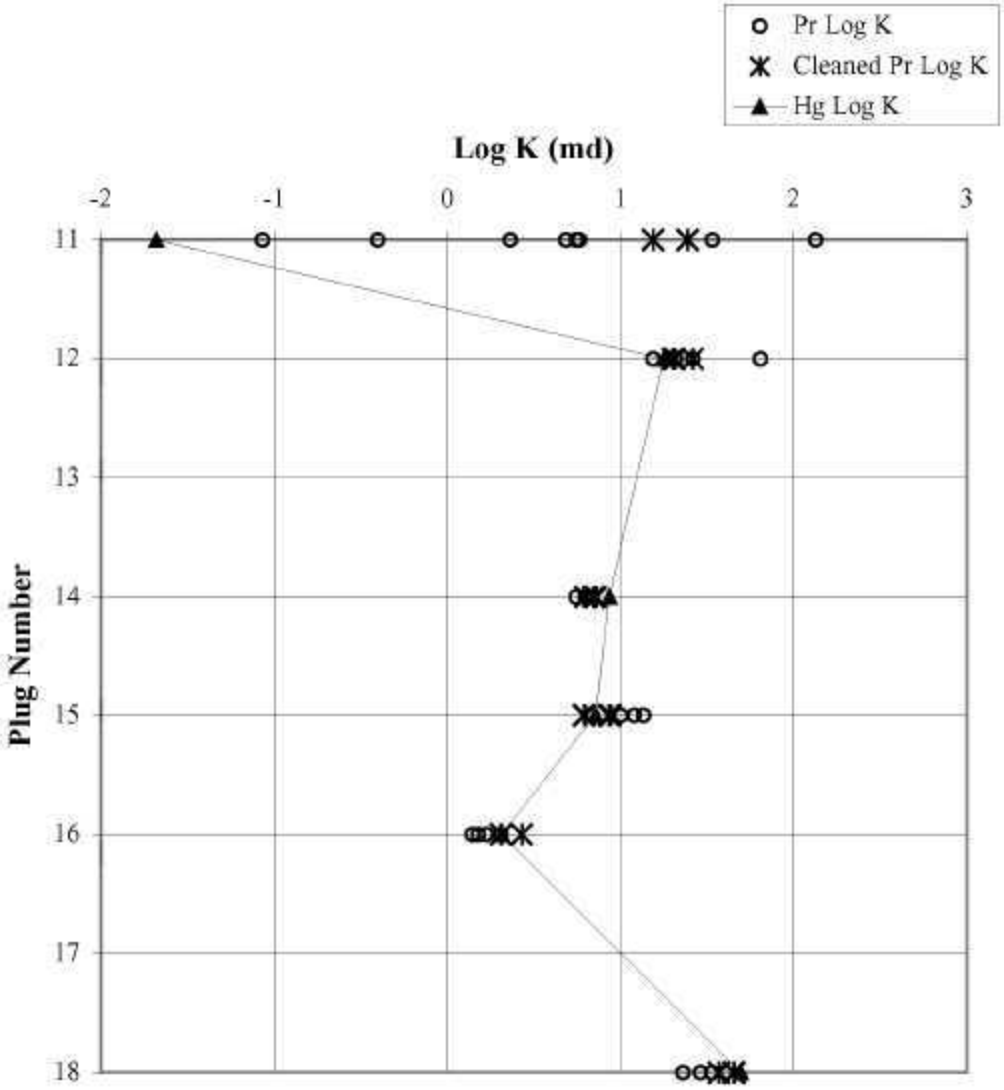

Figure 46. Comparison of log permeabilities derived from various tests for Well Permit 4575B (from Hopkins, 2002).

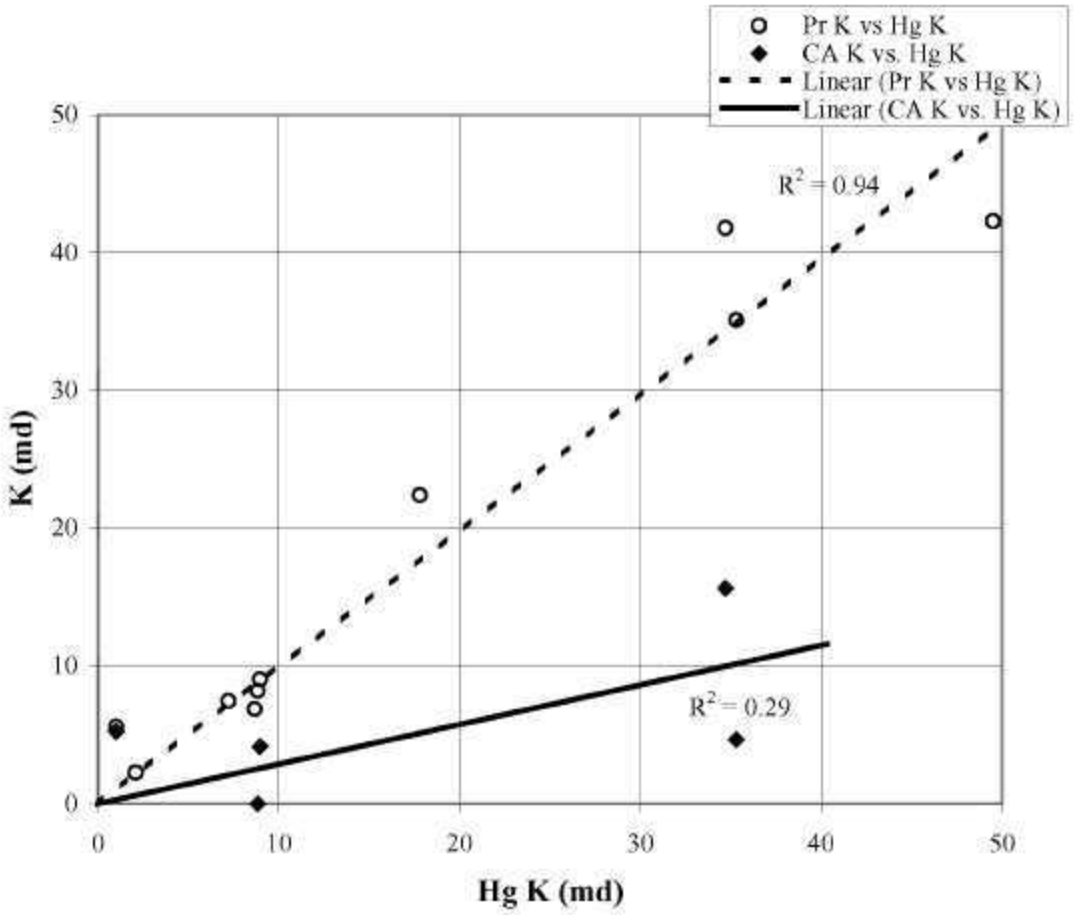

Figure 47. Comparison of mercury derived (Hg), core analysis (CA), and probe permeability (Pr) data (from Hopkins, 2002).

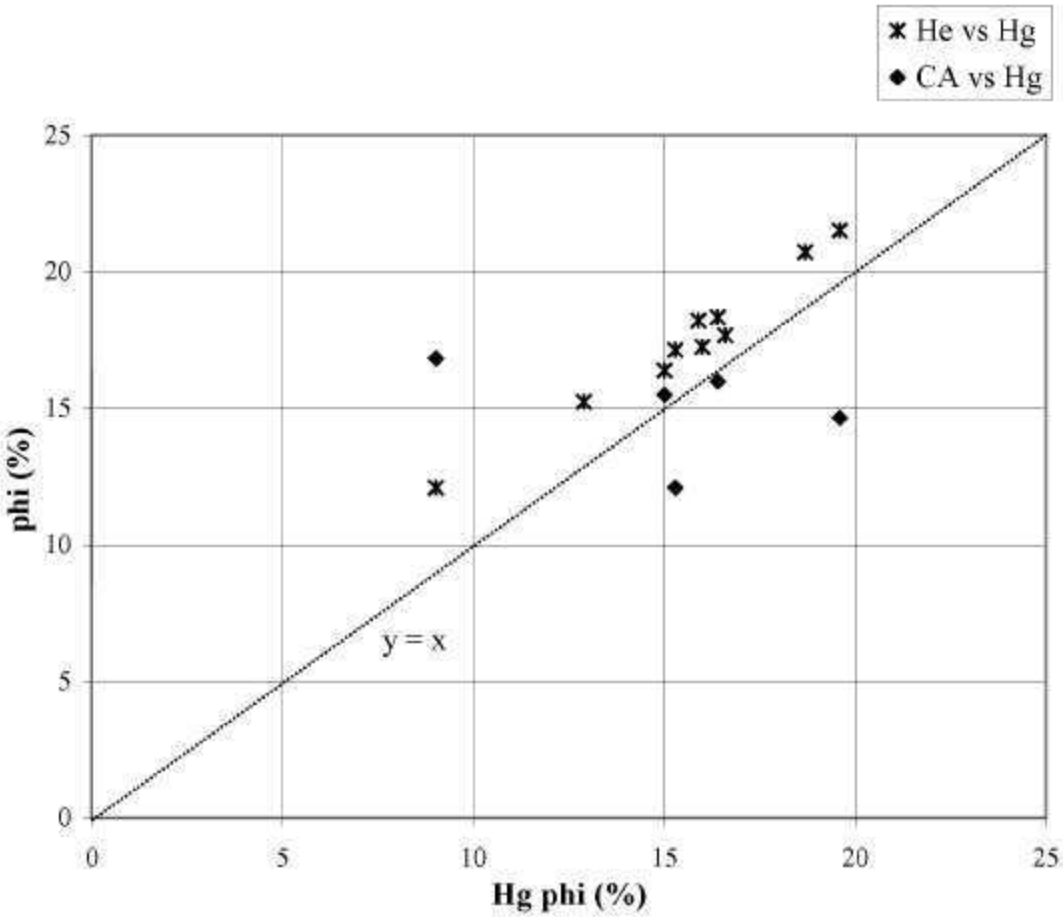

Figure 48. Comparison of helium and core analysis porosities with mercury (capillary pressure) porosity (from Hopkins, 2002).

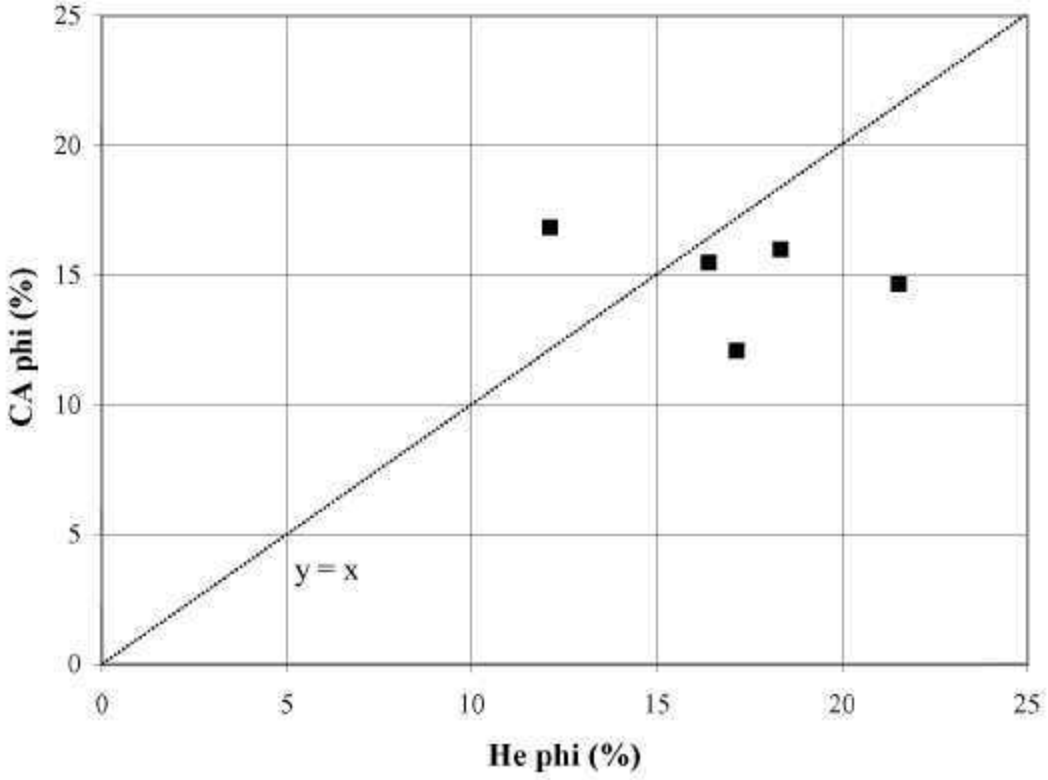

Figure 49. Comparison of core analysis porosity and helium porosity (from Hopkins, 2002).

and 49). There is a general relation between porosity and permeability (Fig. 50). See cross plots of porosity and permeability for the range of correlation values between these two parameters (Figs. 51 through 53). Porosity and permeability predictions by using well log patterns were accomplished by using back-propagation neural network and fractal simulation techniques.

Pore types exhibit general trends to their relation to porosity and median pore throat aperture (Table 4). See Figures 54 through 64 for median pore aperture size distribution for certain depths in well Permits #1591 and 4575B. Median pore throat aperture (MPA) increases with increasing porosity (Fig. 65), and probe permeability and mercury derived permeability strongly correlate with MPA (Fig. 66). The intercrystalline pore system is characterized by the highest porosities.

Capillary pressure data were available for wetting phase (air) saturations. Wetting phase saturation at 77 psia was approximated from its relation with MPA through the equation graphed on Figure 67. No clear relation was observed for entry pressures (displacement pressures) and any parameters. Utilizing a series of equations where porosity, permeability, and capillary radius (=MPA) can be determined, the equation: $y=\tau=(\phi r^2)/8k$ was graphed to solve for π or tortuosity (Fig. 68). Figure 68 shows that tortuosity increases with increasing MPA. This relation is related to pore type: the larger MPA and tortuosity values are observed to be associated with intercrystalline pores. Figure 69 shows that entry pressure conditions can be predicted using the inverse of the pore throat radius.

Results from studies of the pore systems of the Smackover reservoir facies using petrographic image analysis, mercury injection capillary pressure, and nuclear magnetic resonance show the following. Typically, 60 to 80% of the depositional interparticle pores of the grainstone facies are 100 to 1,000 μm^2 in size and round in shape, 20 to 40% of the pores are 1,000 to 10,000 μm^2 in size and moderately non-circular in shape, and 1 to 10% of the pores are

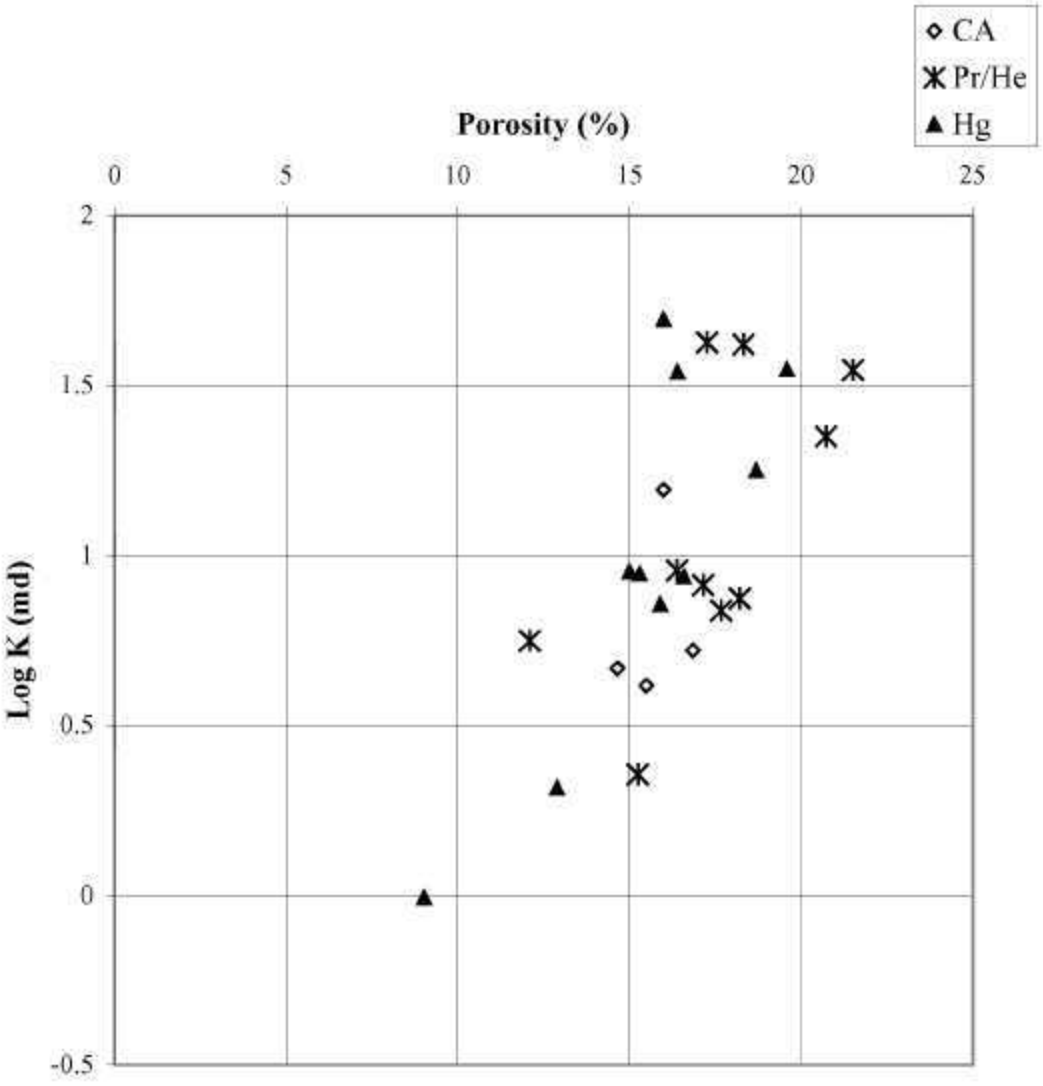

Figure 50. Comparison of porosity and permeability relationships from each method used. CA=core analysis porosity and permeability, Pr/He=plugs measured with the probe permeameter and helium porosimeter, Hg=mercury derived porosity and permeability (from Hopkins, 2002).

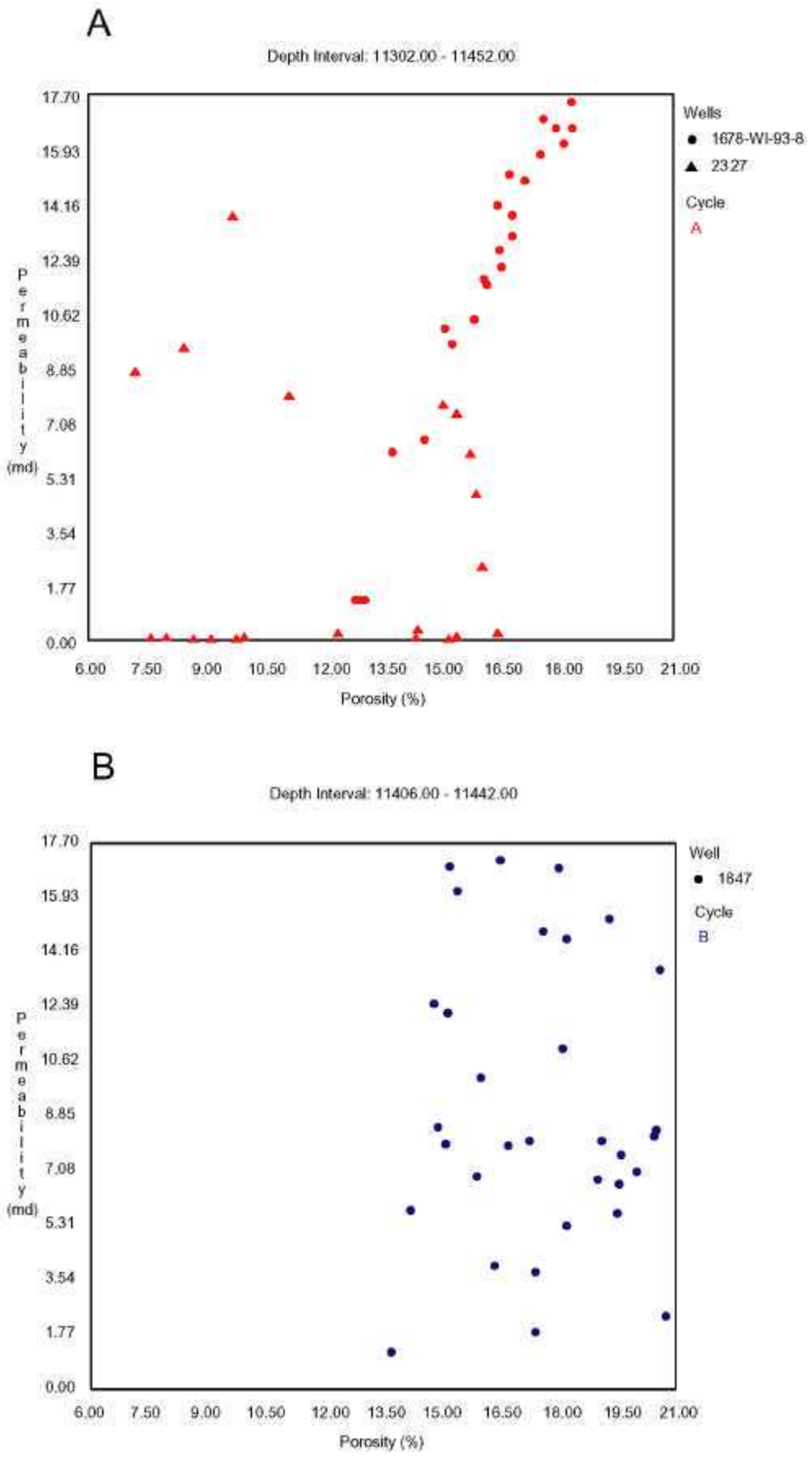

Figure 51. Porosity vs. permeability plots for: (A) Cycle A for wells, Permit # 1678, high production well and Permit #2327, low production well, (B) Cycle B for well, Permit #1847.

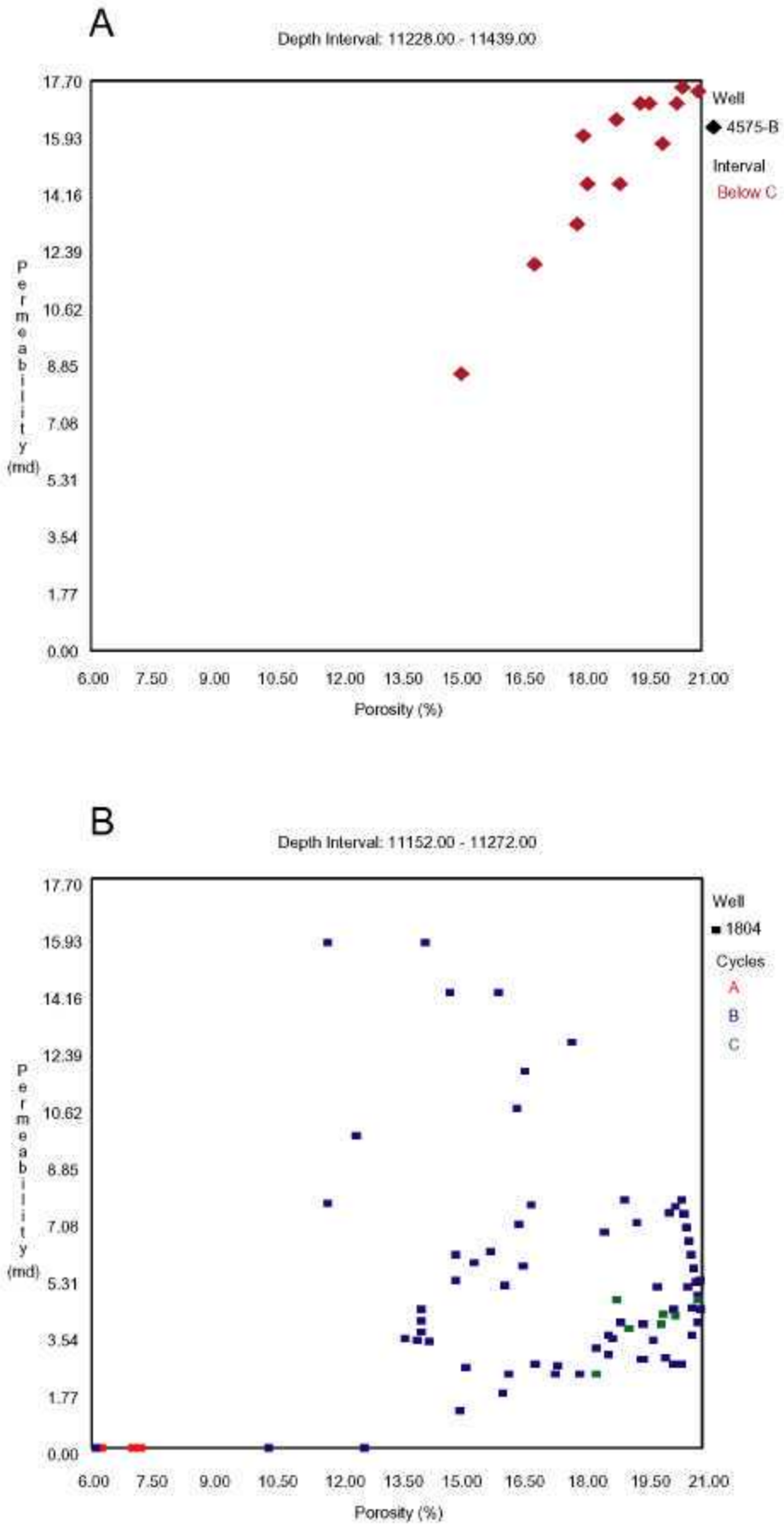

Figure 52. Porosity vs. permeability plots for: (A) Interval immediately below Cycle C for well Permit #4575B, (B) Cycles A, B, and C for well, Permit #1804.

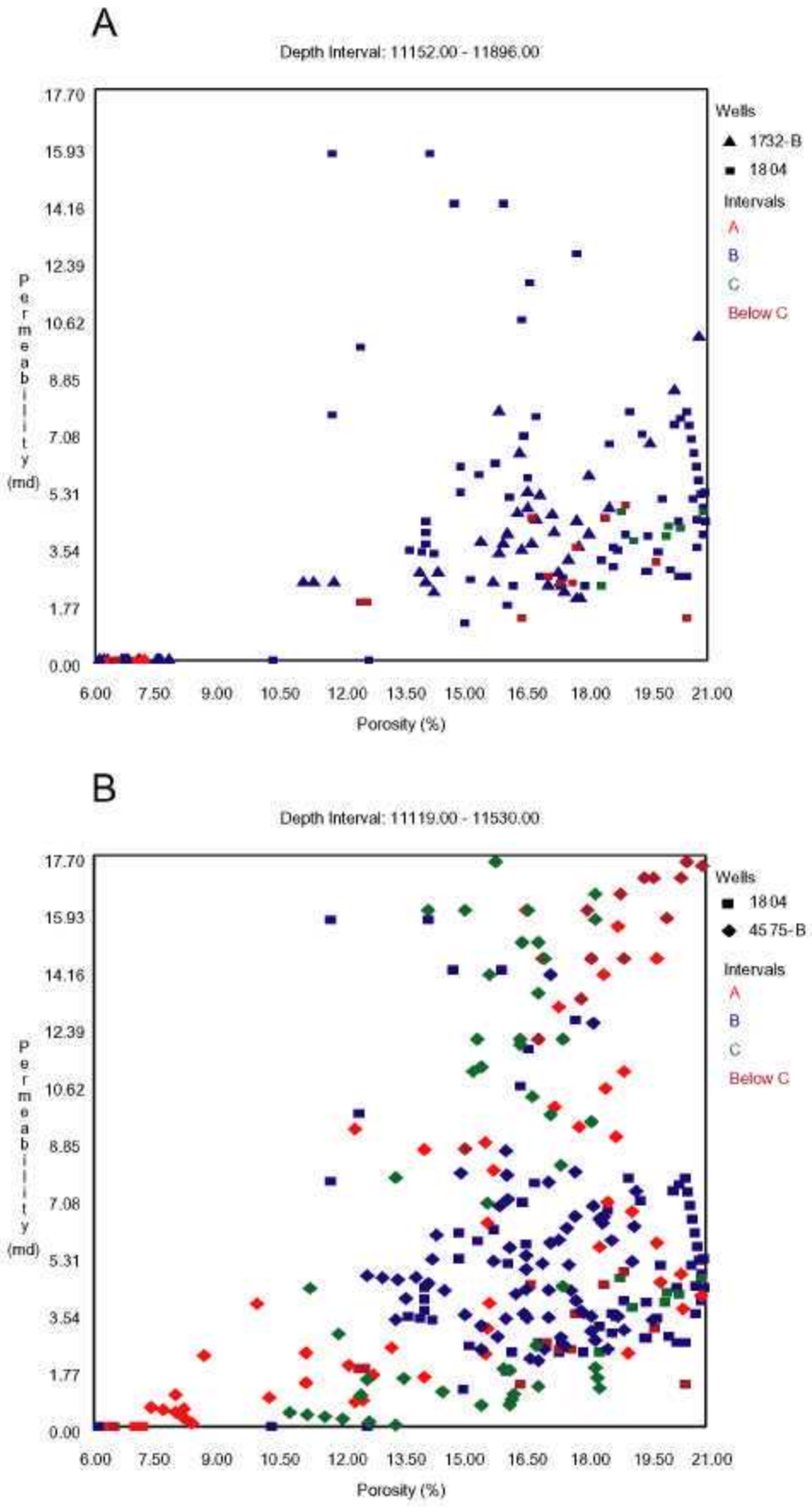

Figure 53. Porosity vs. permeability plots for: (A) Cycles A, B, C and interval immediately below Cycle C for wells, Permit #1732B and Permit #1804, and (B) Cycles A, B, C and interval immediately below Cycle C for wells, Permit #1804 and Permit #4575B. See Figure 8 for location of wells.

Table 4. Common pore type associations in the mercury injection capillary pressure sample set, with the average porosity and median pore throat aperture (from Hopkins, 2002).

Common Pore Type Associations	Average Sample Porosities (%)	Average MPA (μm)
intercrystalline	6.5	4.3
interparticle, intraparticle, moldic	16.3	2.3
interparticle, intraparticle	15.8	2.3
interparticle, vuggy	9.0	1.1
channel, vuggy	2.3	0.3

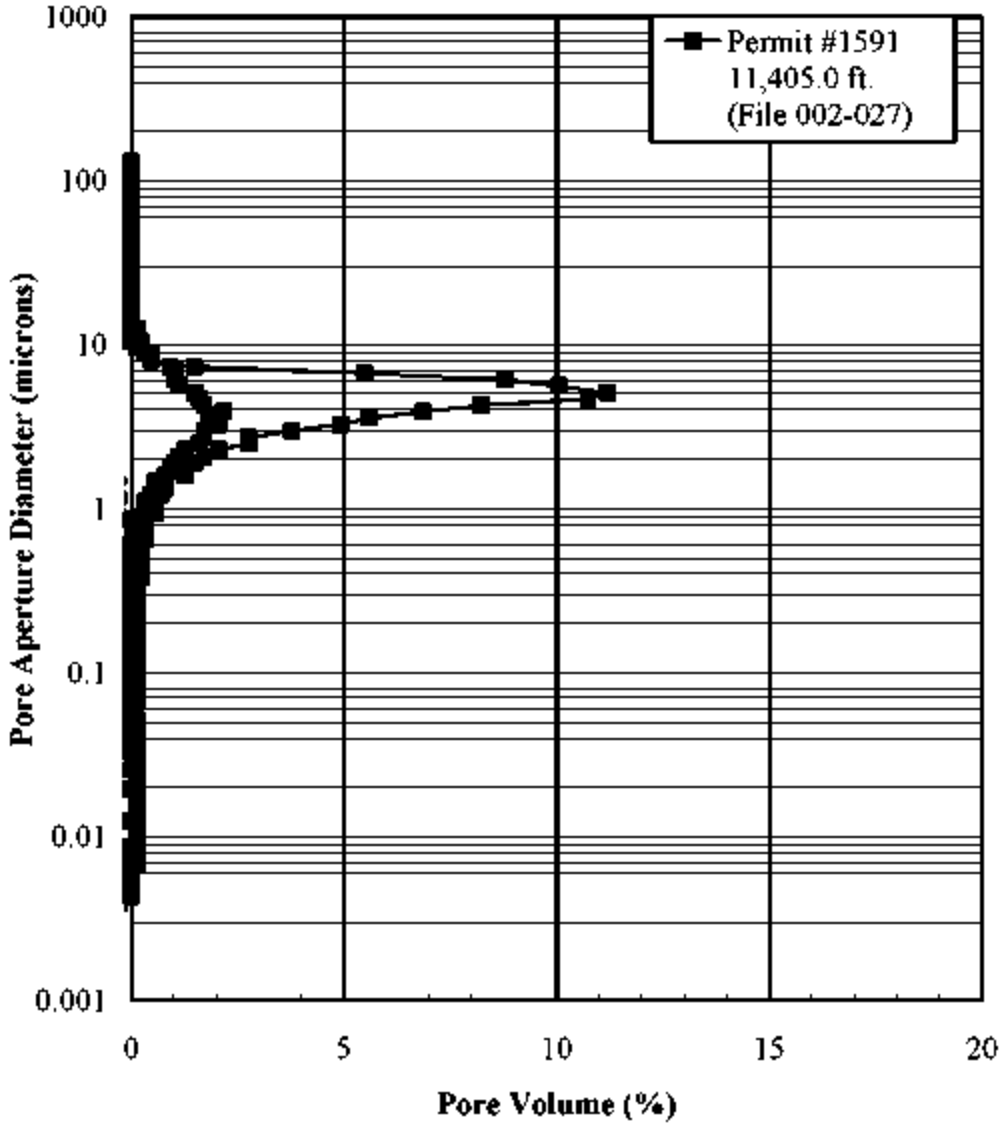

Figure 54. Pore aperture size distribution for Well Permit 1591 at 11,405 ft. (from Hopkins, 2002).

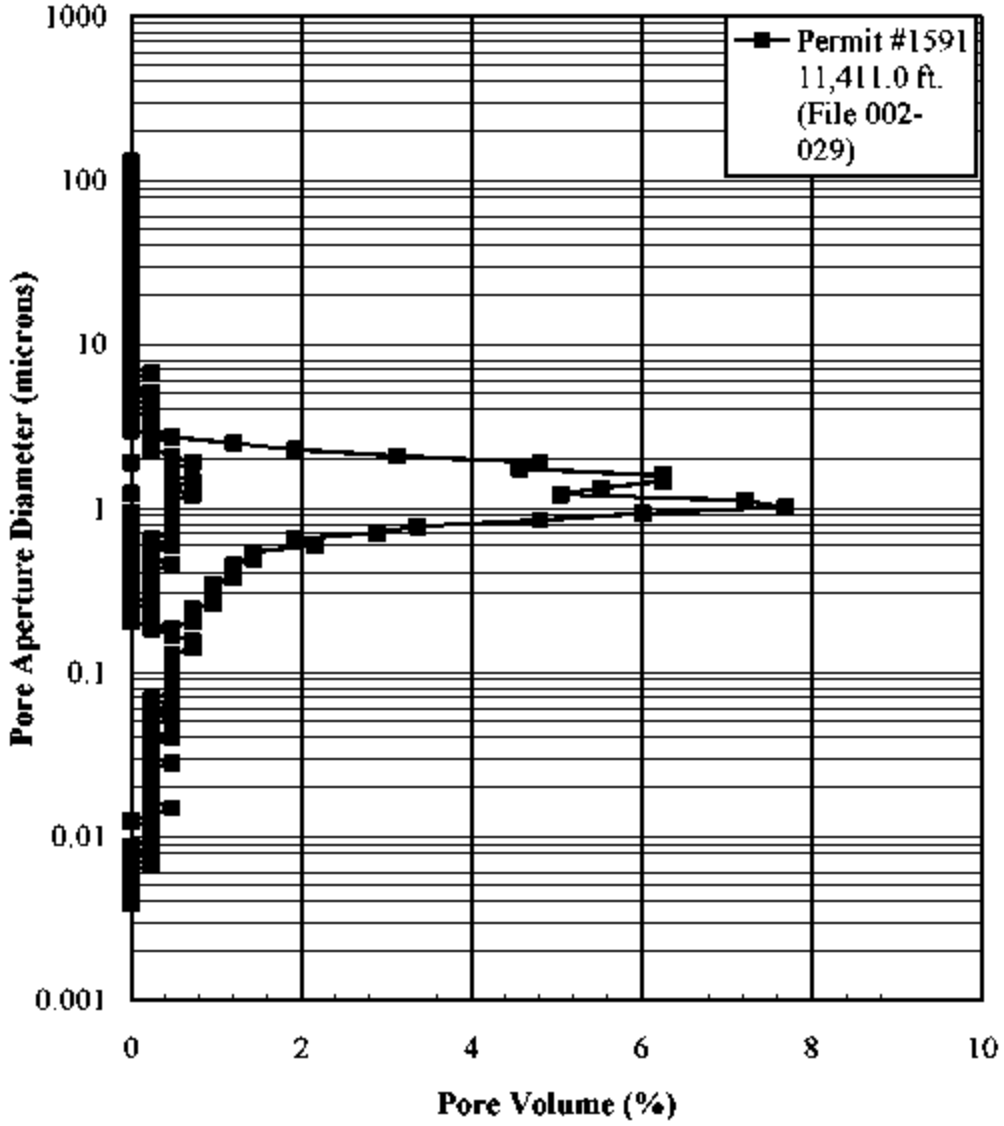

Figure 55. Pore aperture size distribution for Well Permit 1591 at 11,411 ft.

(from Hopkins, 2002).

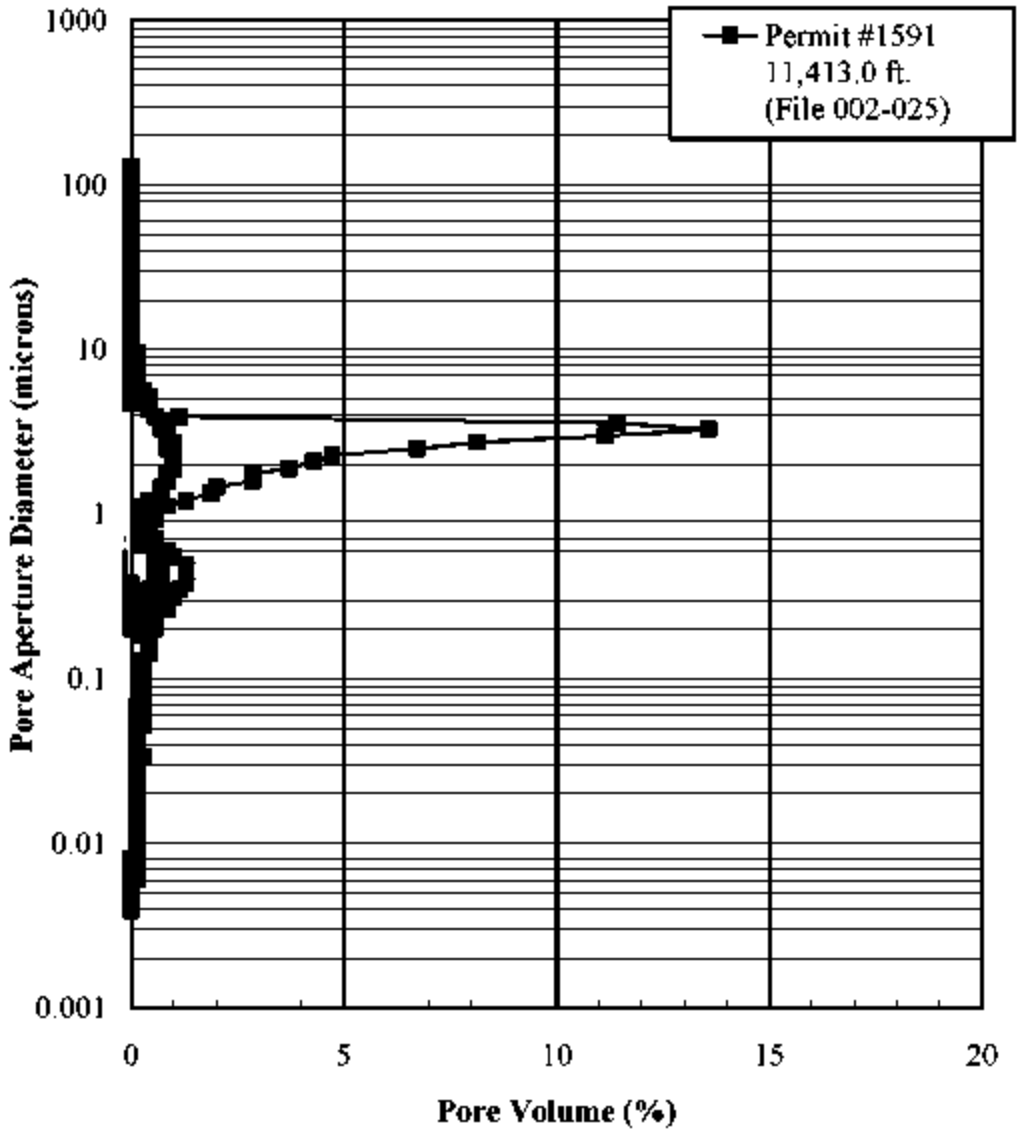

Figure 56. Pore aperture size distribution for Well Permit 1591 at 11,413 ft. (from Hopkins, 2002).

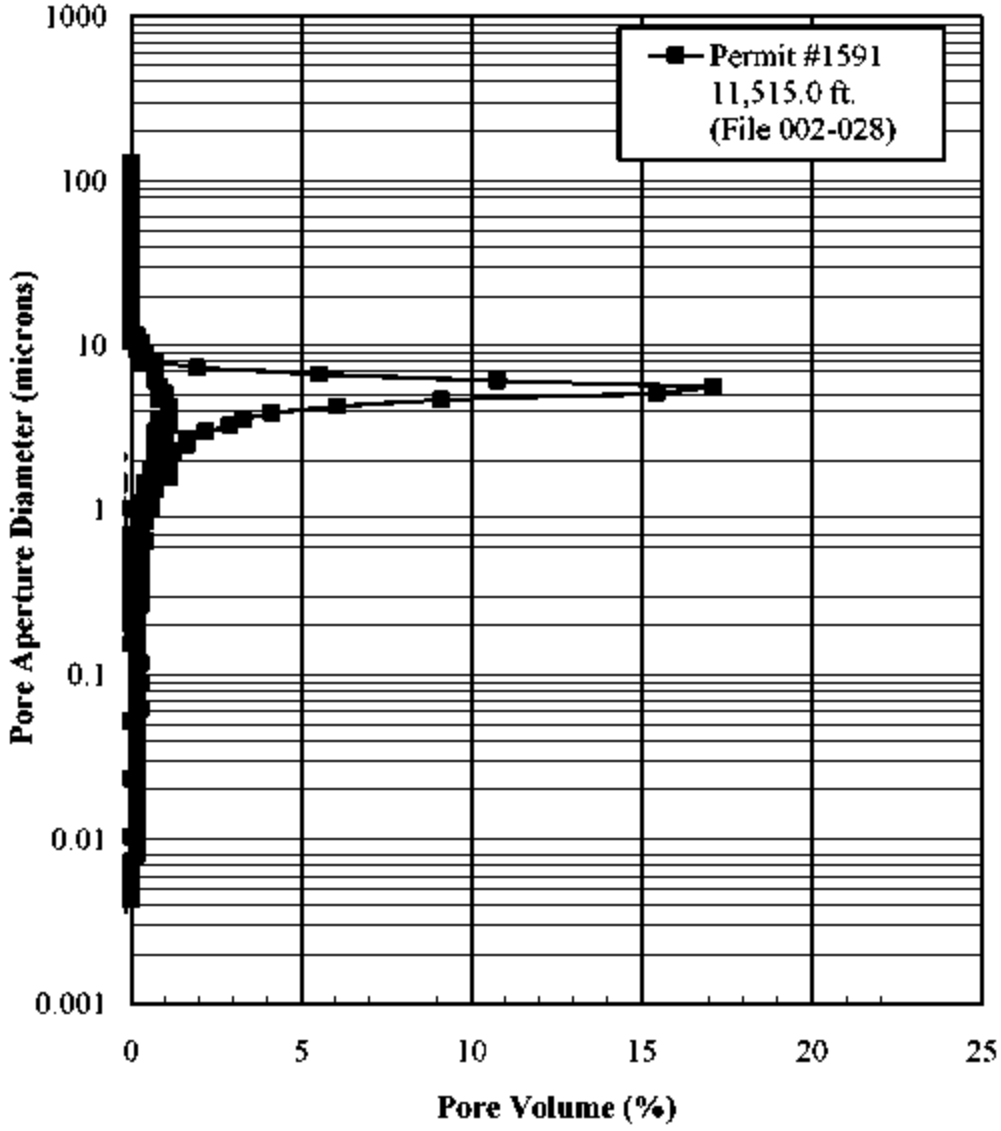

Figure 57. Pore aperture size distribution for Well Permit 1591 at 11,515 ft. (from Hopkins, 2002).

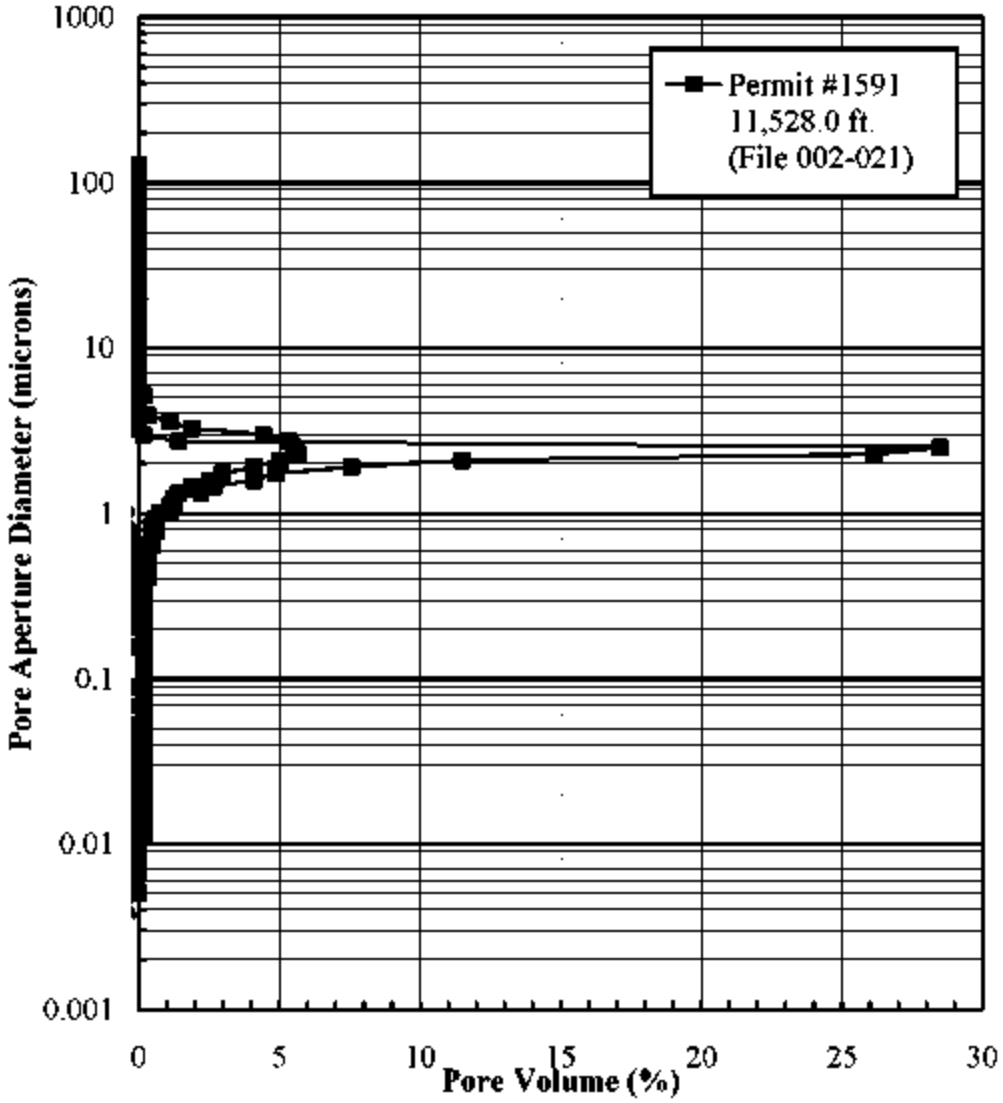

Figure 58. Pore aperture size distribution for Well Permit 1591 at 11,528 ft. (from Hopkins, 2002).

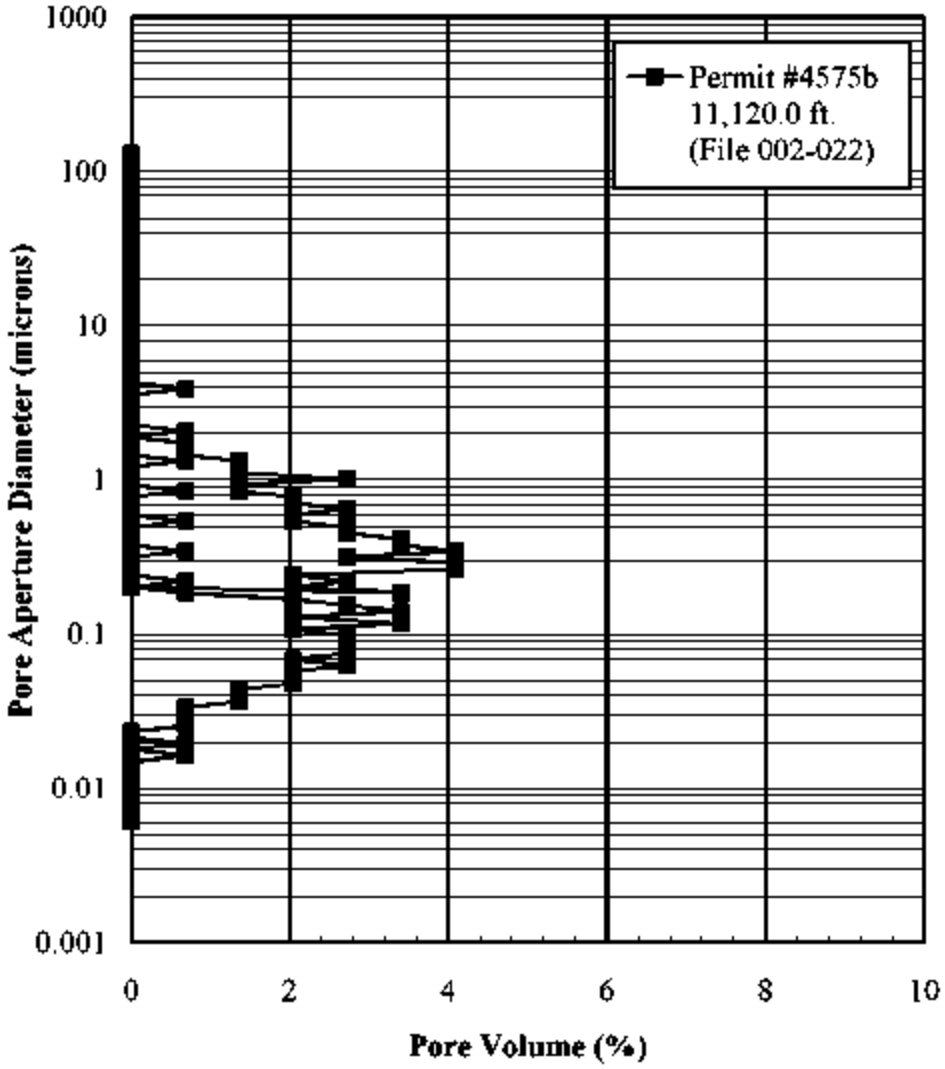

Figure 59. Pore aperture size distribution for Well Permit 4575B at 11,120 ft. (from Hopkins, 2002).

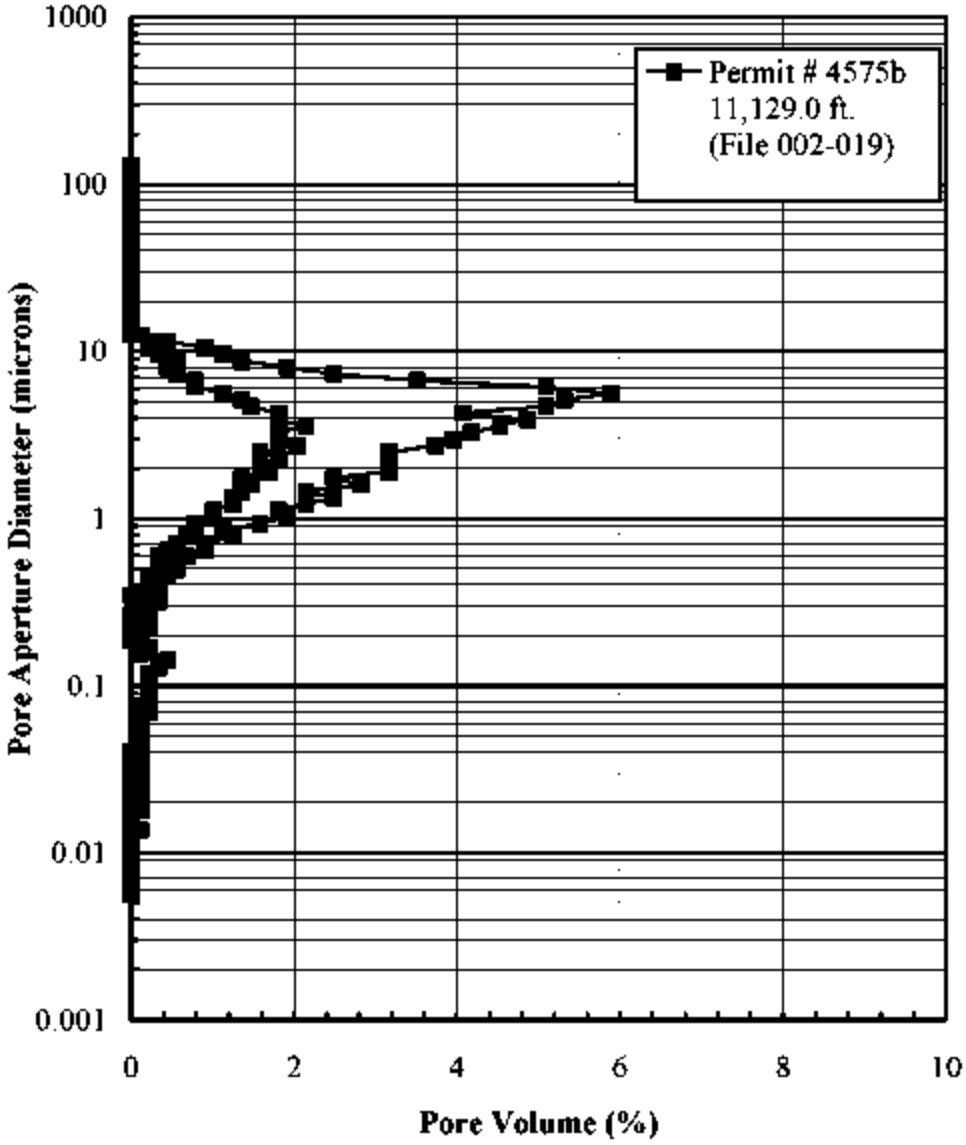

Figure 60. Pore aperture size distribution for Well Permit 4575B at 11,129 ft. (from Hopkins, 2002).

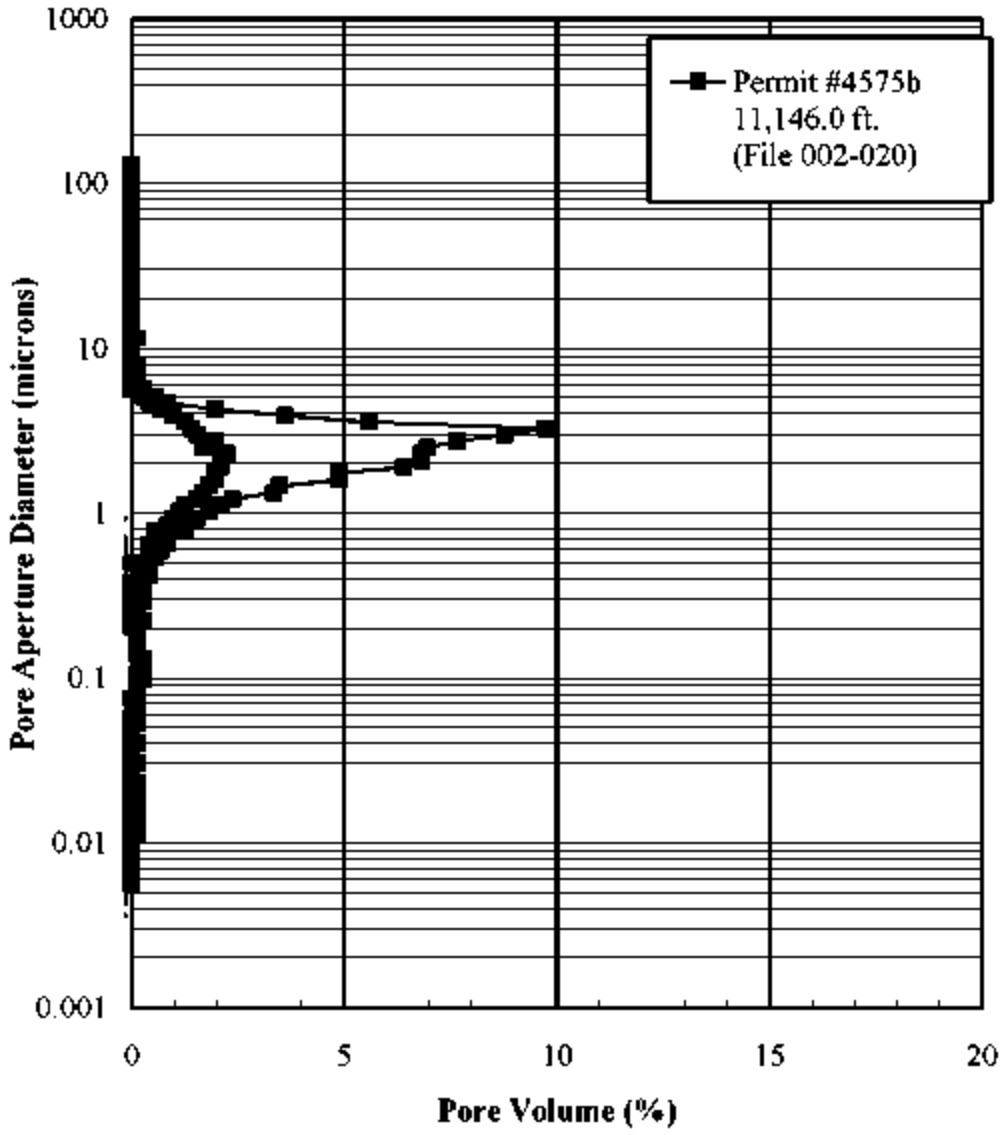

Figure 61. Pore aperture size distribution for Well Permit 4575B at 11,146 ft. (from Hopkins, 2002).

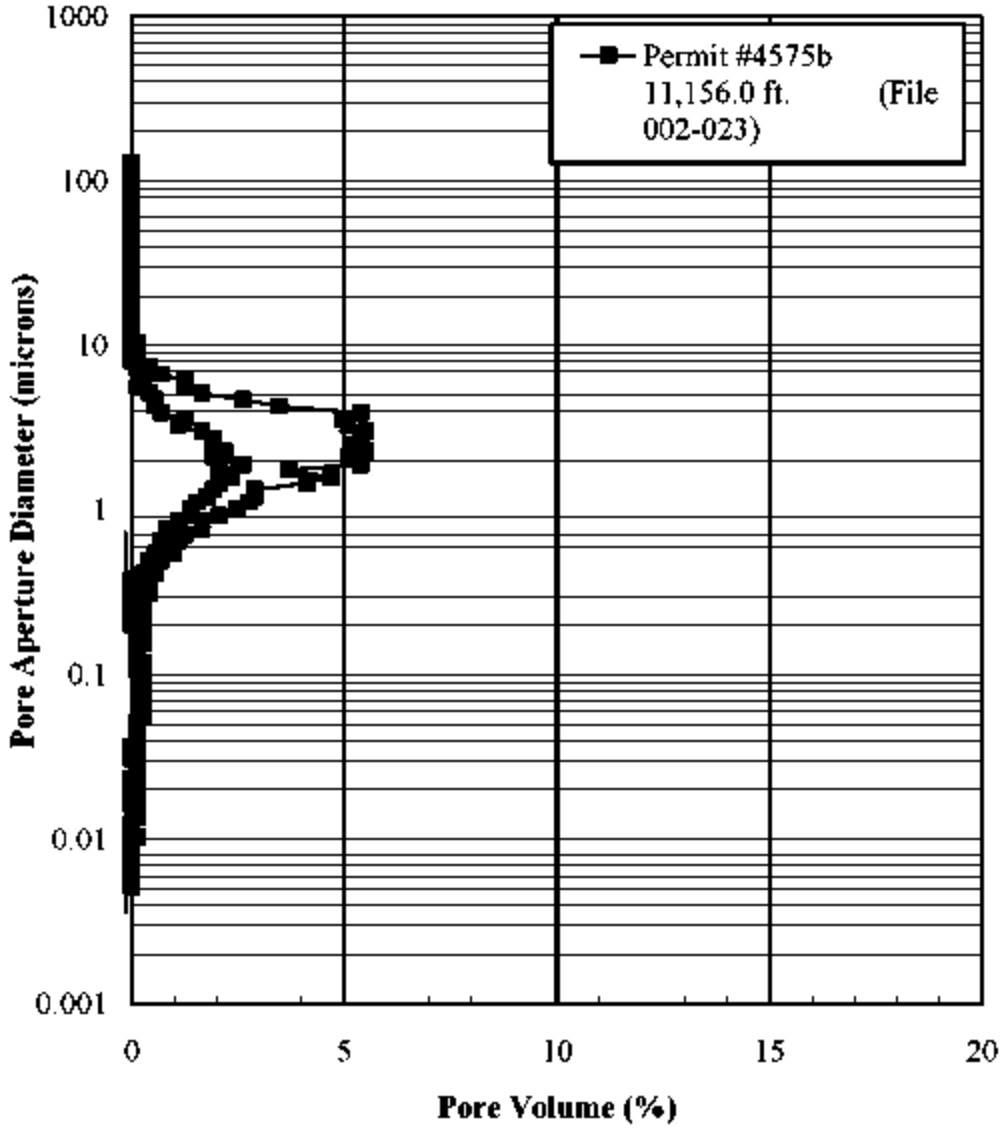

Figure 62. Pore aperture size distribution for Well Permit 4575B at 11,156 ft. (from Hopkins, 2002).

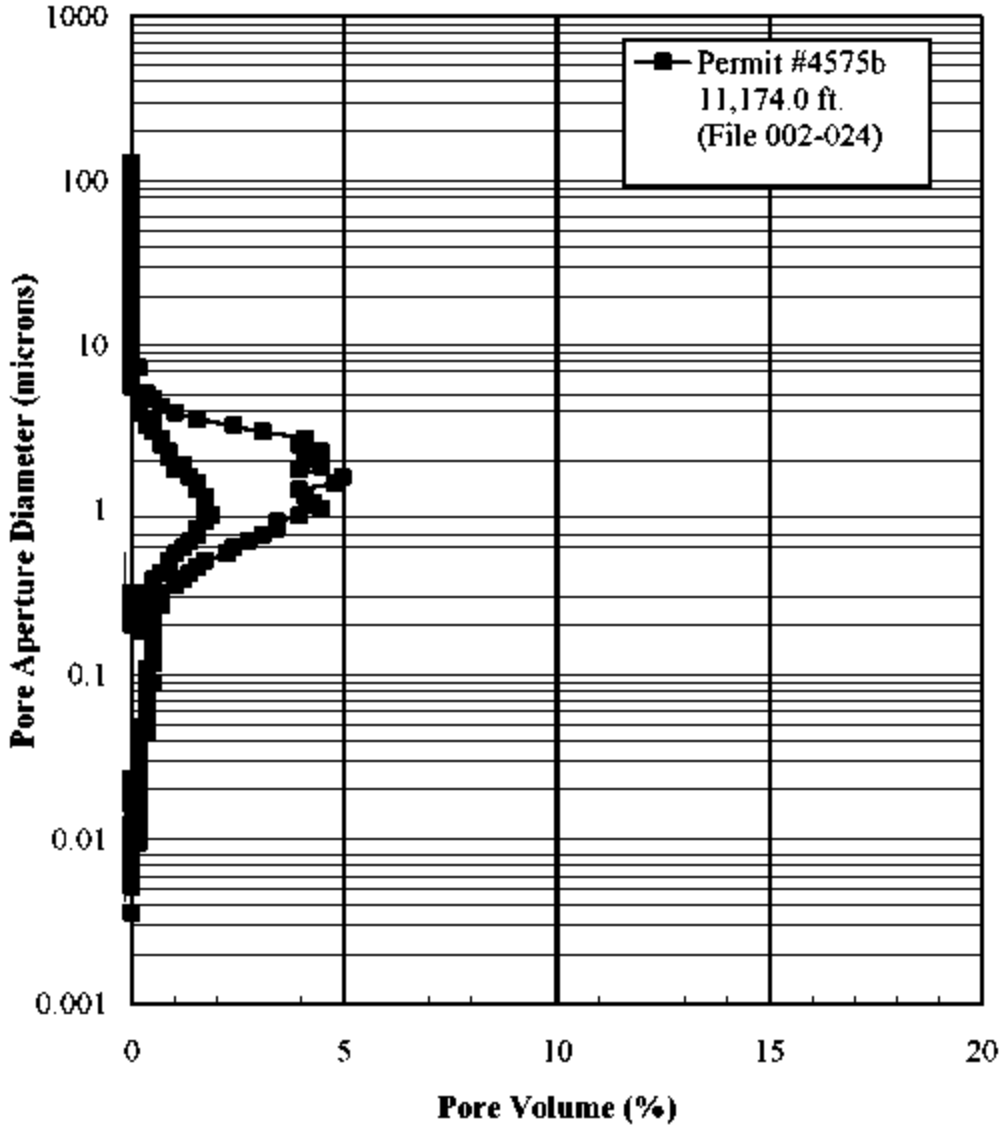

Figure 63. Pore aperture size distribution for Well Permit 4575B at 11,174 ft. (from Hopkins, 2002).

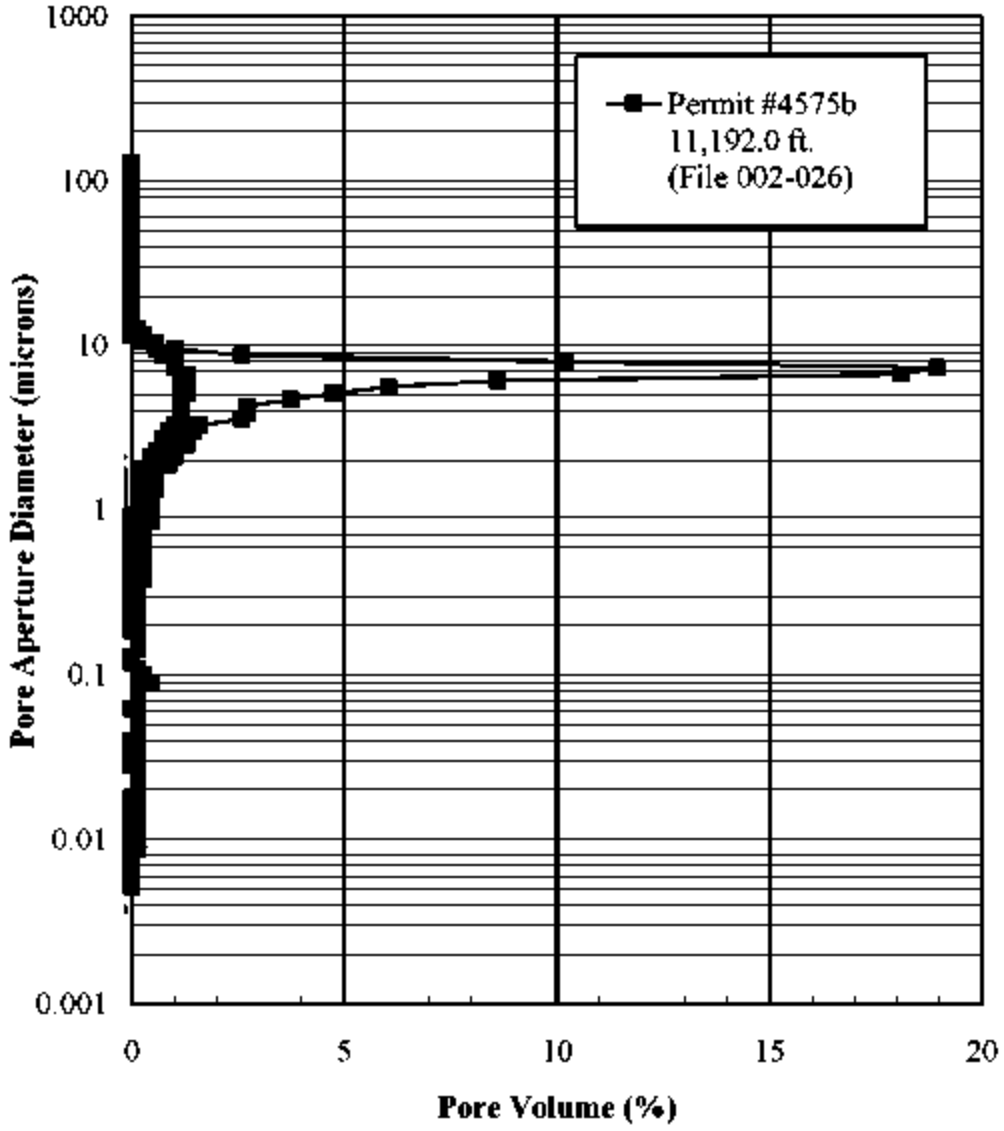

Figure 64. Pore aperture size distribution for Well Permit 4575B at 11,192 ft. (from Hopkins, 2002).

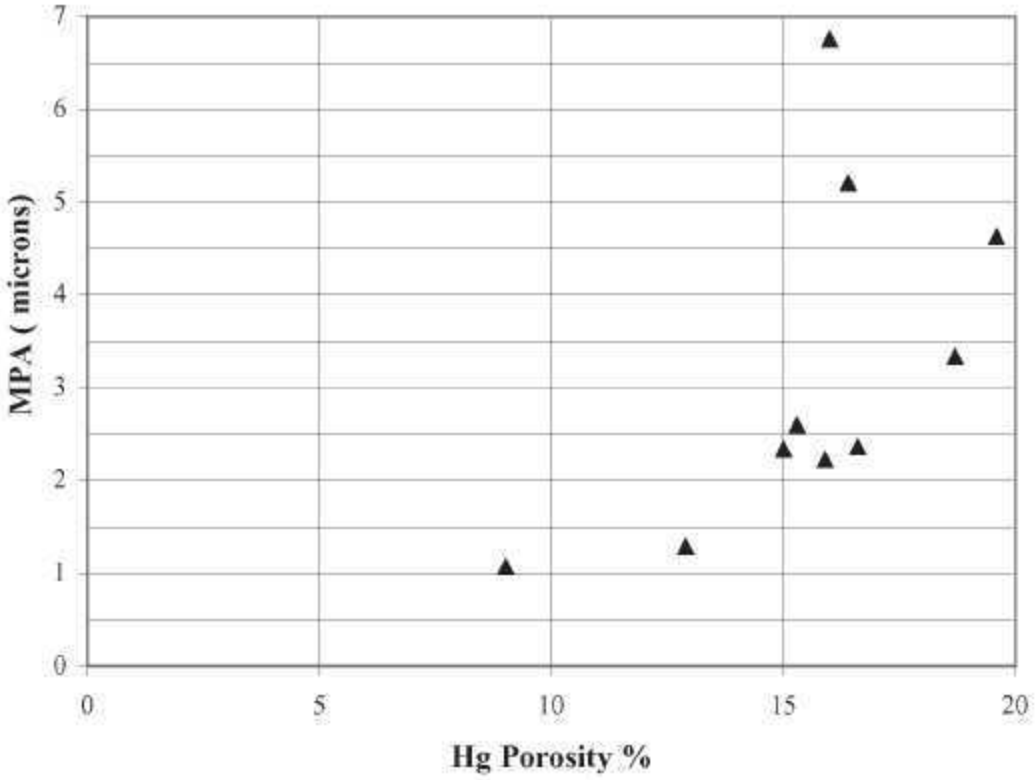

Figure 65. Graph of median pore throat aperture versus mercury derived porosity (from Hopkins, 2002).

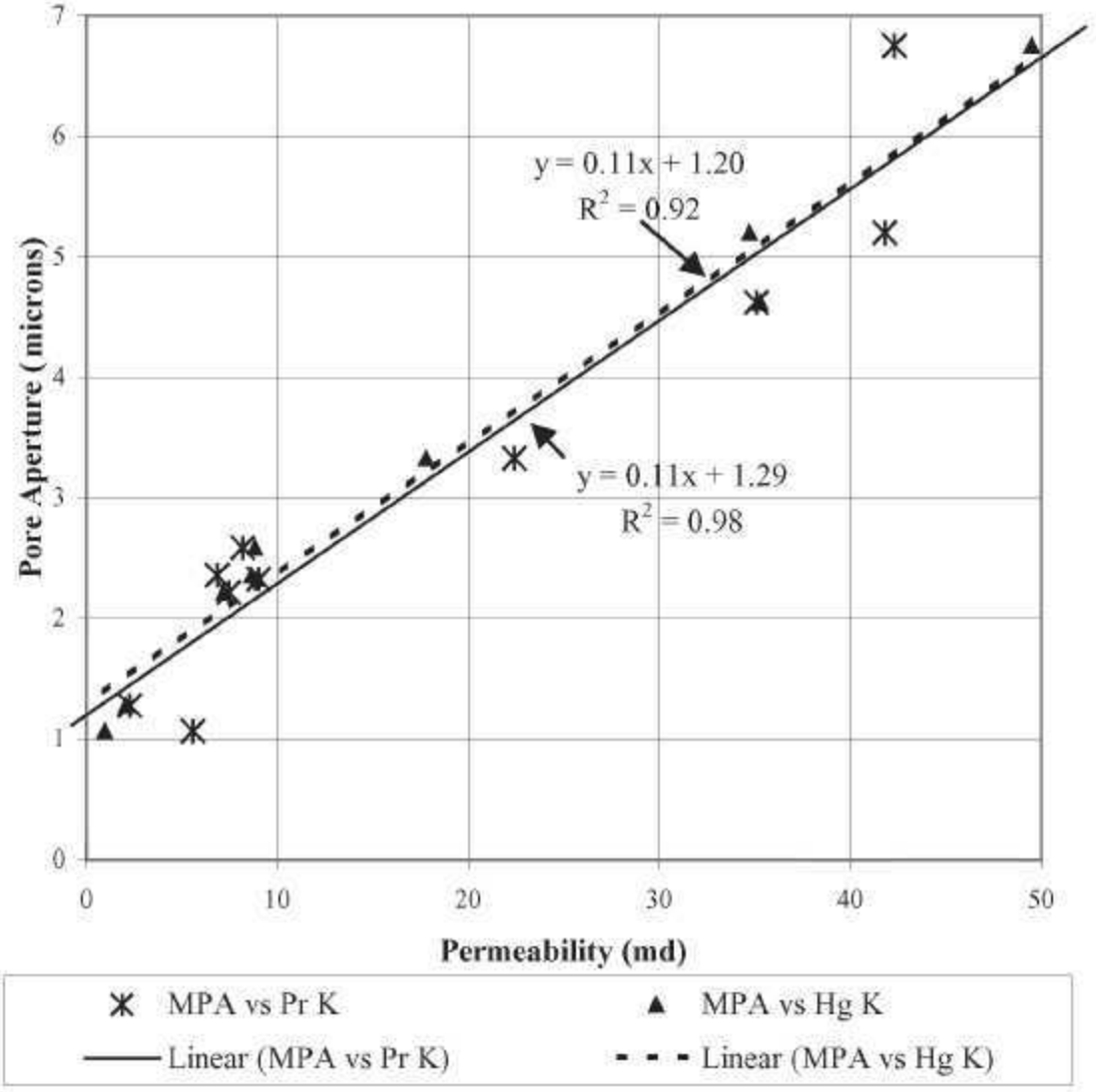

Figure 66. Graph showing the relationship between median pore throat aperture and probe permeability (from Hopkins, 2002).

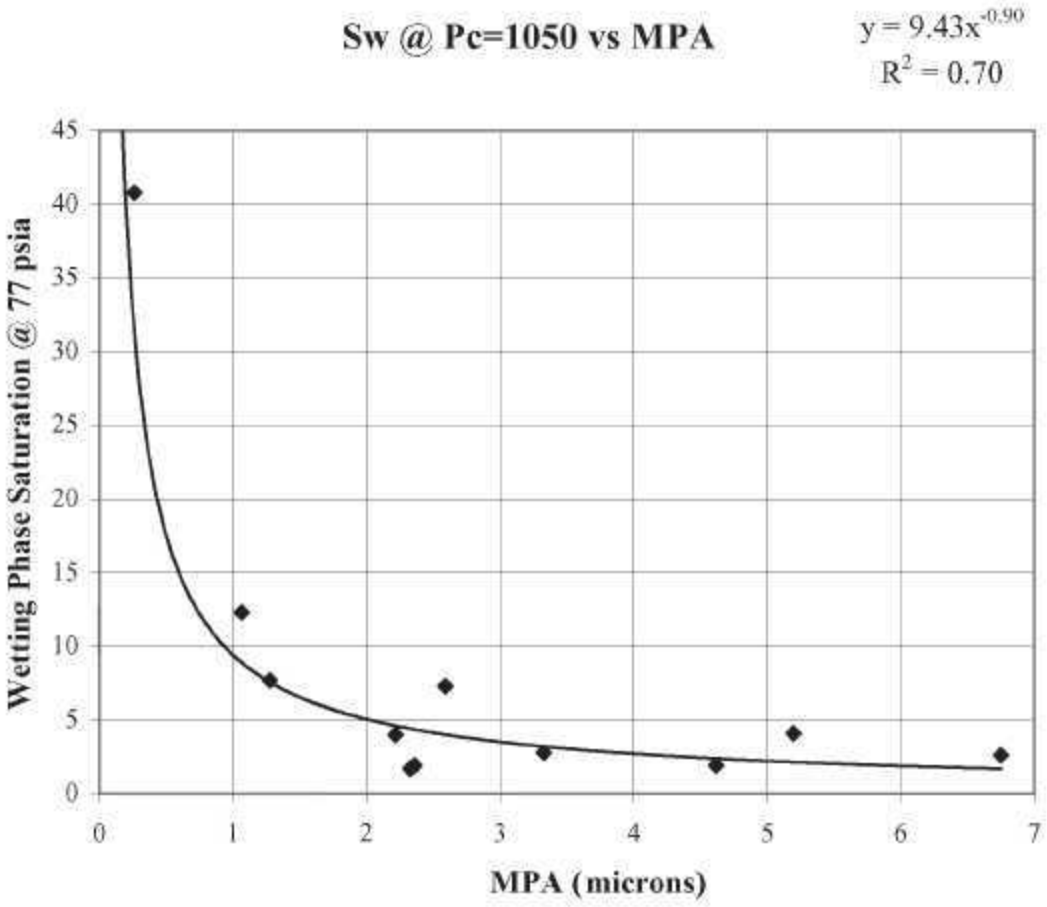

Figure 67. Wetting phase saturation at 77 psia versus median pore throat aperture (from Hopkins, 2002).

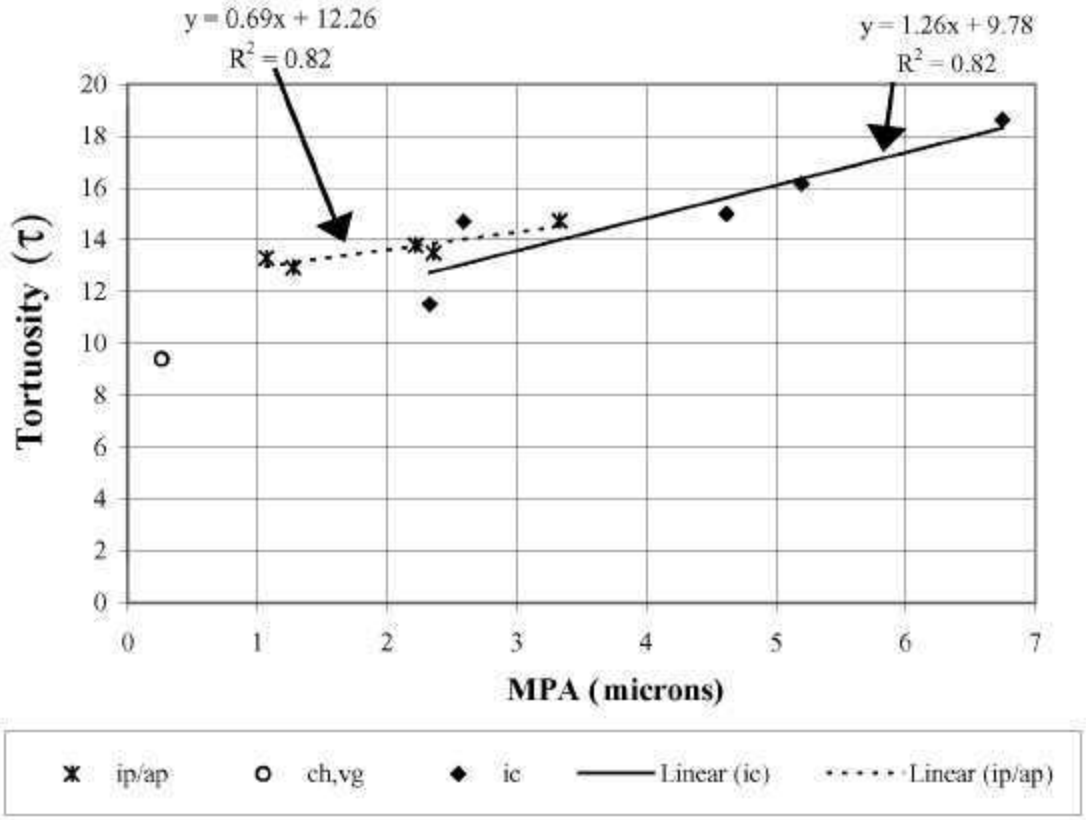

Figure 68. Graph of equation to determine tortuosity (τ) (from Hopkins, 2002).

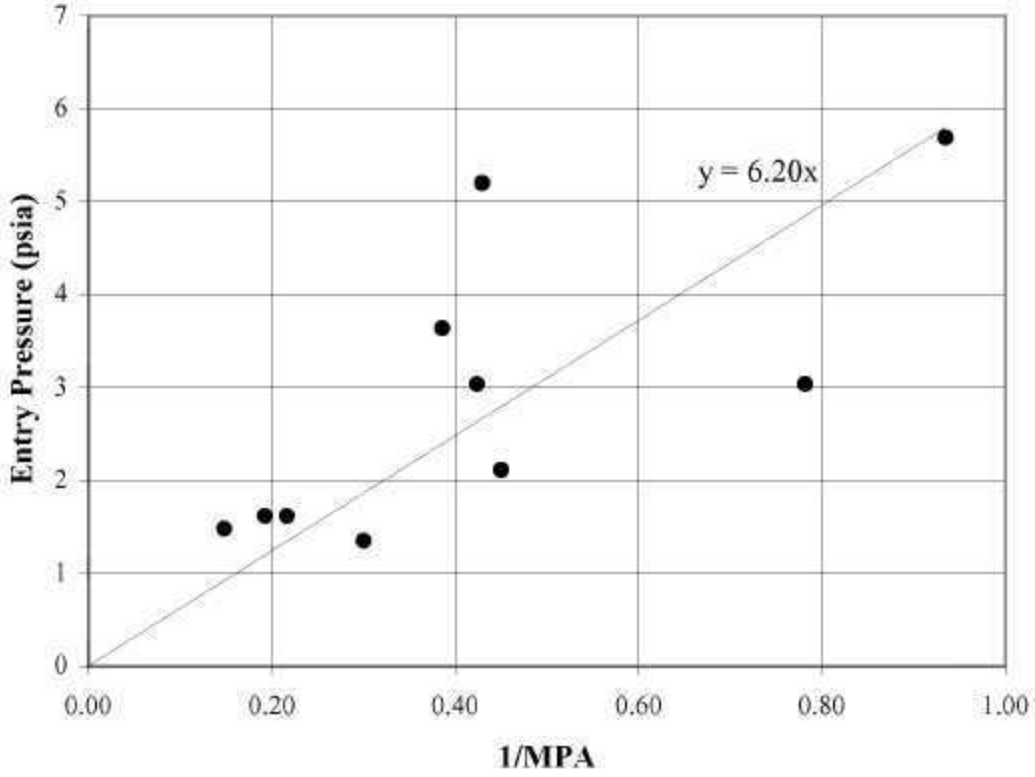

Figure 69. Predicting entry pressure from the inverse of pore throat radius (from Hopkins, 2002).

>10,000 μm^2 in size and non-circular in shape. Grainstone flow units dominated by depositional interparticle porosity have high reservoir potential. Typically, 70 to 90% of the pores of the dolomitized and leached grainstone facies are 100 to 1,000 μm^2 in size and round in shape and 10 to 30% of the pores are 1,000 to 10,000 μm^2 in size and moderately non-circular in shape. Grain moldic pores (<5%) have sizes greater than 10,000 μm^2, are non-circular in shape, and are generally isolated and not connected pores. Leached and dolomitized grainstone flow units dominated by moldic and intercrystalline porosity have lower reservoir potential in that these carbonates have a high percent of small pores and narrow pore throats. Typically, 40 to 70% of the diagenetic pores of the dolostone facies are 100 to 1,000 μm^2 in size and are round in shape, 25 to 45% of the pores are 1,000 to 10,000 μm^2 in size and moderately non-circular to circular in shape, and 1 to 15% of the pores are >10,000 μm^2 in size and are non-circular in shape. Dolostone flow units dominated by intercrystalline and vuggy porosity have the highest reservoir potential.

Burial and Thermal History Study.--Burial and thermal maturation history plots for the well Permit #1639 (9-15) in the Womack Hill Field have been constructed (Figs. 70 and 71) and show that the oil from the field was sourced from outside the field area.

Task RC-2. Petrophysical and Engineering Property Characterization

Description of Work.--This task is designed to focus on the characterization of the reservoir rock, fluid, and volumetric properties. These properties are obtained from petrophysical and engineering data. This task assesses the character of the reservoir fluids (oil, water, and gas), as well as the petrophysical properties of the reservoir rock. The production rate and pressure histories are analyzed for the purpose of estimating reservoir properties. A major goal is to assess current reservoir pressure conditions and develop a simplified reservoir model. New pressure

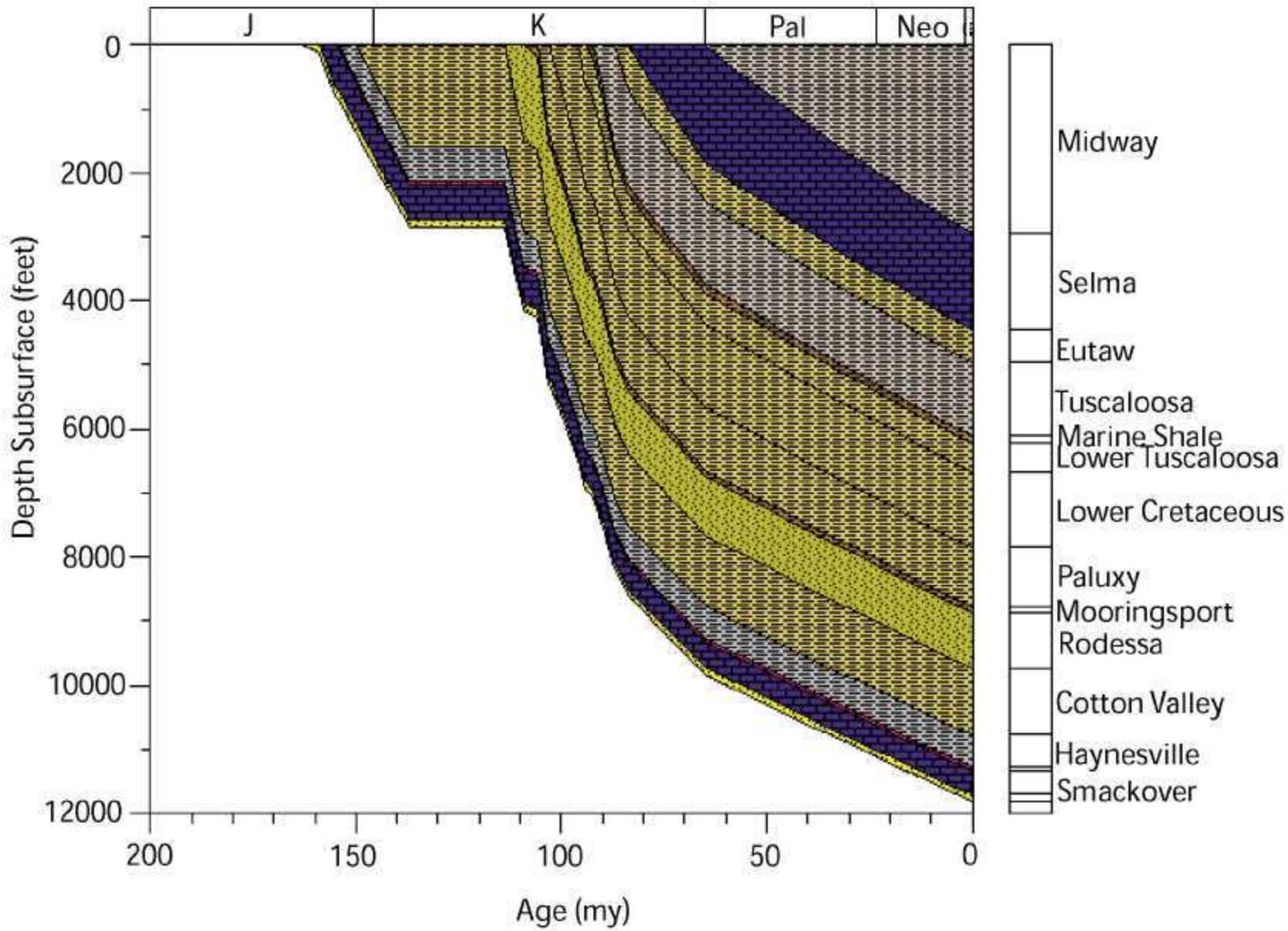

Figure 70. Burial history plot of the 9-15 well.

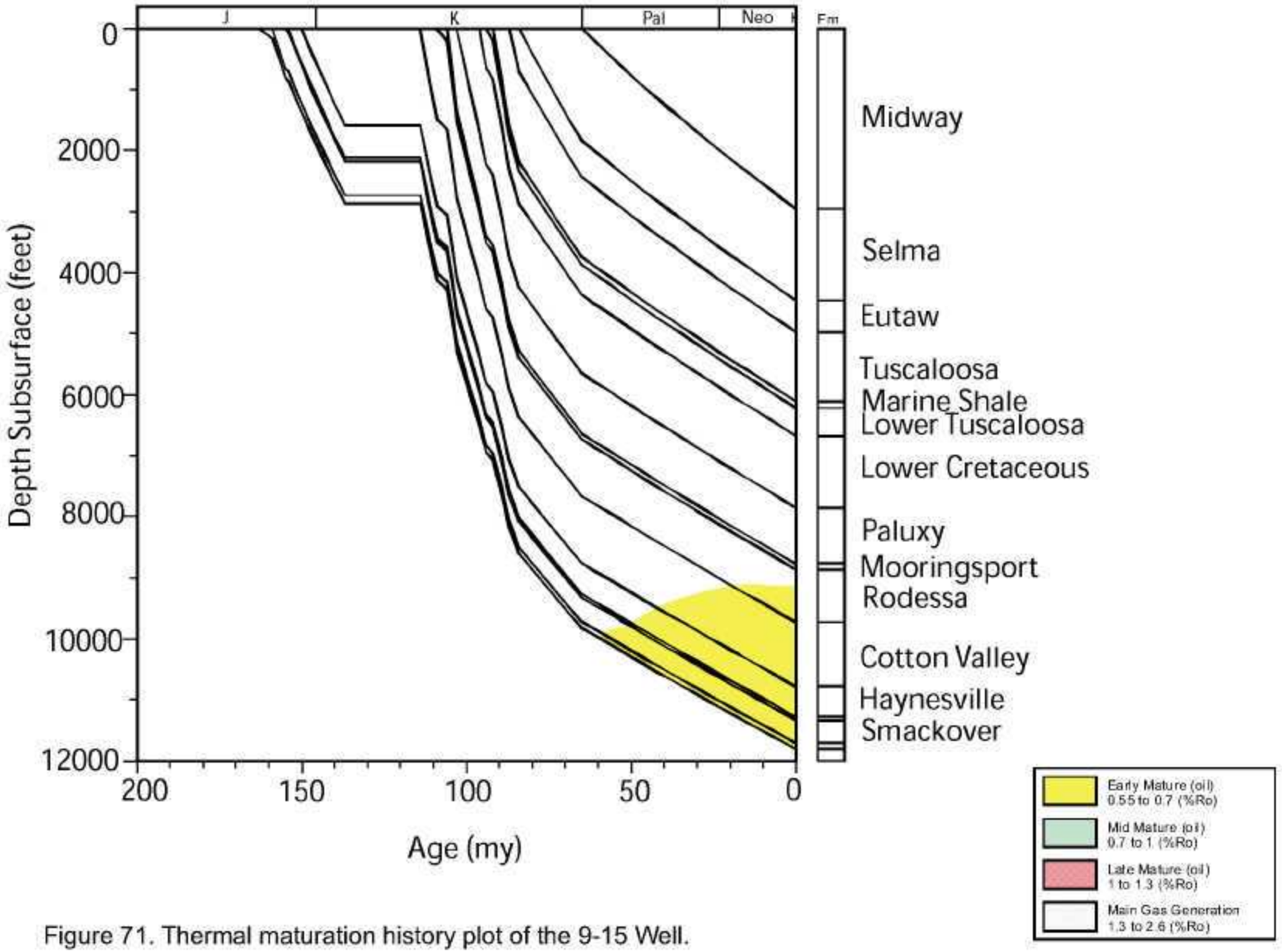

Figure 71. Thermal maturation history plot of the 9-15 Well.

data are obtained to assess communication within the reservoir field-wide. This work serves as a guide and provides bounds for the reservoir simulation modeling.

Rationale.—Petrophysical (core, well logs, etc.) and engineering data (production rate and pressure histories, pressure tests, well completion data) are fundamental to the reservoir characterization process. Petrophysical data are often considered static (non-time dependent) measurements, while the engineering data are considered dynamic. The reservoir characterization concept is (almost by definition) the coupling or integration of these two classes of data. The data are analyzed to identify fluid flow units (reservoir-scale flow sequences), barriers to flow, as well as reservoir compartments. The petrophysical data are essential for defining the quality of the reservoir rock, and engineering data (reservoir performance data) are crucial for assessing the producibility of the reservoir. Coupling these concepts, via reservoir simulation or via simplified analytical models, allows for the interpretation and prediction of reservoir performance under a variety of conditions.

Analysis/Interpretation/Integration Procedure.—Womack Hill Field is a mature oil field (Figs. 72 and 73). Since the discovery of the field production rates have steadily declined. The following tasks are employed as the mechanisms to analyze, interpret, and integrate the petrophysical and engineering data from Womack Hill Field.

1. Collect and catalog the well log, core, and production data.
2. Convert these data into an appropriate electronic format.
3. Develop correlations between core and well log data to predict reservoir permeability using well log responses.
4. Analyze and interpret the reservoir performance data using decline type curve analysis and estimated ultimate recovery analysis.

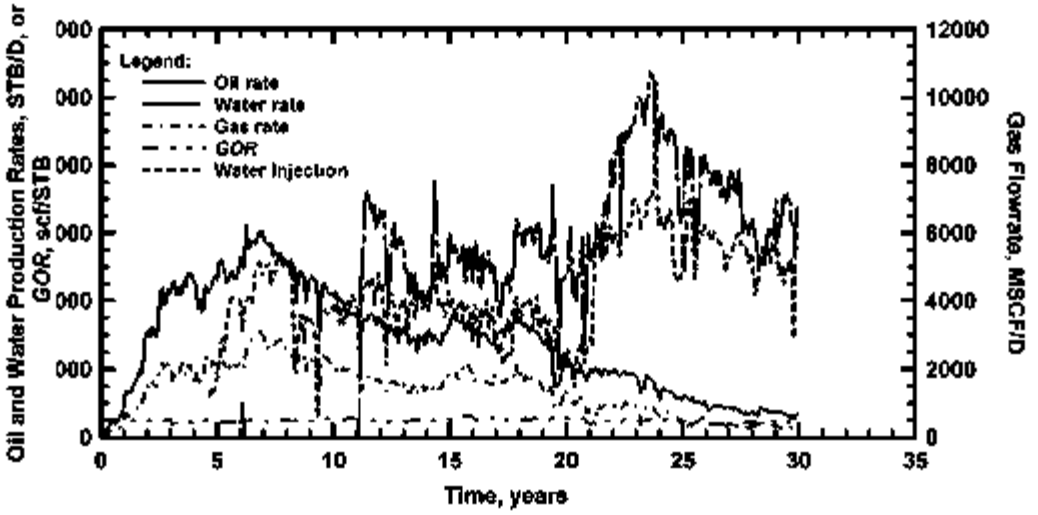

Figure 72 Production history of Womack Hill Field Since 1997, oil and gas rates have steadily declined, while the water production rate has increased *GOR* has remained essentially constant

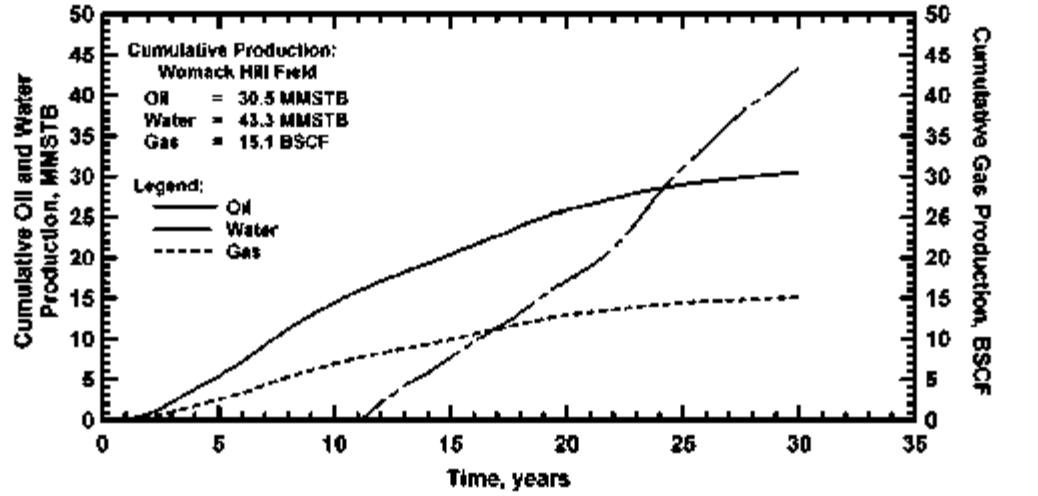

Figure 73 Cumulative production of Womack Hill Field Oil and gas curves are on the plateau and the water continues rising

5. Integrate the geological data and the results of reservoir performance analysis by generating maps of distributions of reservoir properties throughout the field.
6. Establish recommendations to optimize the reservoir management strategies, such as infill drilling.

Correlation of Petrophysical Data—Core-Well Log Data Correlation.--At Womack Hill Field the following well log responses are typically available:

- (SP) Spontaneous potential
- (ILM) Shallow resistivity
- (LLS) Deep resistivity
- (GR) Gamma ray
- (ROHB) Bulk density
- (DPHI) Density derived porosity
- (NPHI) Neutron derived porosity

In addition, substantial volumes of whole and sidewall core data are available. Admittedly, all of these data are 1970's vintage, and we have encountered significant difficulty in trying to correlate the core and well log data.

As an example, in Figure 74 we provide a presentation of the core and well log data—showing the well log data and core permeability profiles for well Permit #1639. The reservoir has been divided into three flow units, based originally on geological data, and we note that our work with the core and well log data also confirmed these assignments. As shown, the core permeability data are quite scattered, giving us an indication of the level of heterogeneity in the reservoir. The wells at Womack Hill Field produce from the upper Smackover carbonate reservoir, which is typically characterized by a high level of heterogeneity. This makes it difficult to find correlations between the petrophysical variables on a regional scale. Therefore, our approach is to establish correlations for the flow units at a local scale (i.e., for individual wells).

As part of our characterization of the petrophysical data, we distributed the core data (porosity and permeability) into the appropriate flow units and aligned the corresponding well

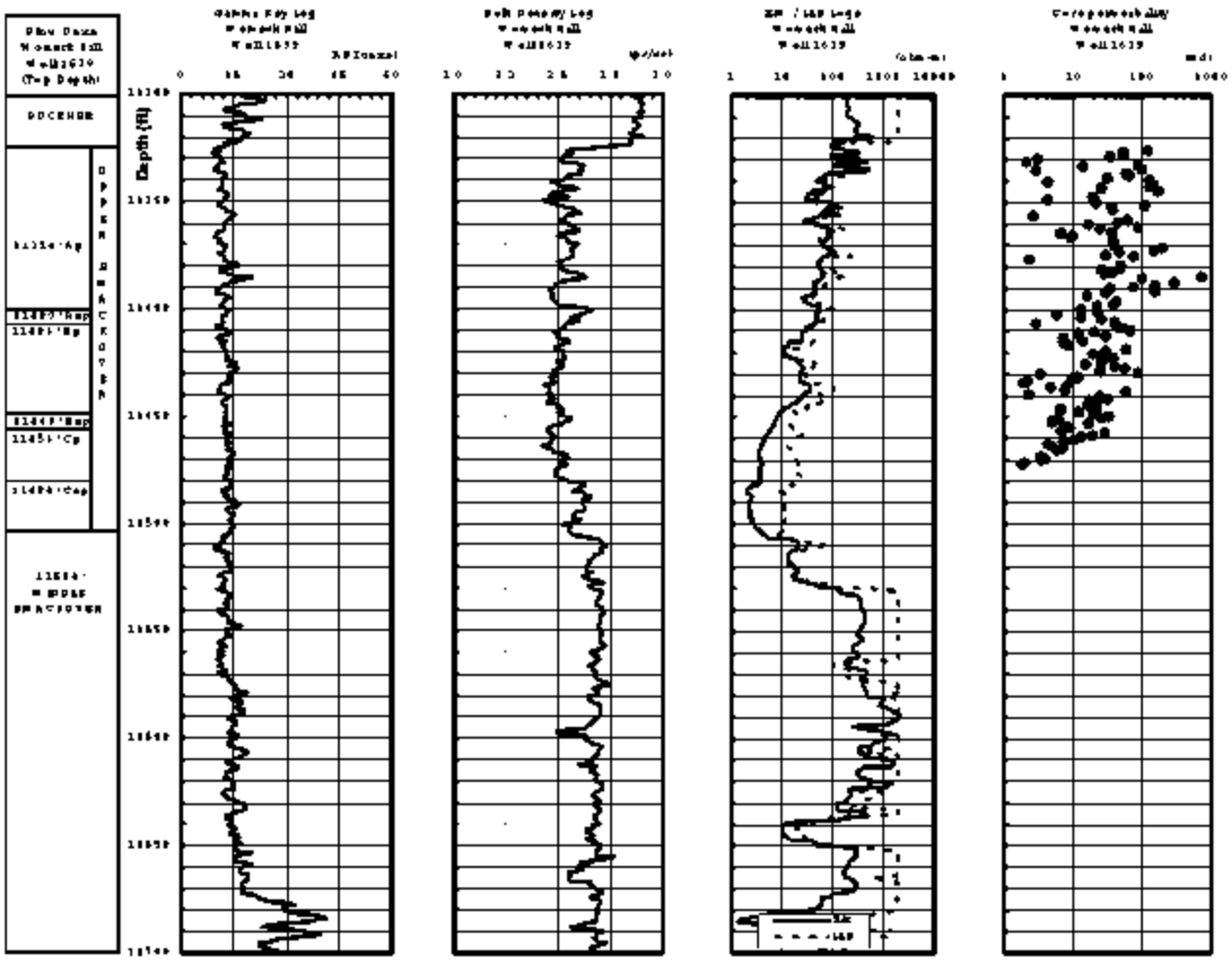

Figure 74 Example of log and core permeability profiles — Well 1639, Womack Hill Field, Alabama

log measurements to construct the data tables for correlation purposes. We selected the core and well log data for 9 wells. We find that there is no consistent suite of well logs for all wells; however, we do note that the GR, LLS and some sort of porosity log are generally available. As such, we selected GR, LLS, and (core) porosity as independent variables to keep the same set of input data for all correlations.

To develop our correlations of the petrophysical data we selected a nonparametric technique that is based on estimating the optimal transformation of each variable (the dependent as well as the independent variables). This method has an advantage over conventional multiple regression algorithms in that it does not require an assumed correlating function (i.e., model) between the variables—where a pre-established model could yield an inaccurate representation. The nonparametric method uses an iterative process involving a set of "alternating conditional expectations" (ACE) to generate a transform value for each data point of the dependent and independent variables. Once the transform for each of the variables has been established, a nonparametric correlation is generated between the dependent variable and the sum of the transform values, this is called the optimal transformation. Parametric correlations can be generated by fitting these curves using the appropriate functions, generally polynomial functions (GRACE program (1996)) The dependent variable is estimated by determining the inverse of the optimal transform. The details for this process are given by Breiman and Friedman (1985).

Our first approach in developing the core-log correlations was to analyze simple relationships between the variables, which could allow us to obtain less complex correlations if a strong relationship is found between these variables. We then studied the relationship between core permeability and each well log signal. Figure 75 presents crossplots of core permeability against GR, RHOB, LLS, and ILM for flow units in well Permit #1639. No single plot indicates

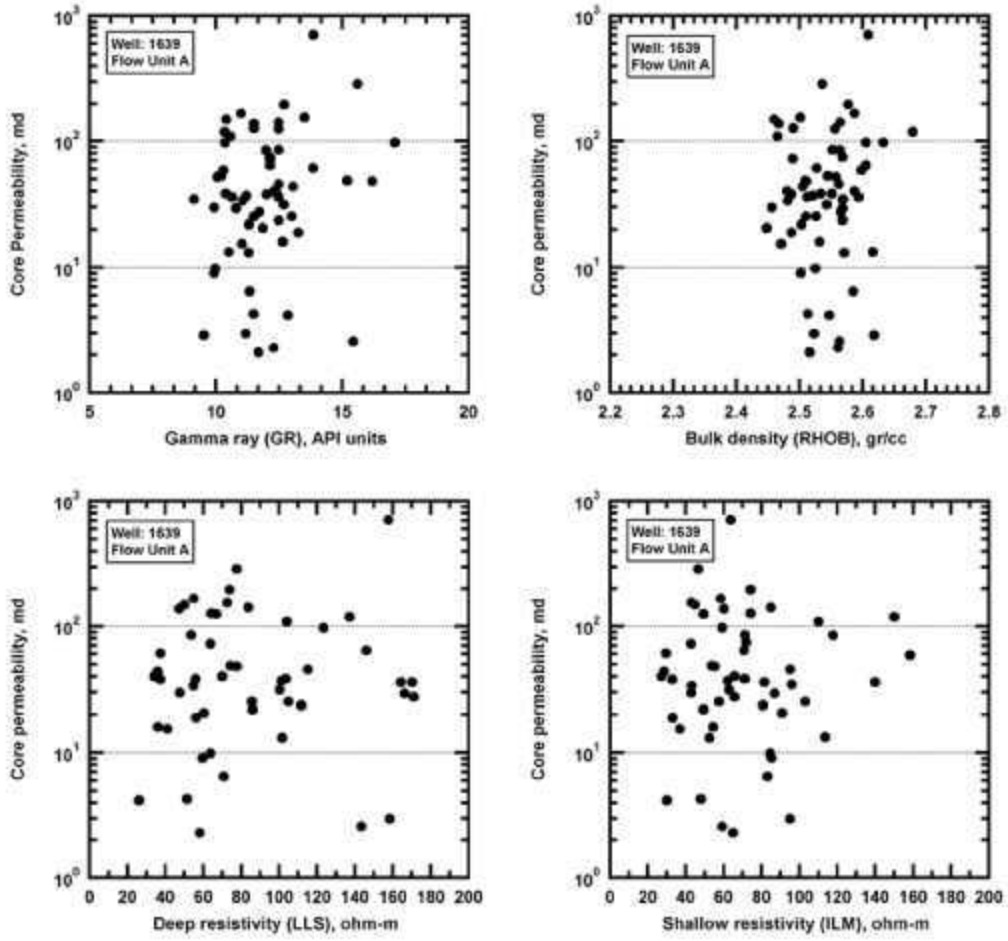

Figure 75. Core permeability univariate correlations — Womack Hill Field, Well 1639 (Flow unit A). No clear trend is present.

a clear tendency between the core permeability and any of the well log variables. GR and RHOB do not provide significant character to the correlation since the behavior of these variables is essentially constant through the section. Although the resistivity data do exhibit some variation, the overall relationship of resistivity with the core permeability is quite random (no clear pattern is evident).

This behavior (i.e., the lack of a univariate relationship) was found in each of the flow units for each well. This observation leads us to pursue the application of regression on several well log variables simultaneously as a mechanism to generate correlations between the core permeability and the well log data. We believe that the use of several well log variables in these correlations will improve the overall behavior of a correlation and establish a more consistent statistical model (when we move to convert the non-parametric relation into a parametric relation).

During the depth shifting effort, we observed that a significant variation exists between the core and well log-derived porosity, over the entire scale of porosity values. As an effort to try to resolve these differences, we considered the relationship between these two variables (core and well log porosity) on the flow unit scale. Figure 76 shows the relation between the porosity derived from the bulk density log and the core porosity for well Permit #1639 (Flow Unit A). We note that the relationship is extremely poor, and that the only positive comment is that the data appear evenly distributed (although randomly) about the 45° line (i.e., the perfect correlation line).

Generally speaking, well log derived porosity values are among the most consistent variables that can be estimated—unfortunately, this is not the case in Womack Hill Field. The use of the well log derived porosity as input data for the correlation would produce significant

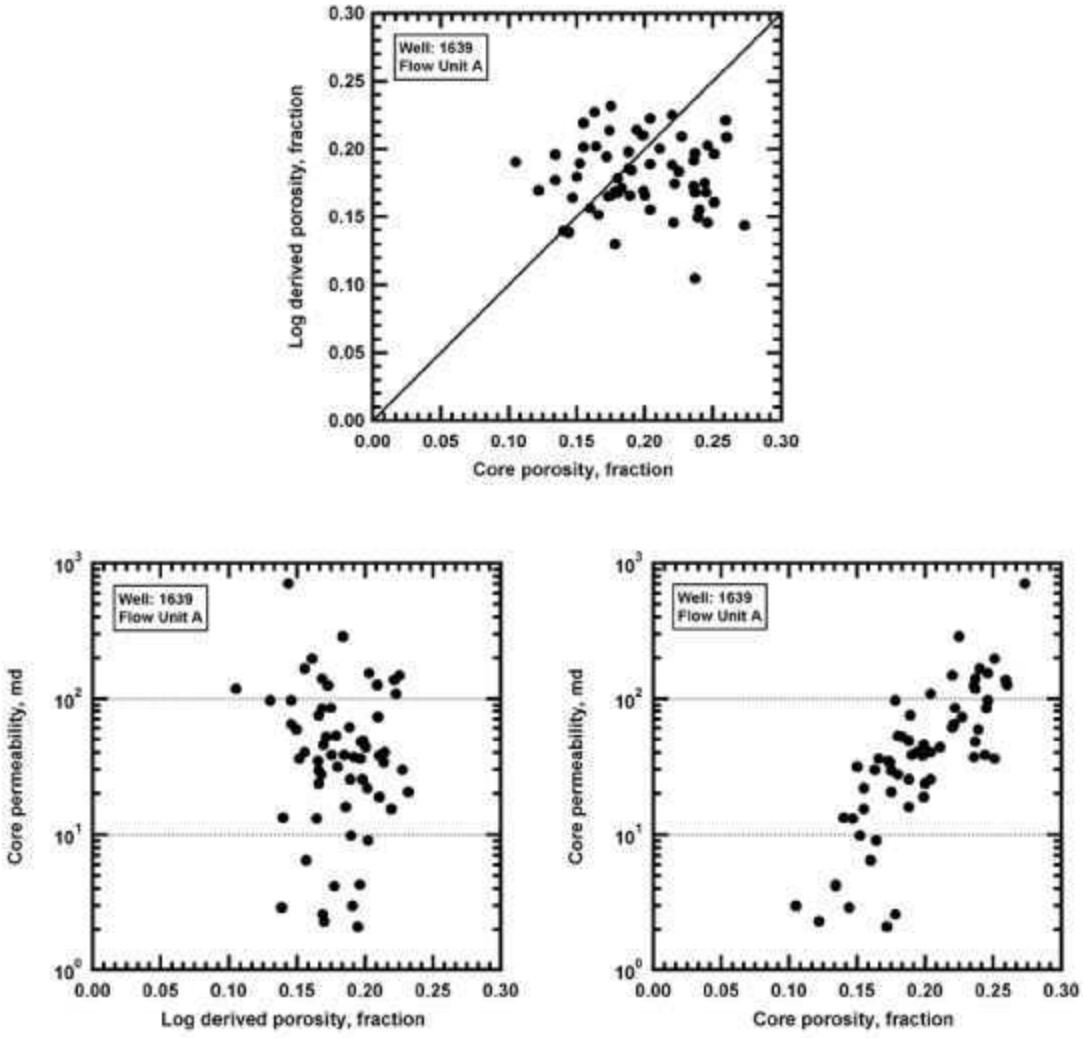

Figure 76. Core permeability and porosity plots — Womack Hill Field, Well 1639 (Flow unit A). Log derived porosity does not match either core porosity or have a clear trend with core permeability — core porosity and permeability show a clear relationship.

errors, as it has little or no relation to the formation permeability. However, a comparison of the logarithm of the core permeability with core porosity yields a reasonably linear trend (Fig. 76). As such, we elected to use the core porosity in lieu of the well log-derived porosity to obtain more consistent results. To generate correlations that can be used for most of the wells, we selected the GR, LLS, and core porosity as input data for the correlations. Although the GR log is thought to have relatively little character, it does provide certain petrophysical characteristics, as the accuracy of the correlation tends to improve when the GR data are included. Typically, the ILM and LLS responses follow essentially the same tracks; however, we prefer the deep resistivity (LLS) over the shallow resistivity (ILM) because the LLS resistivity utilizes information at distances further into the reservoir, and because the LLS is the more common well log acquired in Womack Hill Field.

Having prepared the data sets for correlation, we use the GRACE program (1996) to establish the nonparametric correlations for each variable—generating the corresponding optimal transformations. As we require some functional form, in order to apply the correlation, we utilize parametric correlations that are generated by fitting the data using quadratic polynomials (a feature of the GRACE program). As an example, in Figure 77 we present the transformations for each variable (well Permit #1639—Flow Unit A). Finally, the correlation that is used to predict the dependent variable is obtained by calculating the inverse of the optimal transformation. We noted that the correlating function matches the tendency exhibited by the measured data, which confirms the robustness of the non-parametric method.

Correlation of Petrophysical Data—Statistical Analysis of Core-Data.--In order to generate a petrophysical model of the reservoir we needed to establish a distribution of the formation properties throughout the reservoir drainage area. Our ultimate goal in this effort is to

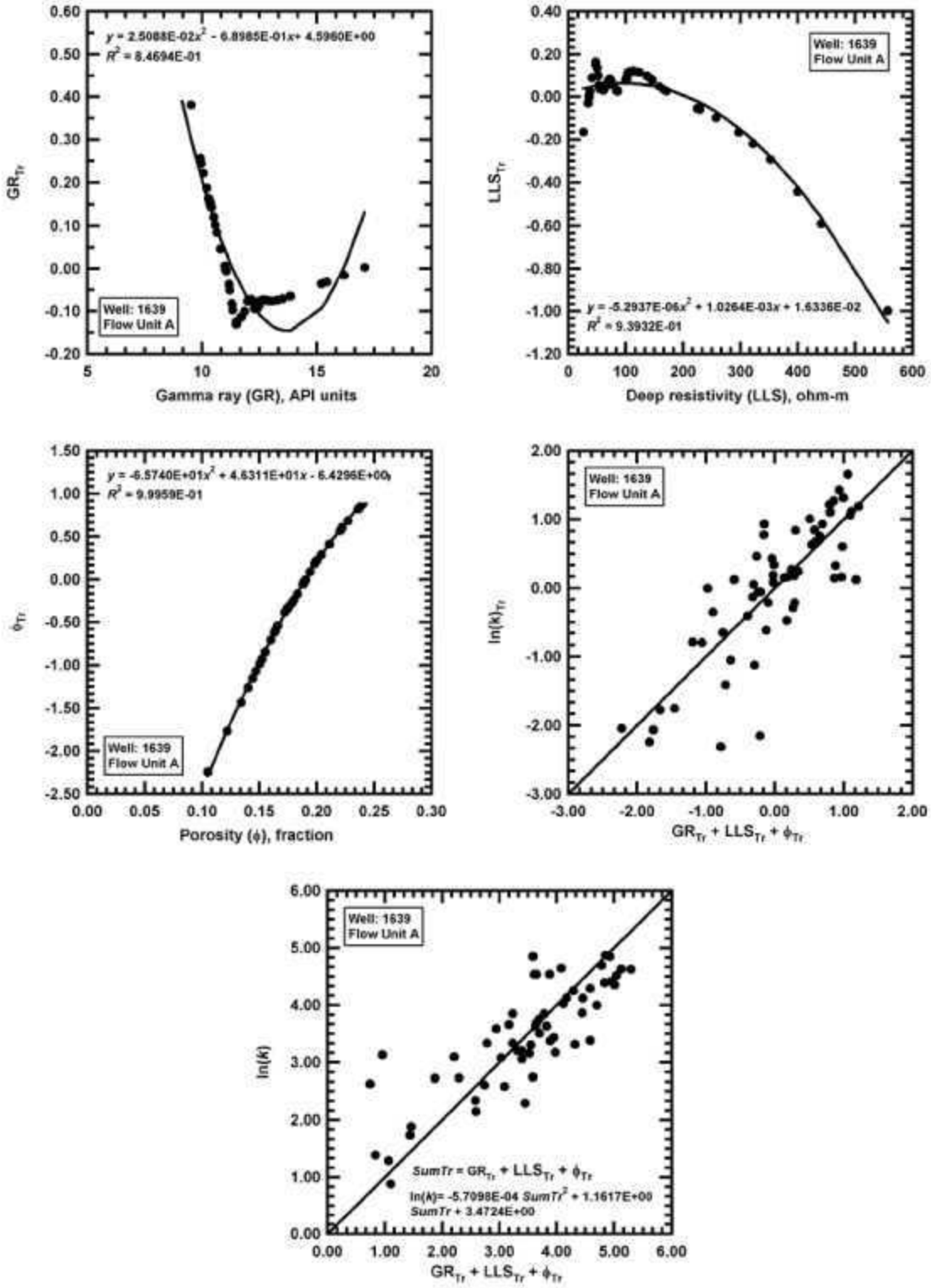

Figure 77. Optimal transformations for independent and dependent variables and core permeability correlation — Womack Hill Field, Well 1639 (Flow unit A).

provide a reservoir description that can be used for numerical simulation. To accomplish this goal, we segregated the data according to flow units and developed histograms of porosity and the logarithm of permeability. These histograms confirm that porosity and the logarithm of permeability both follow a normal distribution.

Figure 78 provides an example of this behavior for well Permit #1639—Flow Unit A. We note that most of the wells in Womack Hill Field yield similar histogram trends. It is our intention to use the mean value of porosity and the logarithm of permeability established from a particular histogram to represent the average for a particular flow unit. Using these results, we developed maps of porosity and permeability based on the average values for each flow unit—which are part of our proposed geological model for numerical simulation.

Well Test Analysis.--In May 2002, a series of pressure transient tests (Fig. 79) were designed and implemented at Womack Hill Field for the express purpose of estimating reservoir pressure, effective permeability, skin factor, and a variety of other properties (e.g., fracture half-length (a surrogate for a high degree of well stimulation due to a rotational series of acid treatments on individual wells)).

The analysis of these well tests was somewhat challenging, particularly because of the need for an accurate production or injection history. As such, we chose to be pragmatic—we analyzed each case (except well Permit #1655) with accounting for the reported production/injection history contemporary with the particular test. Each well test sequence is summarized and discussed below.

Well 1655. Well Permit #1655 is currently producing from the Unit area and has produced since 1971 (Fig. 80a), and we note that the production trend has a number of decline/recovery trends—indicating stimulation, recompletion, or both. The well has been on a constant

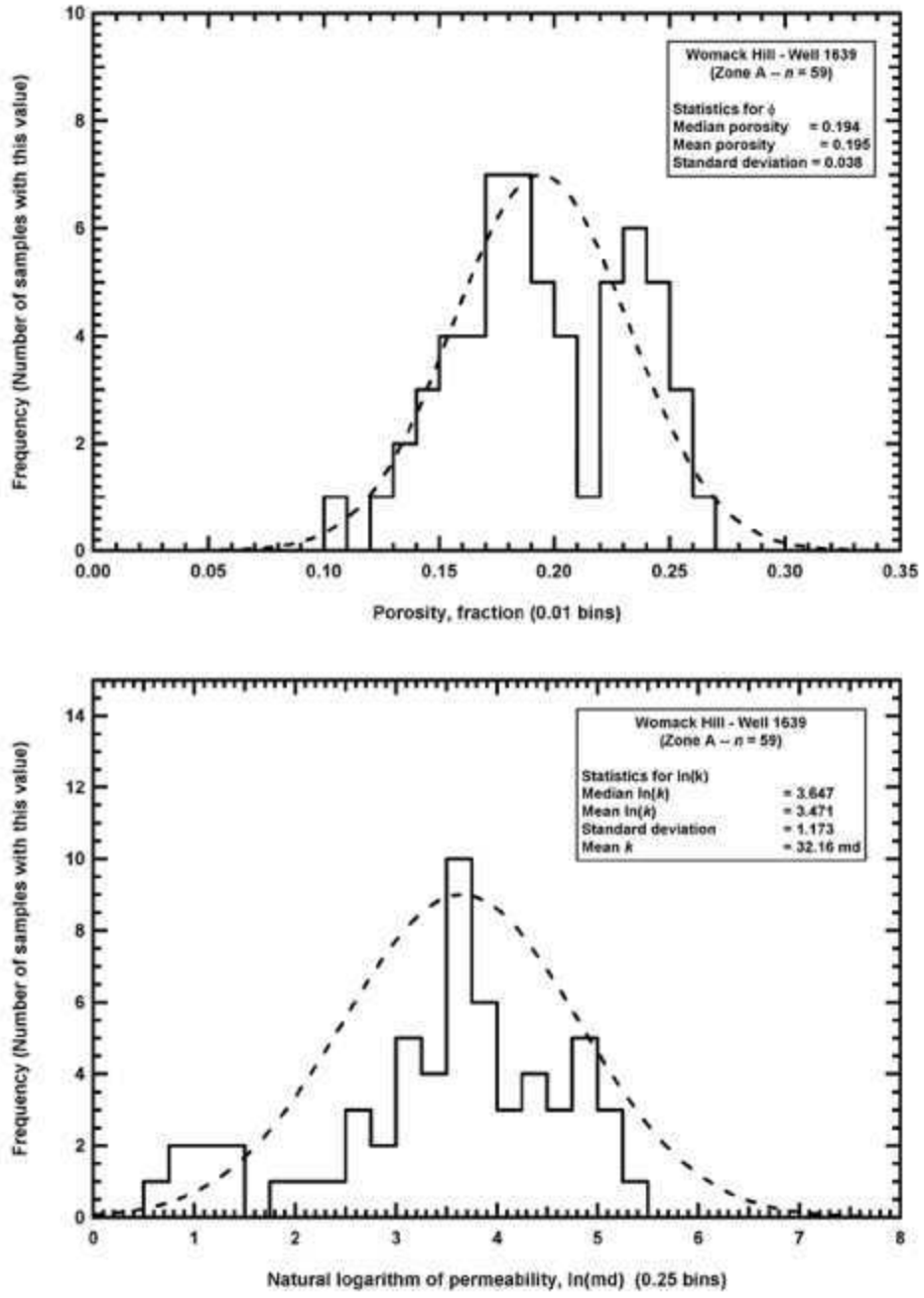

Figure 78. Core porosity and logarithm of core permeability histograms — Womack Hill Field, Well 1639 (Flow unit A). Both porosity and the logarithm of permeability have a normal distribution.

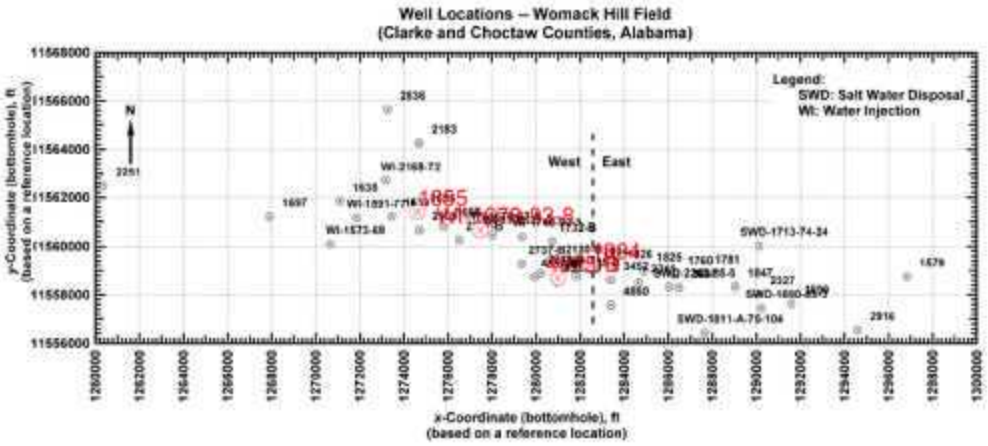

Figure 79. Field Map of Well Locations (bottomhole locations) — Sites of May 2002 Well Tests, Womack Hill Field.

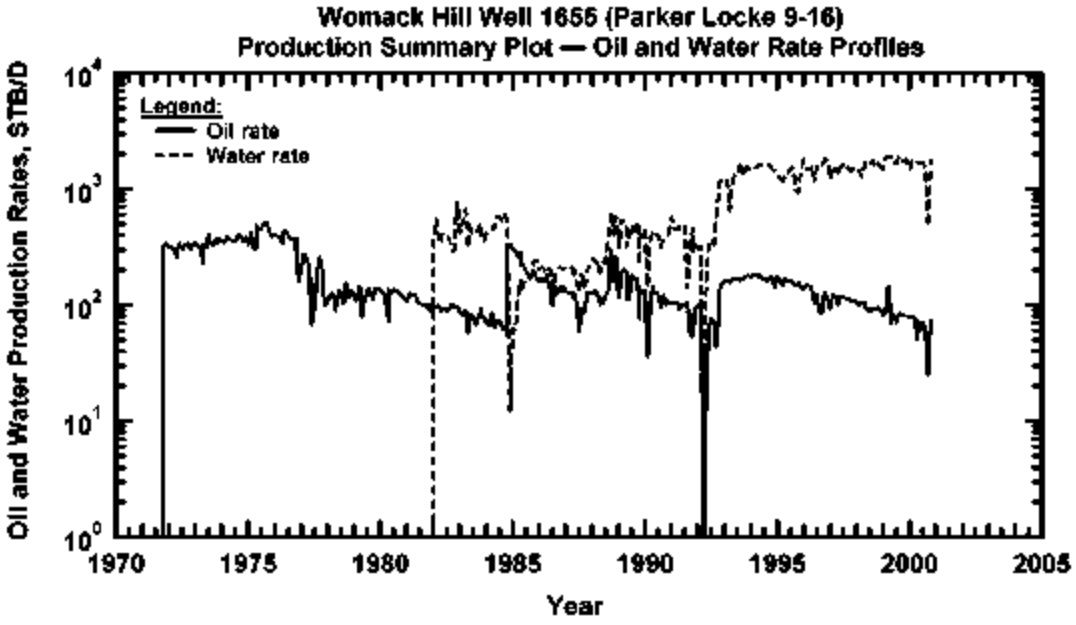

Figure 80a. Production History for Well WH 1655 — Womack Hill Field.

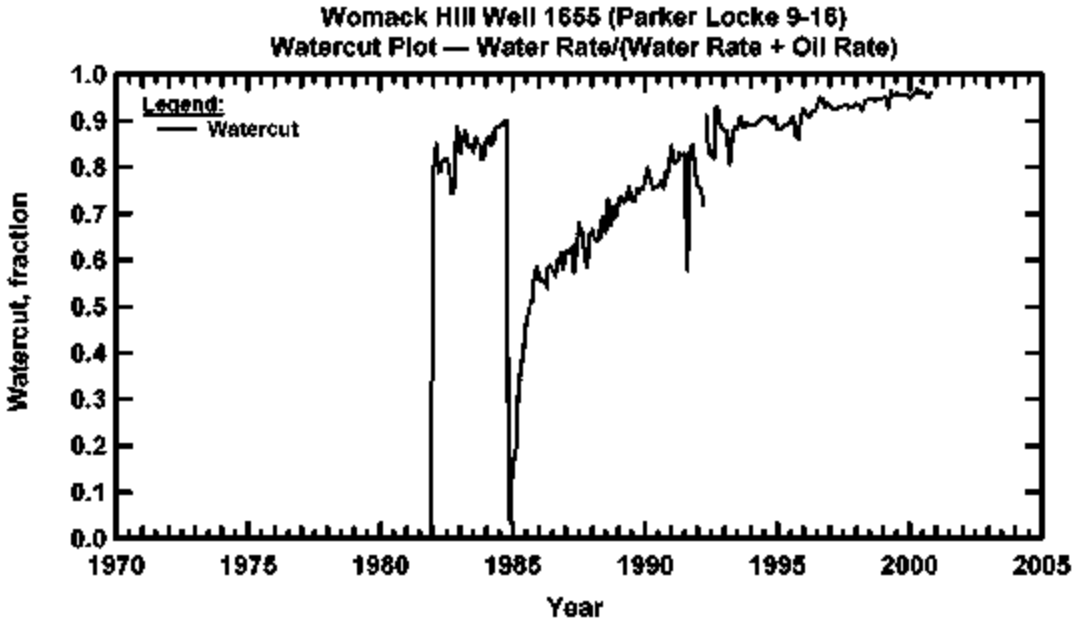

Figure 80b. Watercut for Well WH 1655 — Womack Hill Field.

(exponential) decline in oil production since 1992—while water production was essentially stable in this period (at about 1500-1800 STBW/D). The watercut plot (Fig. 80b) indicates a very high watercut at present, with an apparent stimulation in well performance in 1985. Interestingly, the watercut profile consistently increases from 1985 to present, despite substantial changes in oil and water production performance.

When reviewing the "strip chart" plot (Fig. 80c) for well Permit #1655 the pressure drawdown data appear to indicate unreported rate changes. On the other hand, the pressure buildup data are very smooth (continuously increasing) and contain no spikes or any apparent inconsistencies in the data. In the "summary analysis" plot (Fig. 80d) for well Permit #1655—we note that the pressure derivative function has a "zigzag" character indicative of a changing wellbore storage scenario. We also note an apparent radial flow region as well as an apparent closed boundary feature in the late-time pressure derivative function. The simulated pressure drop and pressure derivative functions match the well test data very well—suggesting a representative model has been developed.

While we must be careful not to "over interpret" a particular scenario, the case for reservoir compartmentalization is supported by the data and the reservoir model. We believe that the well-reservoir model proposed for this case is appropriate and accurate.

Well 1678. Well Permit #1678 has been a water injection well since 1993 and was put on injection as a mechanism for pressure maintenance. We note that well Permit #1678 was put on production in 1972 (Fig. 81a) and produced at a very high watercut (Fig. 81b). The injection rate/pressure summary plot (Fig. 81c) shows consistent trends of injection rates and pressures. It can be argued (based on analogous behavior in other fields) that the general decline in injection

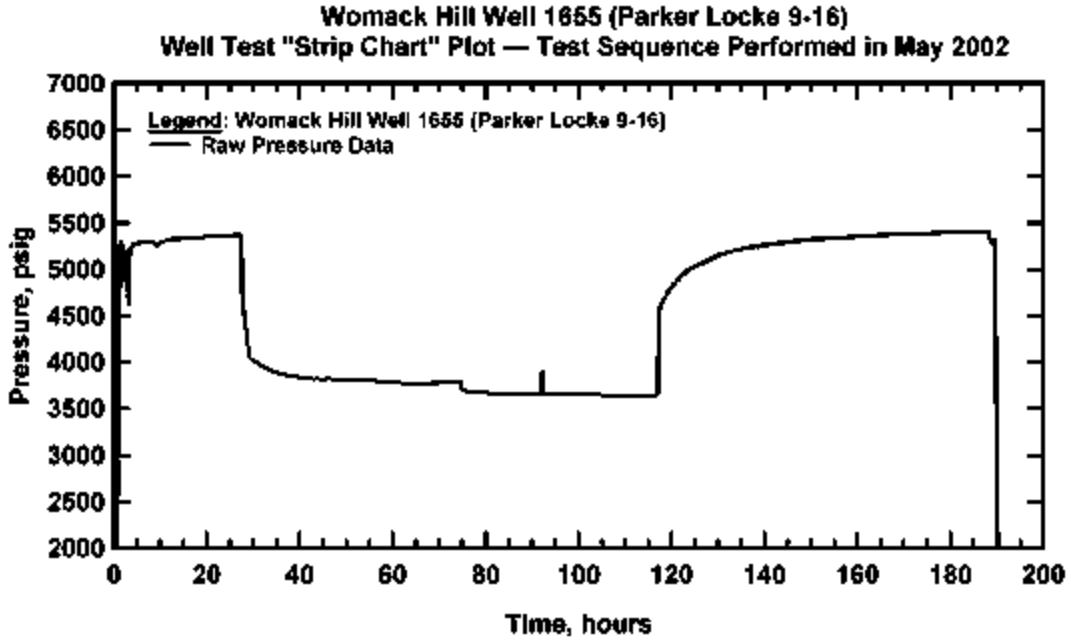

Figure 80c. "Strip Chart" Data Summary Plot (No Analysis) for Well WH 1655 — Womack Hill Field (testing sequence of May 2002).

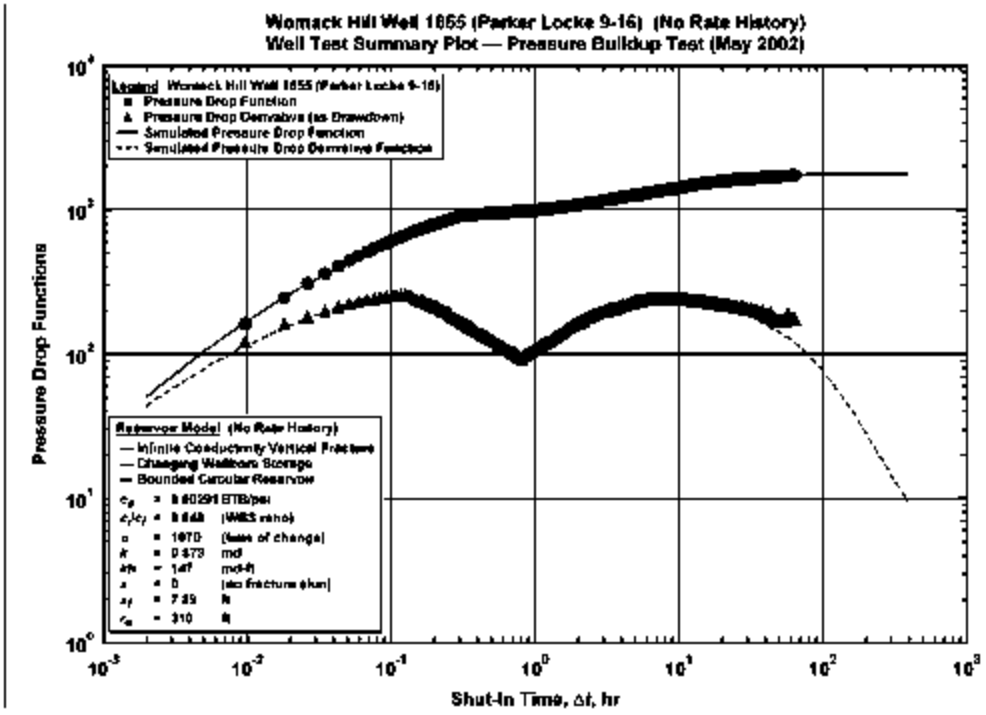

Figure 80d. Summary Plot (No Rate History) for Well WH 1655 — Womack Hill Field (testing sequence of May 2002).

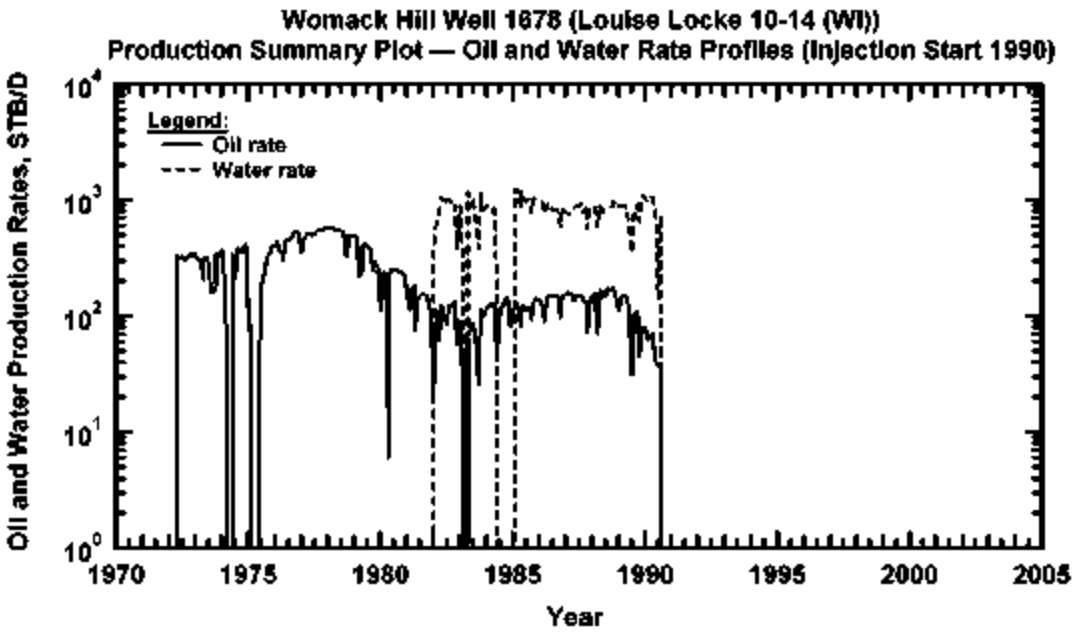

Figure 81a. Production History for Well WH 1678 — Womack Hill Field.

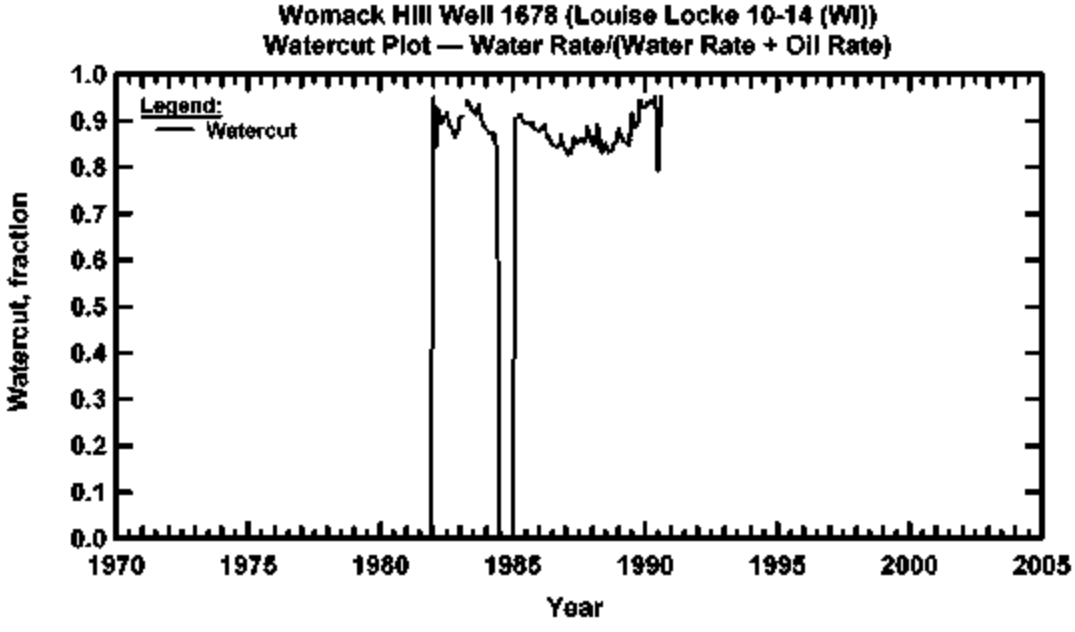

Figure 81b. Watercut for Well WH 1678 — Womack Hill Field.

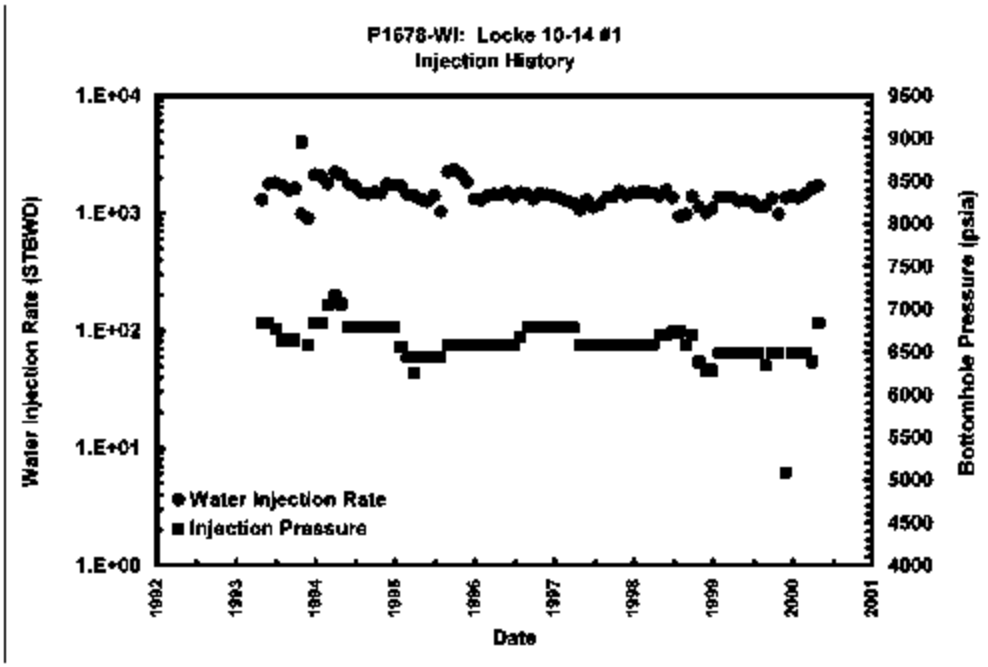

Figure 81c. Injection Data Summary Plot (No Analysis) for Well WH 1678 — Womack Hill Field.

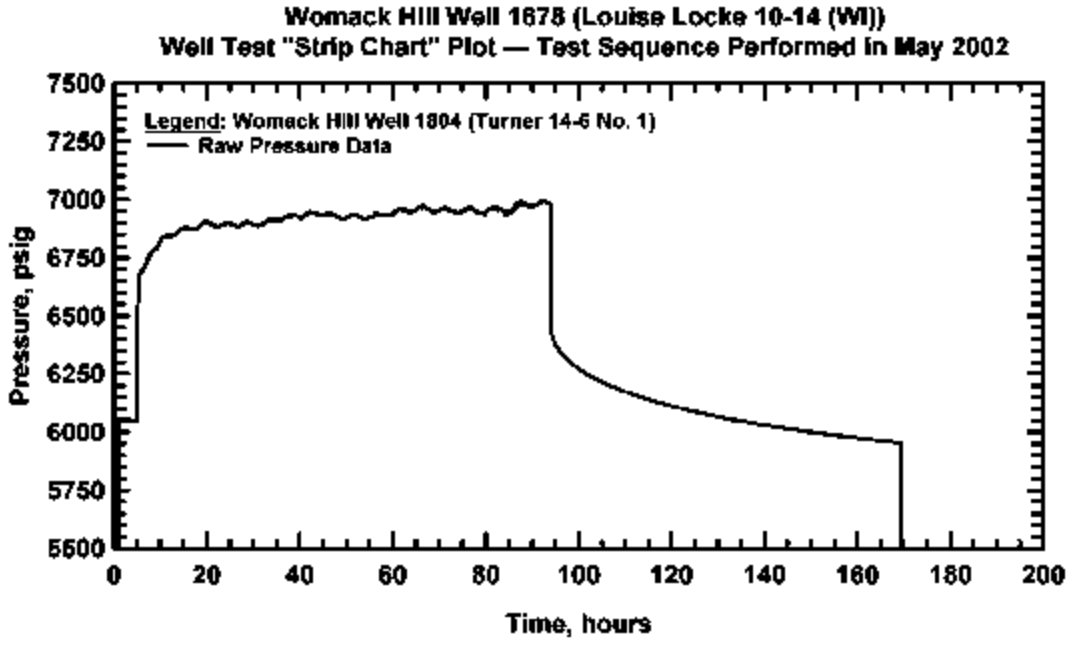

Figure 81d. "Strip Chart" Data Summary Plot (No Analysis) for Well WH 1678 — Womack Hill Field (testing sequence of May 2002).

rates (log scale) with a relatively constant injection pressure (Cartesian scale) is common for an area that is "pressuring-up." In other words, this appears to be a typical injection scenario.

From the "strip chart" plot (Fig. 81d) for well Permit #1678, we note that the injection portion of the data is severely affected by a cyclic pressure profile that is not synchronous with any natural feature (such as tidal motion (for example)). Conversely this behavior is anomalous, and there is no obvious explanation—a representative of the operating company has suggested that this is a surge and release feature caused by the injection pump and manifold system. This is an entirely plausible explanation. Regardless of the cause, the injection portion of the data is rendered invalid for analysis without specific data to "deconvolve" the cyclic pressure features. As such, we have elected to focus solely on the "pressure falloff" portion of the data (we note that these data appear to be smooth and continuous).

The pressure falloff data (Fig. 81e) are analyzed presuming that the given injection profile is appropriate and are analyzed separately without assuming an injection history (other than having a constant injection rate over a protracted time period). Considering the "rate history" case we find that the data appear to indicate a strong component of well stimulation (acidization or fracturing—for this case a small fracture has probably evolved). From the "no rate history" analysis (Fig. 81f), we note that this analysis is essentially identical to the "rate history" case, with the noted difference that the configuration of the presumed boundaries are different in these cases. In particular, the "rate history" analysis presumes "parallel faults" while the "no rate history" case presumes 2 faults at a 90° angle. This analysis confirms our previous contention that the Womack Hill reservoir is more compartmentalized than previously thought. It is also relevant to note that the calculated effective permeability to water is quite high for this case (≈ 6

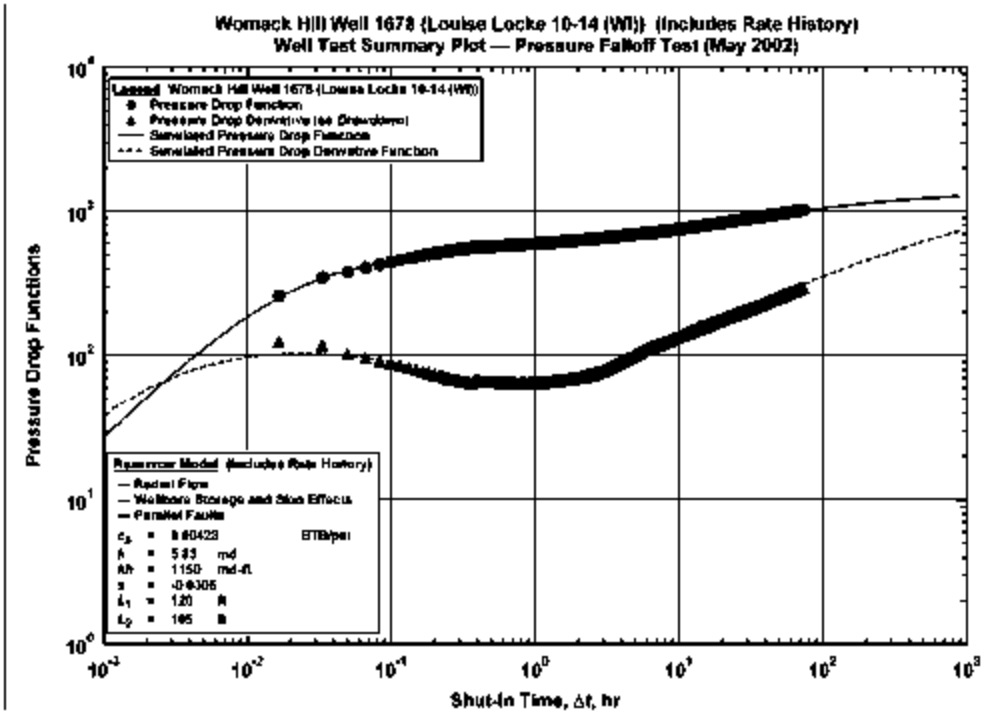

Figure 81e. Summary Plot (Includes Rate History) for Well WH 1678 — Womack Hill Field (testing sequence of May 2002).

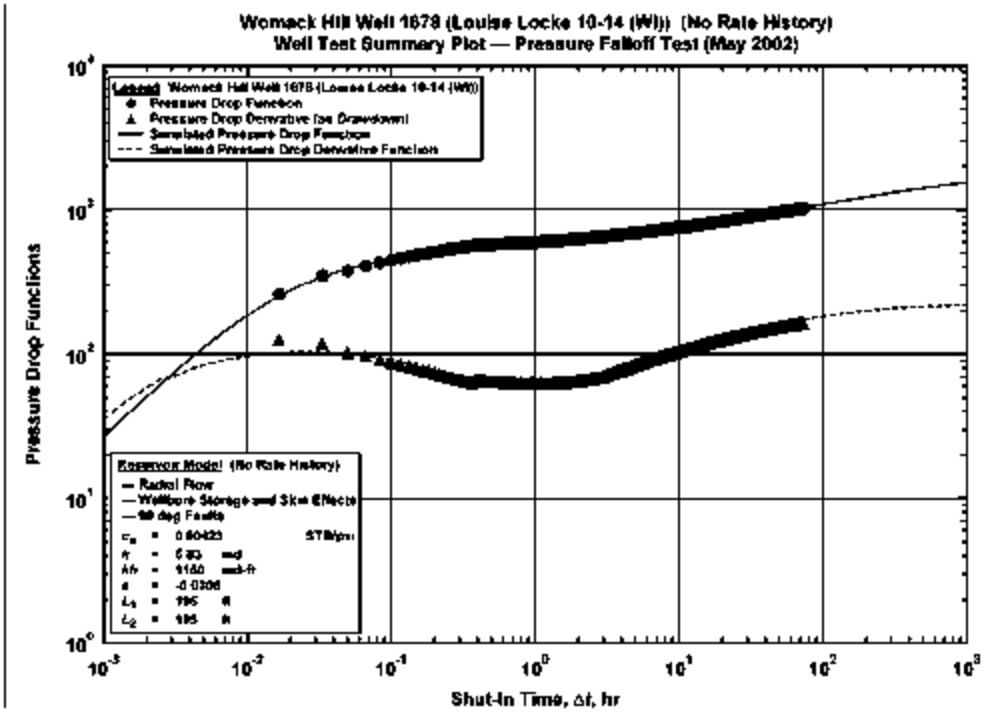

Figure 81f. Summary Plot (No Rate History) for Well WH 1678 — Womack Hill Field (testing sequence of May 2002).

md)—however, such an estimate is not improbable given the water-wet character of the Smackover rock.

Well 1804. Well Permit #1804 is a unique entity in Womack Hill Field—it has been a prolific producer since 1973 (Fig. 82a), with a total cumulative oil production of over 3.4 MMSTB. This well is currently producing from the non-unitized part of the field. We note a unique production history in that the well produced at its physical limit of about 400 STB/D for almost 17 years before going on decline. We also note that the well responds extraordinarily well to stimulation (in this case acid treatments) as can be seen by the production response in 1999-2000. Lastly, this well produced no water until 1990—suggesting that natural water influx is a major factor. A final comment, more subjective than definitive, is that well Permit #1804 appears to be producing from an isolated compartment—the well is not located in close proximity to other wells, and it is not clear that well Permit #1804 has interference of any kind with the wells in its vicinity.

From the watercut history (Fig. 82b) for well Permit #1804, we note that water production did not occur until 1990 (despite our reservations regarding the produced water records, we have confirmed with staff at the operating company that well Permit #1804 did not produce water prior to 1990). The watercut history is well-behaved, and appears to confirm our suggestion that the mechanism for water encroachment is a "slow" water influx.

From the "strip chart" plot (Fig. 82c) for well Permit #1804, we note that the most distinguishing characteristics shown on this summary plot are the pressure increase during the drawdown (most likely the rate is declining during this period) and the very smooth character of the pressure buildup profile. As the rate was reported to be constant during the drawdown (and

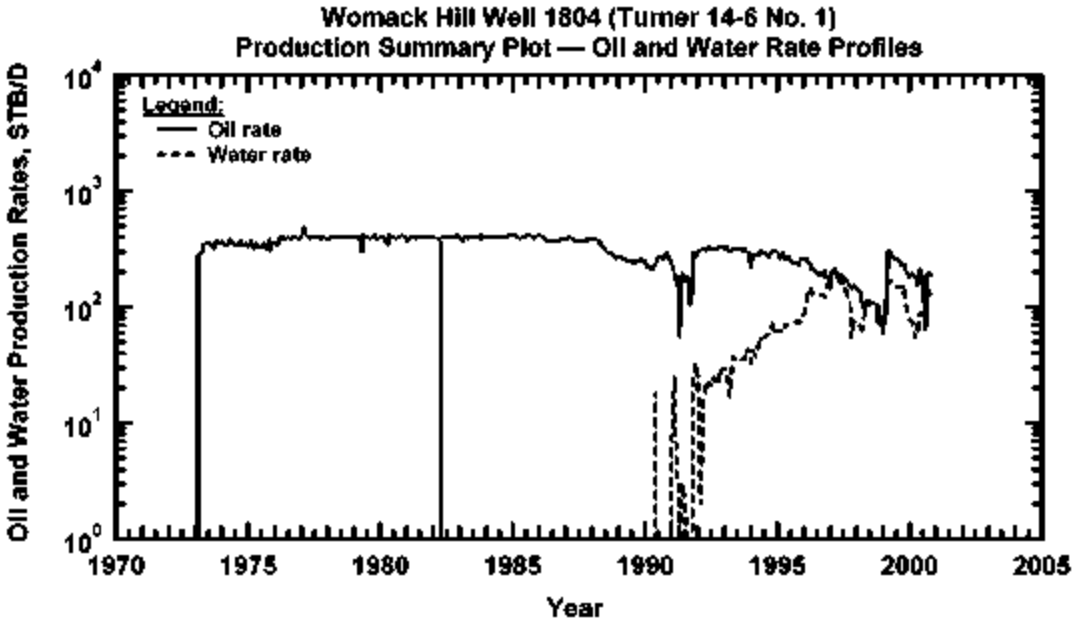

Figure 82a. Production History for Well WH 1804 — Womack Hill Field.

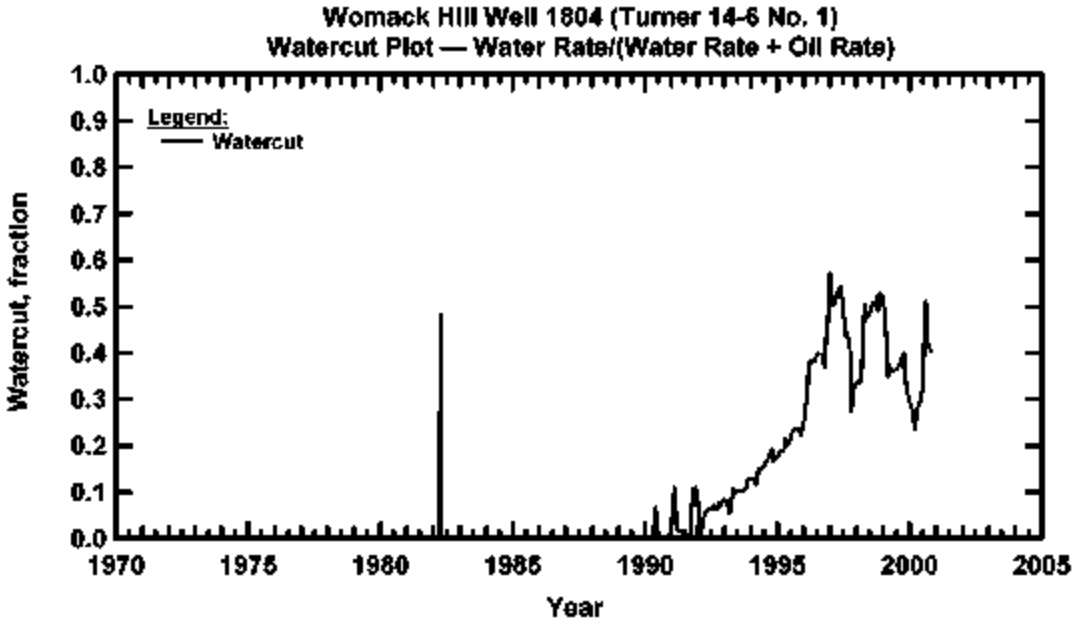

Figure 82b. Watercut for Well WH 1804 — Womack Hill Field.

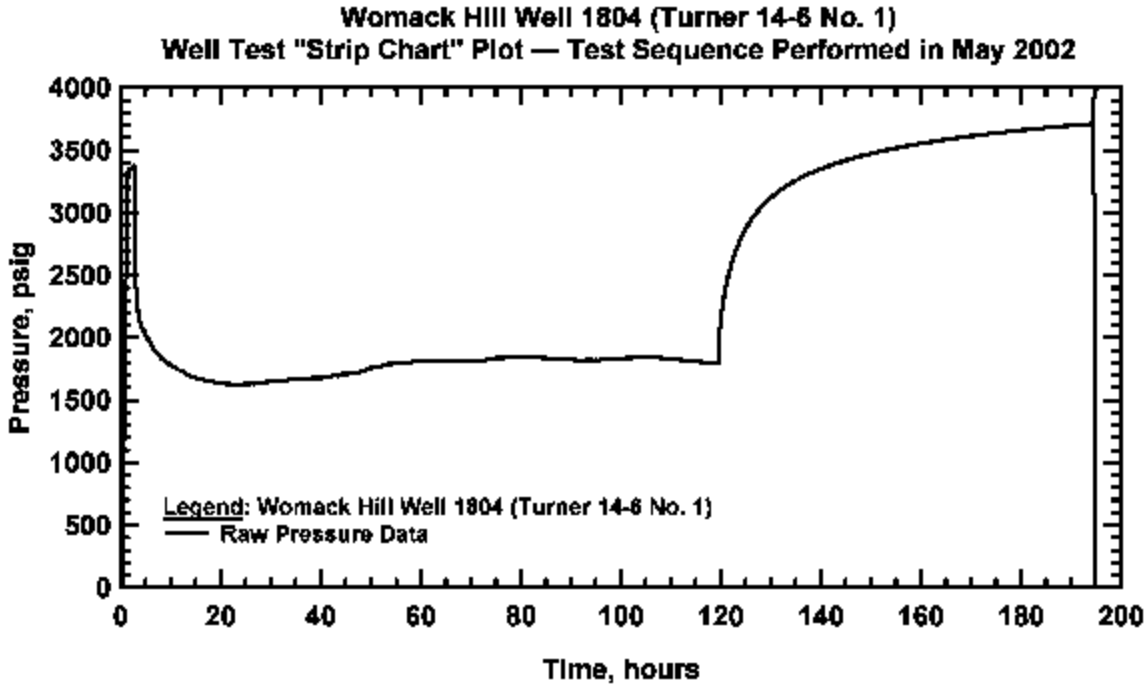

Figure 82c "Strip Chart" Data Summary Plot (No Analysis) for Well WH 1804 — Womack Hill Field (testing sequence of May 2002)

yet the pressure increased during this test sequence), we have concluded that these data can not be analyzed without a more detailed rate history (which is not available).

From the analysis summary (Figs. 82d, e), we note a very strong indication of substantial well stimulation—and our "best match" of the early time data utilizes the model of a vertically fractured well of infinite fracture conductivity. This behavior is almost certainly a product of the well stimulation practices in use by the current operator for the last few years (*i.e.*, acid stimulation). The "later" data suggest two significantly different scenarios—the "includes rate history" case indicates an infinite-acting radial flow behavior (which certainly is plausible), while the "no rate history" case provides a clear indication of a closed reservoir boundary. Unfortunately, these interpretations are somewhat equal in weight as each can be argued from both theoretical and practical considerations.

The inclusion of the rate history (Fig. 82d) is the most rigorous approach—provided that the rate history is accurate. The exclusion of the rate history (Fig. 82e) is often the most practical approach as the rate history is frequently unknown (or is given as a poor representation of the true behavior). While we would be reluctant to label these interpretations as equally probable, both interpretations have strong support—again, from both practical and theoretical standpoints. In the end, it is completely unrealistic that such a prolific well would produce as it has from a compartment of less than 1 acre (as the analysis suggests)—however, if we separate the result from the pressure signature, we must agree that this signature warrants consideration. In summary, we will consider the analysis of the "includes rate history" case as the preferred analysis/interpretation. Given the strength of the theory and the general conclusion that an "uncorrected" signal yields a less viable interpretation, the analysis derived from the "includes rate history" case should be given preference.

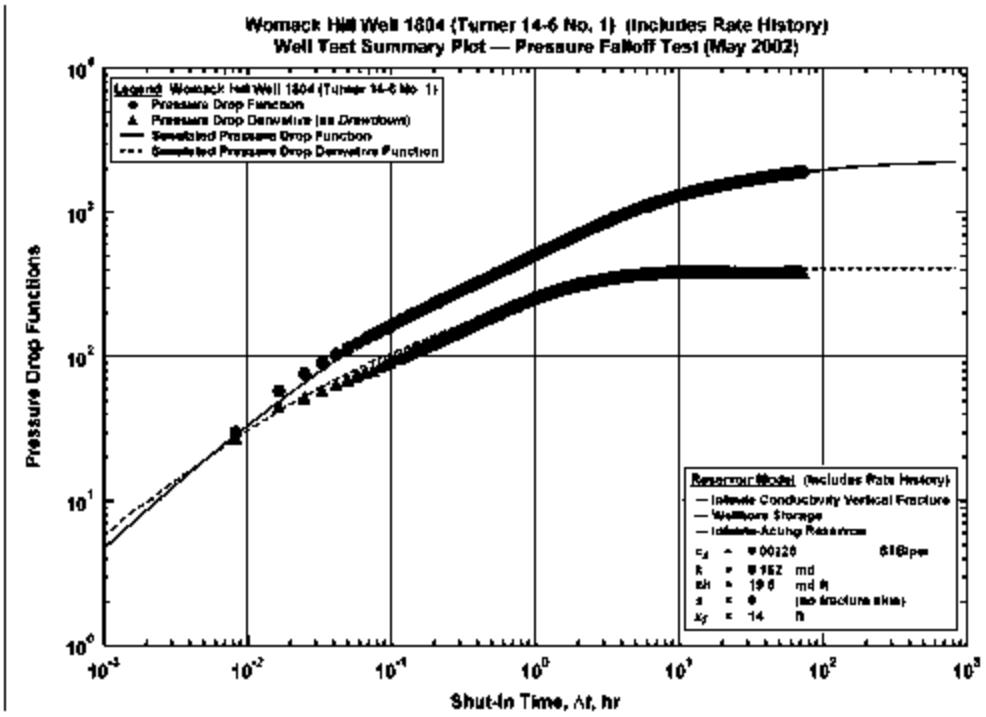

Figure 82d. Summary Plot (Includes Rate History) for Well WH 1804 — Womack Hill Field (testing sequence of May 2002).

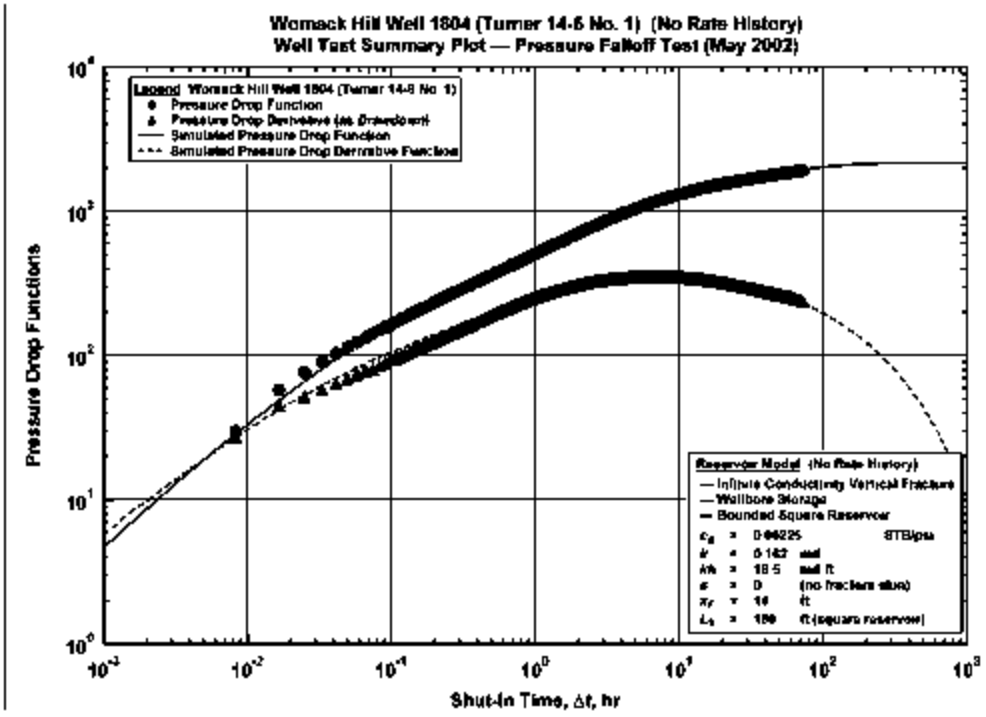

Figure 82e. Summary Plot (No Rate History) for Well WH 1804 — Womack Hill Field (testing sequence of May 2002).

Well 4575-B. Well Permit #4575-B is a replacement well which was drilled and put on production in mid-1985 (Fig. 83a) and is currently producing from the Unit area. We note that this well is also a prolific producer with a sustained production on the order of 500 STBO/D for about the first 10 years of production. From the field map, we note that well Permit #4575-B is located very near the fault that defines the southern limit of Womack Hill Field. We also note that well Permit #4575-B began (abruptly) producing water in 1995 and the water production rate has recently exceeded the oil production rate. We note that the watercut profile (Fig. 83b) is well-behaved, though rapidly increasing.

This behavior suggests that water influx in well Permit #4575-B may be tied to a geologic mechanism—in particular, it appears from well records that well Permit #4575-B is completed in the lowest part of the Upper Smackover sequence (even below the established lower limit of "Zone C"). While we can not resolve all of the production character, we can comment that well Permit #4575-B is a prolific producer, and it appears that water encroachment/influx is a major influence. Our intuition is that the water support is more "from the bottom," but this is an intuitive conclusion, based on the perforated interval. As a final comment, it is clear that the oil production in well Permit #4575-B is declining, and that this decline in oil production is roughly coincident with the onset of water production—we advise remedial action such as production logging to assess points of entry for water and oil, and possibly efforts to isolate zones of high water production.

In reviewing the well test data sequence for this case, we can make a summary comment that the data quality is excellent and that the execution of the test sequence, though marked by an operational issue that required a second drawdown/buildup event, also appears well-coordinated. From the "strip chart" (Fig. 83c) for well Permit #4575-B, we find (as noted above) that two

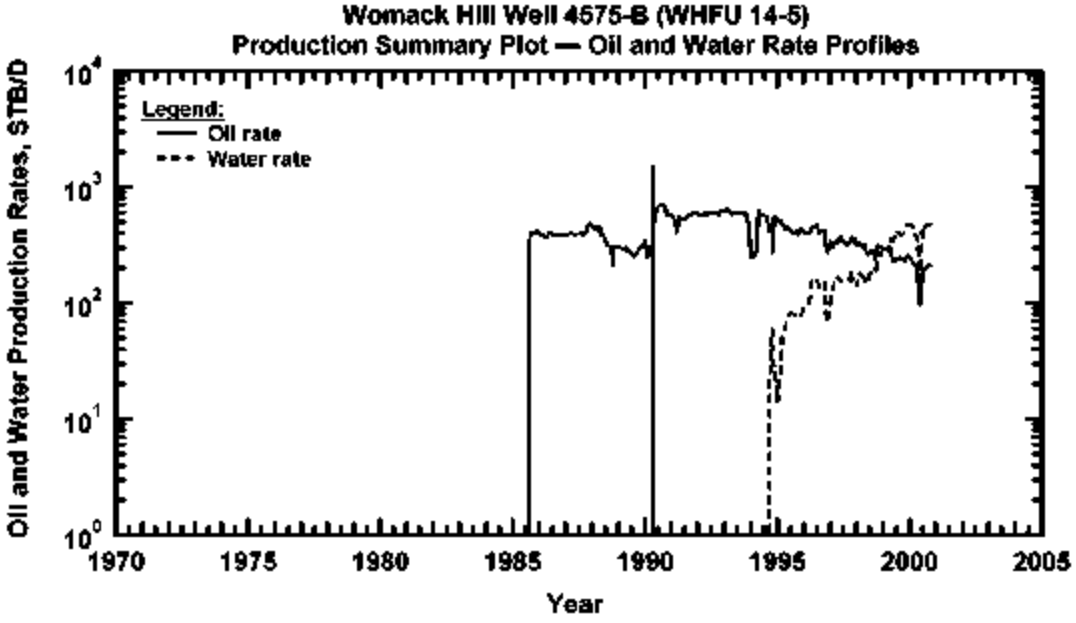

Figure 83a. Production History for Well WH 4575-B — Womack Hill Field.

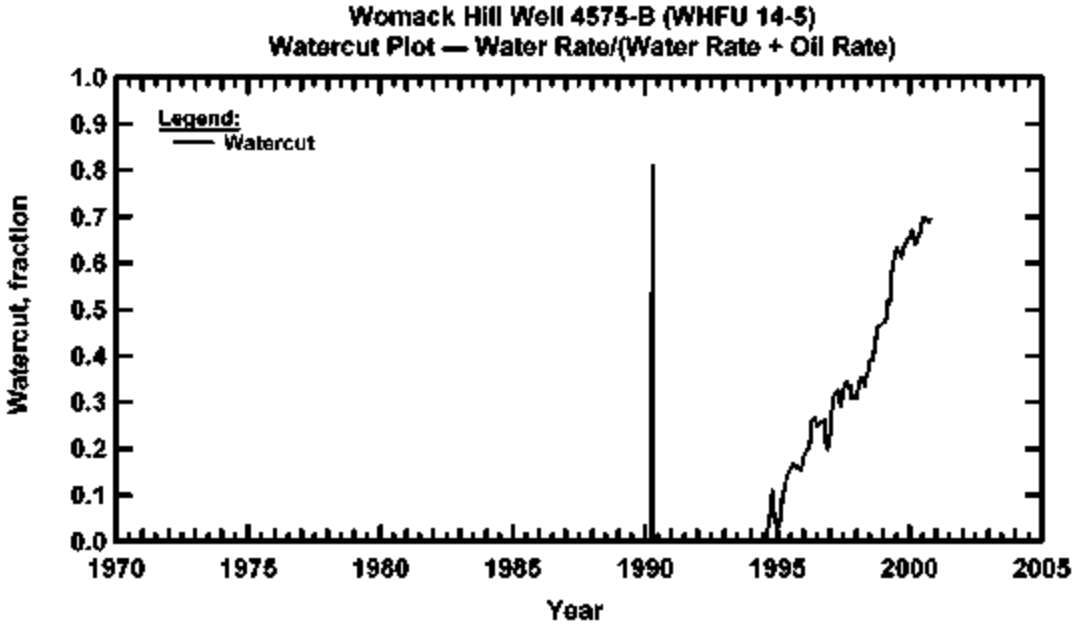

Figure 83b. Watercut for Well WH 4575-B — Womack Hill Field.

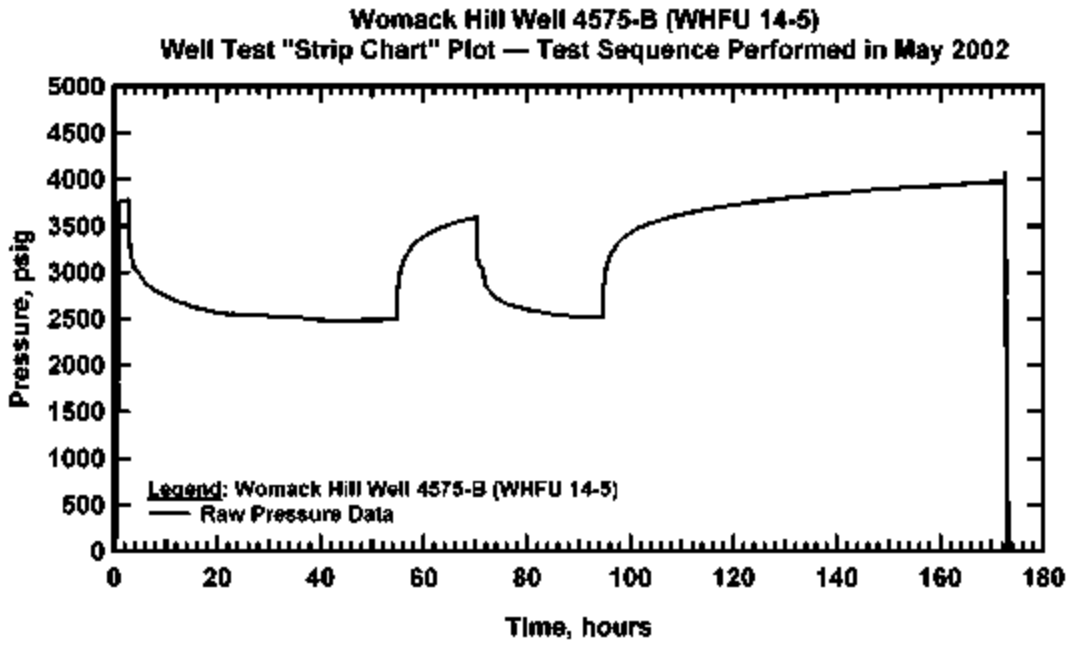

Figure 83c. "Strip Chart" Data Summary Plot (No Analysis) for Well WH 4575-B — Womack Hill Field (testing sequence of May 2002).

separate pressure drawdown/buildup sequences are conducted (again, due to an operational issue). Although both pressure drawdown events appear competent, we focused our activities on the analysis and interpretation of the pressure buildup events—in particular, the second (longer duration) pressure buildup event. We validated that both buildup events are representative—we note a textbook case of a well test sequence with two pressure drawdown/buildup events, in particular, the pressure buildup data for both events overlay exactly (Fig. 83d).

As with our previous work in the analysis and interpretation of the well test data, we again consider the cases of "includes rate history" (Fig. 83e) and "no rate history (Fig. 83f)." These two cases illustrate essentially identical "early time" behavior (as we would expect)—again, we find the behavior of a stimulated well where we have used the model of a fractured well to best represent this behavior (arguably this could also be represented by a large negative skin factor and the radial flow model). We then find that both cases exhibit a radial flow signature in the pressure derivative function during "middle times" (*i.e.*, the horizontal pressure derivative behavior). This flow regime is used to derive the estimate of effective permeability and is one of the most distinctive characteristic behaviors illustrated by the pressure derivative function.

From the "includes rate history" case, we find that the "late time" behavior of the pressure derivative function suggests two parallel, sealing faults. From the "no rate history" case, we find that a "fault signature" exists, but in this case the scenario is that of a single fault (as opposed to two faults). We could debate the merits of including or not including the rate history—and again, we would arrive at the practical issue of whether or not we believe that the rate profile is representative. In contrast to that path, we will simply conclude that the well test data for this case clearly indicate one or more flow obstructions near the well. Given the proximity of well

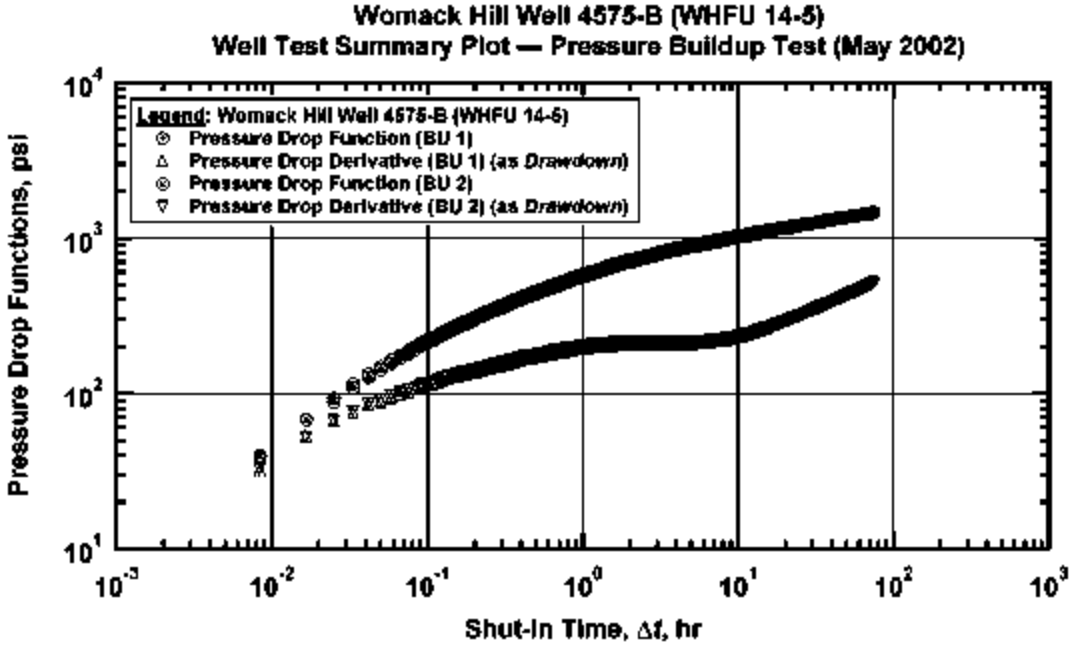

Figure 83d. Well Test Summary Plot (*Both Pressure Buildup Sequences*) for Well WH 4575-B (*Drawdown* Pressure Derivative Functions) — Womack Hill Field (testing sequence of May 2002).

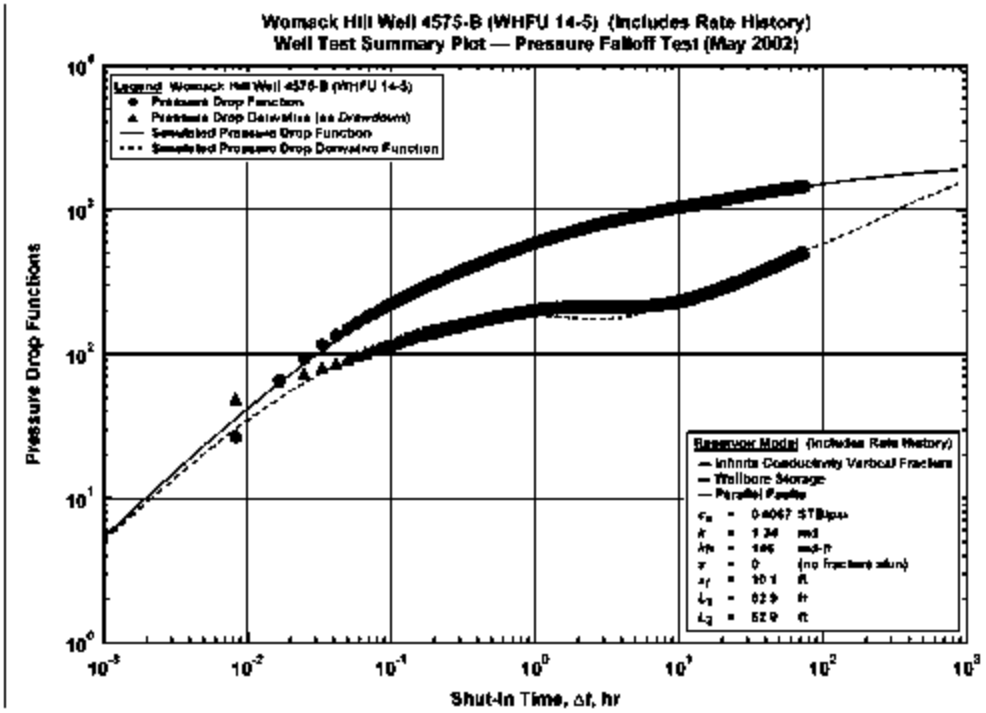

Figure 83e. Summary Plot (Includes Rate History) for Well WH 4575-B (*Second* Pressure Buildup Test Only) — Womack Hill Field (testing sequence of May 2002).

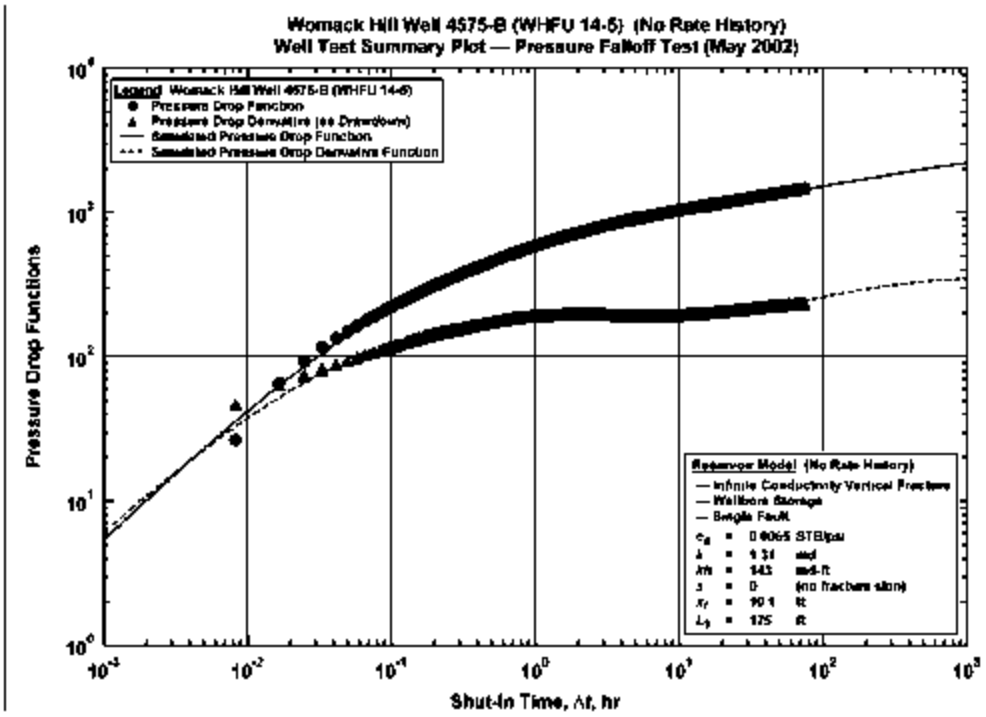

Figure 83f. Summary Plot (No Rate History) for Well WH 4575-B (*Second* Pres-sure Buildup Test Only) — Womack Hill Field (testing sequence of May 2002).

Permit #4575-B to the major fault at the southern boundary of the field, we can simply conclude that this is conclusive evidence of that feature.

Summary of Well Test Results. The results are presented in Table 5 and in Figures 84 and 85.

In Figure 84 we present a crossplot of permeability calculated from production and well test data versus the harmonic average of the permeability from core analysis. Granted these data are of different types (the core data are "air permeability" values which are generally higher than the "absolute" permeability, and the permeabilities derived from production and well test data are "effective" permeabilities (generally to oil)) however, the comparison on a log-log scale suggests that it is simply a matter of a "shift" from one type to another. We obtained a relation that suggests that the *in-situ*, effective permeabilities are on the order of 1/80 of the "air" permeabilities derived from the core data.

Similarly, in Figure 85, we compare the effective permeabilities derived from the production data with the effective permeabilities derived from the well test data. There is a considerable spread of the data, particularly for the case of well Permit #1678 where we compare oil permeability from production data to water permeability from a pressure falloff test sequence. We have placed a trend line arbitrarily through the middle of these data, where this trend suggests that the oil permeability from production data analysis will be on the order of one-half of the oil permeability obtained from well test analysis. Obviously this comparison is an oversimplification given the complexity of the data and the small number of well test cases. Regardless, this work confirms the utilization of production data to estimate reservoir properties, and we also recognize the value of pressure transient testing to assess pressure levels in the reservoir, as well as to distinguish reservoir behavior (boundaries, faults, etc).

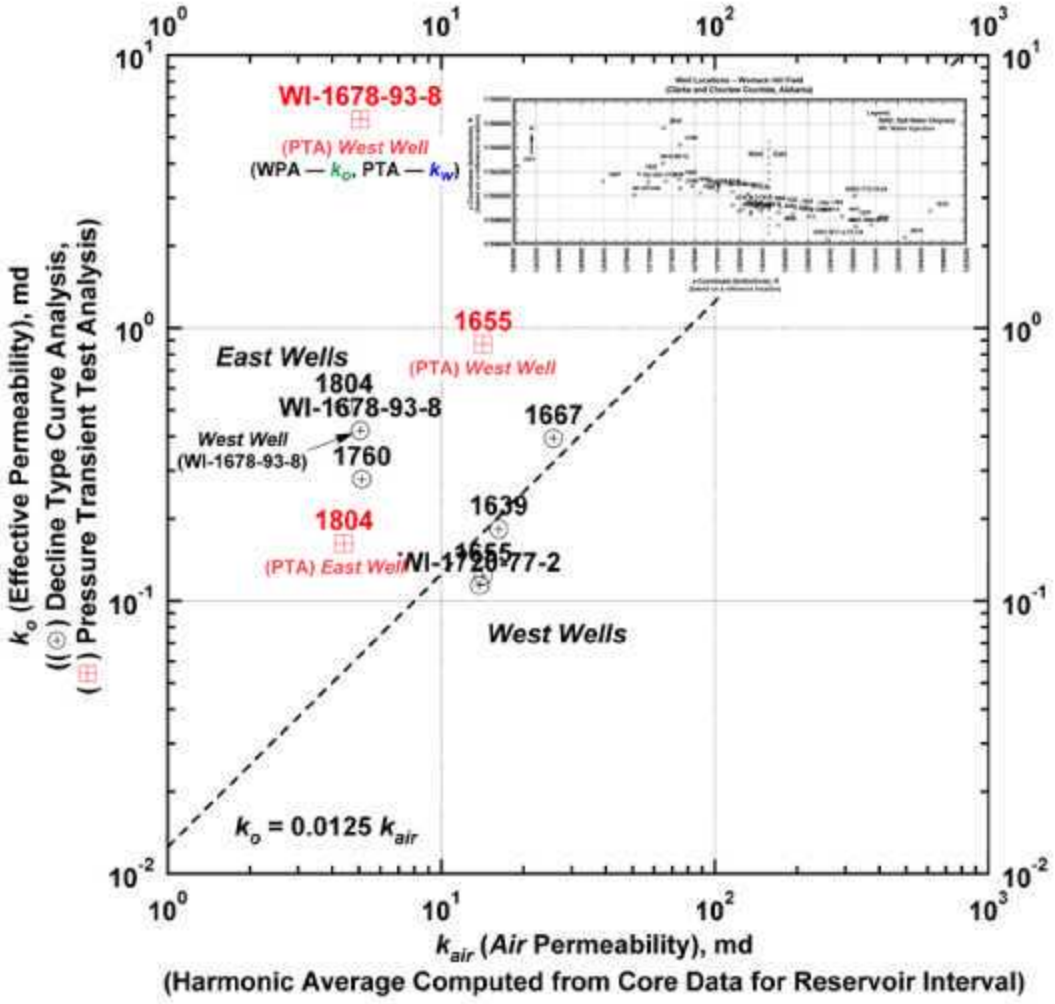

Figure 84. Data Integration Plot for Production, Well Test, and Petrophysical Analysis Results — Womack Hill Field.

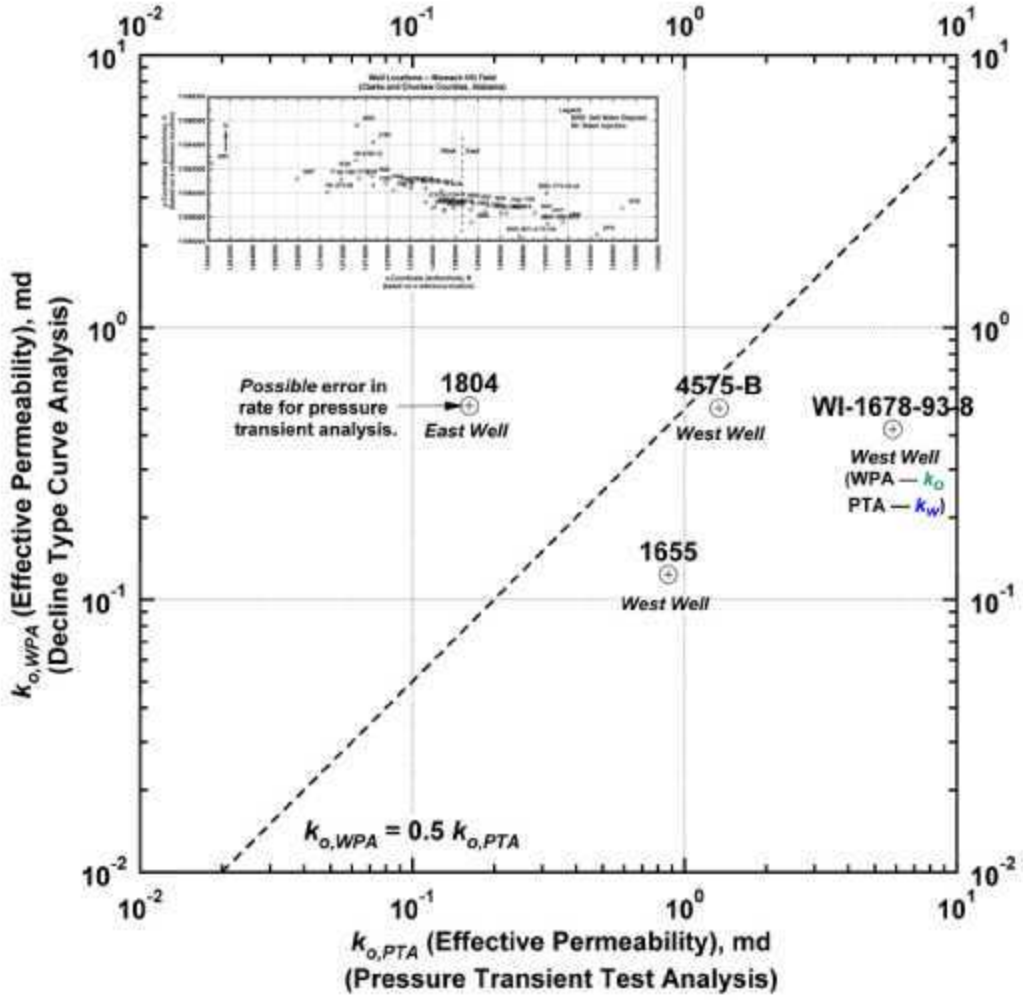

Figure 85. Data Integration Plot for Production and Well Test Analysis Results — Womack Hill Field.

Table 5. Results summary for well test analysis—Womack Hill Field (testing sequence of May 2002).

Well	Rate history	Well/ reservoir model	k_o (or k_w) (md)	k_oh (or k_wh) (md-ft)	s or x_f (dim-less or ft)	Distance to boundary (ft)
1655	No	ICVF-CWBS	0.873	147	7.89 (ft)	310 (r_e (circle))
1678	Yes	RadFlw-WBS-Skin	5.83	1150	-0.031	L_1=120, L_2=105
1678	No	RadFlw-WBS-Skin	5.83	1150	-0.031	L_1=L_2=195
1804	Yes	ICVF-CWBS	0.162	19.5	14.0 (ft)	(infinite-acting)
1804	No	ICVF-CWBS	0.162	19.5	14.0 (ft)	L_1=180
4575-B	Yes	ICVF-CWBS	1.34	146	10.1 (ft)	L_1=L_2=69.2
4575-B	No	ICVF-CWBS	1.31	143	10.1 (ft)	L_1=175

Analysis of Reservoir Performance—General.--Figure 70 presents the historical behavior of the oil, gas, and water production rates at Womack Hill Field since production began in December 1970. Oil and gas production peaked in 1977 at 6,200 STB/D and 3,200 MSCF/D of oil and gas, respectively. Since then, oil and gas flow rates have steadily declined, while the water rate has consistently increased. This production decline has reduced the profitability of the field—which leads to the current program of production optimization and field management strategies to improve the performance and overall recovery. Currently there are 3 injection wells (in the Smackover) which are active, although there are also some injection wells which are also used periodically. The producing gas-to-oil ratio (GOR) has remained relatively constant (approximately 500 scf/STB) indicating that the reservoir pressure remains above the bubblepoint pressure (approximately 1925 psia).

Figure 73 presents the field-wide cumulative production for oil, gas, and water. The oil and gas curves are nearing their respective "plateaus" and should not be expected to change their behavior without substantial intervention (i.e., infill drilling, well stimulation, improved artificial lift, etc.). We also note from Figure 73 that the cumulative water production curve is still increasing at a substantial rate although it does appear to be trending towards a plateau (probably

in the range of 55-60 MMSTB of water). To date, the total oil production is 31.1 MMSTB, along with 50.3 MMSTB of water and 15.4 BSCF of gas. The field is divided into two areas—the eastern and western areas, based presumably on geological information. In Figure 86, we present the production profiles for the eastern area, and in Figure 87 the hydrocarbon production for the western unitized area is presented.

In Figure 88, we present a curve of the logarithm of the fractional flow of water (f_w) versus cumulative oil production (N_p)—these plots are widely used for evaluation and prediction of reservoir performance—in particular, to estimate total recovery at 100 percent water production. The technique only applies at later times and presumes a log-linear relationship of WOR (or fw) and oil recovery, which allows us to extrapolate the presumed straight-line trend to any desired water cut in order to determine the corresponding oil recovery. In our case, this extrapolation yields an oil recovery of approximately 34.5 MMSTB, which is consistent with the result obtained by the hyperbolic extrapolation of the cumulative oil curve (34.6 MMSTB).

Another way to estimate remaining reserves is using "estimated ultimate recovery" (or *EUR*) analysis on the production performance for each well. *EUR* analysis is a semi-empirical technique that consists of extrapolating the production rate (q_o) versus cumulative production (N_p) curve to q_o=0. The corresponding value of N_p at q_o=0 represents the "recoverable" oil ($N_{p,max}$). In Figure 89, we illustrate this process for well Permit #1591. For the wells at Womack Hill Field, the recoverable oil estimate is often close to current cumulative production because of the lateness in the productive life of an individual well (as well as the field). We performed this analysis on all of the producing wells in the field as a mechanism to estimate the remaining field-wide recoverable oil at current conditions.

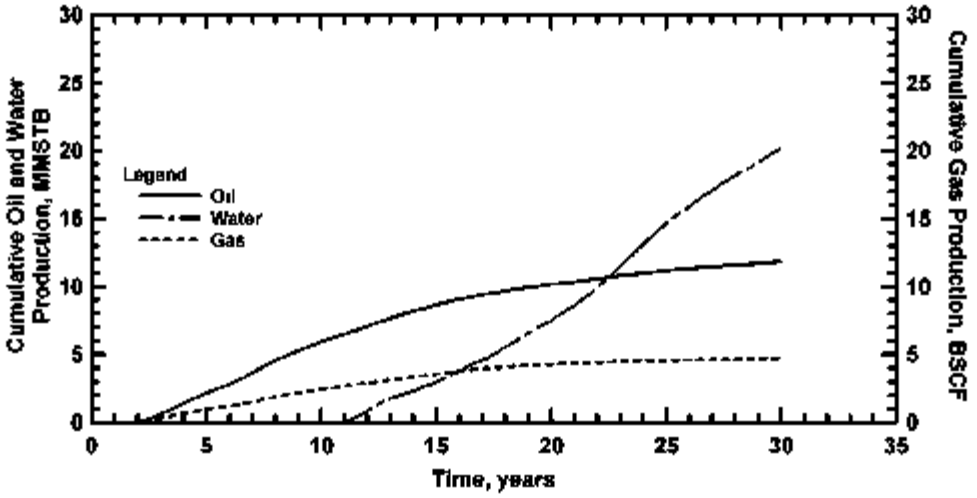

Figure 86 Cumulative Production in Eastern Area — Womack Hill This area produces 38 7 percent of total oil production

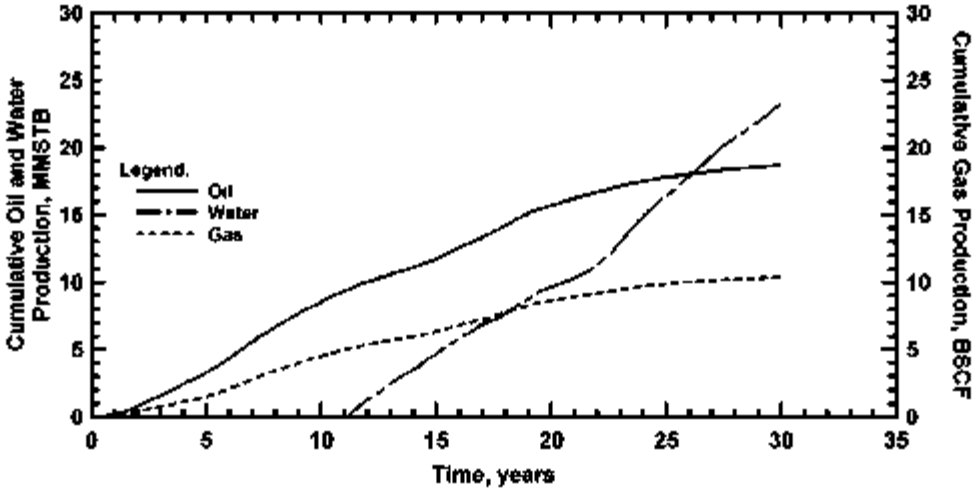

Figure 87 Cumulative Production in Western Area — Womack Hill This area produces 61 3 percent of total oil production

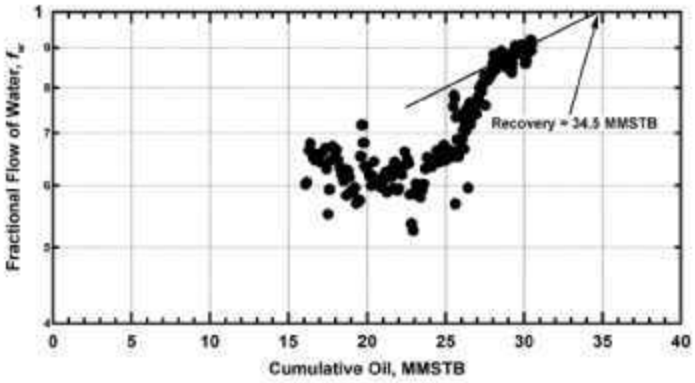

Figure 88. Logarithm of the fractional flow of water versus cumulative oil production. The straight-line extrapolation at f_w=1 yields an oil recovery of 34.5 MMSTB.

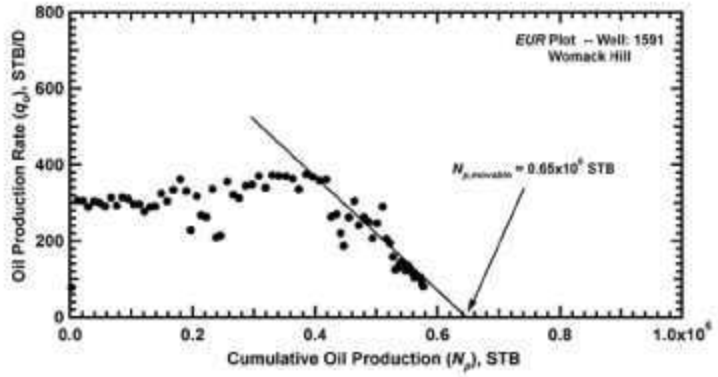

Figure 89. *EUR* plot for Well 1591 — Womack Hill Field. Cumulative production is approaching total recoverable oil.

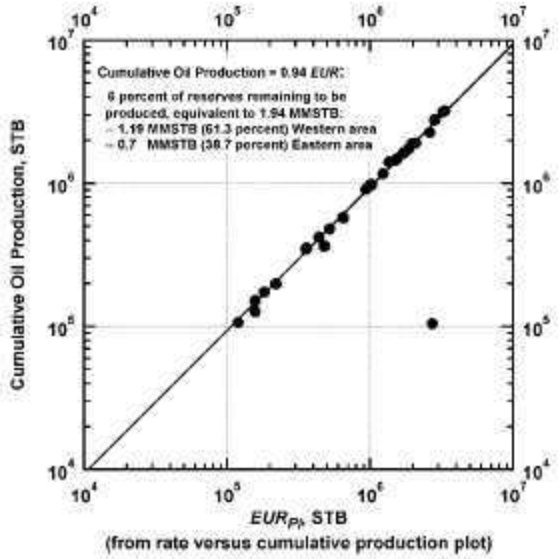

Figure 90. Summary of *EUR* Analysis — Womack Hill Field. Strong correlation — likely a consequence maturity of production.

In Figure 90, we summarize the *EUR* analysis results by plotting the cumulative oil production (N_p) for each well against its corresponding *EUR*. As expected, a strong correlation of N_p with *EUR* emerges because of the mature status of the field. The slope of this curve represents the percentage of oil produced with respect to the total recoverable oil. As a field-wide average, we estimate that about 90 percent of the total oil at current conditions has been recovered—which means that about 10 percent of recoverable oil remains to be produced.

Analysis of Reservoir Performance—Field-Scale Flow Behavior.--Early in the productive life of Womack Hill Field a concept emerged that the field had two compartments (or areas)—one in the west and one in the east. For field management purposes, and based on the belief that a geological division exists in the field, Womack Hill Field has been developed and managed in two independent areas. It appears, however, that some pressure support is benefiting wells in the eastern area, while all of the injection wells are in the western unitized area.

A "flow barrier" in the Womack Hill Field area was identified early in the development of the field and was used as demarcation to separate the western Unit area from the eastern area. It is important to note that all of the water injection wells are located in the western Unit area, so the water injection influence should not affect the eastern area if a "barrier" exists. Figure 71 shows that the water injection rate has always exceeded the oil production rate—the cumulative water injected has reached 42 MMSTB, which is 11.5 MMSTB higher than the oil withdrawal. So, the amount of injected water appears to be more than sufficient to maintain the reservoir pressure. Figures 91 and 92 present the limited pressure data available for the western Unit and eastern areas, respectively. Figure 91 illustrates clearly the pressure increase (or maintenance) in the western Unit wells due to the water injection. However, the pressure maintenance has not been as effective in the eastern area (Fig. 92), where the pressure in most of the wells has

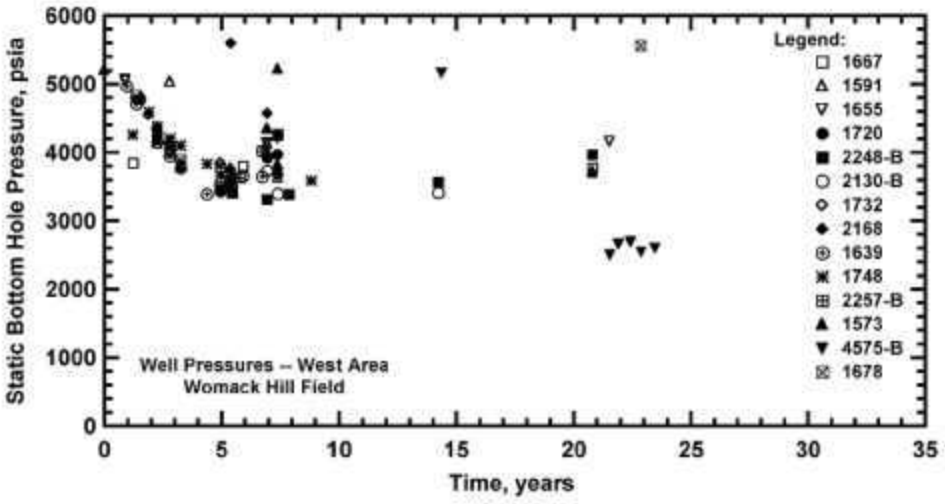

Figure 91. Well pressures in Western Area — Womack Hill Field. The effect of water injection is clearly shown from year 5.

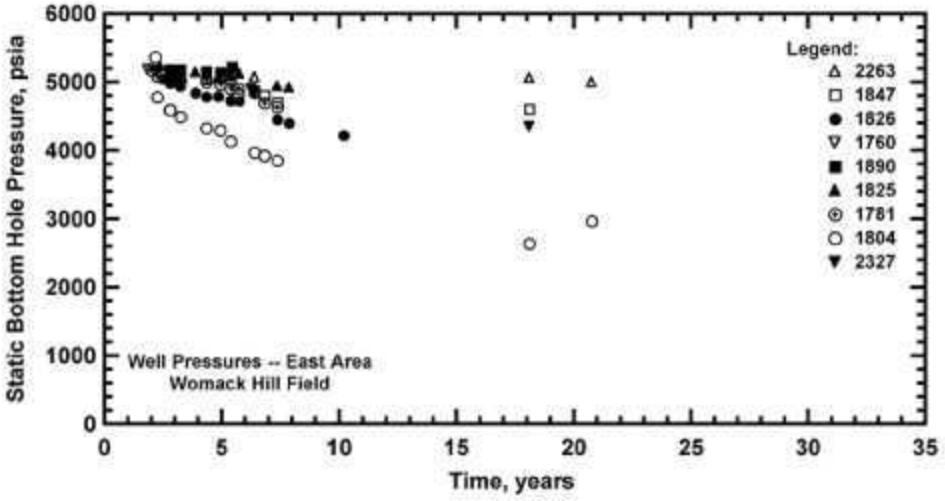

Figure 92. Well pressures in Eastern Area — Womack Hill Field. Despite water injection, well pressures for some wells are declining "normally," while other wells appear to be receiving pressure support.

declined (although there are exceptions). This pressure data suggest that a geological separation could exist between the two areas—but it does not serve to confirm this concept. As noted, some of the wells in the eastern area have experienced pressure maintenance—which suggests that the "barrier" is not completely sealing and that some flow paths may communicate to both areas.

Figure 93 presents the historical field-wide oil production and water injection rates. We first note that from the beginning of the water injection program up to about year 20 (1990), the reservoir performance was approximately a 1:1 ratio (the volume of injected water per volume produced oil). Since then the injected water has increased steadily and the oil production has declined. This sharp change almost certainly cannot be attributed to a reservoir mechanism—it is far more likely to be a consequence of operational practices. In fact, in 1990 the operator first installed hydraulic "jet pumps" in the production wells in order to improve the productivity—but as revealed in Figure 91, this installation has not been as effective as desired.

We also consider the phenomenon of "overproduction" of water where the ratio of water production rate to water injection rate ratio versus time is presented in Figure 94. This profile shows a ratio over unity—so the volume of produced water is higher than the volume of injected water. Water coning, water channeling, and/or strong water influx can cause this phenomenon. Empirical evidence from a site visit to Womack Hill Field suggests the possibility of water channeling and water influx.

Analysis of Reservoir Performance—Decline Type Curve Analysis.--To analyze and interpret the well production profiles for each well we used the decline type curve technique (Fetkovich, 1980; Doublet *et al.*, 1994; Doublet and Blasingame, 1996). The application of this methodology is based in theory, but in practice we must often apply the technique without

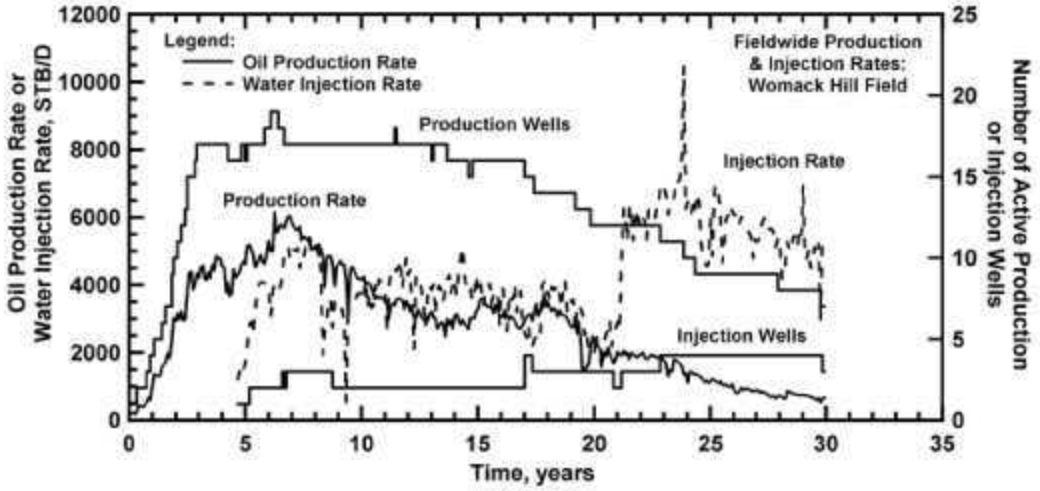

Figure 93. Water injection and oil production rate profiles — Womack Hill Field. Water injection appears to be less efficient over the last 10 years.

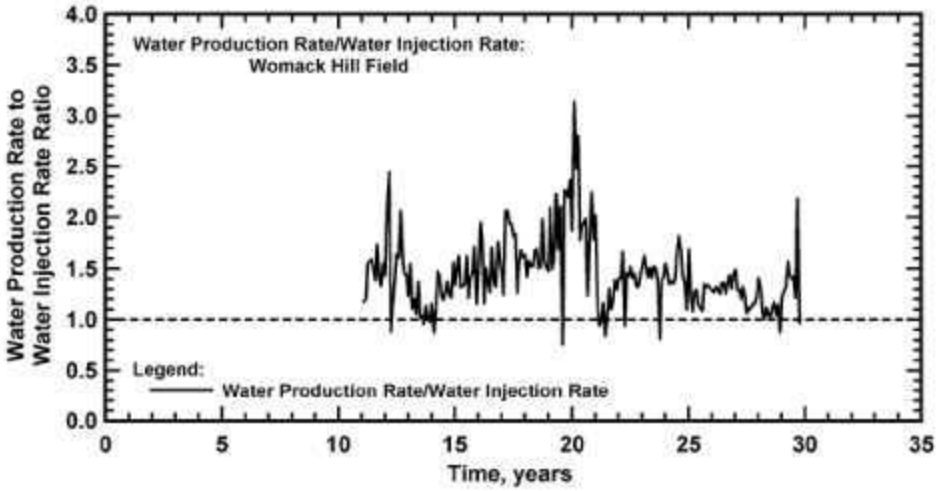

Figure 94. Water production rate to water injection rate ratio — Womack Hill Field. The higher volume of produced water is likely due to water coning or a strong water influx.

certain data — typically wellbore pressure data are not available. This is a limitation, and it is the case for our analysis of the production performance at Womack Hill Field.

For this work we have specifically used the Fetkovich-McCray family of decline type curves (Doublet, *et al.*, 1994) where these type curves are formulated based on pseudosteady-state (or boundary-dominated) flow behavior. We use pressure-drop normalized rate functions as well as a "material balance time" formulation to eliminate the constant p_{wf} constraint associated with the original Fetkovich method. In addition, by adding the rate integral and the rate integral-derivative functions to this analysis technique, we are able to achieve much more consistent (*i.e.*, unique) type curve matches and we generally obtain better matches of transient data for the estimation of formation flow properties.

The software *WPA* (Blasingame, *et al.*, 1998) provides us a mechanism to apply this technique. The input data required for the *WPA* program consists of a table containing the following production data functions:

Time, t (days)	Flowing bottomhole pressure, p_{wf} (psia)	Flow rate, q (STB/D)
XXX	XXX	XXX
XXX	XXX	XXX
XXX	XXX	XXX
XXX	XXX	XXX

In addition to production data, we also require reservoir and fluid properties, as well as an estimate of the initial reservoir pressure. Once the analysis process is completed in the *WPA* software, we are able to obtain estimates of the following parameters:

Flow terms:	Volumetric results:
•Effective permeability, k_e, md	•Reservoir radius, r_e, ft
•Skin factor for near-well damage/stimulation, s	•Drainage area, A, acres
•Fracture-half length, x_f	•Nc_t product, STB/psi

Figure 95 illustrates the type curve match we obtained for well Permit #1847. As shown, the $q/\Delta p$, the "integral" of $q/\Delta p$, and the "integral-derivative" of $q/\Delta p$ are matched against the corresponding type curves. We note that most of the data lie in the "boundary-dominated flow region"—which is logical since the "transient flow region" contains few (if any) representative data (due to the proration of the field). Further, a lack of wellbore pressure data amplifies the problems encountered with the transient flow region—we simply have to provide a "best guess" analysis in this region, which really implies that the "flow property" results are qualitative at best.

As noted, we can only use the transient "flow property" results qualitatively, but we can utilize the "volumetric" results in a somewhat more quantitative fashion because for each well analyzed we clearly observe the late-time "harmonic" trend—which confirms the material balance correctness of this technique. Unfortunately, the parameters estimated using the "late time" data are tied to the value of total compressibility (c_t) specified for the analysis—this is not a value for which we have substantial confidence. Having prescribed a value for c_t we can calculate the oil-in-place (N) and the reservoir drainage area (A). In this particular case we believe that it may be more valuable to report the Nc_t-product because our estimate of c_t yields estimates of N and A which are clearly unrealistic. Our intention is to obtain a "tuned" value of c_t and calibrate our analysis.

Therefore, for this case, we will use the Nc_t product as a surrogate variable to represent the distribution of oil in the reservoir. Figure 96 presents a crossplot EUR_{PI} versus Nc_t for all of

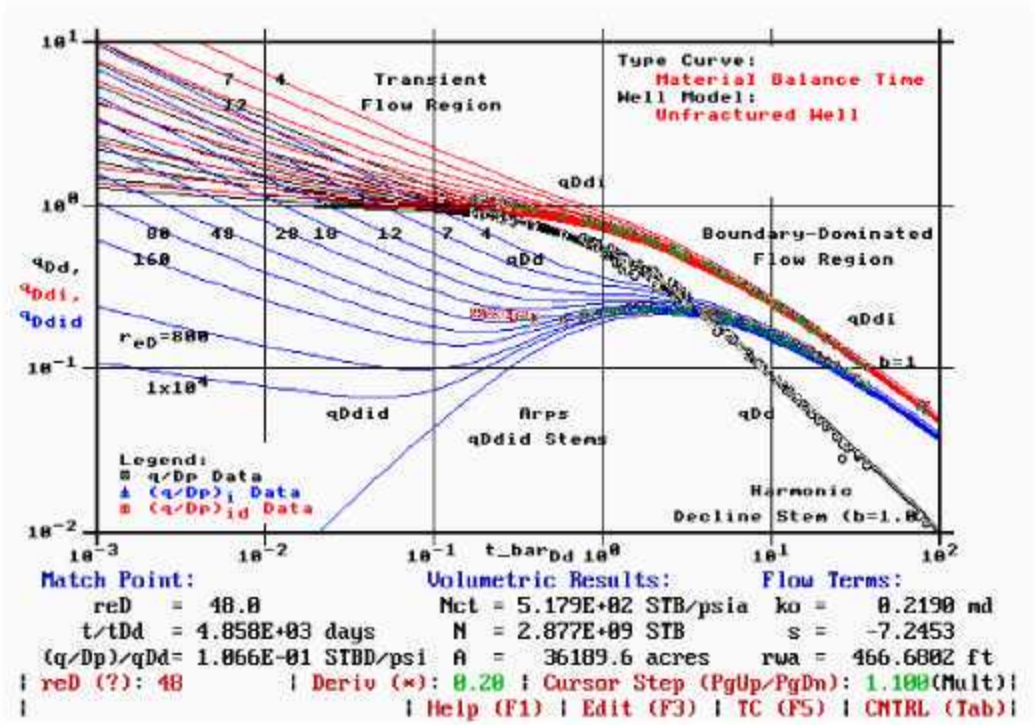

Figure 95. Decline type curve analysis — match plot, Womack Hill Field Well 1847. Most of the data lie in the boundary-dominated flow region 1848. The transient flow regime is less well-defined.

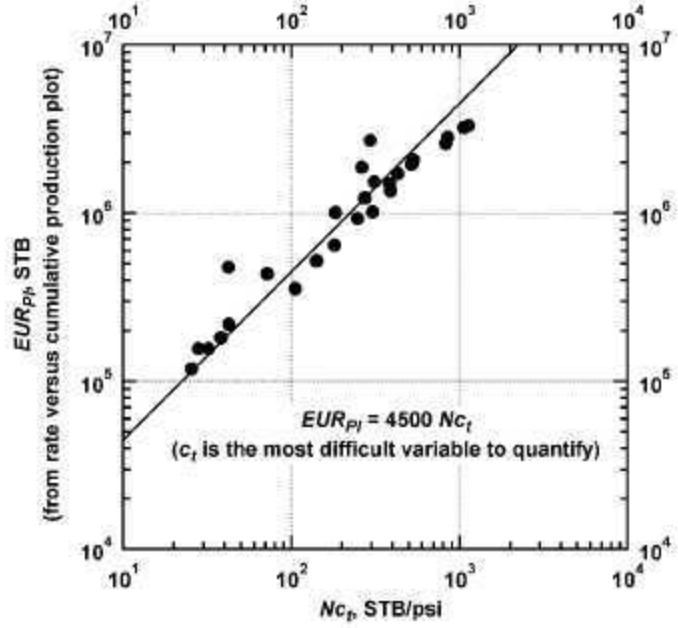

Figure 96. EUR_{PI} versus. Nc_t — Womack Hill Field. EUR_{PI} and. Nc_t are estimated using independent mechanisms — however, these variables are clearly correlated.

wells that were analyzed. As shown, this plot shows a very strong correlation between EUR_{pf} and Nc_t, even though these results are estimated independently. EUR_{pf} is estimated from the rate versus cumulative production plot and Nc_t from using decline type curve analysis. The observation of this strong relationship is logical, and it suggests that the recovery is proportional to the fluid-in-place (which is logical — but this evidence does confirm this behavior).

In Table 6, we present a summary of the results we obtained using decline type curve analysis for each well. The "flow properties," effective permeability (k_o) and skin factor (s) are only qualitative estimates at best due to the lack of competent data in the transient flow region. The N and A estimated depend on an accurate estimate of c_t, and these values are also suspect since a "tuned" estimate of c_t has not been defined. At this point in our work, the Nc_t-product is our most reliable variable for representing oil-in-place.

Analysis of Reservoir Performance—Material Balance.--As Womack Hill Field is still producing at pressures above the bubblepoint, we elected to attempt a material balance calculation using the production and pressure data. The material balance equation for a slightly compressible liquid in a volumetric reservoir is given by Dake (1977):

$$p_i - \bar{p} = \frac{1}{Nc_t}\frac{B_o}{B_{oi}} N_p \qquad (1)$$

On a plot of $\bar{p}$ versus N_p the extrapolation of the straight-line trend to $\bar{p} = 0$ yields the "recoverable" oil, $N_{p,max}$. Figure 97 presents a material balance plot constructed for Womack Hill Field. This plot yields an estimate of $N_{p,max}$ of 76 MMSTB—which appears to be quite high. The slope of the straight-line trend can be used to estimate the original oil-in-place (N), but once again an accurate estimate of c_t is required. This high estimate of recoverable oil suggests that the reservoir pressure is too high for a volumetric model, and may be receiving external energy

Table 6 Summary results for decline type curve analysis — Womack Hill Field

Well permit	Region	N_p (STB)	Nc_t (STB/psi)	N (STB)	A (acres)	k_o (md)	s
1639	West	977305	183 30	1 02E+07	6688 80	0 1833	-6 401
1655	West	1772155	261 80	1 46E+07	11135 80	0 1235	-7 195
1667	West	1168145	272 80	1 52E+07	12443 70	0 3950	-1 372
1760	East	349215	104 60	5 81E+06	10697 30	0 2792	-6 125
1781	East	1923054	529 90	2 94E+07	48353 80	0 3605	-4 577
1804	East	3217813	1083 00	6 01E+07	80988 80	0 7045	-2 309
1825	East	364831	42 10	2 34E+06	3184 90	0 1854	-5 519
1826	East	981820	304 00	1 69E+07	65494 40	0 2521	-7 542
1847	East	1901848	517 90	2 88E+07	36189 60	0 2190	-7 245
1899	East	152230	32 10	1 78E+06	4096 80	0 0821	-6 695
2109	West	1637015	420 10	2 33E+07	27513 00	0 7026	-5 904
2327	East	421841	71 80	3 99E+06	30376 40	0 6467	-5 954
2341	East	1417137	387 30	2 15E+07	41360 70	0 4650	-7 312
3452	East	481699	141 30	7 85E+06	16665 20	1 2105	-1 518
3657	East	127460	29 10	1 62E+06	8168 80	0 3776	-6 501
1732-B	West	198755	42 40	2 36E+06	2675 70	0 2383	-4 739
2130-B	West	2793767	800 00	4 45E+07	194229 70	0 7249	-10 011
2248-B	West	3177666	1057 00	5 87E+07	41355 40	0 2514	-7 851
2257-B	West	1443996	382 30	2 12E+07	34397 20	0 6226	-7 220
4575-B	West	2280222	829 00	4 61E+07	66367 20	0 5044	-7 549
SWD-1890-83-3	East	106874	26 60	1 48E+06	2221 00	0 0689	-7 775
SWD-2263-85-5	East	352008	104 30	5 79E+06	44128 90	1 2025	-6 834
WI-1573-69	West	105302	294 30	1 64E+07	11621 30	0 1041	-6 677
WI-1591-77-1	West	576835	180 10	1 00E+07	6043 80	0 1648	-3 537
WI-1678-93-8	West	1489082	309 90	1 72E+07	20128 80	0 4208	-4 139
WI-1720-77-2	West	174337	38 10	2 12E+06	1699 30	0 1139	-6 255
WI-1748-92-1	West	909261	247 10	1 37E+07	16818 90	0 3155	-5 658

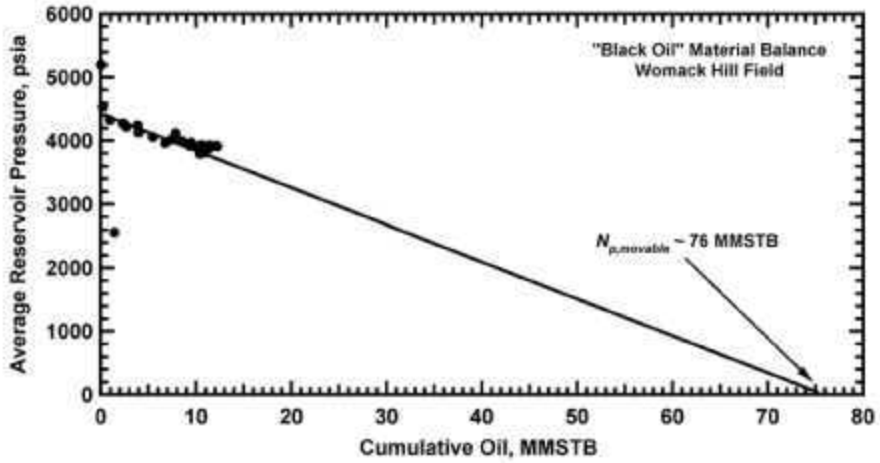

Figure 97. Material balance plot — Womack Hill Field. The straight-line trend produces an estimate of oil-in-place that is presumed to be high due to injection support and possible water influx.

support. The most logical source of this "external" energy would be an aquifer. Again, this exercise was for confirming the external energy than for estimating the oil-in-place.

Integration of Results.--In this section, we present the integration of the results we obtained from the petrophysical and production data analyses. We utilized contour maps in order to establish spatial relationships of reservoir properties and to compare performance-derived parameters with other data such as geological and petrophysical descriptions. Reservoir structure based on the "top of structure" for the upper Smackover shows two highs, one in the eastern area and another in the eastern portion of the western Unit area. Most of the wells are located on these highs, the water injection wells are located on the periphery in the western Unit area of the reservoir. The anhydrite of the Buckner Anhydrite Member provides the reservoir seal, and laterally, the reservoir is bounded on the south by a fault and controlled on the west, east, and north by the water-oil contact.

In Figures 98 through 100, we present the porosity distributions generated using the statistical analysis of data for Flow Units A, B, and C, respectively. The contours show a homogeneous trend in Flow Unit A; however, in Flow Unit C there is insufficient data to produce a meaningful map. We can conclude that a porosity estimate of 18 percent would serve as a reasonable average value for the entire Smackover sequence (Flow Units A, B, and C). Likewise, Figures 101 to 103 present the permeability distributions generated using the statistical analysis on the core data given for Flow Units A, B, and C. Again, the shortage of data in Flow Unit C prohibits us from making any conclusions. However, in Flow Units A and B the contours show a apparent permeability contrast between the eastern and western Unit areas.

Permeability reaches a maximum for the field just on the western Unit high area and its minimum on the south of the eastern high area. The pressure data suggest that a flow barrier may

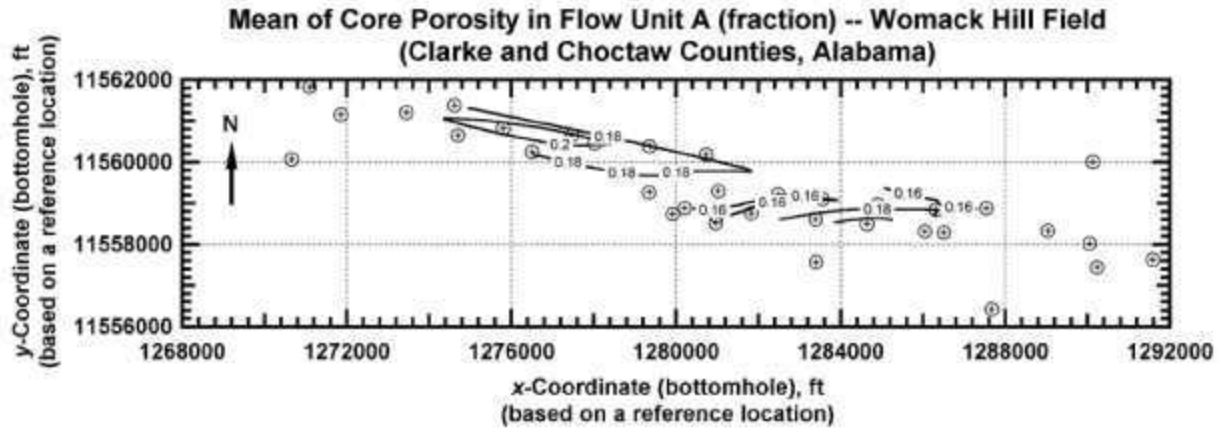

Figure 98. Flow Unit A — Core porosity distribution obtained from statistical analysis (histogram for each well) —the contours tend to indicate a homogeneous reservoir model.

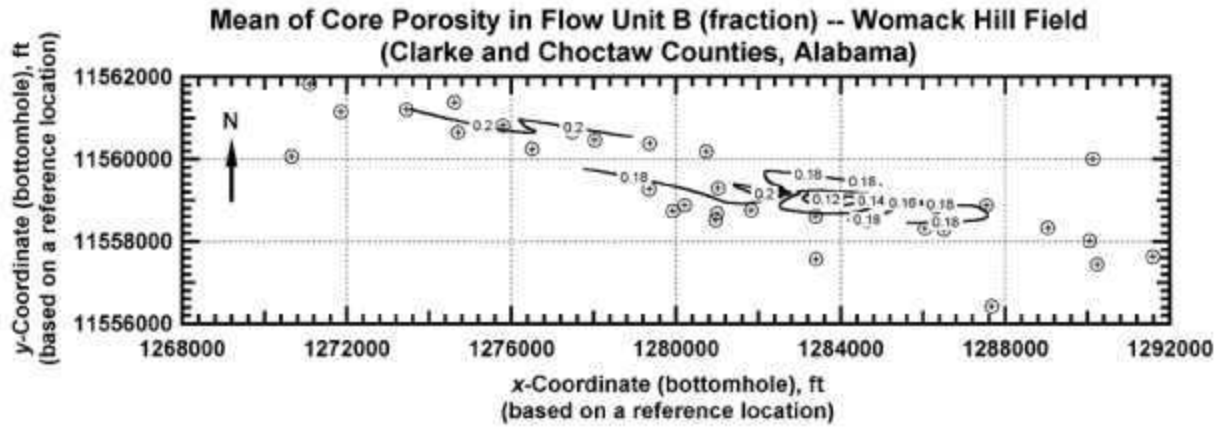

Figure 99. Flow Unit B — Core porosity distribution obtained from statistical analysis (histogram for each well) —the contours tend to indicate a homogeneous reservoir model.

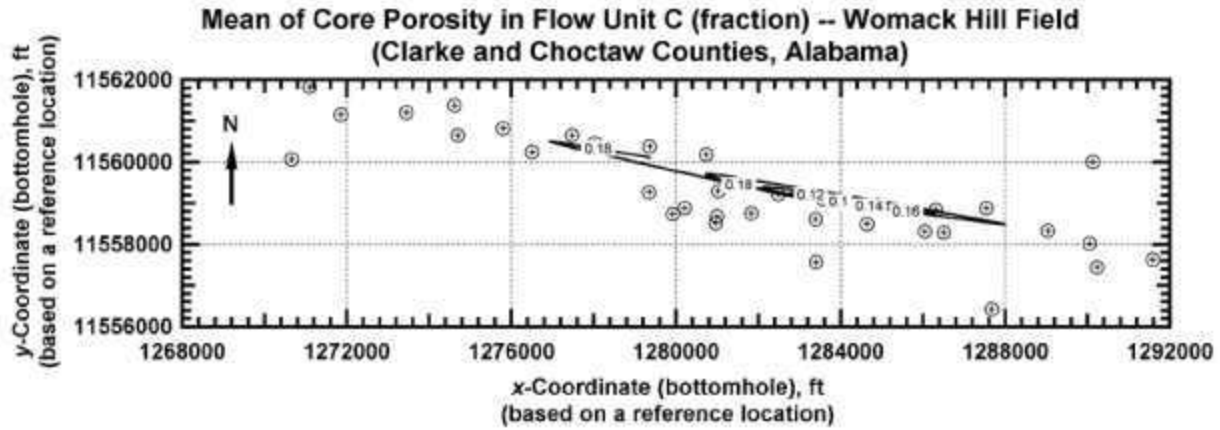

Figure 100. Flow Unit C — Core porosity distribution obtained from statistical analysis (histogram for each well) — insufficient data.

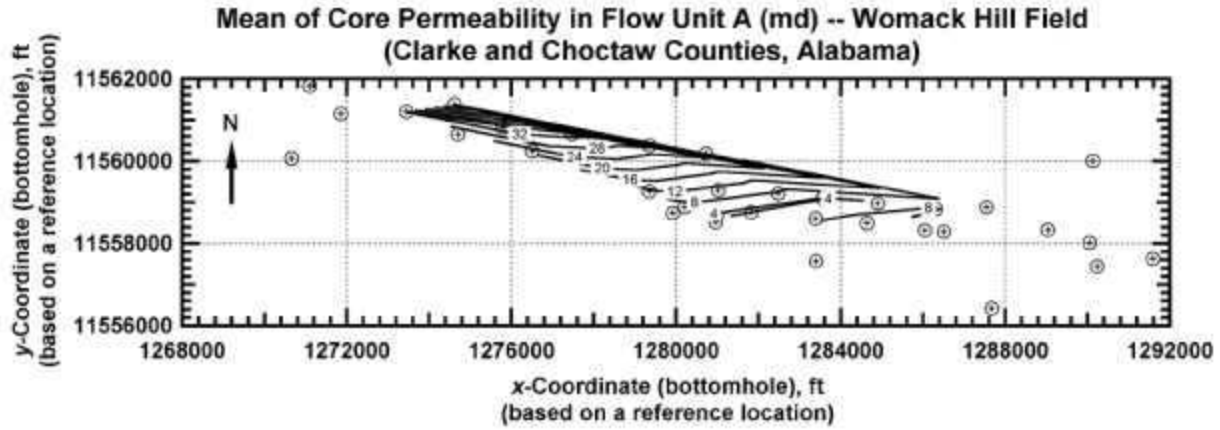

Figure 101. Flow Unit A — Core permeability distribution obtained from statistical analysis (histogram for each well) — a permeability contrast is evident between the Eastern and Western areas.

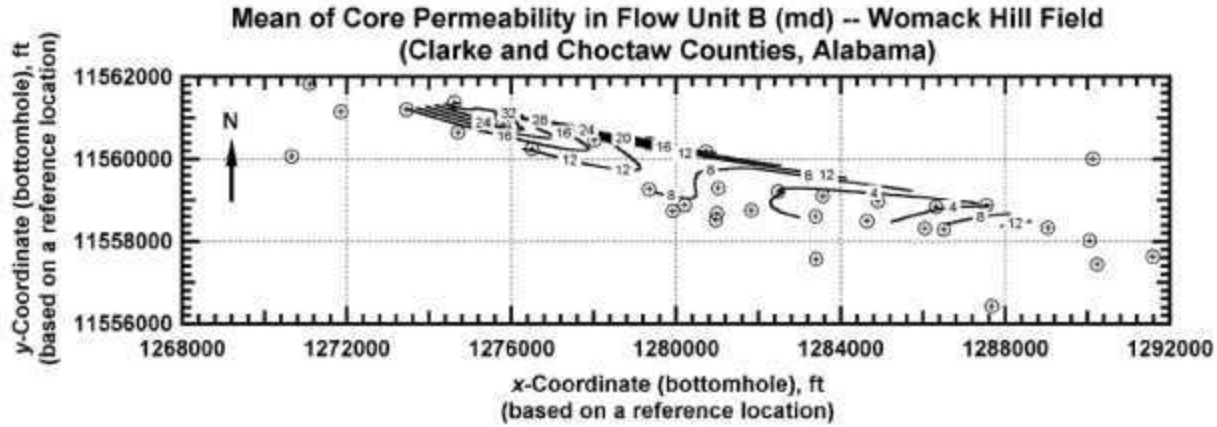

Figure 102. Flow Unit B — Core permeability distribution obtained from statistical analysis (histogram for each well) — a permeability contrast is evident between the Eastern and Western areas.

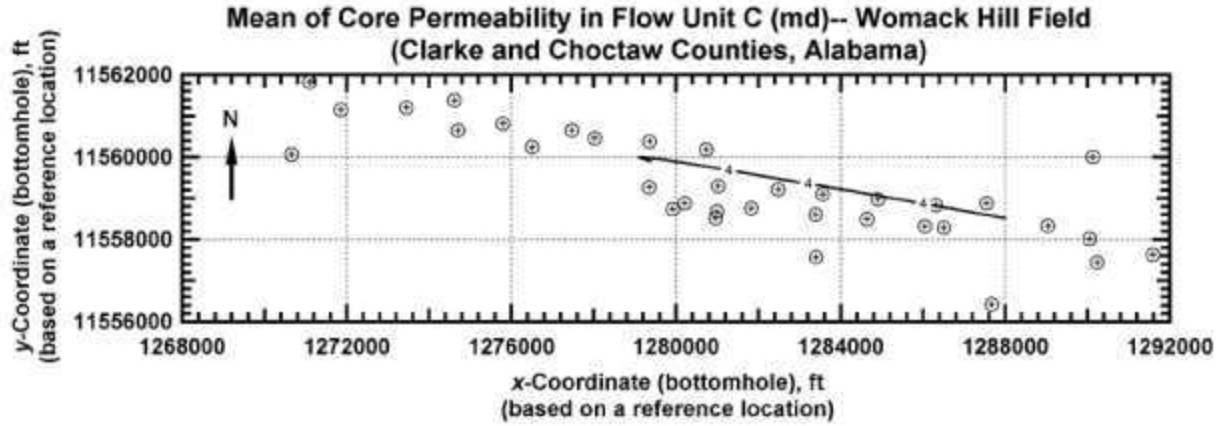

Figure 103. Flow Unit C — Core permeability distribution obtained from statistical analysis (histogram for each well) — insufficient data.

exist between both areas, and the permeability distributions tend to confirm this hypothesis. This permeability contrast has to be considered as the "barrier" between the two areas. Using pressure transient tests (production or injection wells), we can attempt to quantify the existence/influence of this of this barrier. In summary, the "barrier" could simply be a reduction of permeability that was caused by a change in mesoscopic heterogeneity (depositional facies), a change in microscopic heterogeneity (diagenetic changes), or a combination of the two processes.

Figure 104 shows the distribution of the cumulative oil production throughout the field area—this plot shows that the best production is in the western Unit area (where the formation is thicker and permeabilities are higher). In the eastern area the oil production is less, presumably as consequence of the lower reservoir quality. Figure 105 shows the 3-month initial oil rate distribution, this variable behaves consistently throughout most of the reservoir area (probably because of regulatory constraints), and only a few values lie out of the average range (350-450 STB/D)—these values are in the margin of the eastern area, where the gross pay thickness is relatively small.

A map of the *EUR* estimated from the rate versus cumulative production plots is presented in Figure 106; this map revels that the highest recovery is in the vicinity of the eastern high area, reaching a maximum value of 3 MMSTB per well. However, this higher recovery is very localized, and is surrounded by contours of much lower magnitudes. Towards the west, the distribution is more consistent and averages 1.5 MMSTB per well. As we saw earlier, *EUR* and the Nc_t-product correlate quite well—in Figure 107 we can see that the area with higher Nc_t-products generally coincides with the area of higher *EUR*. The distribution reflects the fact that most of the oil-in-place lies in the area associated with the two highs in the field. Outside of this area, the Nc_t-product is significantly lower. Finally, we note in Figures 105 and 107 evidence of

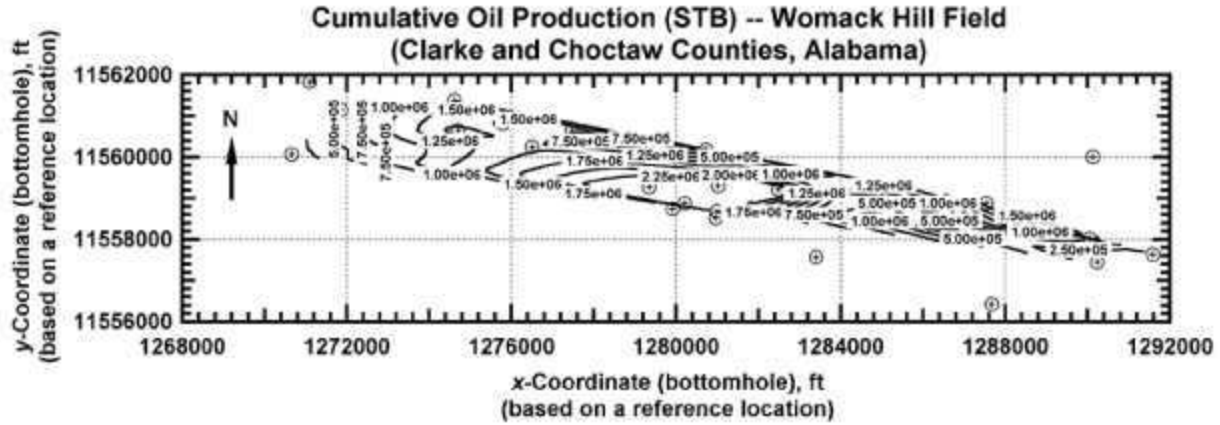

Figure 104. Distribution of cumulative oil production — the best productive area is the Western part of the structure, this area is presumed to have the highest reservoir quality.

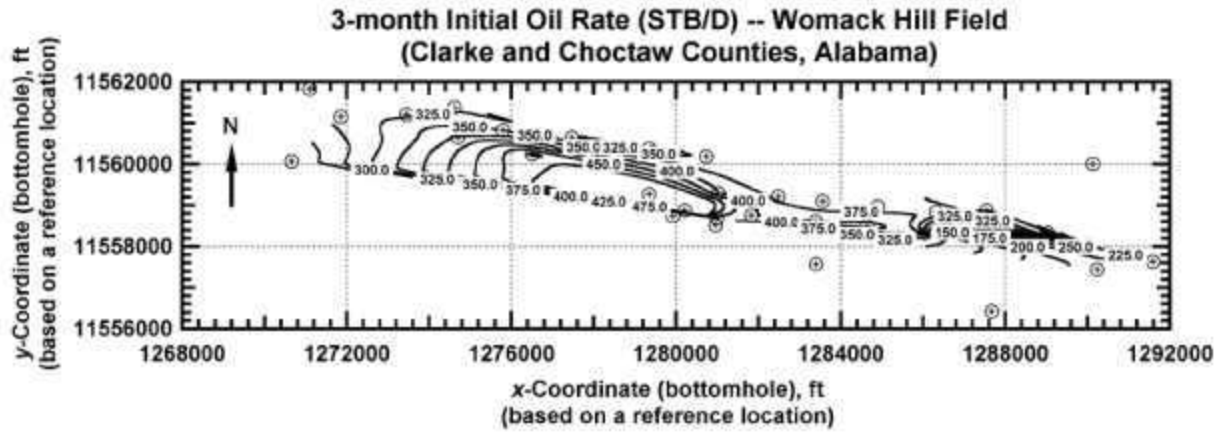

Figure 105. Distribution of the 3-month initial (oil) production (IP) — the trend is consistent throughout most of the field, with the exception of the Eastern edge of the structure.

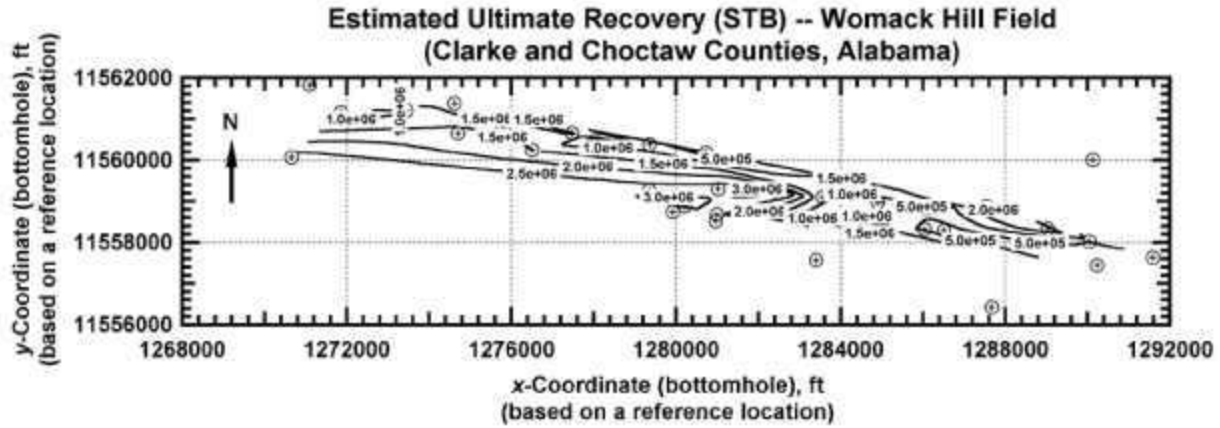

Figure 106. Distribution of estimated ultimate recovery (*EUR*) — note that the zone with the highest *EUR* is around the Eastern ridge of the structure.

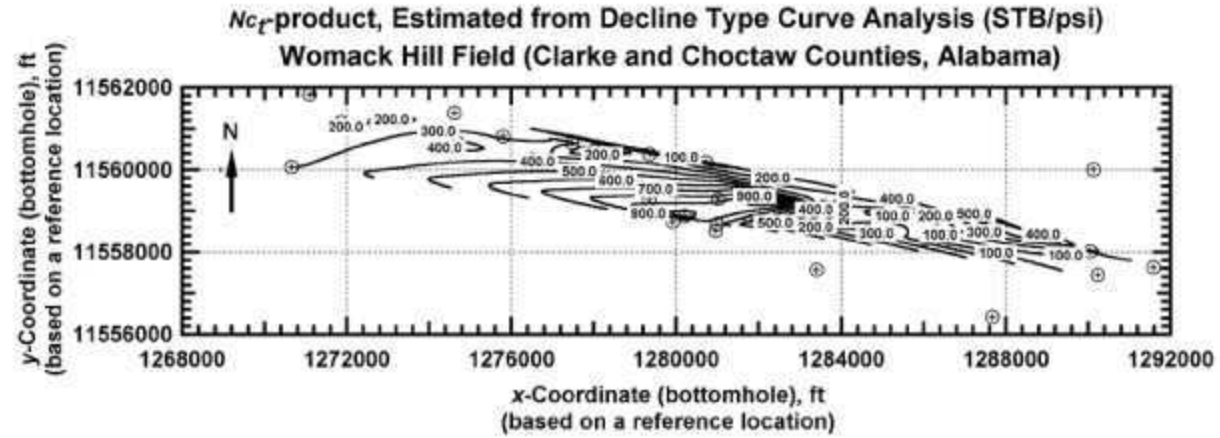

Figure 107. Nc_f-product estimated using decline type curve analysis — Nc_f-product correlates very well with *EUR*.

irregular performance behavior at Womack Hill Field as the zone with higher *EUR* and N_{cp} products is in the area of lower permeability and variable reservoir thickness.

Task RC-3.–Microbial Characterization

Description of Work.--This task determines whether *in-situ* micro-organisms are present in the Smackover carbonate reservoir at Womack Hill Field and determines through laboratory experiments the ability of these microbes to produce a single by-product (acid) by supplying them with only enough nutrients to sustain the cells but not enough to support cell proliferation.

Rationale.–Researchers at Mississippi State University have demonstrated the cost-effectiveness of utilizing the growth of indigenous microbes in enhancing the efficiency of an active waterflood for the recovery of incremental oil. The technology involves injecting a regulated stream of nutrients into a sandstone reservoir at a subsea depth of -2,300 ft to stimulate indigenous microbe growth. Cell proliferation by these micro-organisms acts to reduce the flow of injected water in more permeable zones of the reservoir by selective plugging, thereby diverting the water to other areas of the reservoir. This diversion and altering of flow patterns in the reservoir serve to enhance the sweep efficiency of the waterflood. This technology is expanded upon in this study by using the ability of these microbes to produce a single by-product (acetic acid).

This immobilized enzyme technology (IET) is applied to the carbonates at a depth of 11,300 ft in Womack Hill Field. It is anticipated that the acetic acid will act to break down the Smackover reservoir through dissolution thereby creating enhanced reservoir connectivity.

Microbial Identification and Characterization.--The objectives of this subtask have been to characterize the microflora present in the Womack Hill Field in terms of their ability to act as a source of enzymes that convert alcohols to acids and to determine the nutritional requirements

to maintain cells in a metabolically active state with minimal replication. When microbial cells are operating in an immobilized enzyme mode they are not reproducing but rather they are serving as a container of enzymes that carry out a specific reaction—namely, the conversion of ethyl alcohol to acetic acid in the current project. The cells will perform only a limited amount of repair during this time and virtually no reproduction will take place in the absence of a supply of nitrogen. Therefore, only a small periodic addition of a nitrogen source to the injection water is required for cell maintenance in order to maintain enzymatic activity. The key to success is to supply a sufficient amount of nitrogen to the cells for repair, and perhaps a small amount of reproduction, but not enough to allow vigorous growth. Therefore, experiments were conduced to determine the concentration and amount of potassium nitrate to satisfy the above requirements.

Phosphate is required to activate the dormant cells in the reservoir and support growth and is included in the early nutrient feedings to activate the dormant cells and support the initial growth. Ethanol is a protein-denaturing agent and therefore it is critical to supply the microflora with the ethanol at a concentration below that which will harm the cells. Obviously, the greater the amount of ethanol added, the greater the amount of acid produced and thus experiments will be conducted to determine the concentration of ethanol that results in the production of the greatest amount of acid.

Four water samples from Womack Hill Field well Permit #1781 (Turner 13-6) and two cores taken from the Womack Hill Field a number of years ago were analyzed for micro-organisms capable of growing at 90°C, but none were found in any of the samples. This was not unexpected since the cores had been exposed to the air for years. Likewise, it was not surprising that no micro-organisms capable of growth at 90°C were found in the water samples since micro-organisms prefer to grow attached to a substrate and consequently may be absent in the water. At

the time that these samples were tested, the equipment necessary to maintain an anaerobic environment was inadequate and may have prevented the growth of strict anaerobes. A Coy® Anaerobic Flexible Vinyl Chamber, which efficiently maintains an anaerobic atmosphere, was purchased and resolved the problem.

In order to design the amounts and schedule for the introduction of nutrients into the injection wells for the field demonstration of the immobilized enzyme technology, cultures from the Smackover Formation were required. Attempts to obtain a core from a well being drilled near the Womack Hill Field were unsuccessful for several reasons. As an alternative, cuttings and drilling mud were obtained from Crosby's Creek Oil Field located in Washington County, Alabama, that is situated near Womack Hill Field.

When attempting to isolate micro-organisms from petroleum reservoirs it is expected that most, if not all, will be in the form of ultramicrobacteria (UMB). They are extremely small in size due to lack of essential nutrients and are metabolically dormant. Specifically, the oil reservoir is deficient in nitrogen- and phosphorus-containing nutrients. Furthermore, UMB's normally cannot be reactivated using conventional strength media and more dilute media must be employed in isolation procedures. Therefore, approximately two g of the cuttings were placed into nine 60 ml volatile organic analysis (VOA) vials containing 20 ml of either $^1/_2$, $^1/_{10}{}^{th}$, or $^1/_{20}{}^{th}$ strength mineral salts broth (MSB). MSB consisted of 1 g KNO_3, 0.38 g K_2HPO_4, 0.20 g $MgSO_4 \cdot 7H_2O$, and 0.05 g $FeCl_3 \cdot 6H_2O$ per liter of distilled water. The pH was adjusted to 7.0 with 10% HCl (vol/vol). Of the nine VOA vials prepared, three contained 20 ml of $^1/_2$-strength mineral salts broth (MSB), three contained 20 ml of $^1/_{10}$-strength MSB, and three contained 20 ml of $^1/_{20}$-strength MSB. To each of the VOA vials, ~100 µl of Womack Hill Field crude oil was added. All 9 vials were incubated under stationary conditions at 90°C.

After 21 days of incubation, growth of micro-organisms was evident in all of the vials. It was next decided to determine if the micro-organisms in these enrichments had the ability to convert the ethanol into acetic acid. Five µl of 95% ethanol was added to each of the nine vials and the vials placed in the 90°C incubator to allow the ethanol to reach equilibrium between the gas and aqueous phases. After equilibration, the concentration of ethanol in the headspace of the vials was determined using a Varians® Model 3800 Gas Chromatograph equipped with a flame ionization detector. Additionally, carbon dioxide was determined using a Fisher dual column, dual detector, gas partitioner fitted with thermal conductivity detectors.

As shown in Figure 108, the enrichments from all three dilutions of media consumed ethanol. The difference in the amounts of ethanol consumed is probably a reflection of a difference in cell concentration rather than a difference in species of micro-organism. It should be pointed out that after four days of incubation, 6.9 mg of bicarbonate was added to each vial to react with the acids to form carbon dioxide. The amount of carbon dioxide produced is a function of the amount of acid produced.

Figure 109 shows the amount of carbon dioxide produced by the enrichments cited above. As may be seen, a large quantity of carbon dioxide was produced by the enrichments and was considerably more than could be accounted for by the reaction of acetic acid with the carbonate. This additional carbon dioxide could be derived from utilization of the ethanol or oil. Also, carbon dioxide may have been derived from organic acids produced from the oil directly reacting with the carbonate.

These enrichment cultures were subcultured into new medium with oil. Also, the original cultures were again tested for their ability to utilize ethanol and the results are given in Table 7. As may be observed, all of the cultures consumed ethanol.

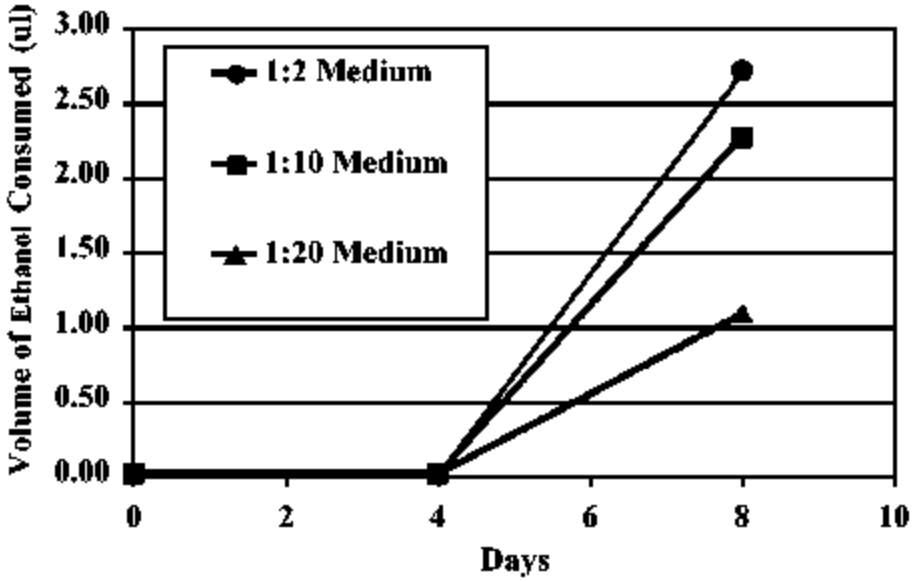

Figure 108. The utilization of ethanol by enrichment cultures.

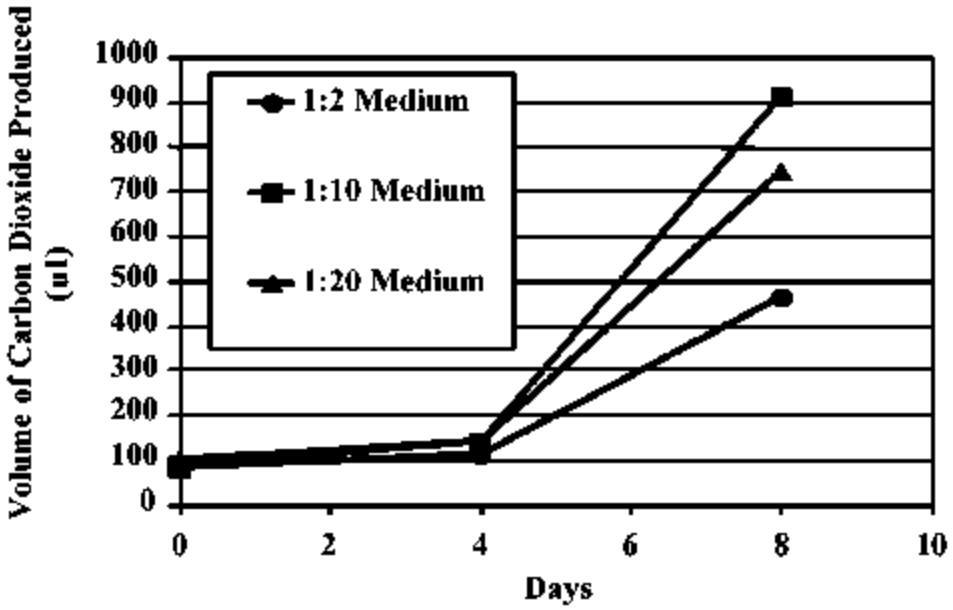

Figure 109. The production of carbon dioxide by enrichment cultures.

Table 7. Utilization of Ethanol by Enrichment Cultures Growing at 90 C Under Anaerobic Conditions

Dilution (MSM:H_2O)	Ethanol Utilization in 5 Days (%)	Ethanol Utilization in 9 Days (%)
1:2	75	88
1:10	74	85
1:20	60	82

Samples of these enrichments were examined using a confocal laser-scanning microscope. In transmitted light, the bacteria are visible within menisci of oil as shown in Figure 110. These bacteria auto fluoresce (fluoresce without staining) when stimulated with the laser (see Figure 111). A reverse negative picture of the cells is given in Figure 112. These findings are highly encouraging and suggest that micro-organisms capable of producing acetic acid from ethanol will be present in the Womack Hill Field reservoir and that they can be induced to grow and be metabolically active at the temperature in the reservoir.

Task RC-4. Integration of Data

Description of Work.--This task integrates the geological, geophysical, petrophysical and engineering data for the Womack Hill Field into a single comprehensive digital database for reservoir characterization, 3-D geologic and seismic modeling, 3-D reservoir simulation, cost-effective field management, and for making operational decisions in the field. Landmark Graphics software, OpenWorks, was used in database construction.

Rationale.--This task serves as a critical effort to the project because the construction of a digital database is an essential tool for the integration of large volumes of data. This task also serves as a means to begin the process of synthesizing concepts. The database also provides a mechanism for quality control in that core and log data can be compared to geophysical, petrophysical and engineering data. These measured and calculated data are utilized in developing predictive algorithms and techniques for calculating variable values for interwell

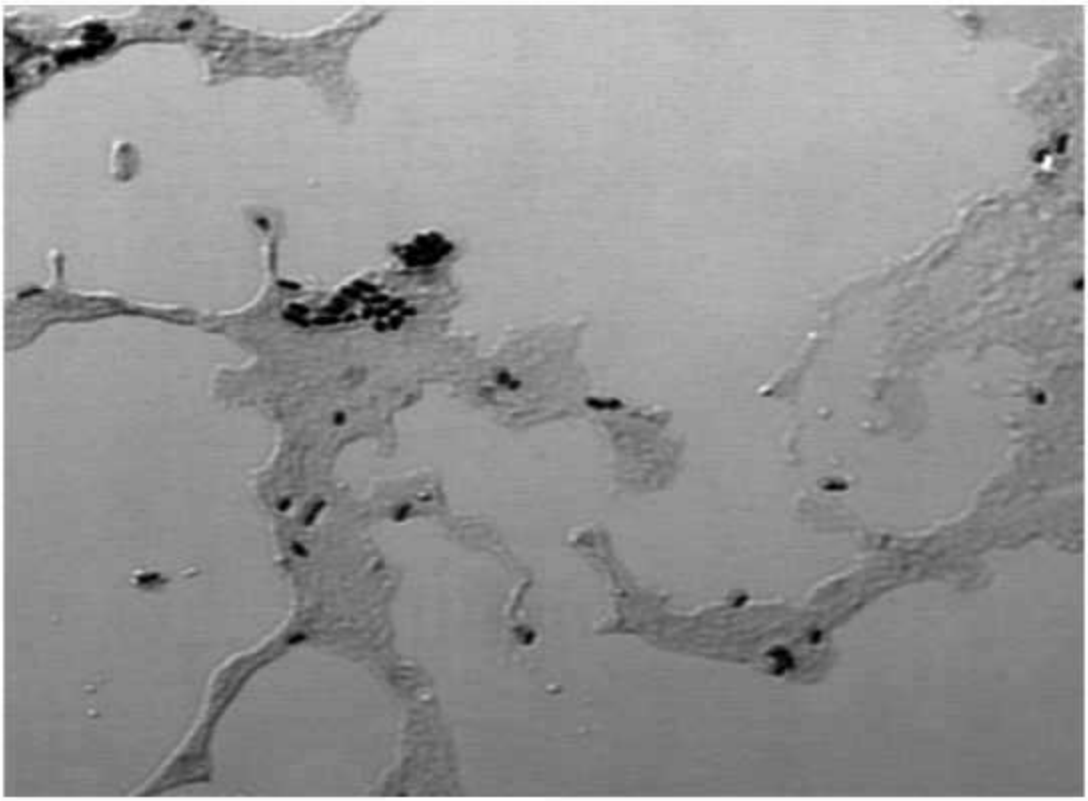

Figure 110. Laser confocal microscope image of oil-degrading grown anaerobically at 90˚C.

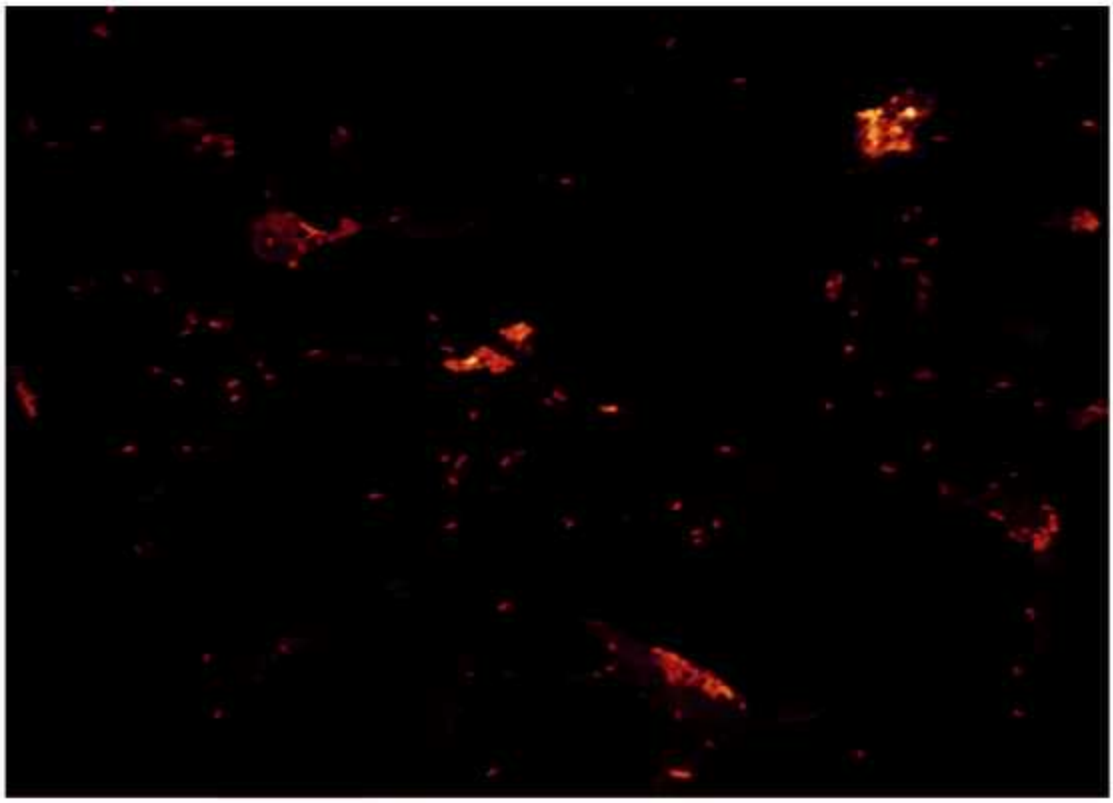

Figure 111. Auto fluorescence of bacteria grown anaerobically at 90°C when stimulated by laser using a confocal laser-scanning microscope.

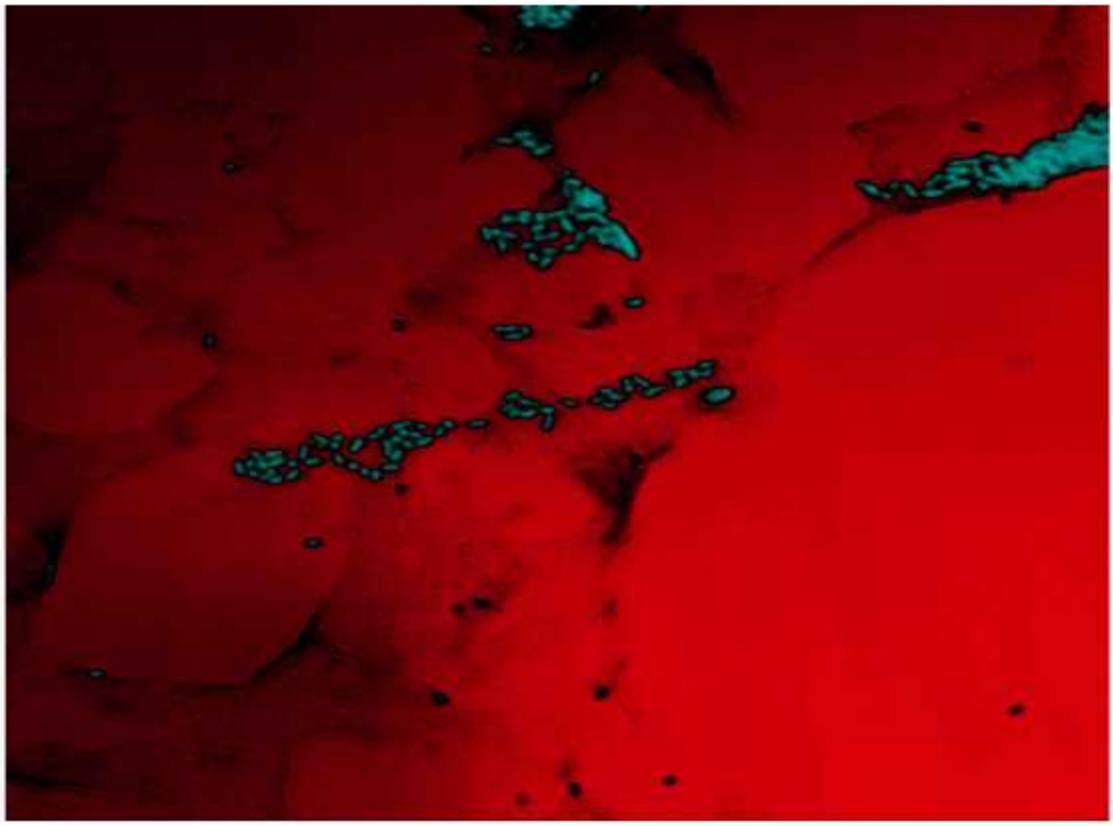

Figure 112. A reverse negative confocal laser-scanning microscope image oil-degrading bacteria grown at 90˚C.

areas. The database serves as an archival record that can be updated in the future. The database is built using a spreadsheet approach. The data are accessed, managed, and analyzed by using standard industry software. The goal is to develop a relevant and transportable database.

Data Integration.--All geological, geophysical, petrophysical and engineering data for the Womack Hill Field have been integrated into a comprehensive digital database. The database has been used in developing predictive algorithms and techniques such as heuristic methods and neural network and fractal permeability for interwell areas.

Recovery Technology Analysis

Task RTA-1. 3-D Geologic Model

Description of Work.--This task involves using the integrated database which includes the information from the reservoir characterization tasks to build a 3-D stratigraphic and structural model of the Womack Hill Field reservoir. Previous reservoir models constructed for the Smackover and for the Permian carbonate shoal reservoirs in West Texas and the depositional modeling of modern ooid sand shoals of the Great Bahama Bank are used as analogs in building the 3-D stratigraphic and structural model for the Smackover shoal reservoir at Womack Hill Field. Landmark Graphics software, Stratamodel, was used to build the 3-D geologic model.

Rationale.--This task provides the framework for the reservoir simulation model. Sequence stratigraphy in association with structural interpretation forms the framework for the model for Womack Hill Field. The model incorporates data and interpretations from the core and well log analysis, sequence stratigraphic, depositional history and structural studies, petrographic analysis, and diagenetic, pore system, and petrophysical and engineering studies. The purpose of the 3-D stratigraphic and structural model is to provide an interpretation for the interwell distribution of systems tracts, lithofacies, and reservoir-grade rock. This work is designed to

improve well-to-well predictability with regard to reservoir parameters, such as primary depositional lithologies, diagenetic features, pore types and systems, porosity and permeability values, and heterogeneity. This layer-based model is built utilizing predictive techniques to populate and distribute property and attribute data. Key data include structural features, physical surfaces, depositional sequences, stratigraphic event beds, sedimentary structures, carbonate textures and mineralogy, diagenetic features, pore types and throats, and porosity and permeability. Geologic modeling sets the stage for reservoir simulation and for the recognition of flow units, barriers to flow and flow patterns in the respective fields. The reservoir model and integrated database are effective tools for cost-effective reservoir management for making decisions regarding operations in the field.

3-D Geologic Model.--Building a 3-D geologic (stratigraphic and structural) model (Figs. 113 and 114) to illustrate the geometry of the reservoir(s) at Womack Hill Field requires understanding of the stratigraphic framework of the reservoir and the structural framework in the field area (Kerans and Tinker, 1997). The Smackover stratigraphic, sedimentologic and petrophysical information (stratigraphic units, carbonate lithologies, lithofacies, cycles, porosities, and permeabilities) obtained from core, well log and thin section studies and from core analysis are fundamental to the construction of the model for this field. These data and information from the subsurface structure and isopach maps and cross sections are integrated into the model to illustrate Smackover cycle distribution, thickness, and reservoir quality and structural configuration. The 2-D seismic data (Fig. 20) for the field provide an independent confirmation of the location of faults in the Womack Hill Field.

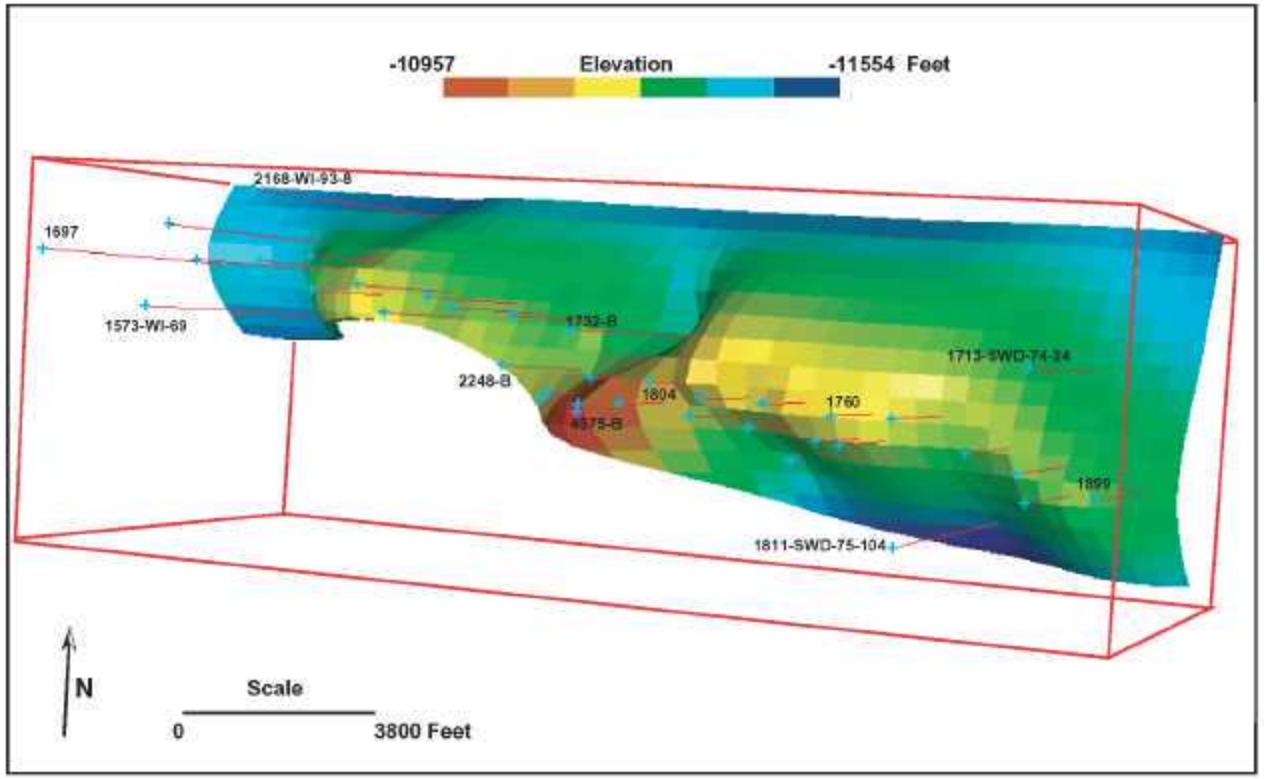

Figure 113. 3-D geologic model of Womack Hill Oil Field. Model depicting elevation of top of Smackover Formation. Model constructed using Stratamodel software. See Figure 8 for location of wells.

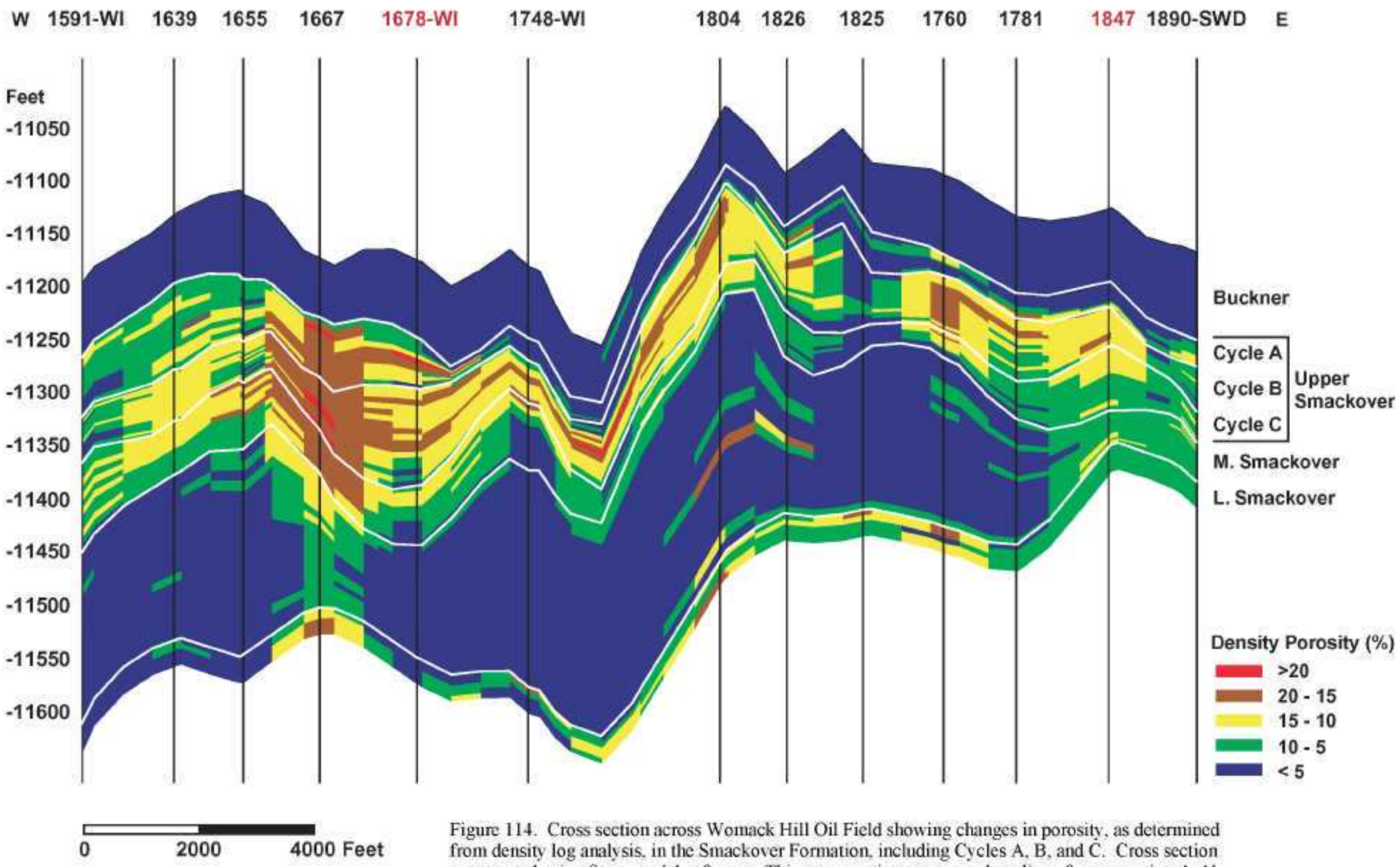

Figure 114. Cross section across Womack Hill Oil Field showing changes in porosity, as determined from density log analysis, in the Smackover Formation, including Cycles A, B, and C. Cross section constructed using Stratamodel software. This cross section corresponds to line of cross section A-A' in Figure 8.

Task RTA-2. 3-D Reservoir Simulation

Description of Work.--This task builds a numerical simulation model for the Womack Hill Field that is based on the 3-D geologic model (stratigraphic and structural framework), petrophysical properties, fluid (PVT) properties, fluid-rock properties, and the results of the reservoir performance analysis. The geological/geophysical model is coupled with the results of the reservoir performance analysis to determine flow units, as well as reservoir-scale barriers to flow. The purpose of this work is to build forecasts for the Womack Hill. Landmark Graphics software, VP Simulator, was used for reservoir simulation.

Rationale.--This task is a critical step for any enhanced oil recovery technology. Reservoir simulation is used to forecast expected reservoir performance, to forecast ultimate recovery, and evaluate different production development scenarios. In itself, modeling of the current scenario at Womack Hill Field is necessary to establish whether or not the existing efforts in reservoir management are sufficient, and if not, how could these activities provide optimal performance. Conceptually, it is important to understand (i.e., be able to model) the current behavior at Womack Hill Field prior to initiating any new activities. Probably the most important aspect of the simulation work is the setup phase. Developing a detailed reservoir model for the Womack Hill Field is essential because this is a geologically complex system, and the long production/injection history has not been evaluated relative to a detailed reservoir description.

3-D Reservoir Simulation.--The static data for the reservoir simulation model, i.e. permeability, porosity and geometry were obtained from the 3-D geologic model. This model was "upscaled" for simulation purposes. This is necessary so that the simulation can be run over the thirty years of field history in a reasonable time (usually 2 to 4 hours). We note that the geologic software only interpolates petrophysical data from known values at the wells. This may

result in the property distributions being too "smooth" *i.e.* small scale interwell heterogeneity is neglected. The permeability of zones A, B and C of the geologic model are shown in Figure 115. The fluid property (PVT) data for the model came from one fluid report on a fluid sample from well Permit #1639 (Table 8). Figures 116 and 117 show the reported oil formation volume factor and oil viscosity functions. Measured relative permeability and capillary pressure were treated as history matching parameters. Sensitivity studies with the simulator show that the simulated results are quite sensitive to the saturation endpoints. The oil-water contact has been reported as 11,360 ft. This was varied during history match. Once the capillary pressure and oil-water contact location were defined in a particular run the simulation was initialized with an initial fluid distribution (Fig. 118). Production data for the study were obtained from the State Oil and Gas Board of Alabama records. Injection data were obtained from Pruet Production Co. Data were reported monthly which may mask some variability. Well completion/perforation depths were also obtained from the State Oil and Gas Board of Alabama records. The dates on which perforations were made (important in the case of recompletions) was obtained from Pruet. We note there have been some significant changes in production operations in the field. In 1990-91 jet pumps were installed in all production wells. We are uncertain whether the increase in the field watercut that occurred at that time is coincidental with this operational change. Acid treatments were also performed periodically in most wells.

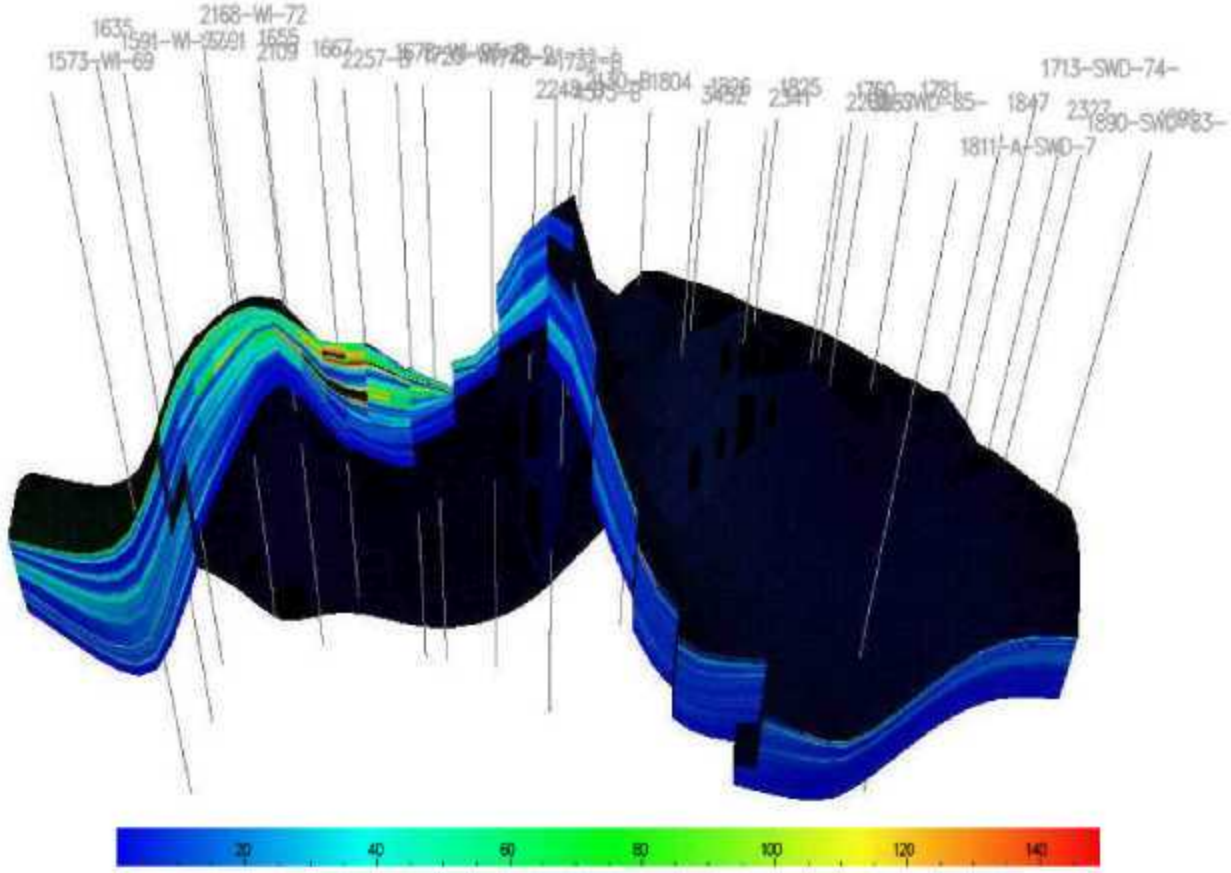

Figure 115. Permeability of A, B and C zones in the geological model.

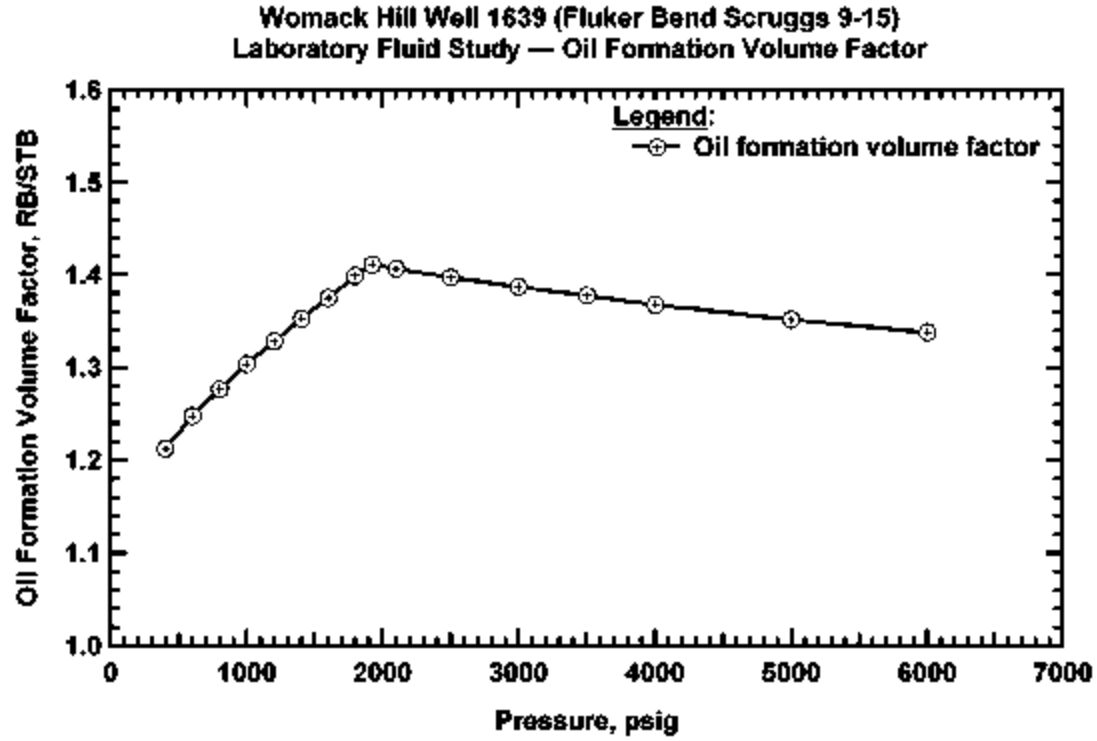

Figure 116. Oil Formation Volume Factor, Well 1639 Womack Hill

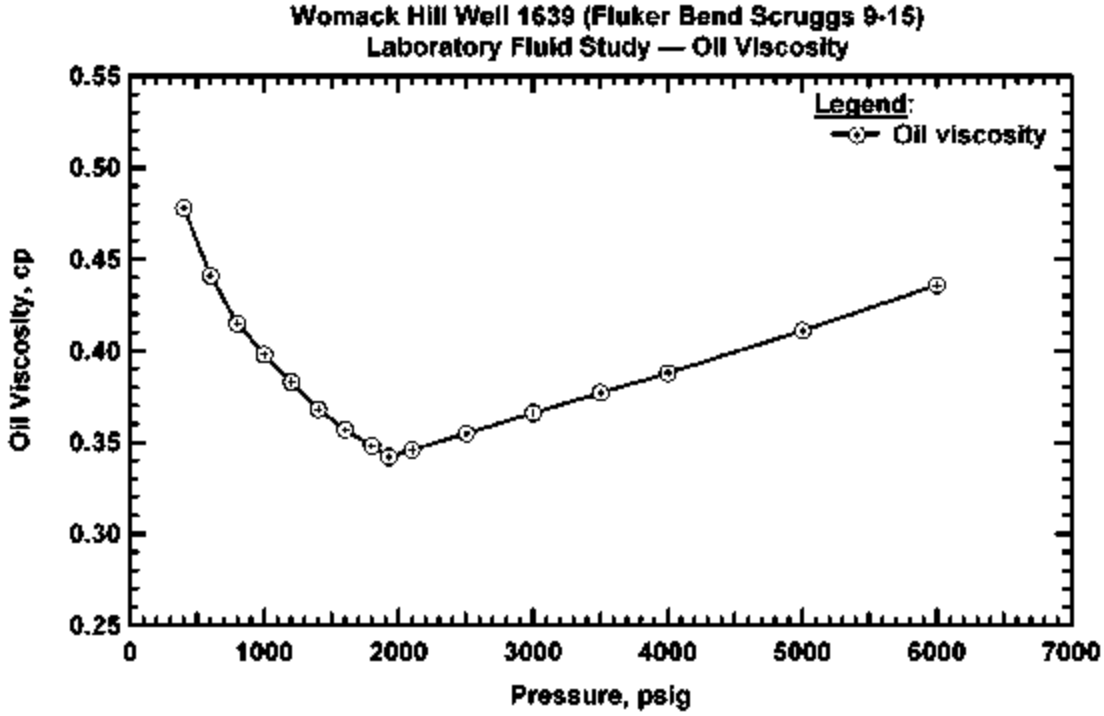

Figure 117 Oil Viscosity, Well 1639 Womack Hill

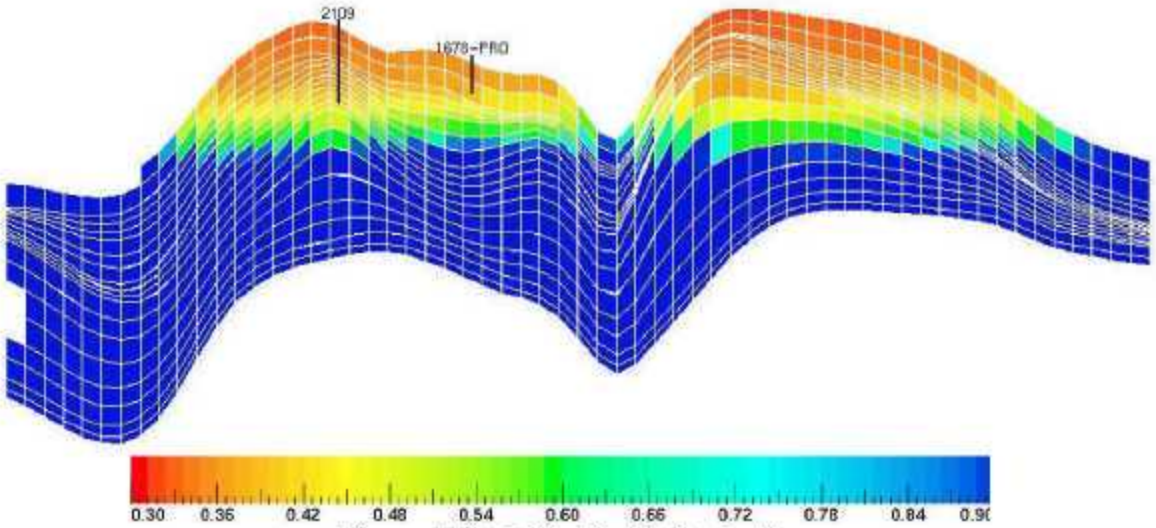

Figure 118. Initial fluid distribution

Table 8. Hydrocarbon analysis of oil from well Permit #1639.

Component	Mol (%)	Density at 60°F (g per cm^3)	API gravity	Molecular weight	Fm vol factor
Hydrogen Sulfide	nil				
Carbon Dxide	0.39				
Nitrogen	4.41				
Methane	19.67				
Ethane	10.54				
Propane	8.73				
Iso-Butane	2.74				
n-Butane	5.04				
Iso-Pentane	3.19				
n-Pentane	2.46				
Hexane	4.47				
Heptane Plus	38.36	.....		.....	
	100.00	0.8487	35.1	189	1.641

Viscosity at 212°F = 0.342 centipoise at saturation pressure to 1.201 centipoise at atmospheric pressure
Gas-oil ratio = 506 SCF/bbl
Saturation pressure (bubble point) = 1925 PSIG at 212°F
Thermal expansion of saturated oil at reservoir temperature:
600 to 4500 psi = 10.79×10^{-6}
4500 to 3000 psi = 12.99×10^{-6}
3000 to 1925 psi = 16.19×10^{-6}
Specific volume at saturation pressure (ft^3/lb) = 0.02407 at 212°F
lb=appreciation for pound

With the completion of the construction of the simulation model for the Womack Hill Field, the task of history matching was undertaken. The history matching process initially made global changes to the model (changing the oil-water contact depth or changing the aquifer strength) in order to achieve the best possible match of the reported water and oil production data. Of particular interest were parameters related to possible communication between the western and eastern areas of the field. To evaluate this communication scenario, a series of reservoir simulation runs were performed based on the following assumptions: a strongly sealing barrier between these two zones, a weak barrier between the zones, and no barrier at all. Reservoir simulation runs were also performed with an aquifer underlying the entire reservoir as well as with an aquifer underlying only the eastern area of the field. In Table 9, we provide the parameters considered in a systematic set of reservoir simulation runs which were designed to

Table 9. Parameters varied in a systematic assessment of global parameters on field-wide performance.

Parameter	Variations
Oil-water contact depth, ft	11,330 ft 11,340 ft 11,350 ft
Aquifer location	Underlying entire reservoir Underlying Eastern portion of the reservoir only
Aquifer	Infinite aquifer Aquifer strength reduced by a factor of 0.1
East/west barrier	Strong (transmissibility reduced by a factor of 0.01) Weak (transmissibility reduced by a factor of 0.1) No barrier

evaluate the influence of the location of the oil-water contact, aquifer orientation, aquifer strength, and the east-west transmissibility barrier.

The results of these parameter variations are shown in the form of a "tornado chart" in Figure 119. The tornado chart is a bit ambiguous for this particular application, so some explanation is in order. Each of the horizontal trends of points in this figure represents a set of simulation runs generated using every possible combination of the four parameters given in Table 9. The runs are coded by symbol and color in each horizontal trend according to the value of a particular parameter.

The data were further analyzed to assess which of the parameter combinations ensured that, as much as possible, the water produced from the field was assigned to the correct wells. Two additional "tornado charts" were produced (as shown in Figures 120 and 121). In Figure 121, we present the data in terms of the total water production misfit (the sum over all wells of the absolute percentage difference in the reported and simulated water production from the well). This error measure is likely to be dominated by wells with large mismatches between simulated and reported water production. This led us to also consider the format shown in Figure 121 which presents the data in terms of the sum of the squared percentage error in water production over all the wells. These "tornado charts" suggest that the distribution of the produced water is predicted best using the oil-water contact depth of 11,350 ft (we note that these results and our conclusions are particular to the set of relative permeability and capillary pressure values used).

The properties of the aquifer and existence of a flow barrier between the eastern and western areas of the field could not be clearly determined from this "tornado chart" analysis. In subsequent runs an aquifer underlying the eastern area of the field only was used in the reservoir

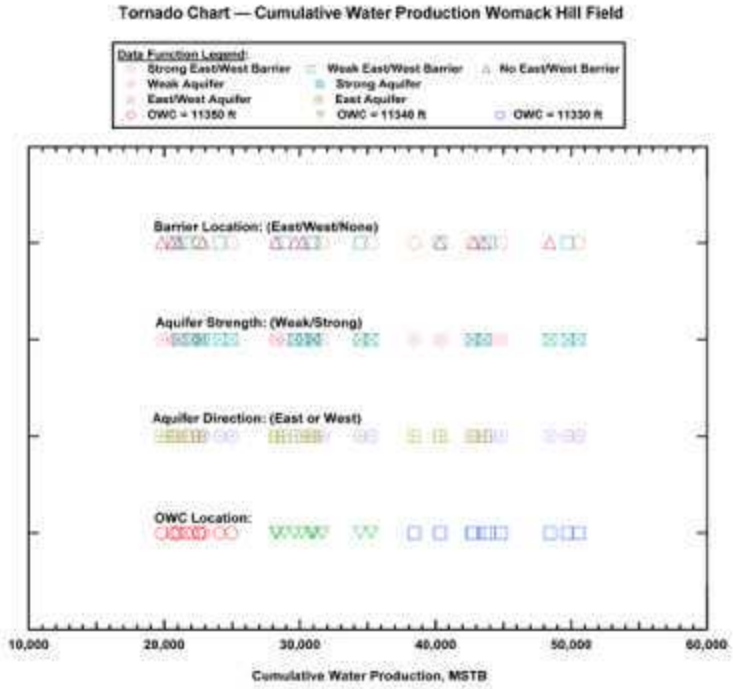

Figure 119. "Tornado chart" representation of the effect of global parameter variations described in Table 9 for cumulative oil production (Womack Hill Field).

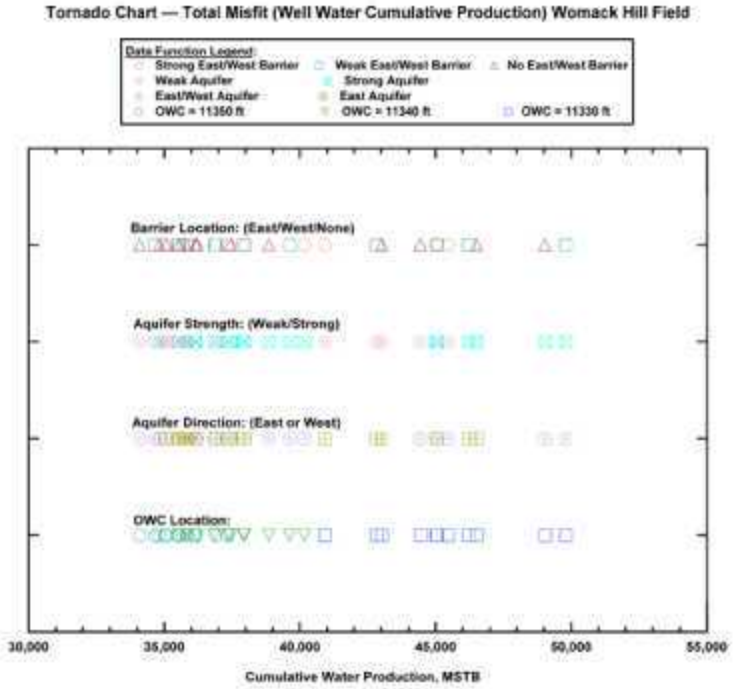

Figure 120. "Tornado chart" representation of the effect of global parameter variations described in Table 9 on the sum of the water production mis-match over all wells in the Womack Hill Field.

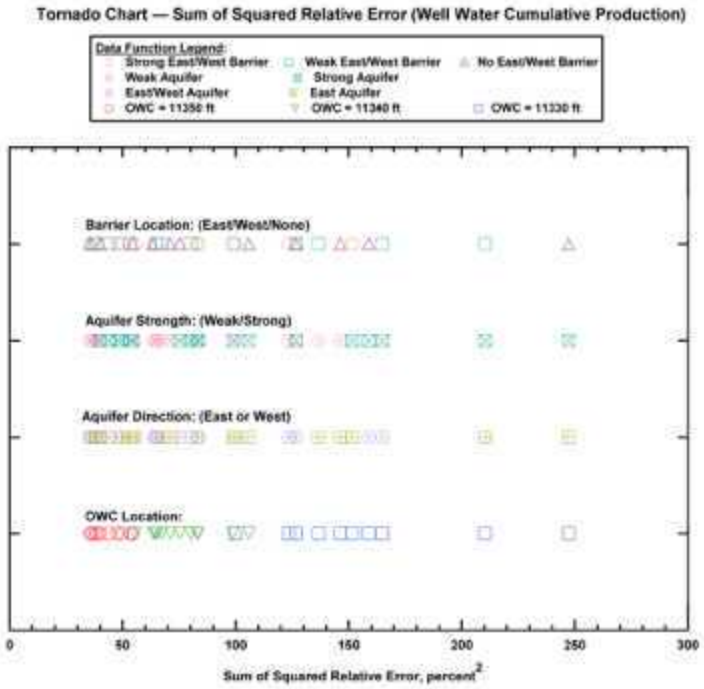

Figure 121. "Tornado chart" representation of the effect of global parameter variations described in Table 9 on the sum of the squared percentage error in water mismatch over all wells in the Womack Hill Field.

simulation (we note that this assumption was supported by the differing pressure behavior in wells from both sides of the field).

After completing our assessment of major factors using the "tornado chart" analysis, we conducted other simulations where we considered "local" changes in various parameters in order to achieve optimal matches for the performance of individual wells. These local property changes typically involved varying the porosity distribution around a given well, and we also considered changes to well productivity indices and the relative permeability curves. We note that both stages of the history-matching process (the refinement of "global" and "local" parameters) are labor and computation intensive.

Table 10 summarizes the match of cumulative water production from the individual wells. It should be noted that water production data were not reported before 1980 and may not have been accurately reported subsequently (at least prior to 1990). Figure 122 shows the match of the field-wide watercut versus time and Figures 123 to 134 show the matches of the historical water production for individual wells (we only present cases that produced over 1,000 MSTB of water). Many of the wells show excellent matches of the historical water rate for at least a portion of their productive life.

The oil saturation maps based on the current version of the reservoir simulation model are shown in Figures 135 to 139. These maps (not to scale) present areal slices through the first five layers of the reservoir model (there are 19 layers) and illustrate the remaining oil saturation (as of October 2000). These maps imply that there may be sufficient remaining oil which could justify a future infill drilling program.

The western portion of the unitized part of the field appears to have little remaining oil and offers little potential for additional drilling. In the south-central (eastern portion of unitized area)

Table 10. Match of cumulative water production from individual wells.

Well #	Actual water production (MSTB)	Simulated water production (MSTB)
1573	0	0
1591	0	3,245
1639	2,219	947
1655	5,750	6,762
1667	1,328	3,667
1678	2,481	3,550
1720	0	14
1732	0	103
1748	243	1184
1760	0	2
1781	2,498	2,982
1804	292	546
1825	0	41
1826	25	102
1847	5,447	2,113
1890	32	15
1899	283	575
2109	5,533	3,118
2130	720	1,263
2248	1,860	158
2257	2,485	2,369
2263	397	296
2327	1,632	297
2341	7,973	3,677
3452	149	141
3657	1,472	931
4575	504	876

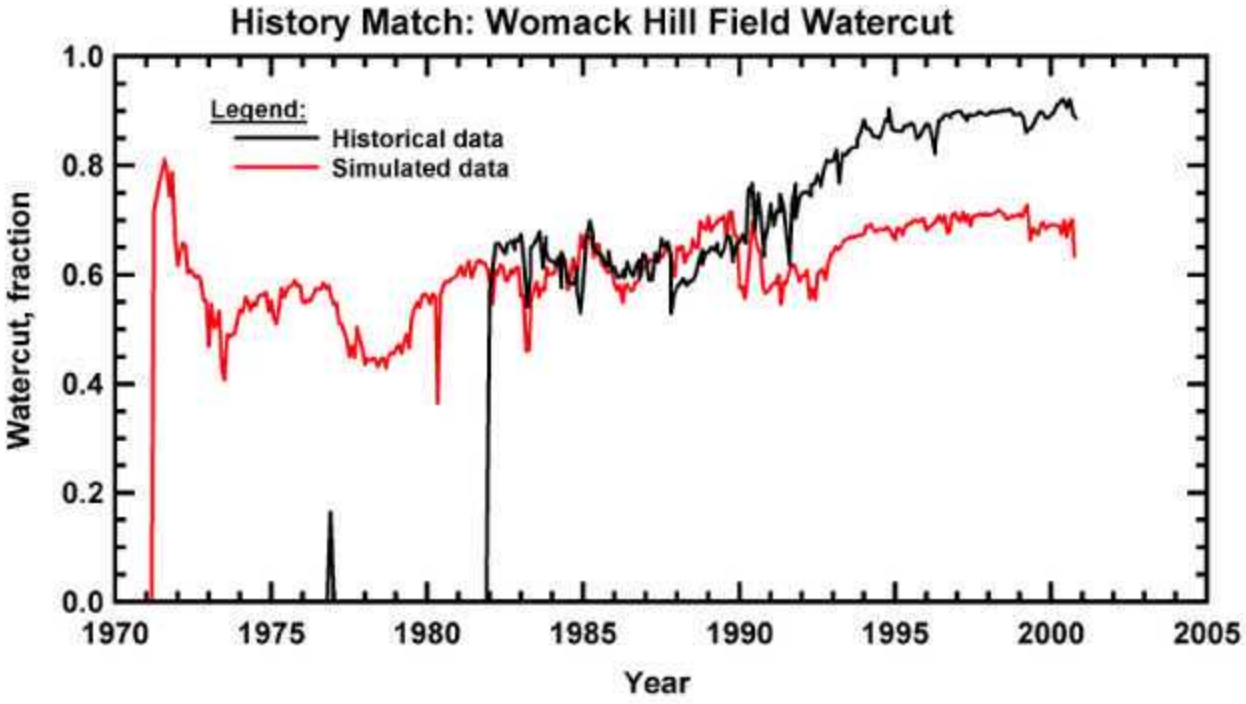

Figure 122. Actual and simulated field-wide watercut versus time in the history matched model.

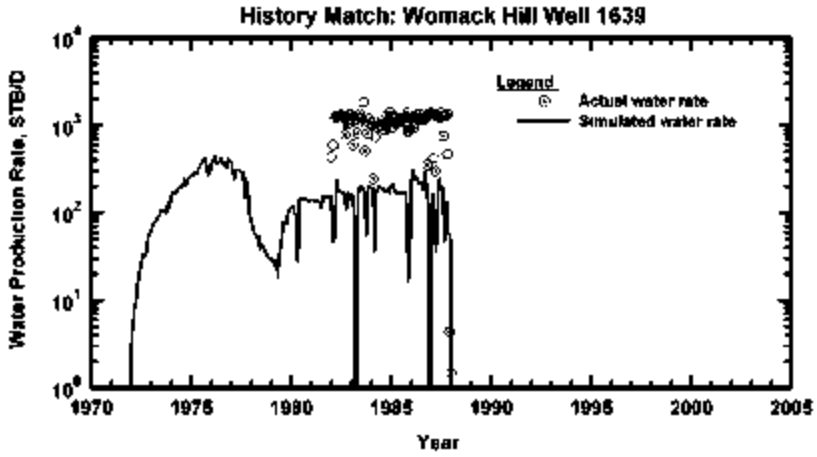

Figure 123 Actual and simulated watercut versus time for well 1639

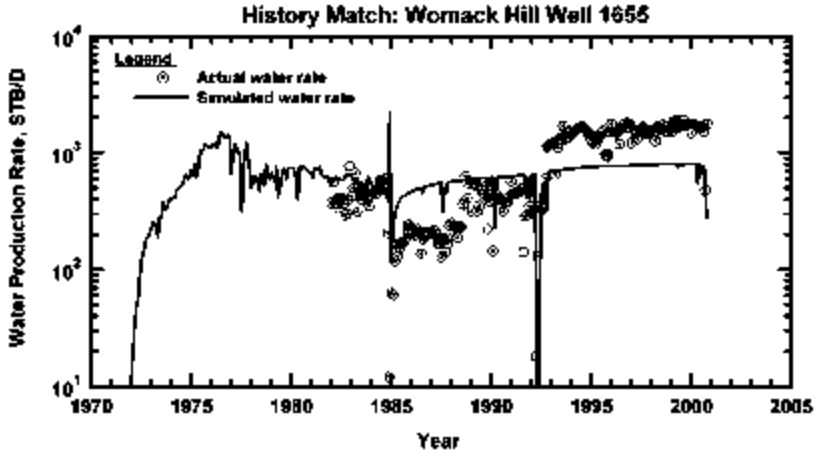

Figure 124 Actual and simulated watercut versus time for well 1655

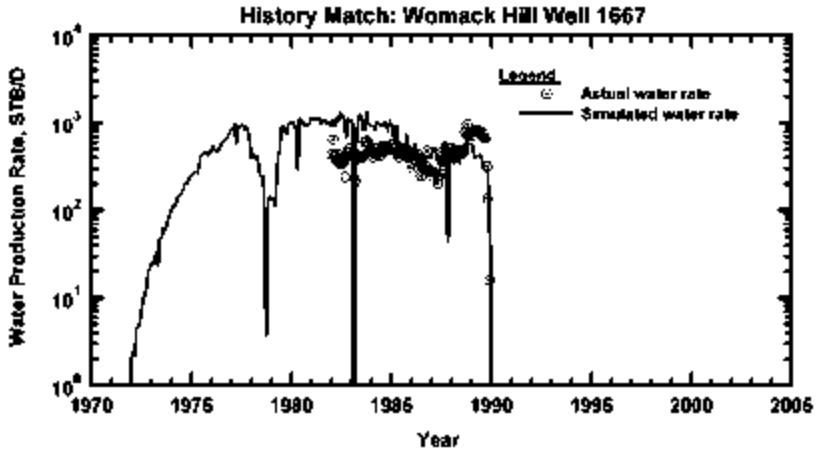

Figure 125 Actual and simulated watercut versus time for well 1667

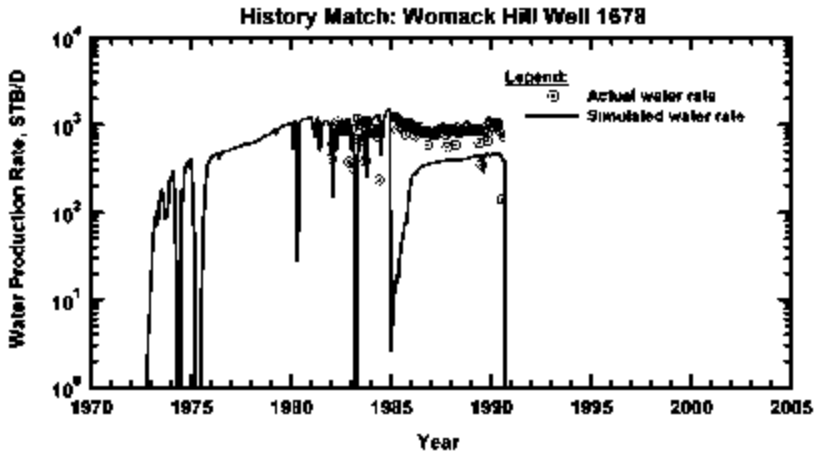

Figure 126. Actual and simulated watercut versus time for well 1678.

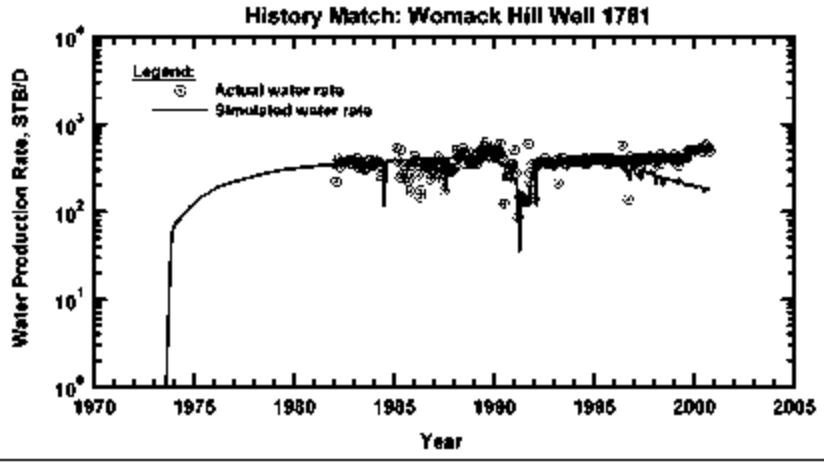

Figure 127. Actual and simulated watercut versus time for well 1781.

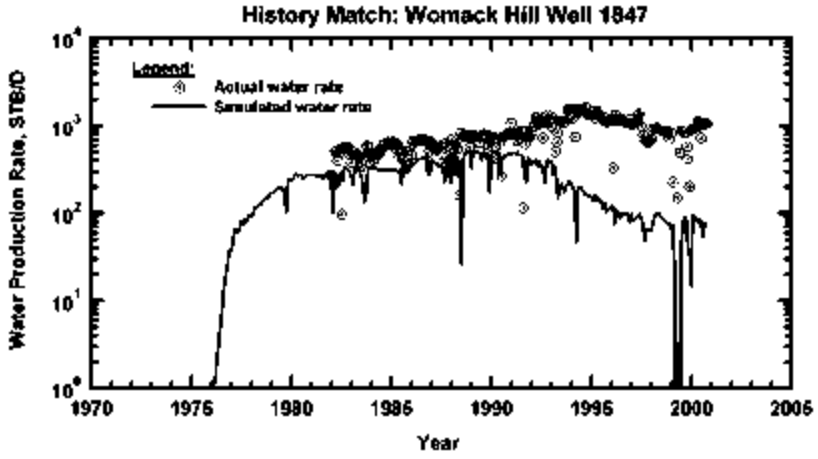

Figure 128. Actual and simulated watercut versus time for well 1847.

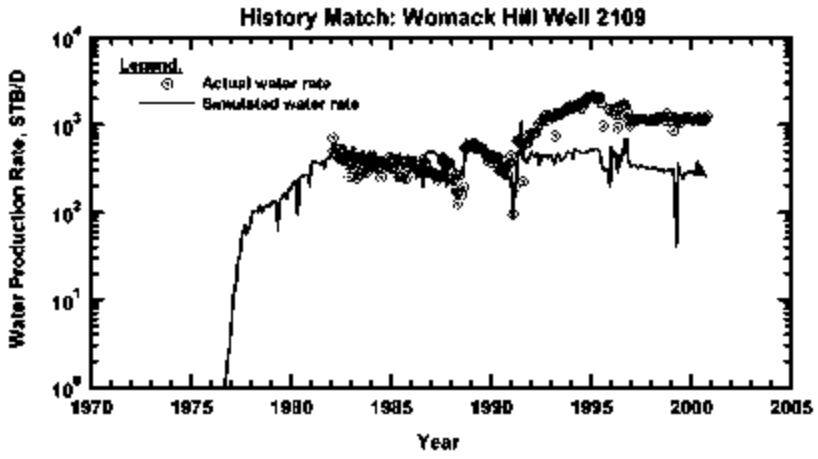

Figure 129. Actual and simulated watercut versus time for well 2109.

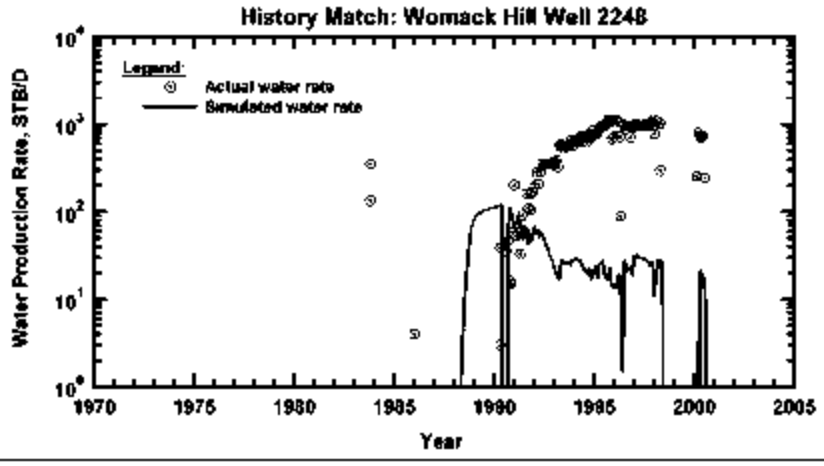

Figure 130. Actual and simulated watercut versus time for well 2248.

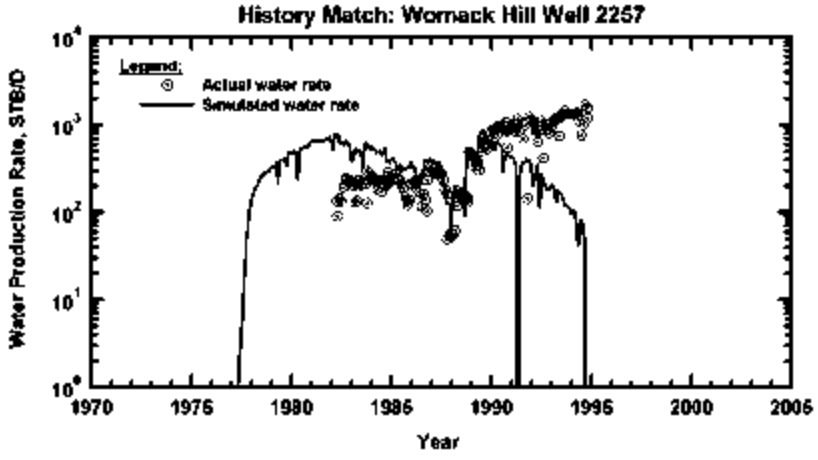

Figure 131. Actual and simulated watercut versus time for well 2257.

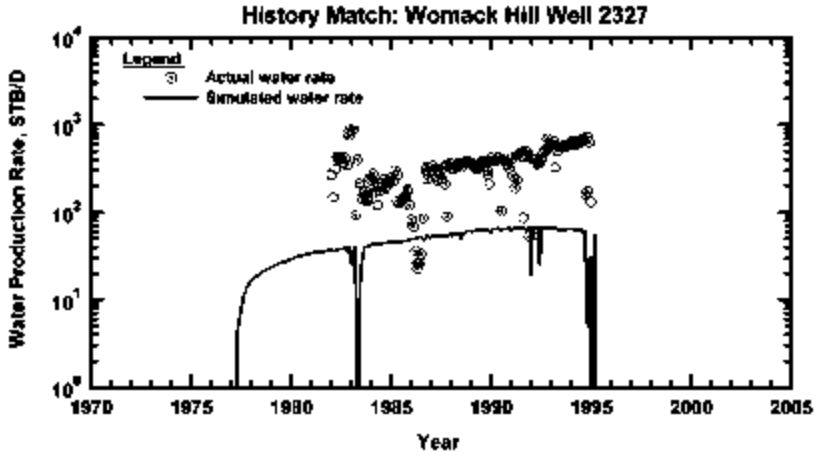

Figure 132 Actual and simulated watercut versus time for well 2327

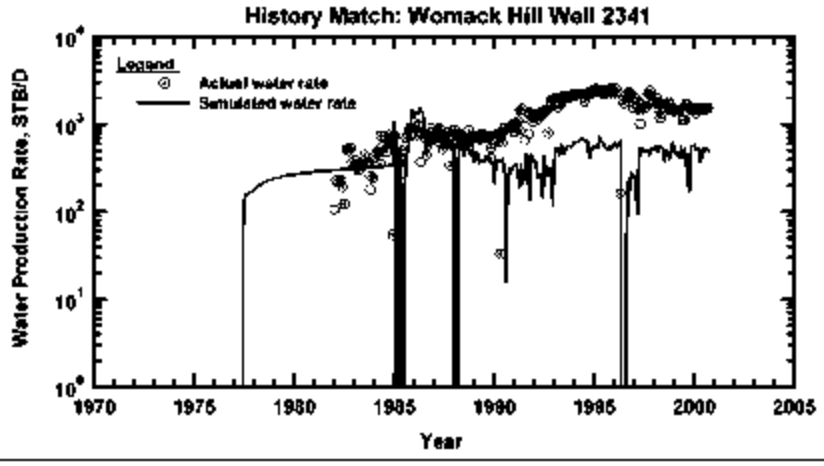

Figure 133 Actual and simulated watercut versus time for well 2341

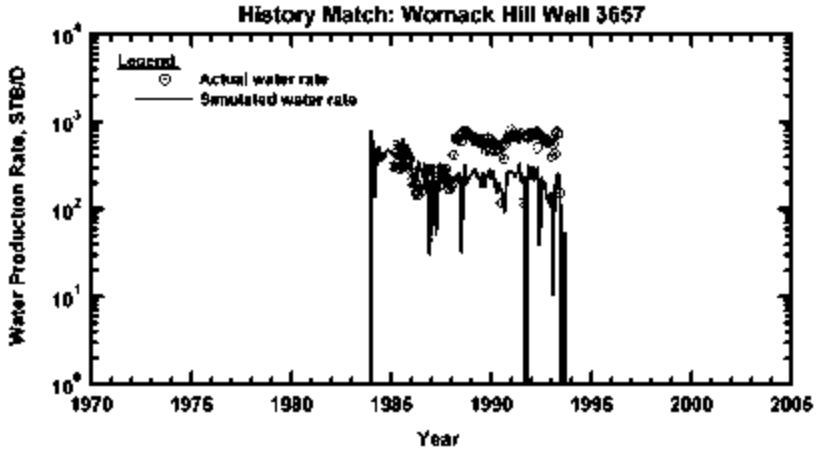

Figure 134 Actual and simulated watercut versus time for well 3657

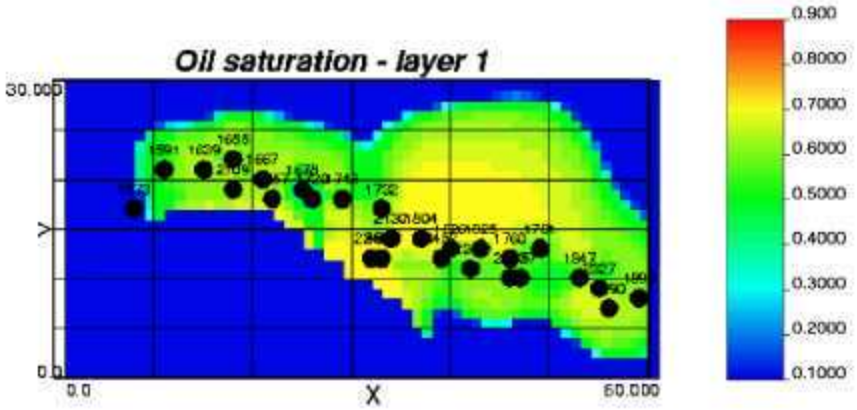

Figure 135. Oil saturation distribution in layer 1 of the history matched model.

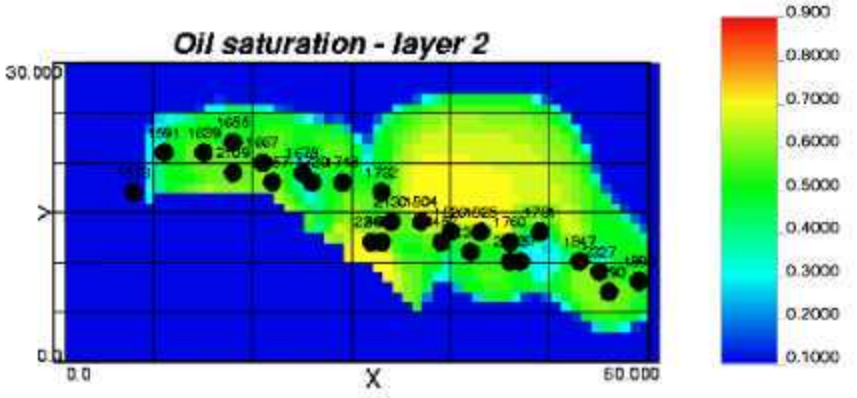

Figure 136. Oil saturation distribution in layer 2 of the history matched model.

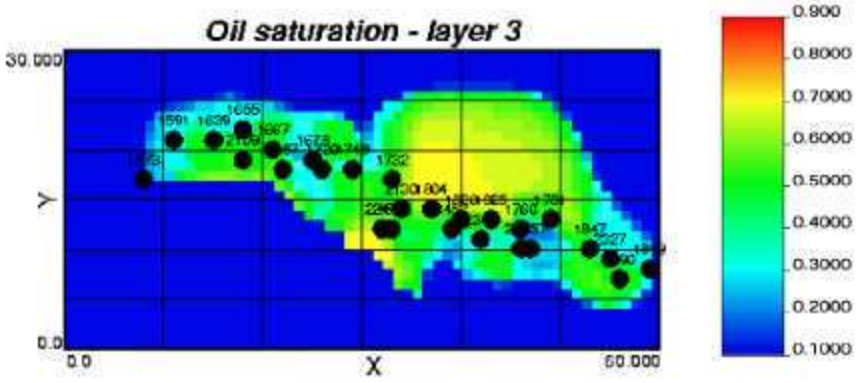

Figure 137. Oil saturation distribution in layer 3 of the history matched model.

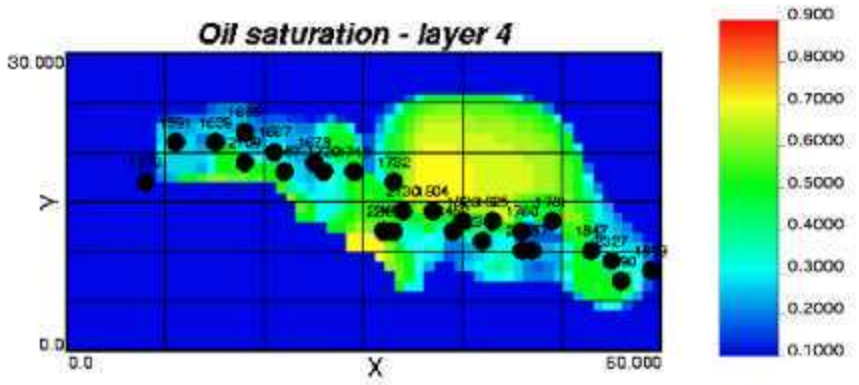

Figure 138. Oil saturation distribution in layer 4 of the history matched model.

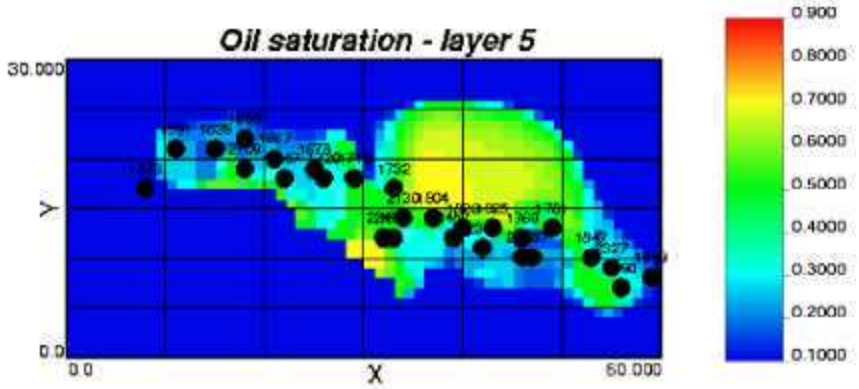

Figure 139. Oil saturation distribution in layer 5 of the history matched model.

and eastern part of the field, there are two areas of interest for infill drilling. The first is in the eastern part of the Unit area, near well Permit #4575B and the fault that forms the southern boundary of the field. Further evaluation of the exact geometry of this fault is recommended using a seismic survey to confirm the location of this fault relative to the existing wells. The second drilling target is approximately 2,900 ft north of well Permit #1826 and about 1,050 ft east of well Permit #1732 in the eastern area of the field. This area appears to possess both structural elevation and remaining oil saturation. As with the first target location, further evaluation is recommended in this zone to confirm the reservoir structure (we also recommend the acquisition and analysis of additional seismic data in this region of the field).

Simulation of a new well in the second target area suggests that oil rates of substantial proportions could be achieved, although it is likely that a substantial associated water production will also occur (as shown in Figure 140). Realization of these production rates from a new well in this area is strongly dependent on the existence of the structural elevation, porosity, and permeability predicted in the geologic model of the reservoir existing in this area. The predicted cumulative production (over five years) for this well is 1,384 MSTB of oil and 172 MSTB of water. We concede that these volumes are estimates, but certainly justify consideration.

We note that simulation of our hypothetical infill well begins in November 2000 and runs for five years. The simulation model has only been history matched to this point because water injection data since that time has not yet been made available. Simulation of the new well assumes that water injection continues into the reservoir at October 2000 injection rates. In November 2002, J. R. Pounds, Inc. drilled and in January 2003 tested well Permit #12762 immediately northwest of well Permit #1826 in the eastern part of Womack Hill Field. Well Permit #1826 produced 981,820 barrels of oil from Cycle A (perforations at 11,236-254 ft) and

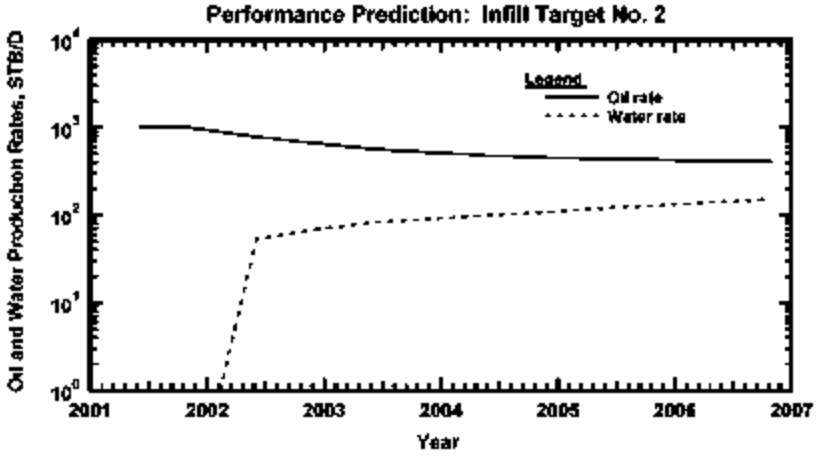

Figure 140 Simulated performance of a new well drilled in infill target No 2

was plugged and abandoned in 1991. Well Permit #12762 tested 160 barrels of oil per day from below Cycle A (perforations at 11,324-36 ft) on January 4, 2003. The shut-in bottom pressure for the well was 4760 psi compared to an original reservoir pressure of 5433 psi. The well has produced 14,237 barrels of oil through September 2003. Original water production for the well was 500 to 650 barrels per month; however, in May 2003, monthly water production increased to 14,400 barrels. Water production has continued at a rate of 13,500 to 15,500 per month. Oil production is 54 barrels per day or 1,582 barrels of oil per month. The increase in water production is believed to be a result of water encroachment into this area of the field. The reservoir simulation developed for Womack Hill Field was modified to accommodate the results from this new well. The results are shown in Figures 141 through 146. Using the revised simulation model, two hypothetical wells were placed in the area north of well Permit #12762. The hypothetical wells were perforated above 11,300 ft and were produced along with the remaining wells in the field for five years. Figures 147 and 148 show the observed production profiles for these wells. Over the five years of production the first well (PROD-001) produced 825 MSTB of oil and the second well (PROD-002) produced 664 MSTB of oil.

A satisfactory history match of the performance of the Womack Hill Field has been developed using integrated reservoir characterization and reservoir simulation. The history matched model implies there is remaining oil in the field which could potentially be accessed by drilling at least one additional well in the eastern area of the field. Further appraisal by acquisition of seismic data is recommended prior to pursuing a drilling program.

Task RTA-3. Microbial Core Experiments

Description of Work.--This task involves the maximization of the chemical addition program using microbial core experiments. Live (freshly taken cores rather than archived cores)

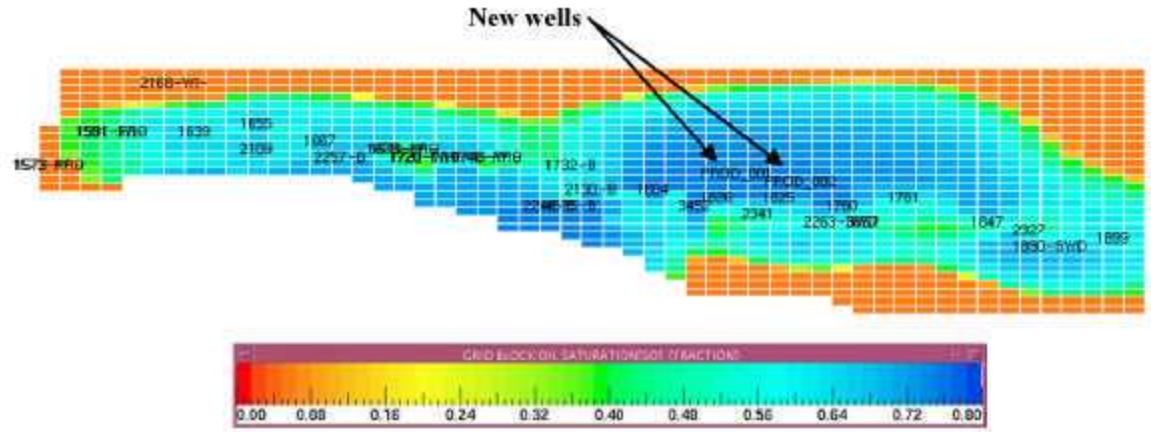

Figure 141— Oil saturation in layer 1 of the simulation model for March 2003.

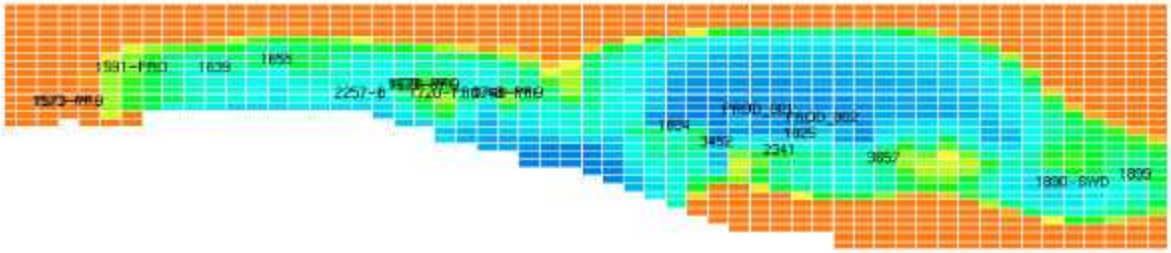

Figure 142— Oil saturation in layer 2 of the simulation model for March 2003.

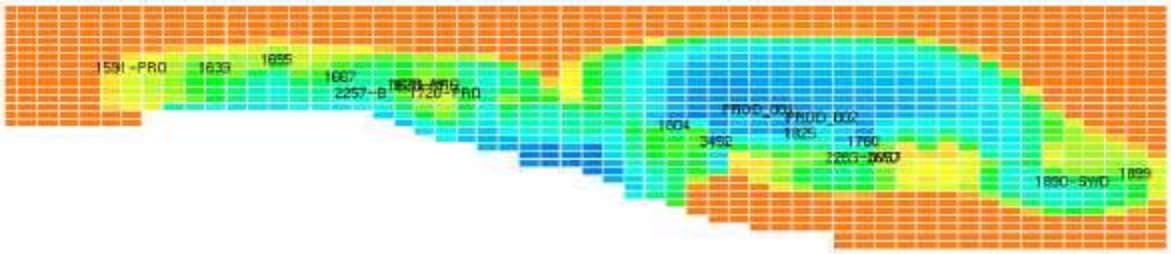

Figure 143— Oil saturation in layer 3 of the simulation model for March 2003.

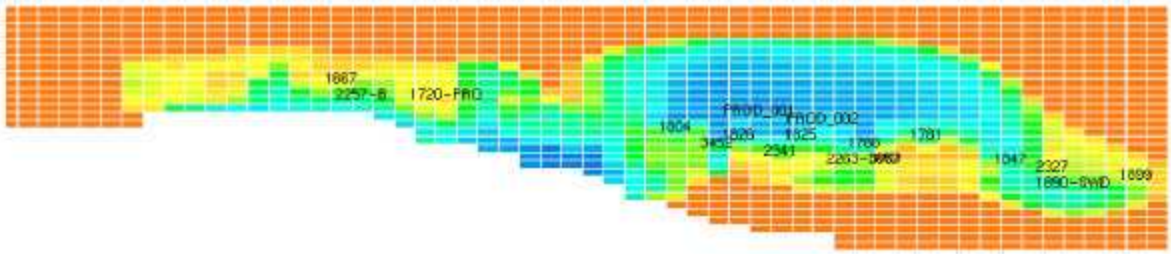

Figure 144— Oil saturation in layer 4 of the simulation model for March 2003.

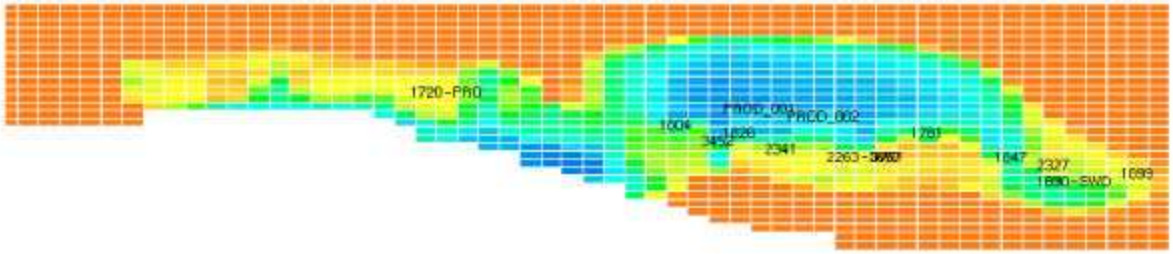

Figure 145— Oil saturation in layer 5 of the simulation model for March 2003.

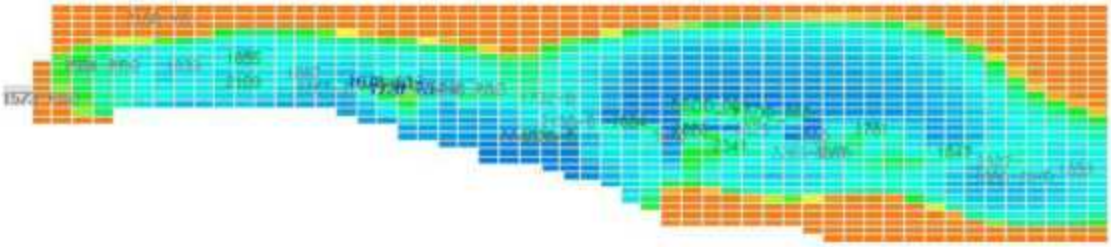

Figure 146— Oil saturation in layer 1 of the simulation model for March 2008.

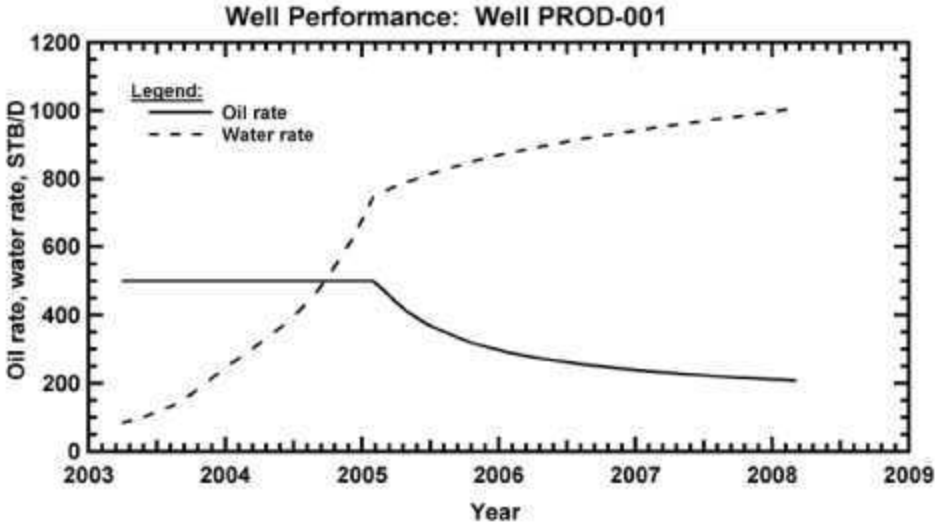

Figure 147— Production profile for infill well PROD-001.

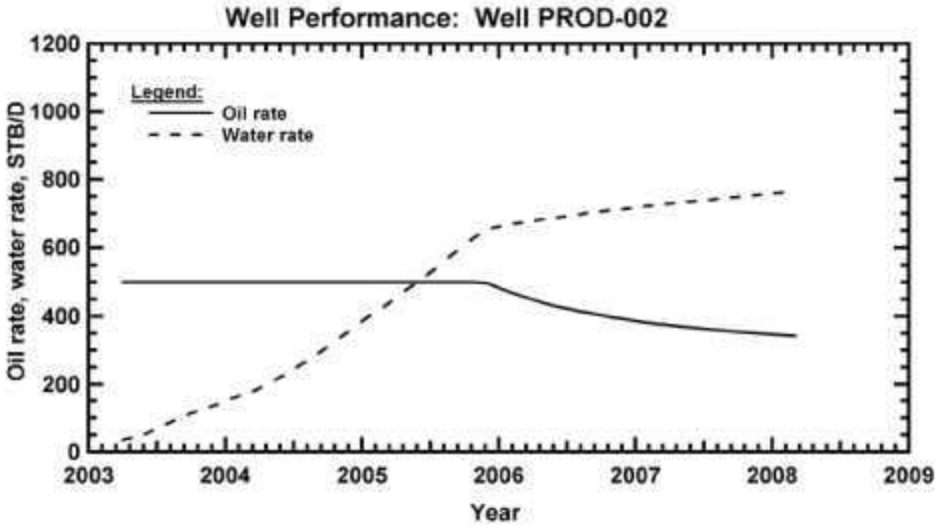

Figure 148—Production profile for infill well PROD-002.

cores are required for use in this work. The cores are incorporated into the core apparatus. The chemical addition program from Task RC-3 is employed initially and changes made to maximize acid production while minimizing cell proliferation. All experiments were conducted under anaerobic conditions at reservoir temperature. These studies finalize the chemical addition program to be implemented in the field demonstration project.

Rationale.--As stated in Task RC-3, researchers at Mississippi State University have demonstrated the cost-effectiveness of utilizing the growth of indigenous microbes in enhancing the efficiency of an active waterflood for the recovery of incremental oil. This technology expands on the previous study by using the ability of *in-situ* microbes to generate acetic acid as a growth by-product. This immobilized enzyme technology (IET) is applied to a carbonate reservoir at a depth of 11,300 ft. It is anticipated that the acetic acid will act to break down the reservoir through dissolution, thereby increasing porosity and permeability in less permeable zones of the reservoir. This should result in reduced reservoir compartmentalization and more contacted oil, thereby increasing producibility of the reservoir.

Microbial Core Experiments.--Core samples from a well drilled into the Smackover Formation by Pruet Production Co. were received from Omni Laboratories in Pearl, Mississippi on June 14, 2002. These samples were crushed under nitrogen and samples placed in a 40 ml vial with 20 ml of liquid. The dilutions of MSM used were 1:2, 1:5, 1:10, 1:15, and 1:20. A range of media concentrations were employed to increase chances of success, since low levels of nutrients are required for activation of ultramicrobacteria in the cores. Several drops of oil from the Womack Hill Field were placed on top of the samples, and work was performed in the anaerobic chamber. The remaining crushed core was placed in jars and stored in the anaerobic chamber. The vials were then placed in a 90°C incubator. To check for cell growth, production of carbon

dioxide in the atmosphere of the vials was determined by gas chromatographic analyses. After one month of incubation, the samples produced carbon dioxide and thus contained viable micro-organisms.

Working at 90°C makes obtaining pure cultures challenging because routine microbiological techniques cannot be employed. Normally, samples of the material from which isolation is attempted is streaked onto the surface of a medium solidified with agar, but unfortunately, agar will not remain solid at this temperature and therefore cannot be employed in this work.

Another approach to obtain a solid medium involved the use of a new type of silica gel medium prepared using Ludox (obtained from E. I. DuPoint De Nemours Co., Inc) as described by Temple (1949). No growth was observed on the surface of the silica gel and the silica gel plates dried out quickly. Also, rapid changes in temperature caused the gel to crack.

The conventional "dilution to extinction" technique can sometimes be employed to obtain pure cultures but was not successful. A modification of the technique of serially diluting a sample in melted agar medium (2) was developed and showed considerable promise. The culture employed was one that had been proven to contain cells. A small amount of this culture was added to ten ml of sterile, melted, oil-saturated mineral salts agar (2%) contained in a 16x150 mm test tube, cooled to 80°C, and mixed thoroughly. Five ml of this suspension was added to five ml of the same medium and thoroughly mixed. The procedure was repeated such that dilutions of 1:2, 1:4, 1:8, 1:16, 1:32, 1:64, and 1:128 of the original agar suspension had been made. An 18-inch piece of sterile 3-mm glass tubing was inserted into the melted agar suspension in each tube and a suction applied to the top of the tube with a rubber bulb. When the tubing was approximately full, it was removed from the test tube and one end of the glass tubing was sealed with Fingertip Rope Caulk (Thermwell Products Co., Inc, Mahwah, NJ). After the

filled tubing equilibrated to 90°C, the other end of the glass tubing was sealed with caulk. Although the medium was not solid, it was viscous and retarded or prevented movement of the entrapped cells. All work was carried out in an anaerobic chamber. The glass tubing was incubated in a 90°C incubator in a flat position. After two weeks, the tubes were removed from the incubator and examined for the presence of colonies in the agar (that had hardened at room temperature). When a well-isolated colony was observed, the glass tubing was wiped with 70% ethanol and scored at that point with a sterile triangular file. The colony was removed with a sterile inoculating needle and placed into a test tube containing sterile mineral salts medium and crude oil. Several of the colonies that were transferred into the mineral salts medium with the crude oil grew as attested to by the fact that the medium became turbid and gram stains of the contents of the tubes revealed the presence of gram positive microbial cells. Transfers of these cultures failed to grow for reasons unknown.

Work to develop a solid medium for the growth of the oil-degrading bacteria at 90°C using Phytagel™ as the solidifying agent instead of agar that begins to liquefy at temperatures above about 45°C is promising. Results to date suggest that it will be a satisfactory solidifying agent once the ionic strength of the medium has been optimized.

Another problem in dealing with these 90°C cultures is that conventional laboratory incubators will not reach 90°C and an oven has to be employed as an incubator. Since even small fluctuations in temperature retard the growth of the bacterial cultures, special arrangements have to be employed in order to maintain a constant temperature. The system chosen for this task consists of a one-gallon paint can containing sand. A one-quart Ball® wide mouth jar is placed in the center of the can and the culture tubes or plates placed in the jar (see Figure 149). The jar lid is placed on top of the jar, covered with sand, and the lid sealed on the can. This arrangement

has resulted in a more rapid growth of the cultures due to the maintenance of a more constant temperature.

Figure 149. Photograph of the system employed for incubating cultures at 90° C.
(One- gallon paint can containing a one-quart glass jar with culture tubes inside.

Experiments designed to develop procedures for imaging organic/inorganic relationships in Womack Hill Field rocks were undertaken. A specific objective of these analyses was to characterize the spatial occurrence of porosity in the rocks before and after enhancement by bacterially-produced acetic acid. This comparison should show the particular geologic components (carbonate grains vs. cements, etc.) that are susceptible to microbial-acid modification, and may yield insight into a facies effect on the process. Smackover ooid and peloid grainstone and packstone and two other limestones have been analyzed using thin section petrography, scanning electron microscopy (SEM) (Figs. 150 and 151), and laser confocal microscopy (Fig. 152).

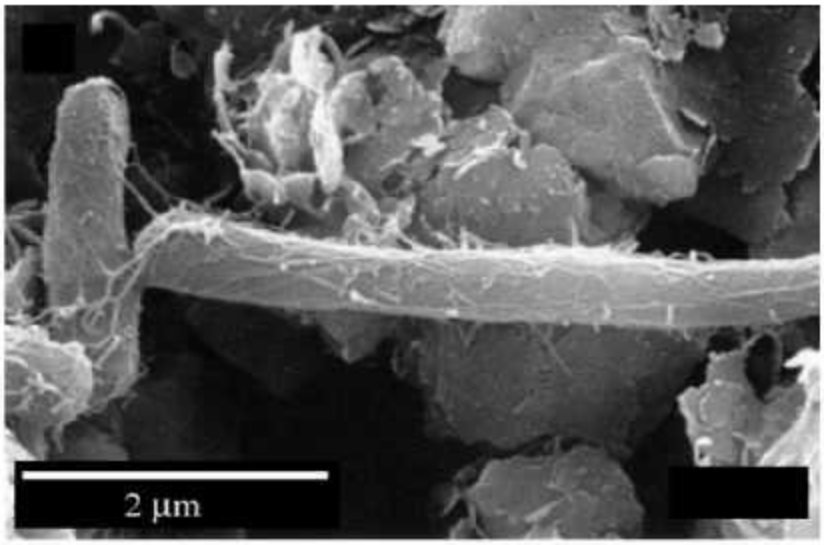

Figure 150. Bacterial bodies well-preserved by ethanol dehydration.

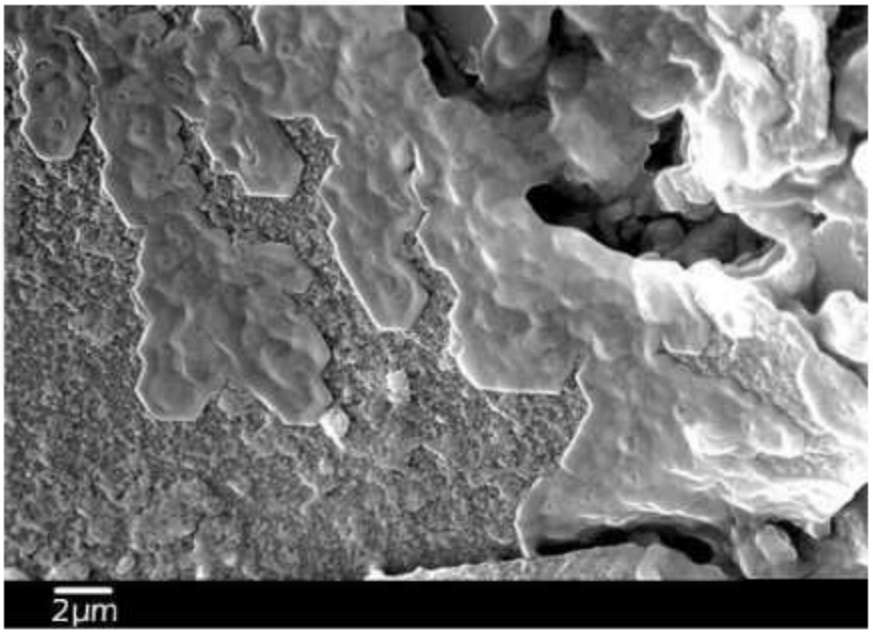

Figure 151. Grain-coating morphology of polysaccharide slime preserved by simple air-drying.

Pieces of 1" diameter core mineralogically similar to the Smackover Formation at Womack Hill Field were used in experiments designed to investigate porosity enhancement by bacterially-produced acetic acid. Live oilfield bacteria were added to the core pieces and then fed phosphate and nitrate food for two weeks to encourage growth. The experiments were performed in a

standard vacuum filtration device modified to accept the limestone core pieces. Acetic-acid production was initiated when 15 micromolar ethanol was introduced into the core. In the first experiment ethanol was added to the core for 4 days.

The results of this first porosity-enhancement experiment were disappointing. Figure 152 is a petrographic image of the Smackover core used in these experiments. It is composed almost entirely of dolomite with minor anhydrite and intercrystalline porosity. The porosity-enhancing experiment was designed and previously tested on limestone.

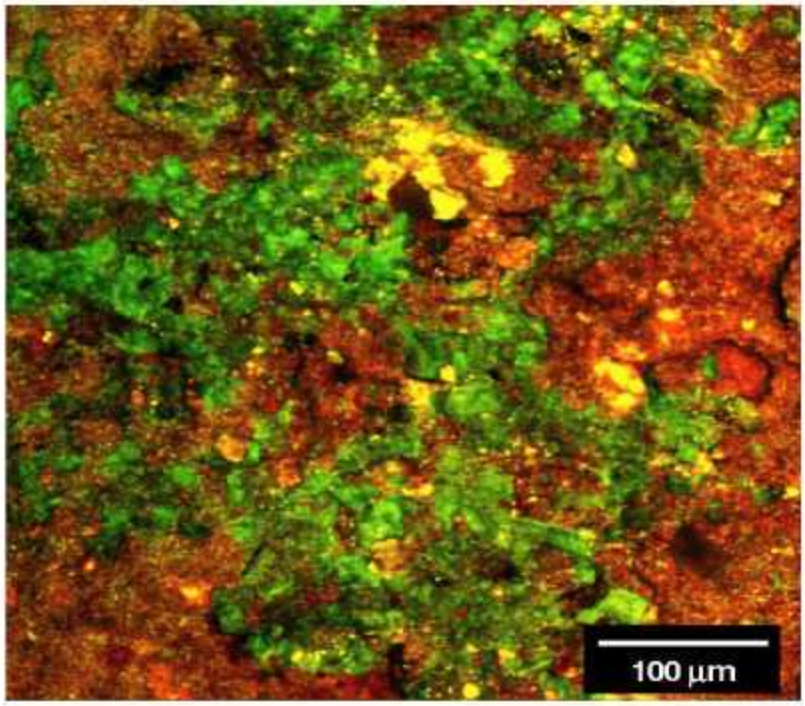

Figure 152. Laser confocal image of red-fluorescing organic matter (bacteria and biofilm) and mineral matrix (green) in a Smackover core sample.

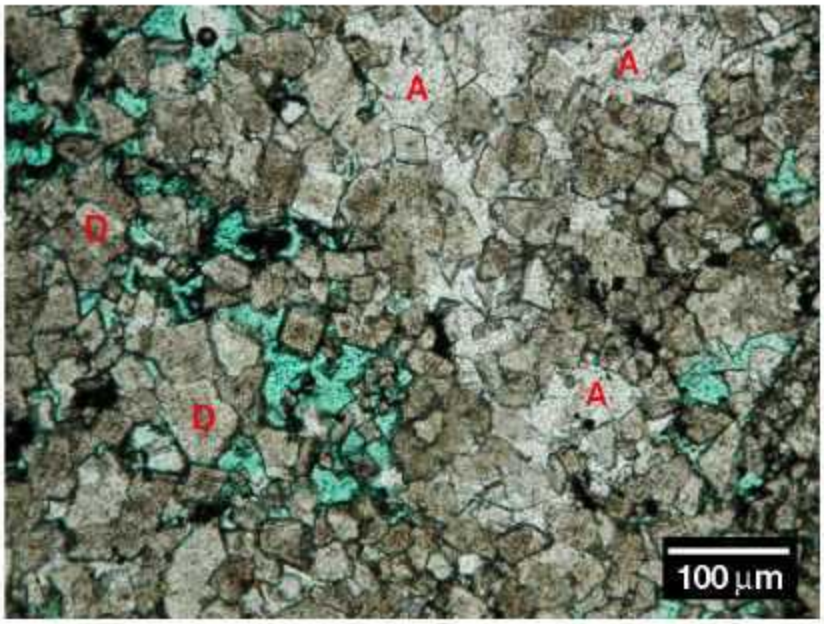

Figure 153. Petrographic image (plain polarized light) of Smackover core used in the first dissolution experiment. Dolomite (D), anhydrite (A), and intercrystalline porosity (blue color) is present.

Calcite, the major mineral component of limestone, is conspicuously absent from the samples tested here.

Figure 153 is a SEM image that shows the most common morphology of dolomite in the core. Smooth and euhedral crystal faces that show little or no sign of etching or dissolution are often covered with organic biofilm.

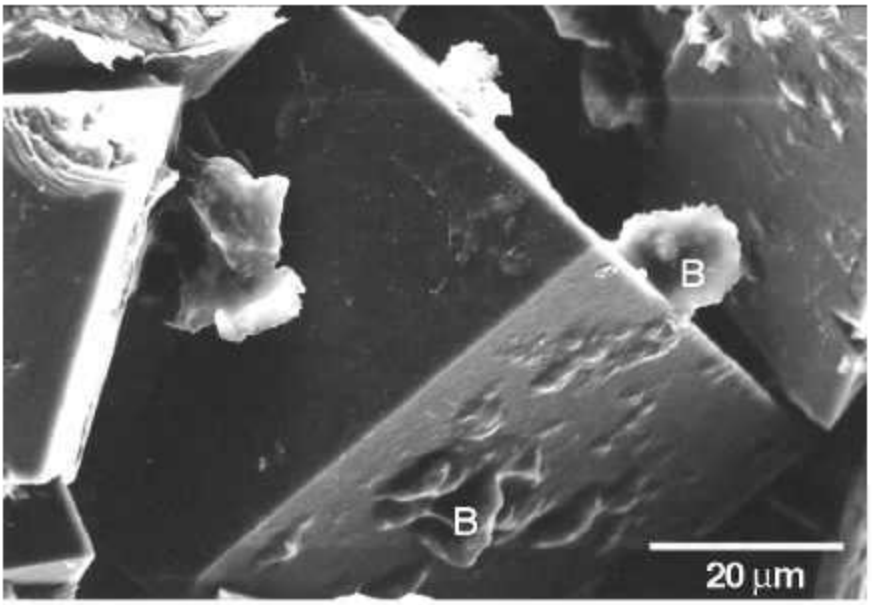

Figure 154. SEM image of unetched dolomite crystal from first acetic-acid production experiment. Smooth crystal faces are differentially covered with organic biofilm (B).

Evidence of minor etching on some crystals is not uncommon, however, it is unclear if that dissolution occurred during or before the experiment (Figures 155 and 156).

There are at least two factors responsible for the failure of this experiment to significantly enhance the porosity of the core. The mineralogy of the core was not what was expected. The solubility of dolomite and anhydrite is significantly less than that of calcite and it may be possible that longer exposure to bacterially-produced acetic acid could produce the desired dissolution. Secondly, Figure 152 clearly showed that the bacteria introduced into the core produced copious amounts of biofilm. This material coated much of the rock surface and the bacteria themselves. Thus, isolated from the ethanol, acetic-acid production was probably minimized.

Flow experiments have been performed using Cretaceous Sligo and Mississippian limestone samples. Preliminary results from these experiments indicate that porosity enhancement does occur in limestones (not dolomites) in which the bacterial production of biofilm has been

minimized by restricted feeding. Longer-term experiments should be performed on dolomite and anhydrite-rich rocks.

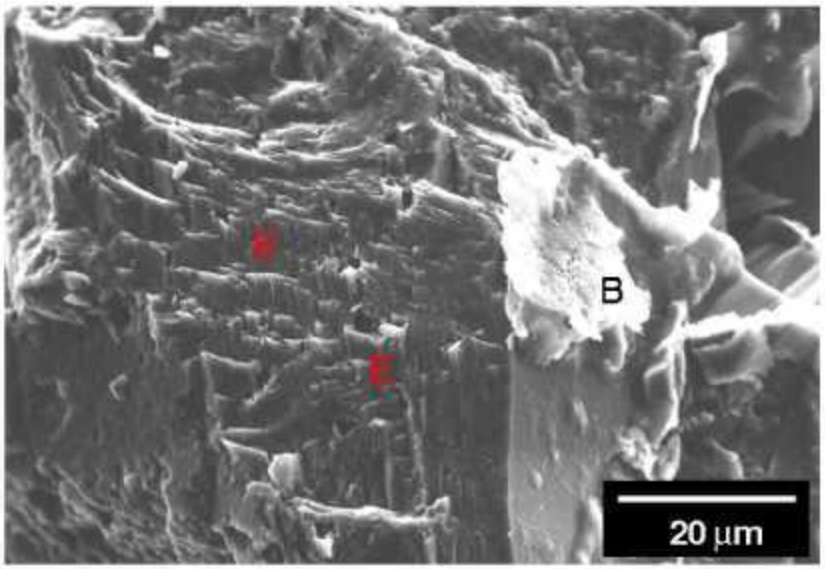

Figure 155. SEM image of a dolomite crystal with minor etching (E). Biofilm (B) is present on an unetched crystal face.

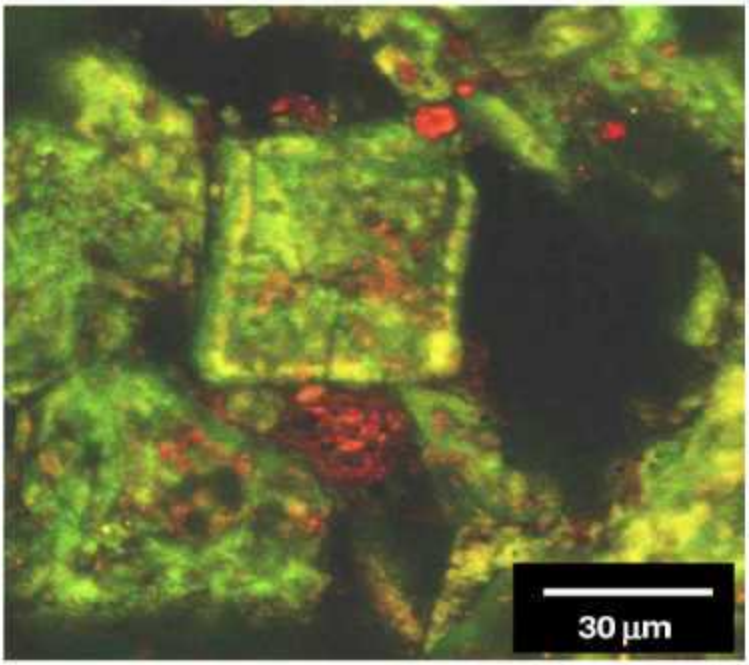

Figure 156. Laser confocal image of red-fluorescing organic matter (bacteria and biofilm) on slightly etched calcite crystal in a Smackover ooid grainstone.

The core plug testing system in the laboratory was designed to operate at ambient temperature and therefore had to be reconfigured for use at 90°C. This has been accomplished and is shown in Figures 157 to 161. The system will accommodate two core plugs at the same time and therefore two cores can be treated differently at the same time but under exactly the same environmental conditions. In the present case that means that while one core receives nutrients (test core), the other core receives only injection water with no nutrients (control core). This is especially important because even slight changes in temperature could have a major impact on the results. Since live cores from the Womack Oil Field are not available, small one-inch cores from the Smackover Formation in Escambia County, Alabama, have been utilized to test the operation of the system. These cores were obtained from Omni Laboratories in Pearl,

Mississippi. The cores had been cut lengthwise and had been exposed to the atmosphere for quite some time. Consequently, viable anaerobic extremeophiles (*i. e.*, micro-organisms that grow in the absence of oxygen at 90°C) are not expected. Trials were coducted to (1) test the operation of the system and (2) determine the impact, if any, of the nutrient solutions *per se* on the cores. The four solutions employed were (1) injection water ($CaCl_2 \cdot 2H_2O$, 14.3 g; $MgCl_2 \cdot 6\ H_2O$, 5.77 g; $BaCl_2 \cdot 2\ H_2O$, 5.38 g; $Na_2SO_4 \cdot 10\ H_2O$, 4.18 g; NaCl, 147 g; 50 liters of distilled water), (2) injection water containing 0.03 % Na_2HPO_4 , (3) injection water containing 0.12% $NaNO_3$, (4) injection water containing 0.9% ethanol (Table 11).

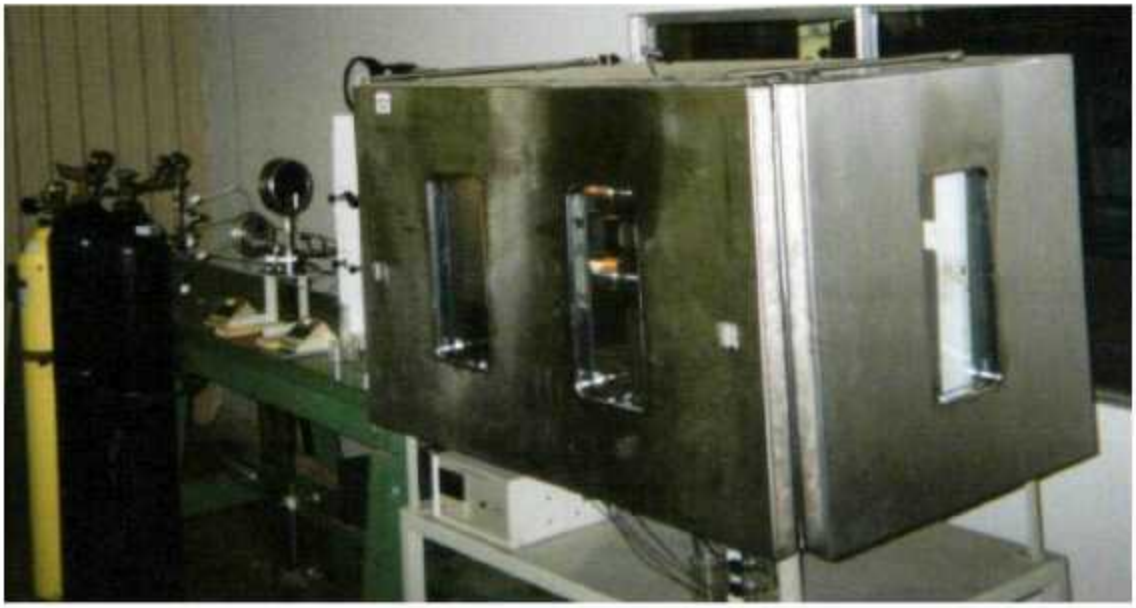

Fig. 157: Core plug testing system including incubator and gas cylinders.

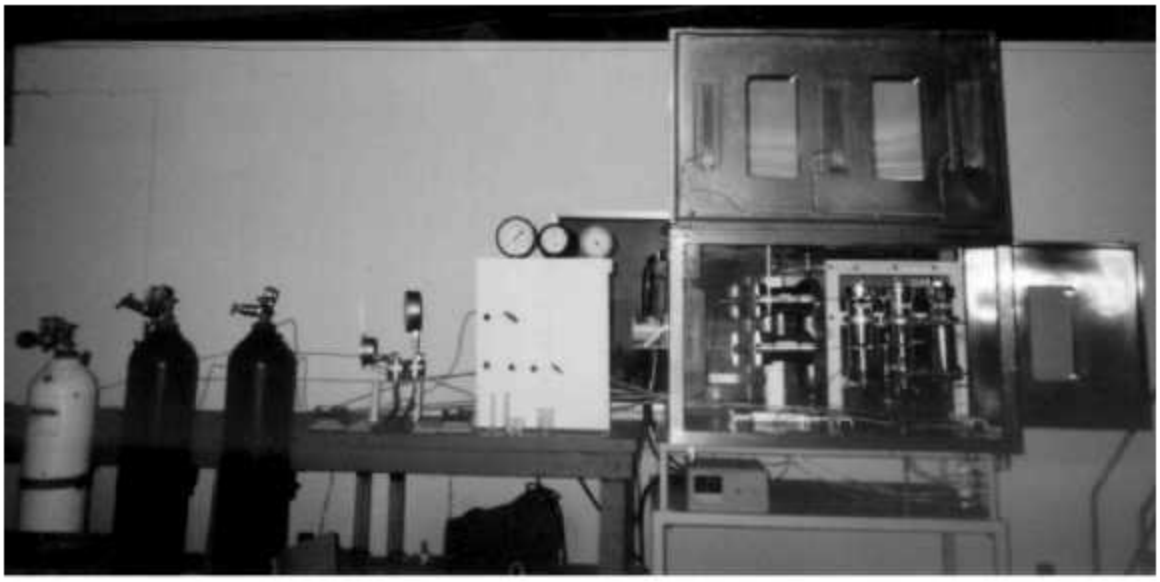

Figure 158. Core plug system with incubator open.

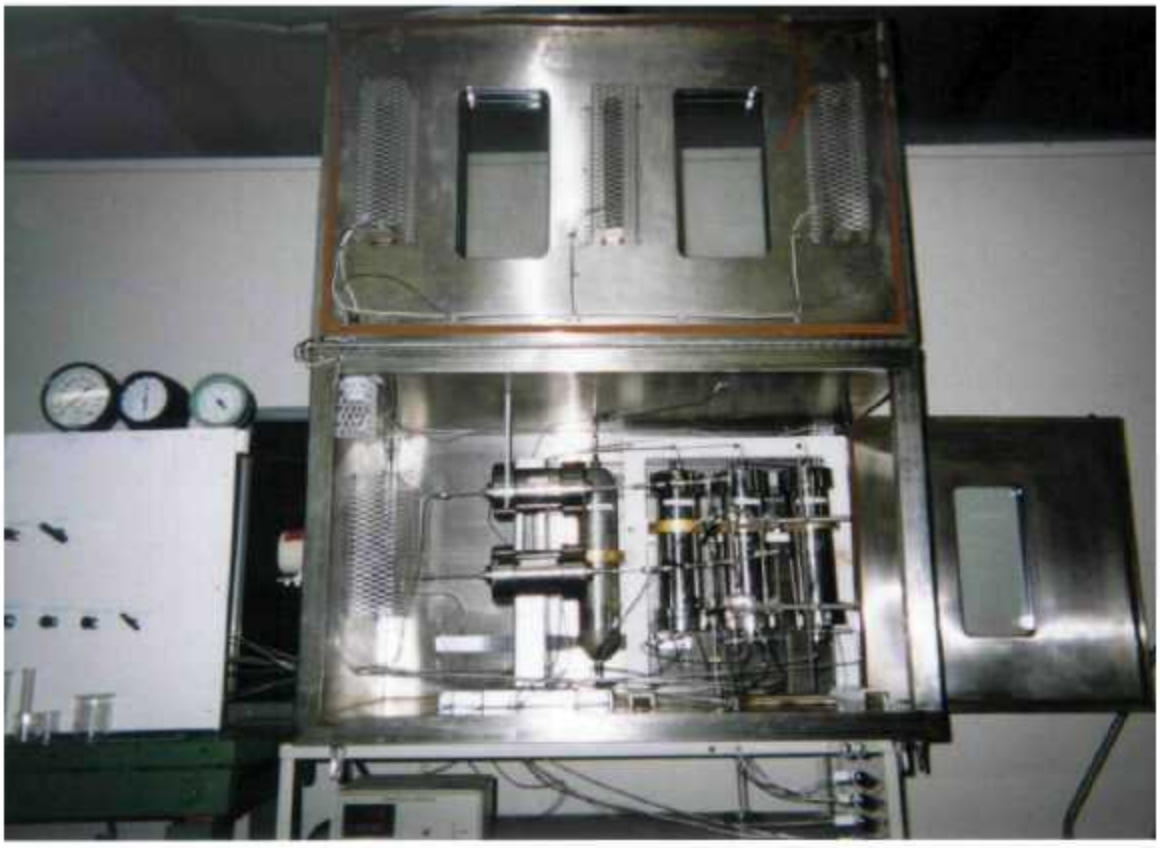

Figure 159. Close up view of opened incubator.
The vertical cylinders hold liquid and the horizontal sleeves hold the cores.

Figure 160. Collection system. Effluent from the cores flows into the graduated cylinders.

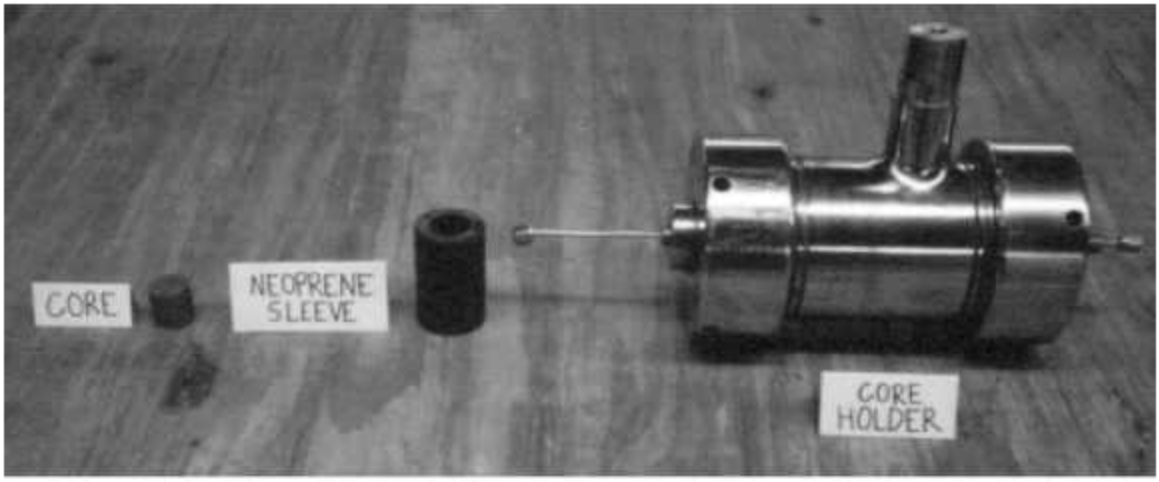

Figure 161. A Hassler sleeve core holder and the neoprene sleeve that holds the core inside the core holder.

Trials of the system were conducted as follows. Two cores measuring 2.5 cm in diameter by 2.7 cm in length were placed in Hassler sleeves in the 90°C oven of the system. An annulus pressure of 350 psi was applied to them. A series of solutions (injection water, injection water containing

phosphate, injection water containing nitrate and a 0.25 µmolar ethanol solution in water) was flushed through each core at 25 psi. The flow rates for each solution through the core were then determined by the time required for 10 ml of solution to flow through the system. The total amount of liquid that flowed through each core was also recorded. The water flow through the cores varied from core to core as expected and in some cases no flow was observed. Generally speaking, the flow rate decreased significantly in all cores and in some cases stopped completely.

Table 11. Treatment of One-inch Core Plugs from the Smackover Formation.

Day	Treatment	Core 1 (ml)	Core 2 (ml)
Monday	Nitrate[1]	100	100
Tuesday	Phosphate[2]	100	100
Wednesday	Nitrate	100	100
Thursday	Phosphate	100	100
Friday	Ethanol[3]	100	0
Friday	Injection Water	0	100
Monday	Nitrate	100	100
Tuesday	Phosphate	100	100
Wednesday	Nitrate	100	100
Thursday	Phosphate	100	100
Friday	Ethanol	100	0
Friday	Injection Water	0	100
Monday	Acetic Acid[4]	100	100
Tuesday	N/A	N/A	N/A
Wednesday	N/A	N/A	N/A
Thursday	N/A	N/A	N/A
Monday	Injection Water	100	100
Tuesday	Injection Water	100	100
Wednesday	Injection Water	100	100
Thursday	Injection Water	100	100
Friday	Acetic Acid	100	100
Monday	Injection Water	100	100
Tuesday	Injection Water	100	100
Wednesday	Injection Water	100	100
Thursday	Injection Water	100	100
Friday	Acetic Acid	100	100

1- Injection water containing nitrate (0.12%)
2- Injection water containing phosphate (0.03%)
3- 0.25 µmolar ethanol in water
4- Acetic acid 1% (v/v) in injection water
N/A – Not applicable

Since the one-inch core plugs that are now being employed do not contain viable micro-organisms that will grow at 90°C, tests for the production of acetic acid from ethanol cannot be conducted at that temperature. Furthermore, there is not a sufficient quantity of the 90°C oil-degrading cultures on hand to inoculate the cores. Therefore, in order to determine the effect of acetic acid on core plugs from the Smackover Formation, the following experiment was conducted. Two one-inch core plugs were placed in Hassler sleeve core holders, the sleeves placed in the core plug system at 90°C, and the core plugs flushed with solutions according to the schedule given in Table 11. The results of this experiment are shown in Figures 160 to 163. It should be noted that the core plugs received the acetic acid solution on three separate occasions.

During some operations, several pieces of the 1/8-inch stainless steel tubing developed leaks and repairs had to be made. After several such experiences, it was concluded that the tubing was defective and new tubing was ordered. In the meantime studies were conducted at 30°C using one-inch core plugs since no tubing breaks have occurred at this temperature. In these studies cores were inoculated with oil-degrading cultures that grow at 30°C. The purpose of these experiments was to determine the optimal concentration of ethanol to be employed.

Figure 162. Inlet end of core plug no. 1 from Smackover Formation after treatment with dilute acetic acid.

Figure 163. Outlet end of core plug no. 1 from Smackover Formation after treatment with dilute acetic acid.

Figure 164. Inlet end of core plug no. 2 from Smackover Formation after treatment with dilute acetic acid.

Figure 165. Outlet end of core plug no. 2 from Smackover Formation after treatment with dilute acetic acid.

Other studies were conducted using small (2.5 mm x 8-9 mm) cores to establish feeding formulations. A sodium nitrate concentration of 0.12% (w/v) and a sodium dihydrogen phosphate concentration of 0.03% (w/v) were found to be satisfactory. Using these

concentrations of nitrate and phosphate, the bacteria were activated and proliferated to the extent that they reduced the flow of injection water. Similarly, a concentration of 0.002% (v/v) ethanol worked effectively for the production of acetic acid. Experimental results suggest that supplemental sodium nitrate for cell maintenance will not be required for at least two months. Figure 166 illustrates the treatment of two limestone cores having different permeabilities with nutrients (nitrate and phosphate) for growth and the subsequent production of acetic acid from ethanol. As may be observed, the permeability in both cores increased with the continued feeding of ethanol over a period of nearly two months. This suggests that after the bacteria are activated they will convert the ethanol to acetic acid without proliferation of numbers to the extent that they begin to block injection water flow.

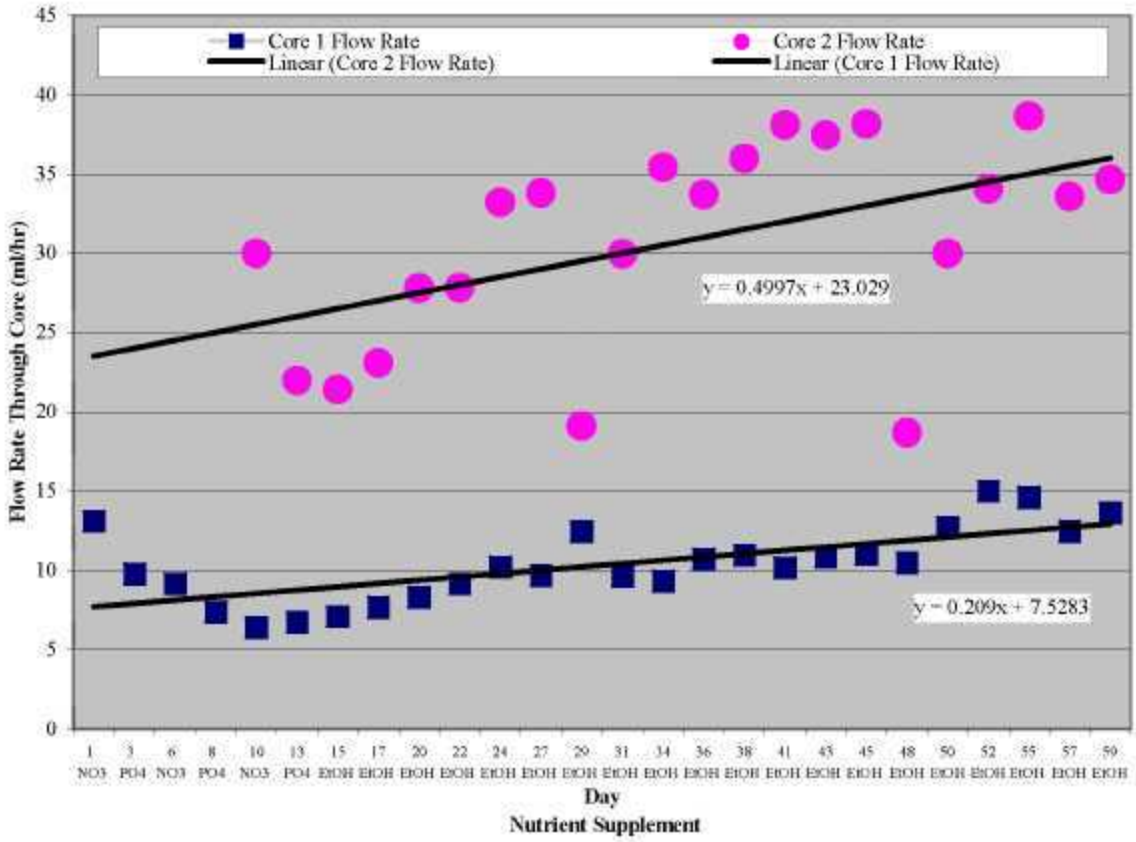

Figure 166. Flow rate of injection water containing various supplements through cores.

Recovery Technology Evaluation

Task RTE-1. Evaluation and Acquisition of 3-D Seismic Data

Description of Work.--This task involves the use of the 3-D geologic model to determine whether there are zones in the Womack Hill Field reservoir where uncontacted oil remains and whether there is attic oil remaining in the field. The task also includes evaluating whether the acquisition of 3-D seismic data is required to confirm the presence of uncontacted oil, including attic oil in the Womack Hill Field and if the 3-D seismic data acquisition is justified by the financial investment. If so, 3-D seismic data will be acquired, processed and interpreted as part of this task to facilitate the implementation of the integrated demonstration project of the Womack Hill Field.

Rationale.--Petroleum companies have been extremely successful in certain areas of the Eastern Gulf Region in exploring for and developing Upper Jurassic Norphlet, Smackover and Haynesville Fields using 3-D seismic data. Utilizing 3-D seismic data, in combination with well logs, has proven to be a powerful tool in imaging Smackover structures and reservoirs in parts of the Eastern Gulf Region. It is anticipated that 3-D seismic imaging of the reservoir structure, in combination with the 3-D geologic model, which incorporates the 3-D structural interpretation of the Womack Hill petroleum trap, will assist in providing the information required to determine whether uncontacted oil and attic oil remain in the Womack Hill Field. SeisWorks is used to perform this task.

Seismic Data.--The results from the geoscientific reservoir characterization and 3-D geologic modeling have been utilized to evaluate areas of the field that would benefit from further assessment by using new seismic data. Four areas were identified from the reservoir characterization and modeling work as priority areas (Fig. 167).

These include the (1) northern part of the northeast quarter of Section 16, south of well Permit #2109, in the unitized portion (western part) of the field, (2) the area around well Permit #4575B in the west-central part of Section 14 in the unitized portion of the field, (3) the northern part of Section 14 and part of the northwest quarter of Section 13, north of well Permits #1804, #1826, #1825 and #1760, in the eastern part of the field, and (4) the center of Section 13, around well Permits #1781 and #1847 and north of well Permit #1811 (dry hole), southwest of well Permit #1713 (dry hole), east of well Permit #1760 (inactive well since 1976 after producing 349,215 barrels, and west of well Permit #2327 (inactive well since 1995 after producing 421,841 barrels), in the eastern part of the field. Well Permit #2109 is a very productive well (cumulative production of 1.703 million barrels), is one of four wells along with well Permits

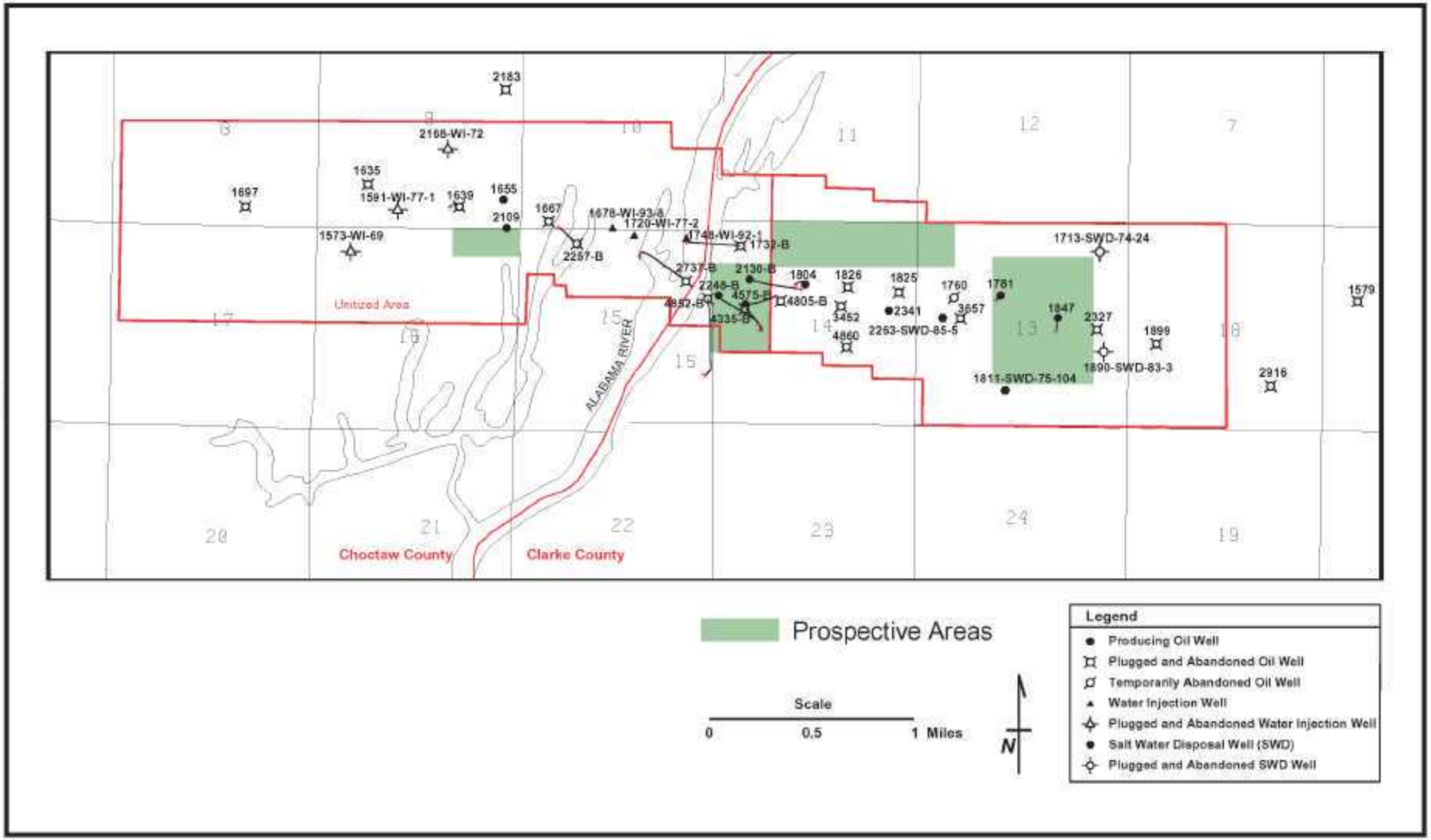

Figure 167. Prospective drilling targets.

#1655, #2248, and #457BB currently producing in the Unit area, and has only been perforated in reservoir zone C. The area south of this well is structurally high and has high potential for unrecovered (attic) oil. The fault trap in this part of the field is the result of a combination of closure against the fault to the south and 3-way dip closure to the north, east and west. Well Permit #4575B is one of the most productive wells in the field (cumulative production of 2.446 million barrels), has not been perforated in zones A, B or C, and is located in the structurally highest part of the field. This part of the field has excellent potential for the recovery of additional oil. Well Permits #1825 (cumulative production of 364,831 barrels and plugged and abandoned in 1978) and #1760 (cumulative production of 349,215 barrels and plugged and abandoned in 1976) are marginally productive; however, productive well Permit #1826 (cumulative production of 981,820 barrels but plugged and abandoned in 1991) located also to the south of the prospective area in Section 14 and the northwest quarter of Section 13 has only been perforated in reservoir zone A. Very productive well Permit #1781 (cumulative production of 1.962 million barrels, currently producing and perforated only in reservoir zone A) and very productive well Permit #1847 (cumulative production of 1.919 million barrels, currently producing and perforated only in reservoir zone B) are located to east of the prospective area, and well Permit #1804 (cumulative production of 3.374 million barrels, currently producing and the most productive well in the field) is located to the southwest of the prospective area. The prospective area in Section 14 and the northwest quarter of Section 13, therefore, has high potential for unrecovered oil. The trap in this part of the field is a salt anticline with 4-way dip closure, and the prospective area appears to be structurally high to the area of well Permits #1781 and #1847 located to the east and to the area of well Permits #1826, #1825 and #1760 located to the south. The prospective area in the center of Section 13 has high potential for

unrecovered oil in that this area includes the very productive well Permits #1781 and #1847. Only well Permits #1804, #1781, #1847, #2341 and #12762 are currently producing in the eastern area of the Womack Hill Field.

The project management team met at the offices of Pruet Production Co. on February 6, 2003, to review the project results to date. The team concluded that at least four areas of the Womack Hill Field were prospective for the recovery of additional oil from the field. Two of the prospective areas in the Unit area probably could be drained by perforating porous and permeable zones in the upper part of the reservoir in well Permits #2109 and #4575B, respectively. The prospective areas in the eastern part of the field in Section 14 and Section 13 will require the drilling of new wells. The acquisition of new 2-D or 3-D seismic data are required to locate strategically the drill sites of the new wells. J. R. Pounds, Inc. drilled a new well in Section 14 in a prospective area immediately northwest of well Permit #1826. This well Permit #12762 tested 160 barrels of oil on January 4, 2003. Pruet, therefore, decided to focus on the prospective area in the center of Section 13, as a potential infill drilling site.

Pruet Production Co. contracted with Boone Exploration, Inc., for the acquisition of new seismic data for an area in the eastern part of Womack Hill Field (Fig. 168). However, we estimated that the acquisition, processing, interpretation and evaluation of the new seismic data would require several months of work beyond the scheduled completion date of Phase I of the project. The drill site location selection for a new well in the field would require additional months of work. The project team members, including Pruet Production Co., were interested in drilling this new well in the field if the seismic data confirm that additional commercial quantities of oil could be recovered from the field. A no-cost extension for Phase I of the project was requested and granted by DOE to complete this work.

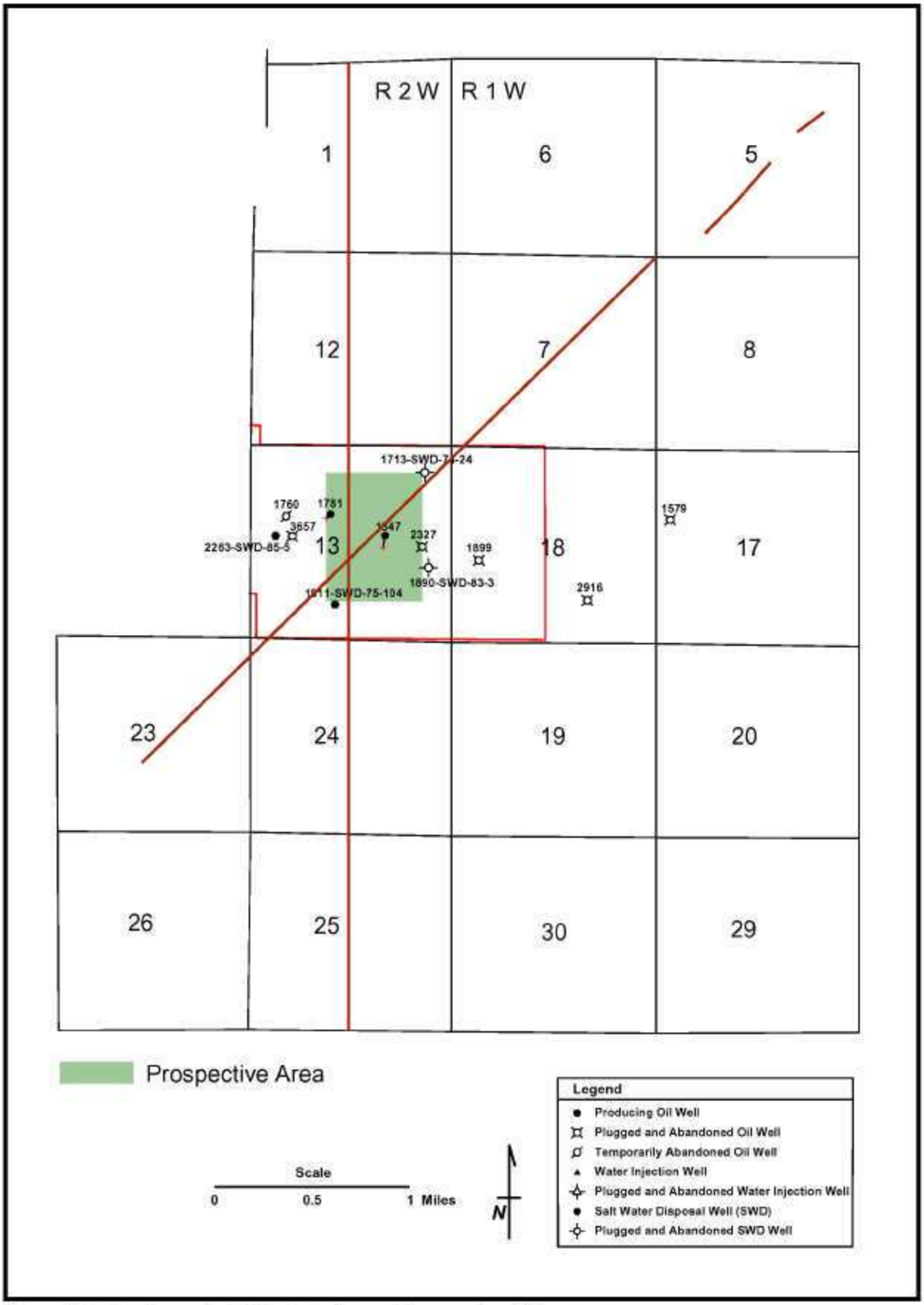

Figure 168. Newly acquried 2-D seismic lines and prospective drilling targets.

Seismic Data Acquisition.--The University of Alabama requested a no-cost extension on February 13, 2003, to acquire new 2-D or 3-D seismic data from the Womack Hill Field to assist Pruet Production Co. in their decision-making process of whether and where to drill a new well in the Womack Hill Field. The no-cost extension was granted by DOE to September 30, 2003.

Pruet decided to acquire new high-quality 2-D seismic data rather than 3-D seismic data for a portion of the eastern part of Womack Hill Field. Their decision was based on their experience and the recent experiences of others that have shown that the fault shadow associated with the major fault in Choctaw and Clarke Counties, Alabama (southern bounding fault at Womack Hill Field), caused imaging problems which could result in the drilling of a dry hole. Pruet believes that high quality 2-D seismic data would be effective for determining whether they could drill a new productive well in the Womack Hill Field.

DOE was first informed verbally of Pruet's decision and received in writing on September 16, 2003, a request to approve the acquisition of 2-D rather than 3-D seismic data for a portion of the Womack Hill Field area. DOE expressed support for this modification in the Phase I project work tasks for Budget Period 1 (acquiring 2-D rather than 3-D seismic data) on September 17, 2003. DOE also granted a no-cost extension of Phase I of the project to December 31, 2003 to complete this work.

Boone Exploration, Inc. of Huntsville, Texas, completed the field acquisition of two high-quality 2-D seismic lines in Womack Hill Field. Boone Geophysical used its Opseis Eagle radio telemetry system to record the data with the following parameters:

Instrumentation	Opseis Eagle
Source	Dynamite
Charge size	5.5# Pentolite, single capped
Source array	Single hole
Hole depth	100'-150' range
Source interval	330'
Receiver interval	110'
Sample rate	2 MS
Record length	6 seconds
# Geophones per group	6
Total shotpoints	160
Total stations	470

Line one is a NE-SE line. The length of the line is 4.8125 miles, and it contains 231 stations (Fig. 168). Maximum fold is 101 and average fold is 58. The line runs through Sections 5 and 7, T. 10 N., R. 1 W. and Sections 13 and 23, T. 10 N., R. 2 W., Clarke County. Line two is a N-S line. The length of the line is 4.9792 miles, and it contains 239 stations. Maximum fold is 82 and average fold is 60. The line runs through Sections 1, 12, 13, 24 and 25, T. 10 N., R. 2 W., Clarke County.

Geo-Seis Processing, Inc. of Pearl, Mississippi, processed the data. Geo-Seis processed the data with a 4-millisecond sample rate through the DMO migration stage.

Pruet's seismic interpreter describes the data as better by far than previous data shot in the Womack Hill Field area. There is still a fault shadow effect from the major fault to the south but that was expected. The interpretation and integration of the seismic data with well log control has been completed.

Task RTE-2. Evaluation of the Pressure Maintenance Project

Description of Work.—This task is designed to evaluate the effectiveness of the existing pressure maintenance activities being conducted at Womack Hill Field Unit. Efforts will be made to evaluate pressure and fluid communication in the field and to review injection/production behavior to verify pressure support in a particular area. The short-term goal of this work is to determine if modifications are required for the injection strategy. The

long-term goal is to establish the practices and procedures for implementing optimal pressure maintenance.

Rationale.--Profitability is currently down at Womack Hill Field Unit because production is declining and the cost of operations is escalating. The operator has cited water loss due to the heterogeneous nature of the Smackover reservoir as a major source of the production decline. Modification of the existing pressure maintenance project and/or the addition of an advanced oil recovery technology has the potential to extend the life of this reservoir by increasing profitability.

Multiwell Productivity Analysis.--The multiwell productivity analysis approach provides a mechanism to assess the performance of wells relative to one another. The major limitation to the Valko et al. (2000) method, which is used to perform this analysis, is that this method presumes that pseudosteady-state flow conditions exist in the entire reservoir sequence. This is generally a reasonable assumption; however, in the case with the reservoir at Womack Hill Field the production is influenced substantially by water injection in the western unitized part of the field and water influx in the eastern (non-unitized) part of the field where a strong water drive exists. These conditions are not modeled by the Valko et al. (2000) method. Thus, the application of this method to Womack Hill Field indicates that the production performance for each well in the field is increasing with time. This probably is not the case. Examination of the water injection and observed water influx behavior clarifies this observation. The boundaries for this analysis are presented in Table 12 and the results of the analysis are included in Figures 169 through 197. Figure 169 represents the case of total (oil and water) rates, and Figure 170 summarizes the results generated by using only the oil rates.

Table 12

Reservoir, Fluid and Production Parameters for the Dimensionless Multiwell Performance Index (*DMPI*) — Womack Hill Field (Alabama, USA)

Reservoir Properties:	
Wellbore radius, r_w	= 0.33 ft
Average net pay thickness, h	= 104 ft
Formation permeability, k	= 0.3 md
Average porosity, ϕ	= 0.132 (fraction)
Total reservoir dimensions	= 20,930 ft by 4,000 ft
Initial reservoir pressure, p_i	= 5500 psia
Fluid properties:	
Oil formation volume factor, B_o	= 1.36 RB/STB
Oil viscosity, μ_o	= 0.4 cp
Production parameters:	
Constant bottomhole pressure, p_{wf}	= 100 psia (assumed)

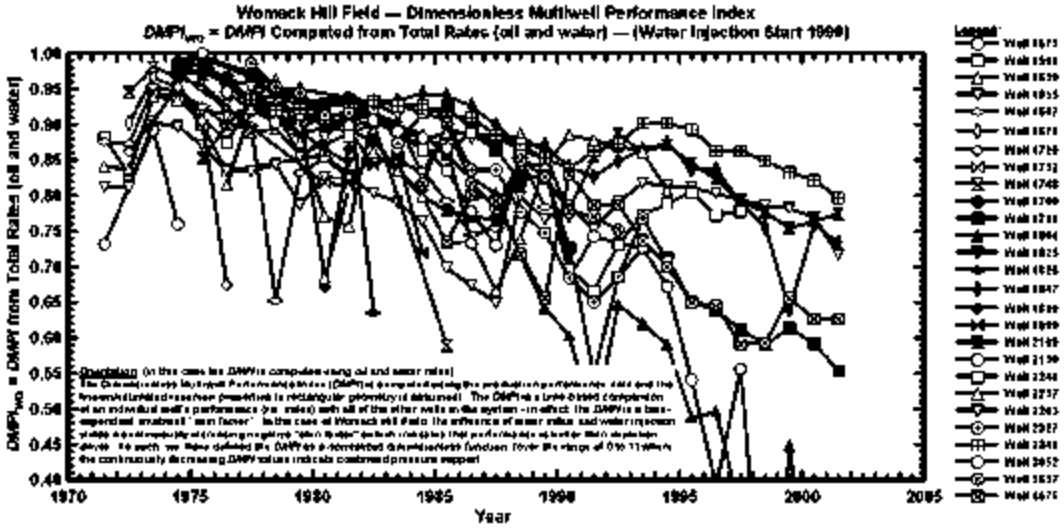

Figure 169 — Dimensionless multiwell performance index (*DMPI*) computed for Womack Hill Field — Total rates (oil and water) are used in this calculation.

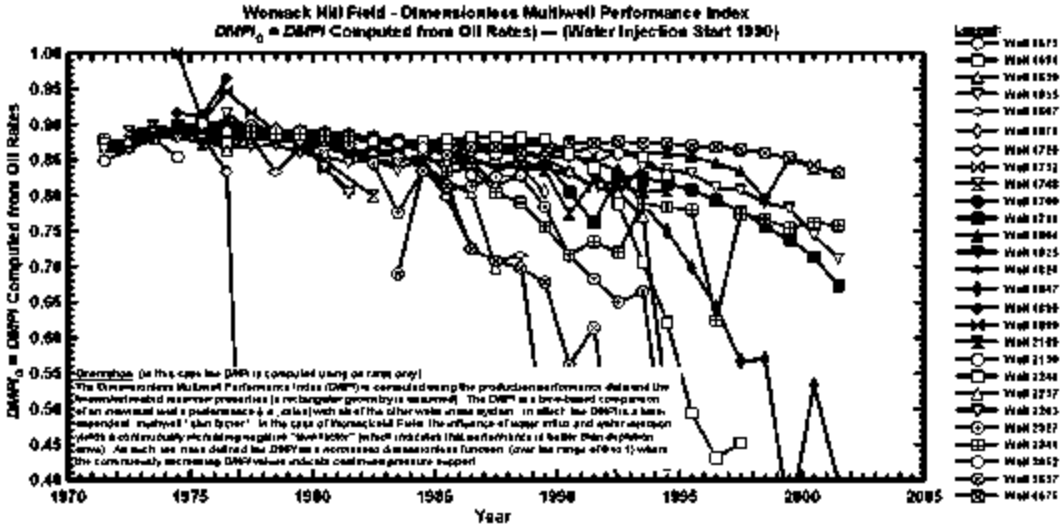

Figure 170 — Dimensionless multiwell performance index (*DMPI*) computed for Womack Hill Field — Oil rates are used in this calculation.

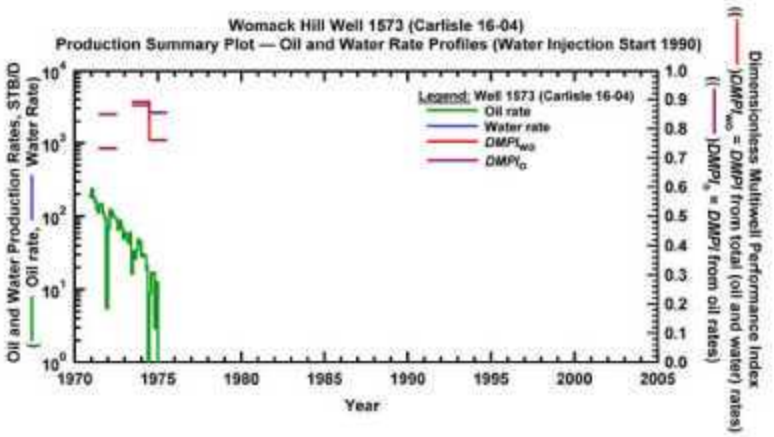

Figure 171 — Plot of the dimensionless multiwell performance index (*DMPI*) (total and oil rate cases) and the oil and water production rate histories — Womack Hill We11 1573.

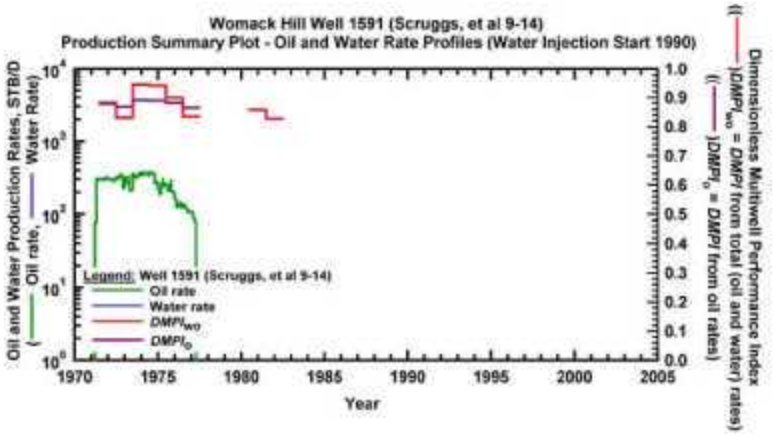

Figure 172 — Plot of the dimensionless multiwell performance index (*DMPI*) (total and oil rate cases) and the oil and water production rate histories — Womack Hill We11 1591.

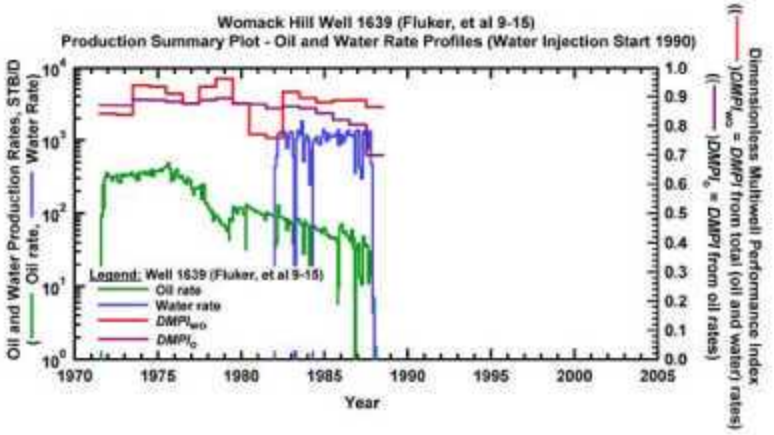

Figure 173 — Plot of the dimensionless multiwell performance index (*DMPI*) (total and oil rate cases) and the oil and water production rate histories — Womack Hill We11 1639.

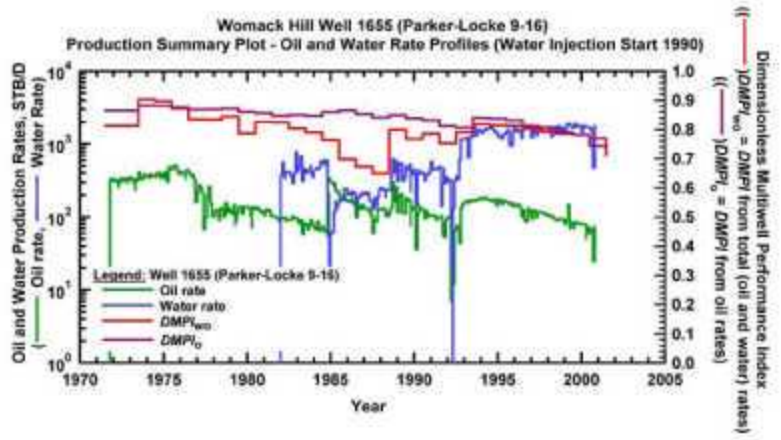

Figure 174 — Plot of the dimensionless multiwell performance index (*DMPI*) (total and oil rate cases) and the oil and water production rate histories — Womack Hill We11 1655.

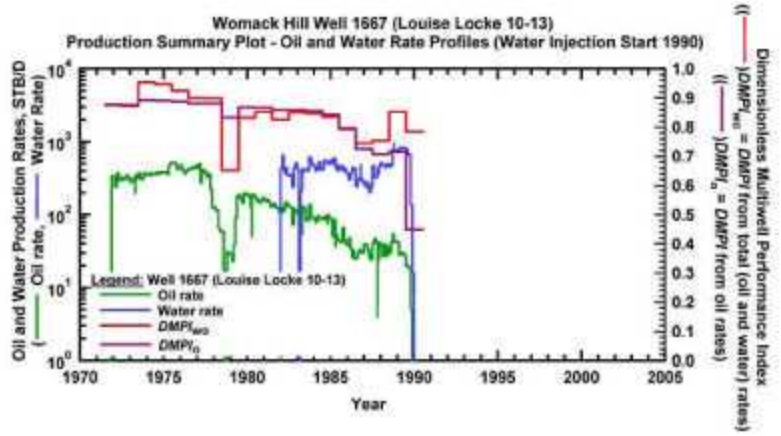

Figure 175 — Plot of the dimensionless multiwell performance index (*DMPI*) (total and oil rate cases) and the oil and water production rate histories — Womack Hill We11 1667.

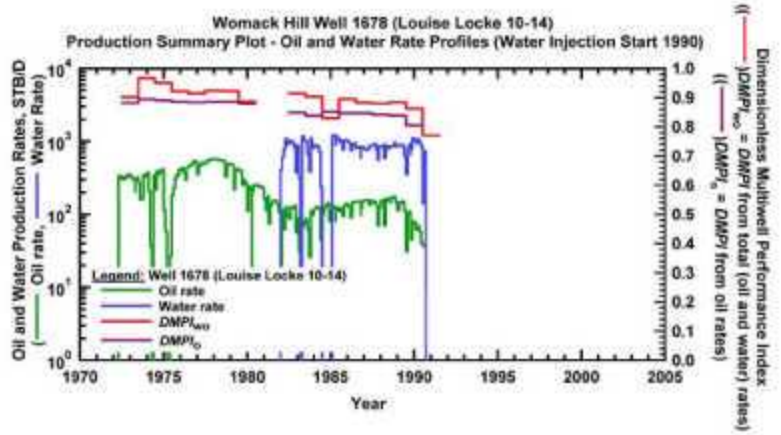

Figure 176 — Plot of the dimensionless multiwell performance index (*DMPI*) (total and oil rate cases) and the oil and water production rate histories — Womack Hill We11 1678.

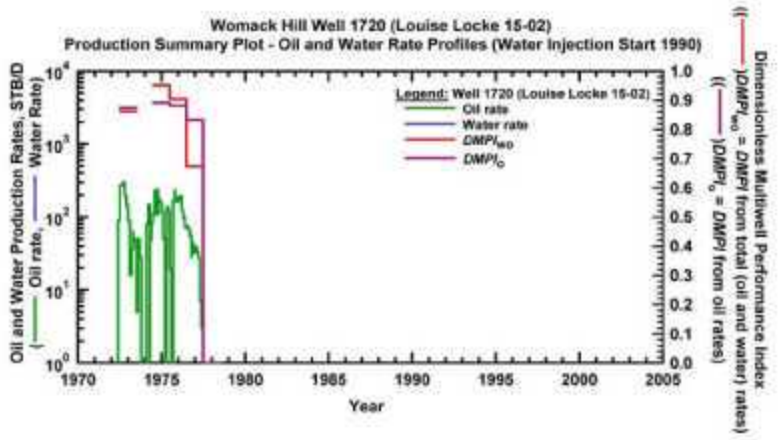

Figure 177 — Plot of the dimensionless multiwell performance index (*DMPI*) (total and oil rate cases) and the oil and water production rate histories — Womack Hill We11 1720.

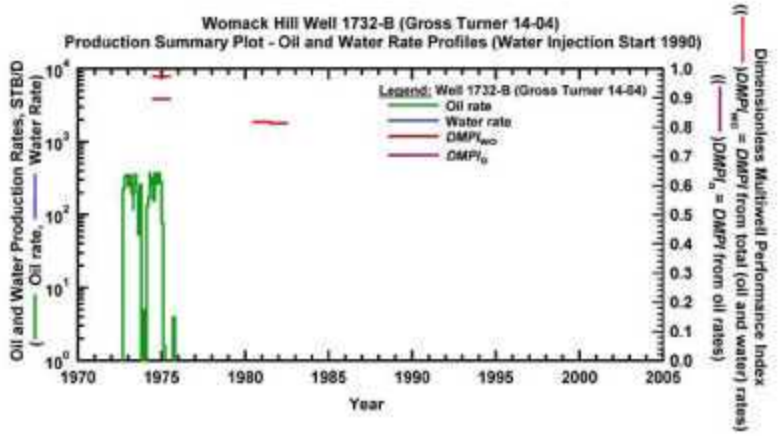

Figure 178 — Plot of the dimensionless multiwell performance index (*DMPI*) (total and oil rate cases) and the oil and water production rate histories — Womack Hill We11 1732.

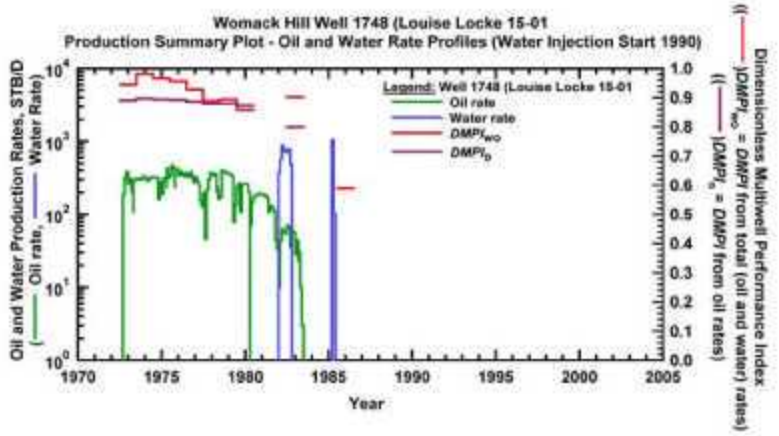

Figure 179 — Plot of the dimensionless multiwell performance index (*DMPI*) (total and oil rate cases) and the oil and water production rate histories — Womack Hill We11 1748.

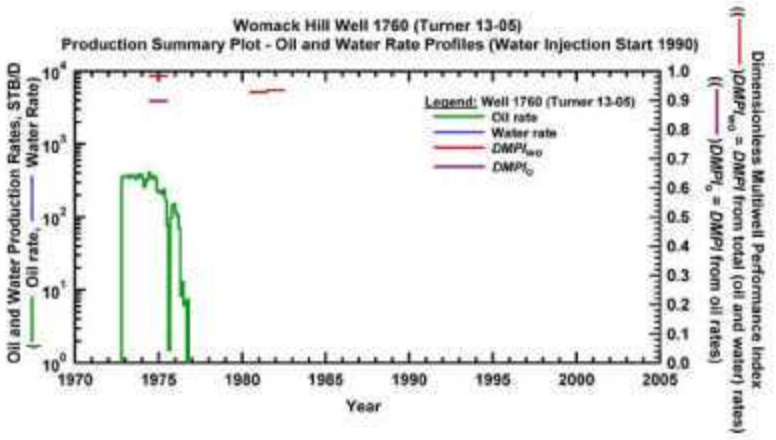

Figure 180— Plot of the dimensionless multiwell performance index (*DMPI*) (total and oil rate cases) and the oil and water production rate histories — Womack Hill We11 1760.

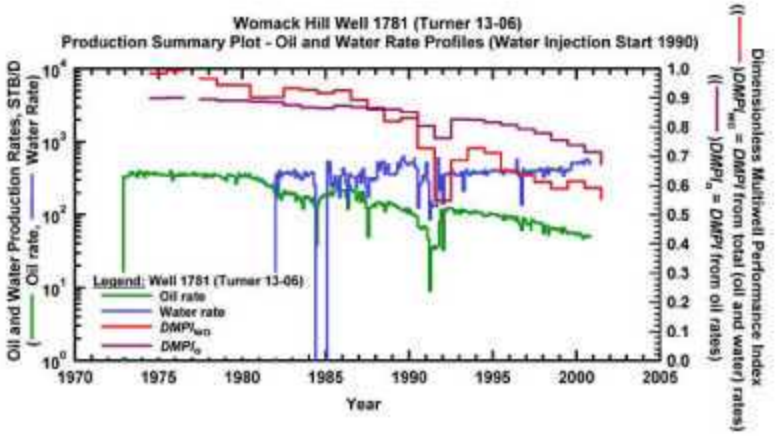

Figure 181 — Plot of the dimensionless multiwell performance index (*DMPI*) (total and oil rate cases) and the oil and water production rate histories — Womack Hill We11 1781.

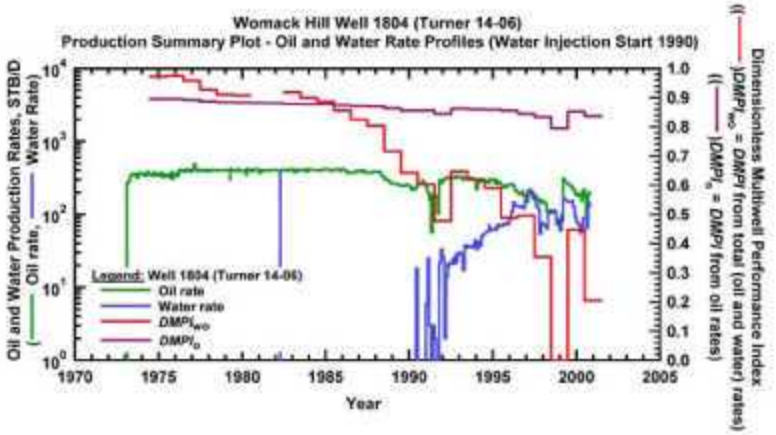

Figure 182— Plot of the dimensionless multiwell performance index (*DMPI*) (total and oil rate cases) and the oil and water production rate histories — Womack Hill We11 1804.

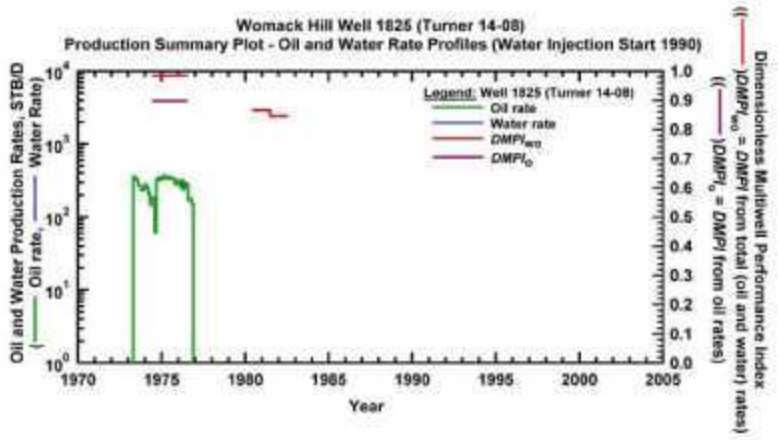

Figure 183 – Plot of the dimensionless multiwell performance index (*DMPI*) (total and oil rate cases) and the oil and water production rate histories — Womack Hill We11 1825.

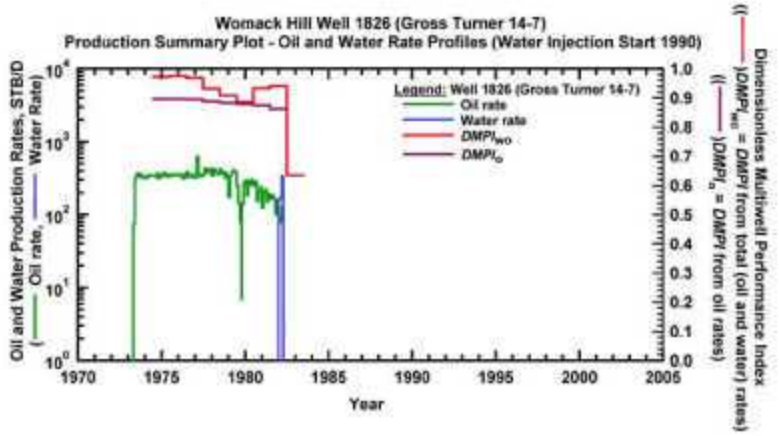

Figure 184 — Plot of the dimensionless multiwell performance index (*DMPI*) (total and oil rate cases) and the oil and water production rate histories — Womack Hill We11 1826.

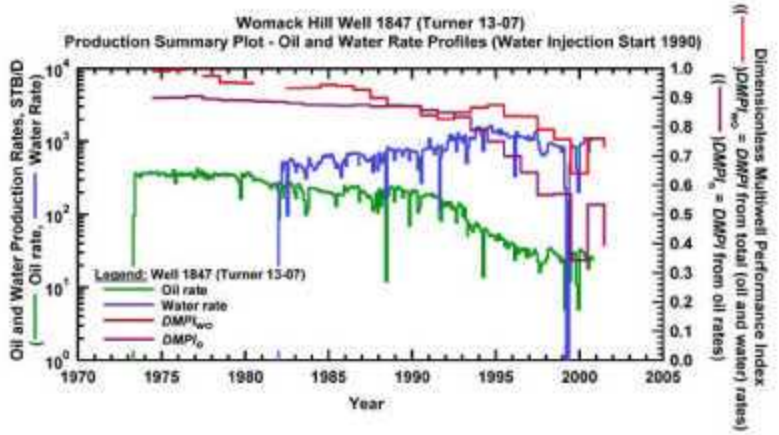

Figure 185 — Plot of the dimensionless multiwell performance index (*DMPI*) (total and oil rate cases) and the oil and water production rate histories — Womack Hill We11 1847.

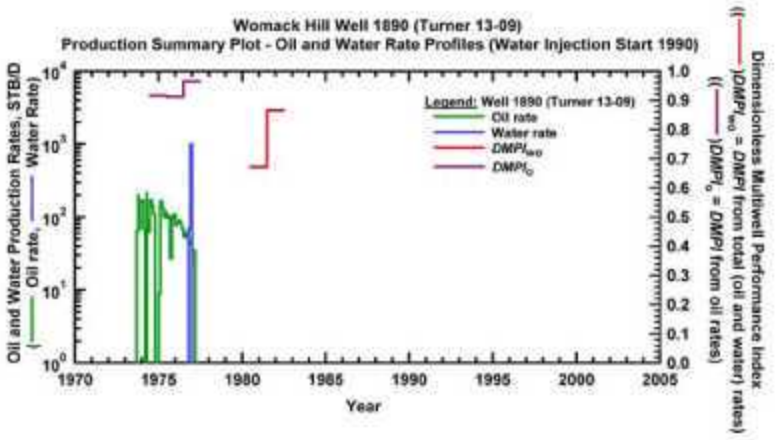

Figure 186— Plot of the dimensionless multiwell performance index (*DMPI*) (total and oil rate cases) and the oil and water production rate histories — Womack Hill We11 1890.

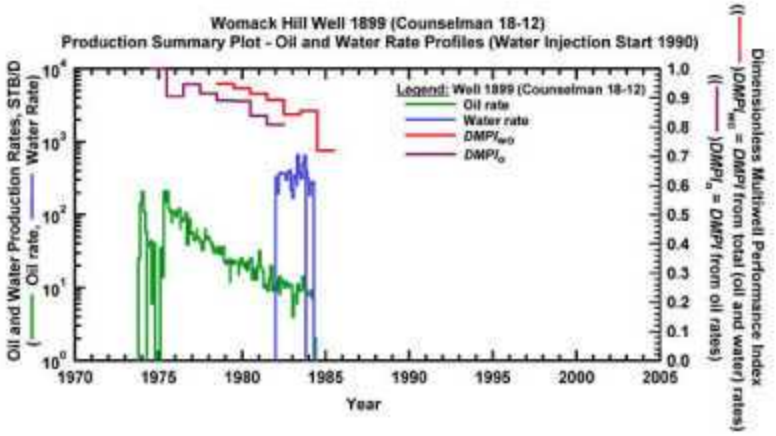

Figure 187 — Plot of the dimensionless multiwell performance index (*DMPI*) (total and oil rate cases) and the oil and water production rate histories — Womack Hill We11 1899.

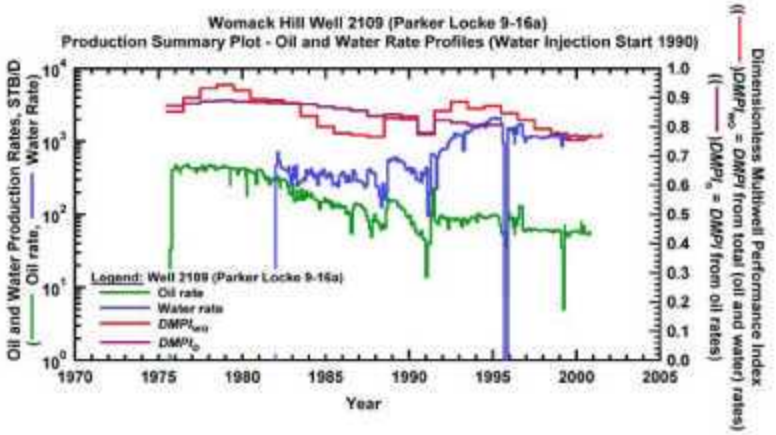

Figure 188— Plot of the dimensionless multiwell performance index (*DMPI*) (total and oil rate cases) and the oil and water production rate histories — Womack Hill We11 2109.

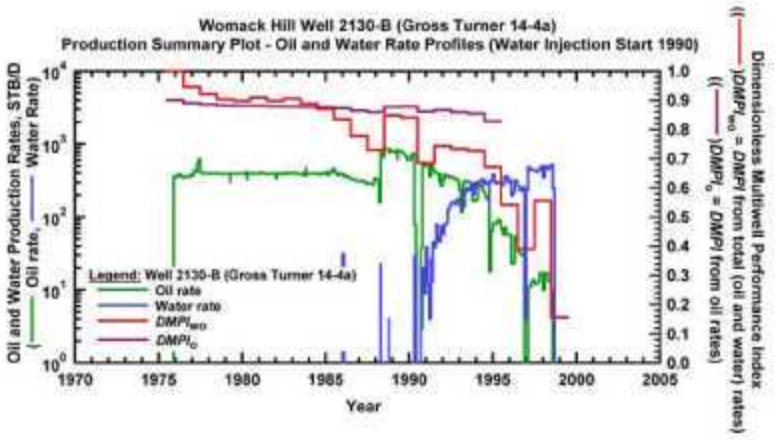

Figure 189 — Plot of the dimensionless multiwell performance index (*DMPI*) (total and oil rate cases) and the oil and water production rate histories — Womack Hill We11 2130.

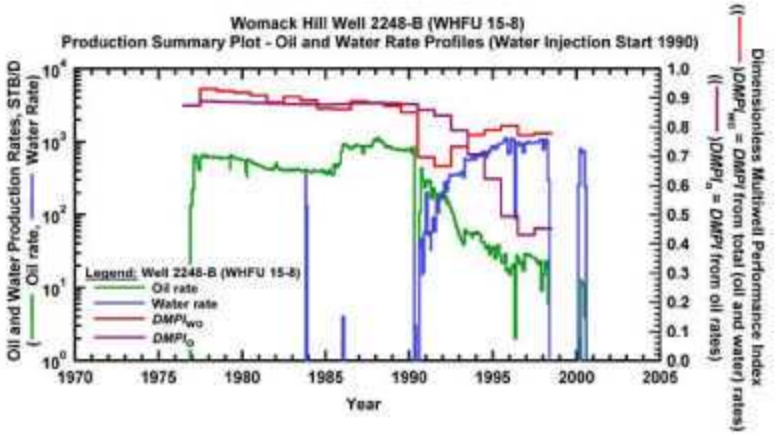

Figure 190— Plot of the dimensionless multiwell performance index (*DMPI*) (total and oil rate cases) and the oil and water production rate histories — Womack Hill We11 2248.

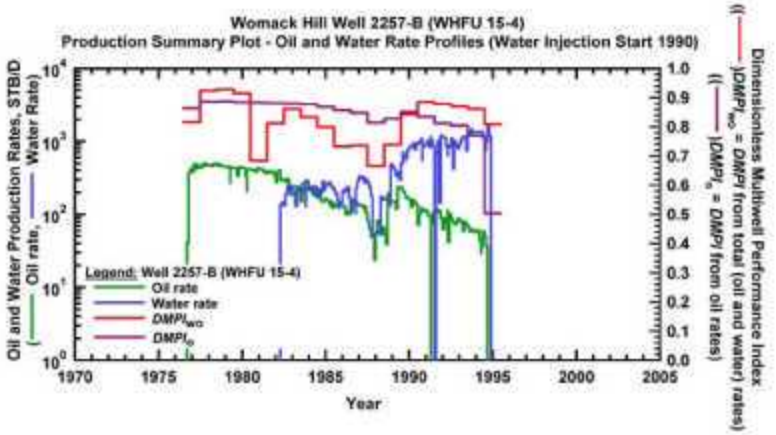

Figure 191— Plot of the dimensionless multiwell performance index (*DMPI*) (total and oil rate cases) and the oil and water production rate histories — Womack Hill We11 2257.

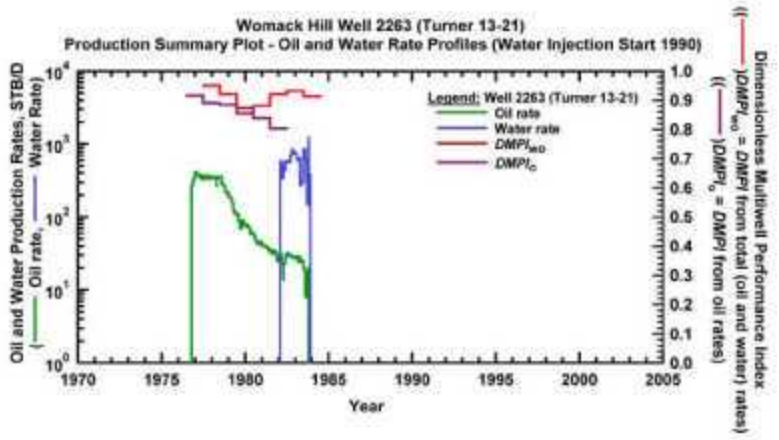

Figure 192— Plot of the dimensionless multiwell performance index (*DMPI*) (total and oil rate cases) and the oil and water production rate histories — Womack Hill We11 2263.

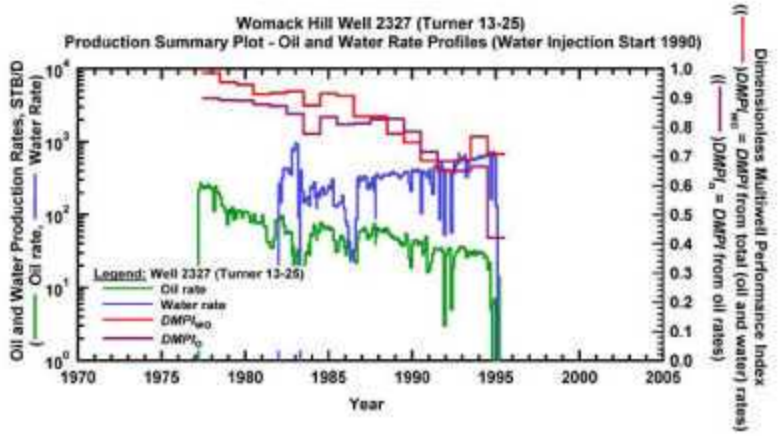

Figure 193— Plot of the dimensionless multiwell performance index (*DMPI*) (total and oil rate cases) and the oil and water production rate histories — Womack Hill We11 2327.

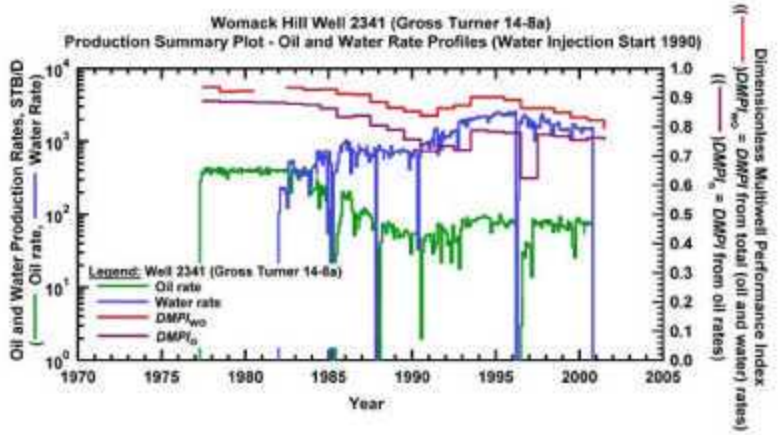

Figure 194— Plot of the dimensionless multiwell performance index (*DMPI*) (total and oil rate cases) and the oil and water production rate histories — Womack Hill We11 2341.

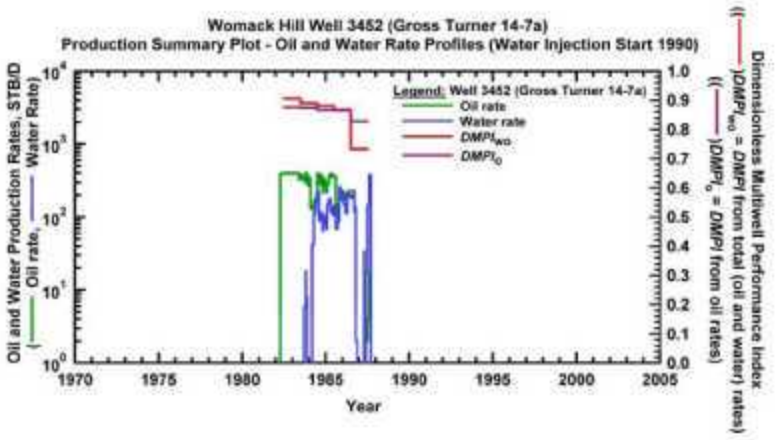

Figure 195— Plot of the dimensionless multiwell performance index (*DMPI*) (total and oil rate cases) and the oil and water production rate histories — Womack Hill We11 3452.

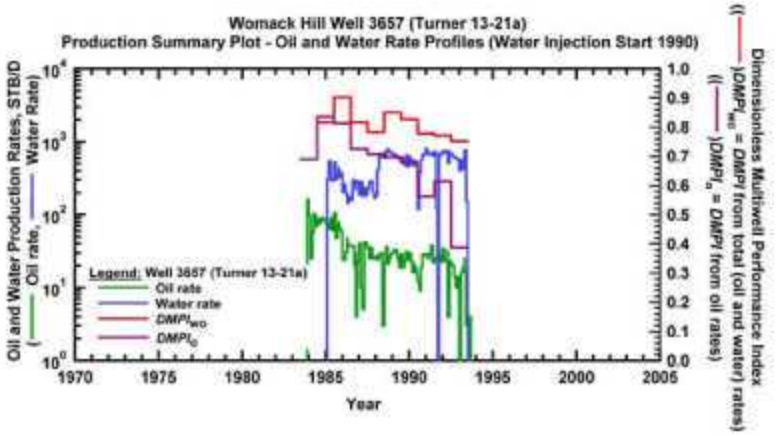

Figure 196— Plot of the dimensionless multiwell performance index (*DMPI*) (total and oil rate cases) and the oil and water production rate histories — Womack Hill We11 3657.

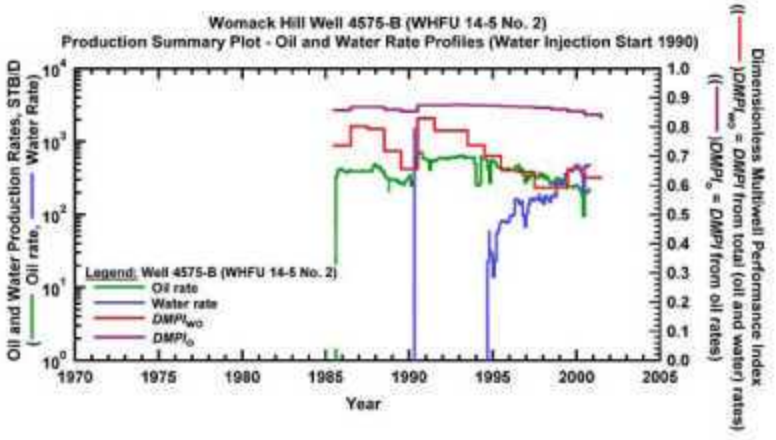

Figure 197 — Plot of the dimensionless multiwell performance index (*DMPI*) (total and oil rate cases) and the oil and water production rate histories — Womack Hill We11 4575.

The results from this analysis show that the dimensionless multiwell performance index (DMPI) is a useful method in identifying and evaluating the effect of water injection and water influx in Womack Hill Field even though this method was not designed to consider these effects specifically. For example, the DMPI based on total production (oil and water) rates is almost linear with time for well Permit #1781 which began production in 1973 and continues to be a producing well in the eastern part of the field (Fig. 181). This trend indicates that water support is stable. Thus, the historical water production data for this well indicates that well Permit #1781 has experienced strong water support. This well is in the eastern part (non-unitized) of the Womack Hill Field where a strong water drive exists. The DMPI based on oil rates shows a continuous decrease with time for well Permit #1655 which began production in 1971 and continues to be a producing well in the Unit area (Fig. 174). This trend indicates the performance of the well is affected by combination of pressure support as well as other wells coming on and off of production. This well is in the western part (unitized) of the Womack Hill Field. The unitized area is experiencing support by means of pressure maintenance through water injection. Therefore, the DMPI method shows the strong influence natural water influx and water injection have had on sustaining well production performance at Womack Hill Field.

Correlation of Production Performance.--Results from the analysis of the production data for each well in Womack Hill Field is summarized in Table 13. By using the correlation of production behavior as a mechanism, a "type rate plot" or generic model for production at this field can be established. However, no single model resulted, but rather we were able to correlate production behavior for each well relative to an exponential or harmonic rate model. The "type curve" models for the exponential and harmonic rate profiles are shown in Figure 198. A histogram with a distribution model for the summary analyses of the initial production rate for

Table 13

Summary Correlation of Production Performance (Model Comparison) — Womack Hill Field (Alabama, USA)

Well	Unit	Rate Decline Model	q_i (STB/D)
Well 1573 (Carlisle 16-04)	West	Exponential	200
Well 1591 (Scruggs, et al 9-14)	West	Harmonic	350
Well 1639 (Fluker, et al 9-15)	West	Exponential	475
Well 1655 (Parker-Locke 9-16)	West	Harmonic	340
Well 1667 (Louise Locke 10-13)	West	Exponential	575
Well 1678 (Louise Locke 10-14)	West	Exponential	475
Well 1720 (Louise Locke 15-02)	West	Exponential	300
Well 1732-B (Gross Turner 14-04)	West	Exponential	380
Well 1748 (Louise Locke 15-01	West	Exponential	350
Well 1760 (Turner 13-05)	East	Exponential	420
Well 1781 (Turner 13-06)	East	Exponential	410
Well 1804 (Turner 14-06)	East	Harmonic	500
Well 1825 (Turner 14-08)	East	Exponential	400
Well 1826 (Gross Turner 14-7)	East	Exponential	410
Well 1847 (Turner 13-07)	East	Exponential	440
Well 1890 (Turner 13-09)	West	Exponential	220
Well 1899 (Counselman 18-12)	West	Exponential	250
Well 2109 (Parker Locke 9-16a)	West	Exponential	480
Well 2130-B (Gross Turner 14-4a)	West	Exponential	425
Well 2248-B (WHFU 15-8)	West	Exponential	550
Well 2257-B (WHFU 15-4)	West	Exponential	490
Well 2263 (Turner 13-21)	East	Exponential	450
Well 2327 (Turner 13-25)	East	Harmonic	190
Well 2341 (Gross Turner 14-8a)	West	Exponential	450
Well 3452 (Gross Turner 14-7a)	East	Exponential	420
Well 3657 (Turner 13-21a)	East	Harmonic	180
Well 4575-B (WHFU 14-5 No. 2)	West	Exponential	875

The statistics for this analysis.

Statistics: n=27

Median q_i Value	= 420 STB/D
Average q_i Value	= 407.6 STB/D
Standard Deviation	= 142.5 STB/D

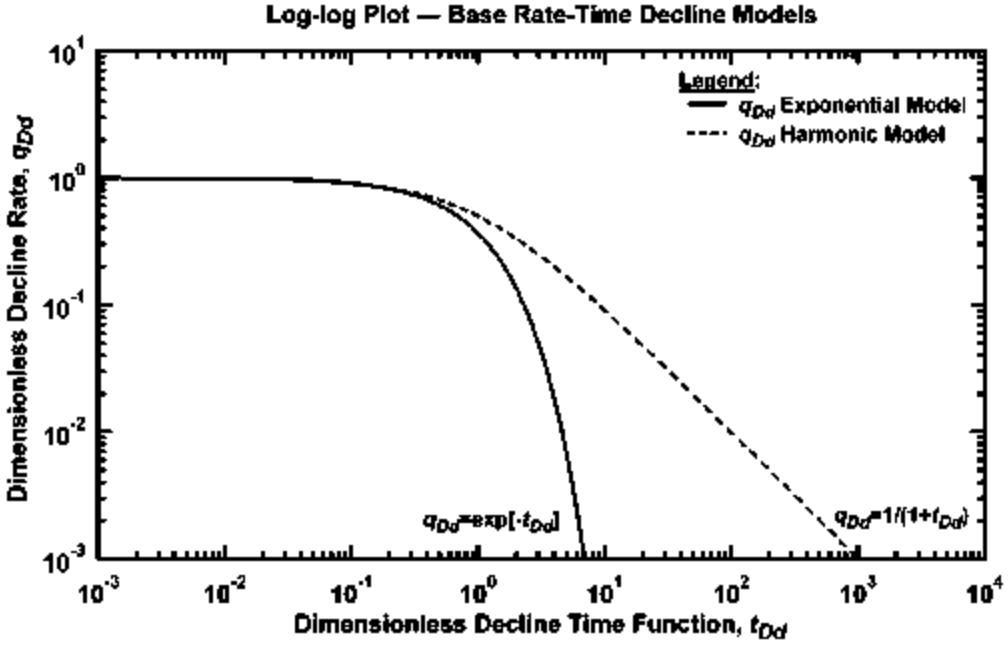

Figure 198 — Dimensionless production rate-time "type curve" — exponential and harmonic rate decline models.

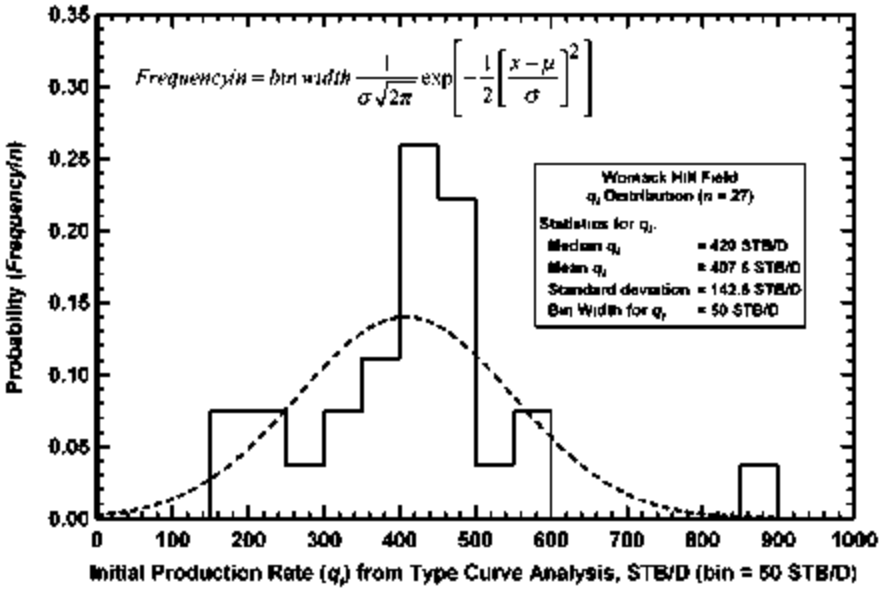

Figure 199 — Histogram of "Initial Production Rate" (q_i) determined using the dimensionless production rate-time "type curve." In this work the selection of the exponential or harmonic rate decline models was based on whichever model appeared to best fit the data.

all wells in the Womack Hill Field is presented in Figure 199. The average initial production rate in the field for the 27 wells studied is on the order of 400 STB/D. Summary plots for exponential and harmonic rate cases for the western unitized part of Womack Hill Field are given in Figures 200 and 201. Summary plots for exponential and harmonic rate cases for the eastern part of the field are shown in Figures 202 and 203. Rate-time plots and dimensionless rate-time "type curve" plots for individual wells for Womack Hill Field are presented in Figures 204 to 257.

Effectiveness of the Pressure Maintenance Program.--To evaluate the effectiveness of the pressure maintenance program involving water injection, Figures 258-261 were constructed. Associations between water production and injection are evident in Figure 258 for the western unitized area of the field. A correlation of oil production, water injection, and "Top of Smackover" is shown in Figure 259. This figure shows that the best oil production in the field is correlated with reservoir structure (*i.e.*, the "Top of Smackover"). Water injection also appears to be correlated with oil production, and we have classified oil production as having "strong," "good," or "no evidence" of water injection support in Figure 260. This correlation is drawn from observations taken from Figure 259, but is confirmed independently in the data cross plot (*EUR* versus oil permeability from decline curve analysis (k_o)) as shown in Figure 260. This classification/correlation is not perfect, but does at least confirm the apparent relation of water injection and enhanced oil production. The conclusion which can be drawn from this comparison is that water injection, reservoir structure, and effective permeability to oil have an influence on oil recovery. In examining the injection pressure history for Womack Hill Field in Figure 261, it can be concluded (at least qualitatively) that the area under injection in the western unitized area of the field was in some hydraulic communication for most of the last 10

years (note the similarity of the injection pressure profiles during this time period). It is, therefore, recommended that water injection should be continued and conducted down-dip and focused (generally) towards regions of the field which are structurally low to maximize the effect of water injection for pressure maintenance.

Task RTE-3. Evaluation of the Immobilized Enzyme Technology Project Concept

Description of Work.--This task involves the evaluation of the laboratory results of the proposed immobilized enzyme technology (IET) project at Womack Hill Field Unit to determine whether it is feasible to implement an IET field-scale demonstration project at Womack Hill Field Unit.

Rationale.--MEOR technology has been determined to be profitable at North Blowhorn Creek Field Unit, Alabama. The reservoir at this field is a sandstone at a depth of –2,300 ft. The application of this biological technology to Smackover carbonates at a depth of 11,300 ft has the potential to increase oil production at Womack Hill Field Unit, thereby increasing profitability and saving this endangered mature field from premature abandonment.

Evaluation of Laboratory Results.--Bacteria that grow at 90°C have been found in well cuttings from an oil field near Womack Hill Field. These bacteria convert ethanol to an acid that reacts with carbonates. Standard petrographic, laser-confocal, and scanning electron microscope techniques to image organic/inorganic relationships in reservoir carbonates have been developed and tested. Dissolution experiments have been performed.

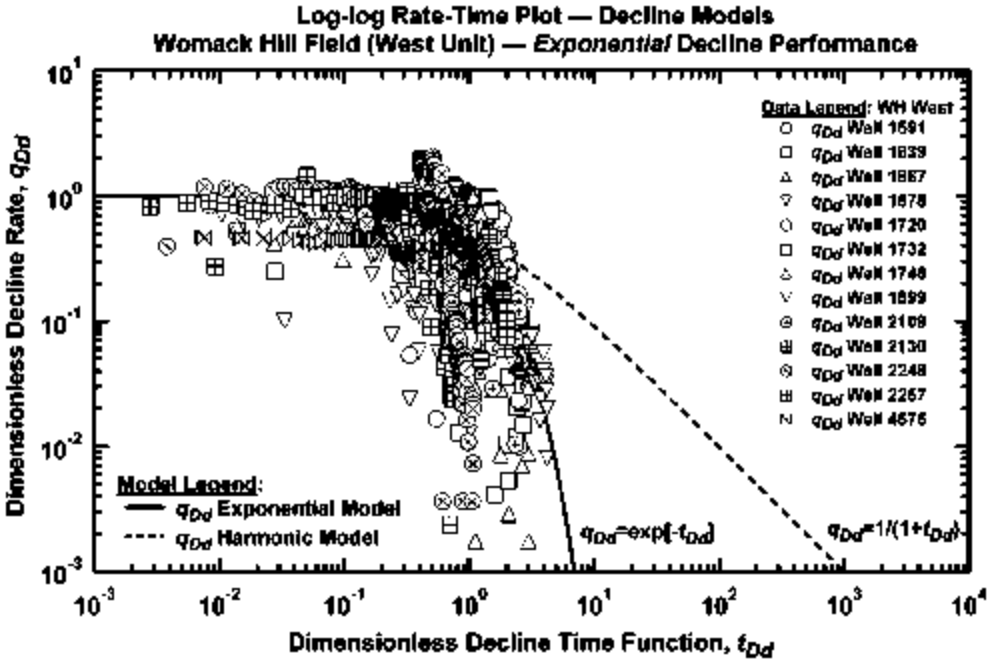

Figure 200 — **Dimensionless production rate-time "type curve" — exponential rate decline model compared to production data from Womack Hill Field (West Unit). The exponential trend is the solution for normal reservoir depletion (for constant pressure production).**

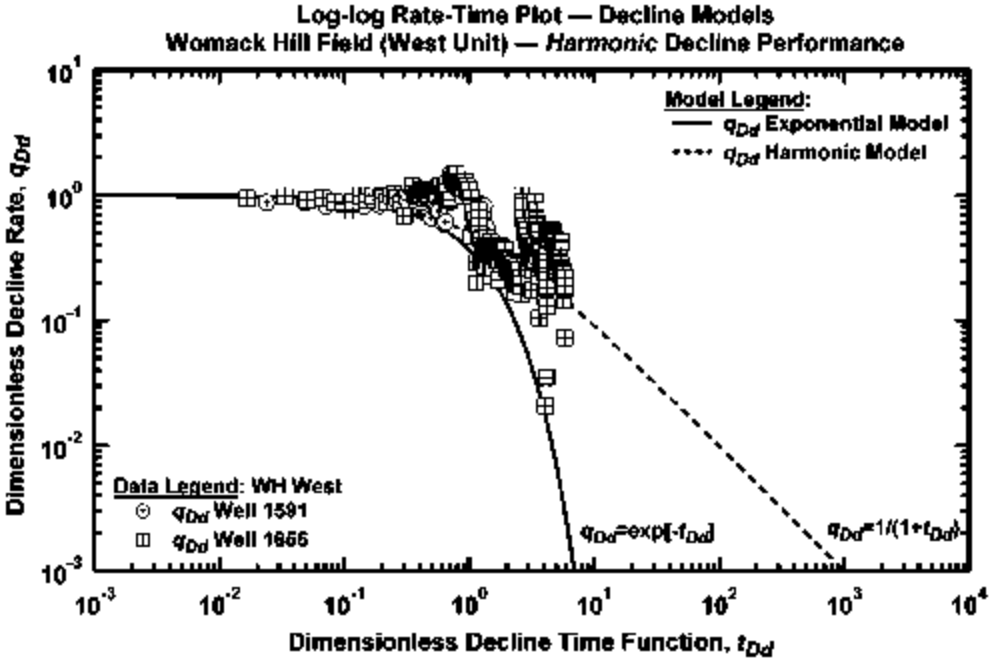

Figure 201 — **Dimensionless production rate-time "type curve" — harmonic rate decline model compared to production data from Womack Hill Field (West Unit). A very general conclusion is that "harmonic" cases indicate water influx/water injection support.**

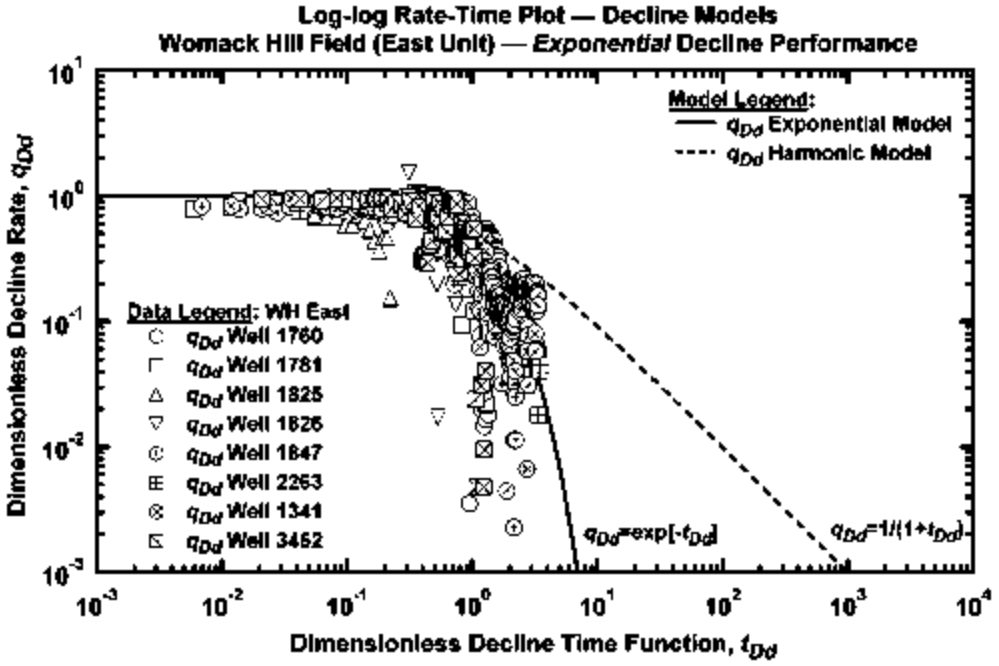

Figure 202 — **Dimensionless production rate-time "type curve" — exponential rate decline model compared to production data from Womack Hill Field (East Unit). The exponential trend is the solution for normal reservoir depletion (for constant pressure production).**

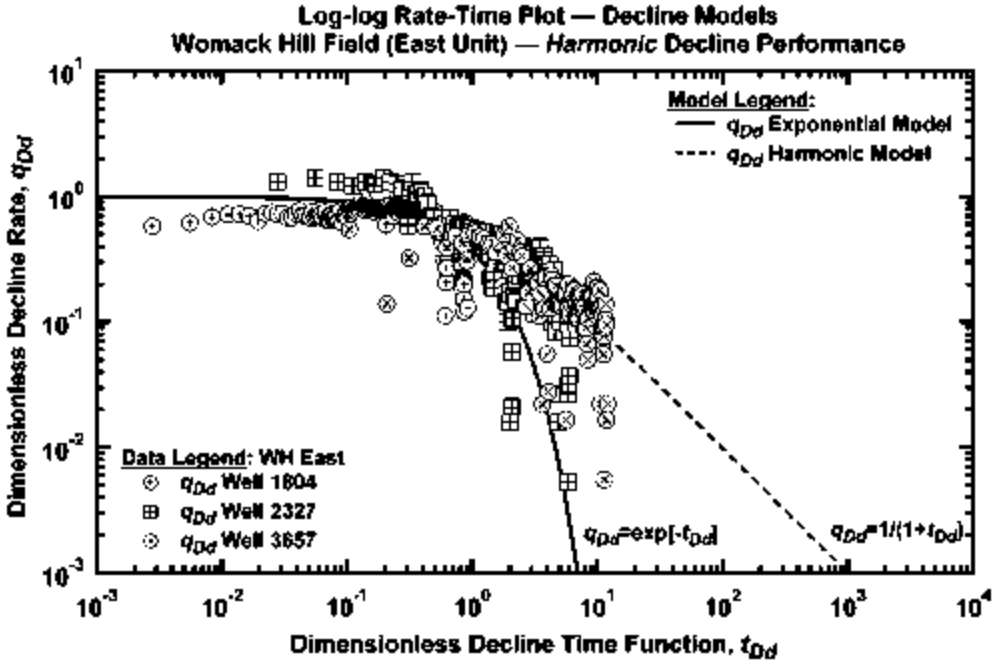

Figure 203 — **Dimensionless production rate-time "type curve" — harmonic rate decline model compared to production data from Womack Hill Field (East Unit). A very general conclusion is that "harmonic" cases indicate water influx/water injection support.**

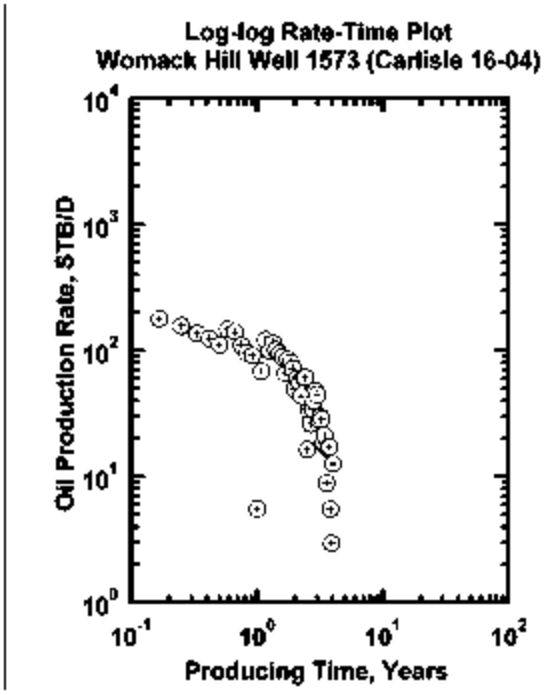

Figure 204 — Log-log rate-time plot — Womack Hill We11 1573.

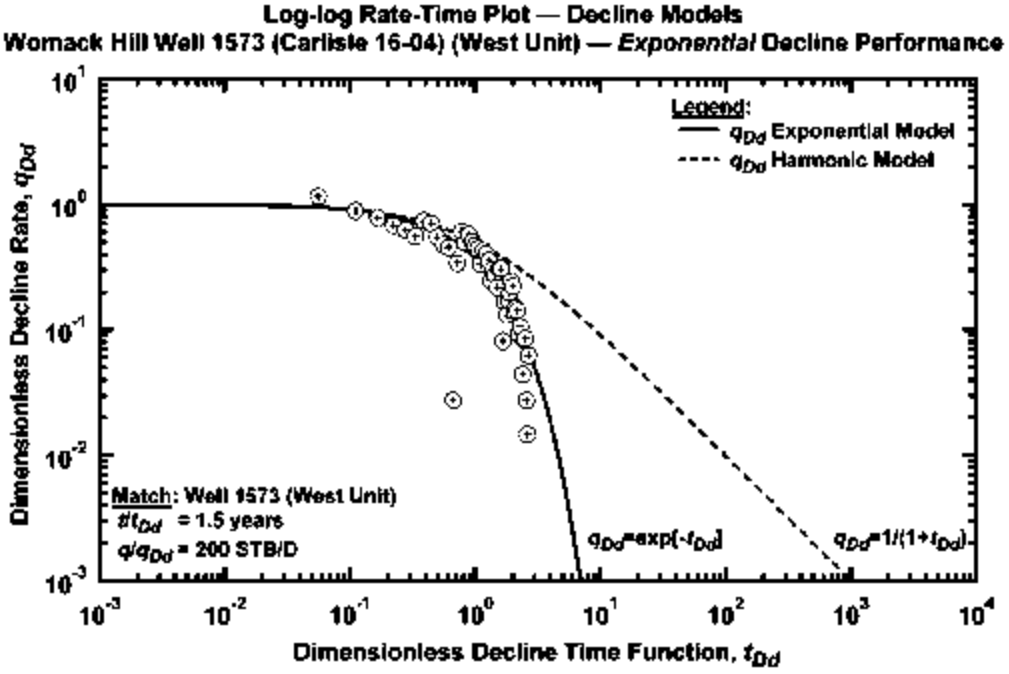

Figure 205 — Dimensionless log-log rate-time "type curve" plot — Womack Hill We11 1573.

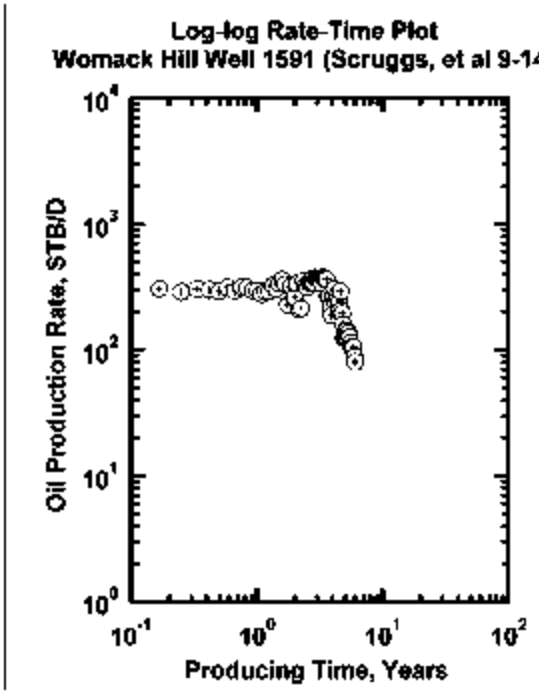

Figure 206 — Log-log rate-time plot — Womack Hill Well 1591.

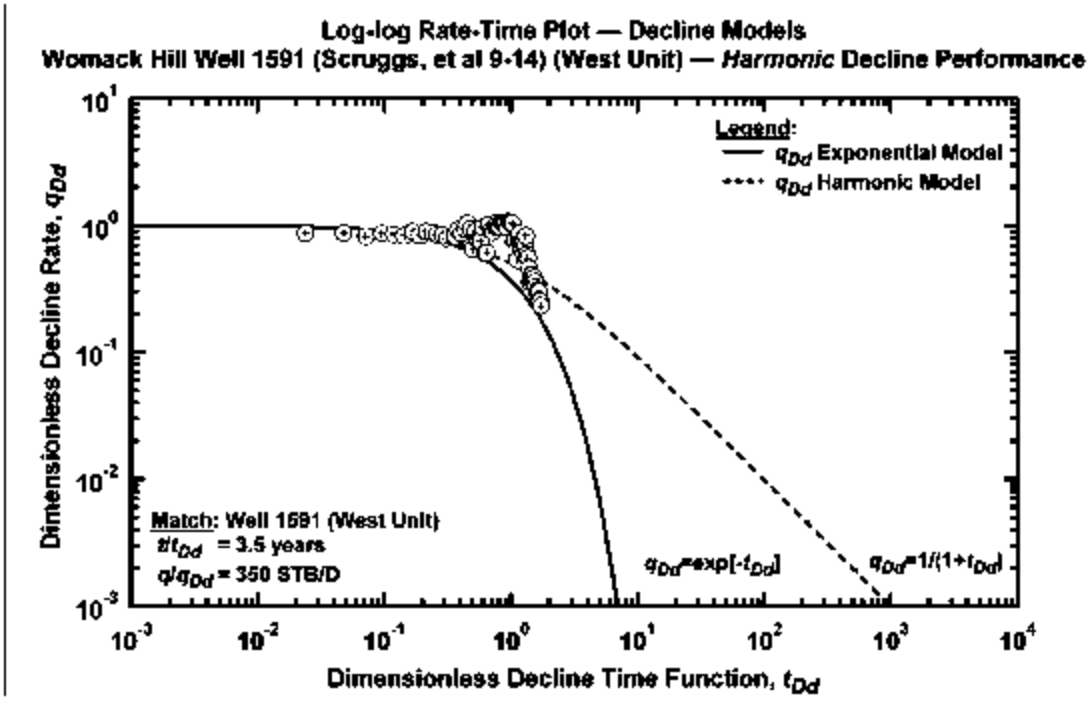

Figure 207 — Dimensionless log-log rate-time "type curve" plot — Womack Hill Well 1591.

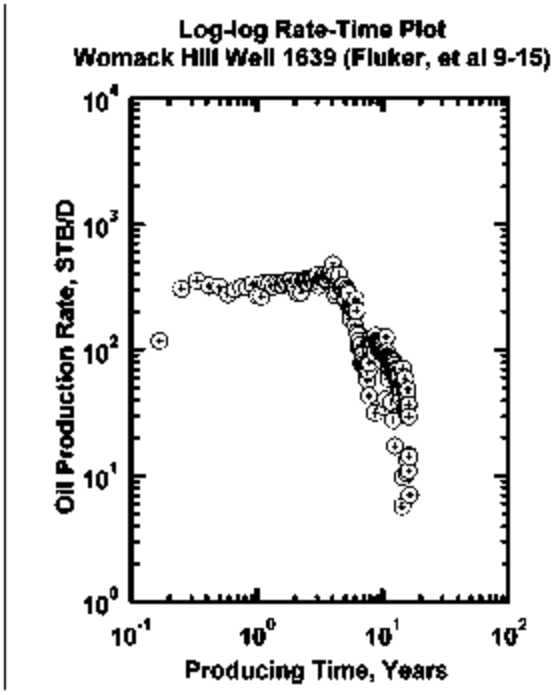

Figure 208 — Log-log rate-time plot — Womack Hill We11 1639.

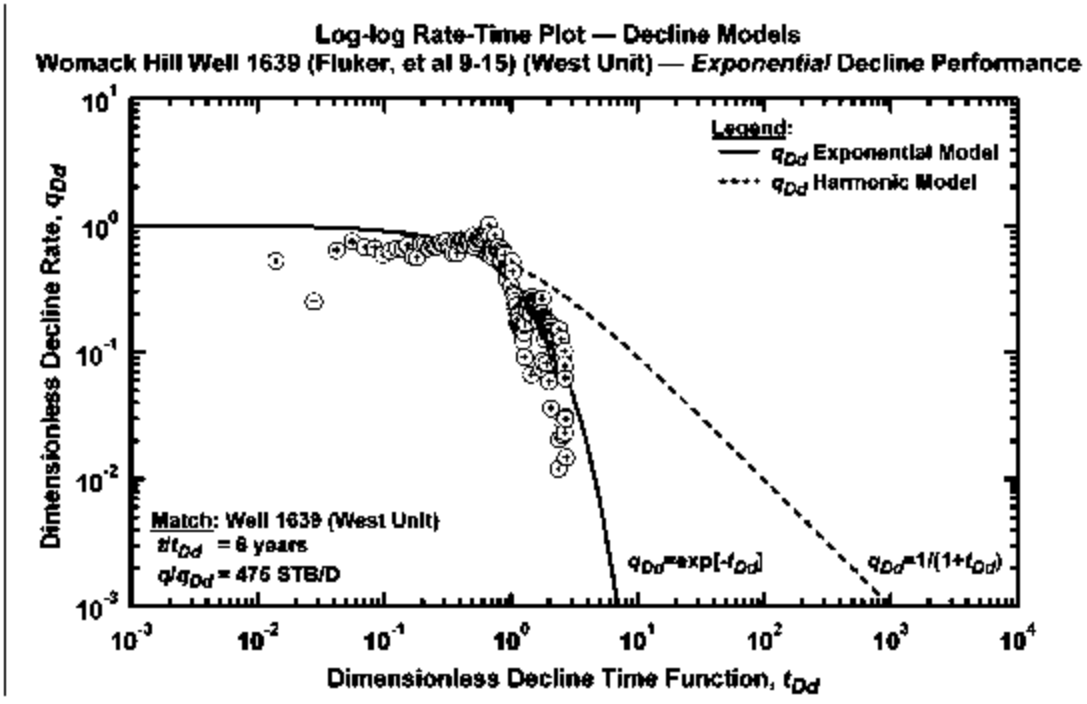

Figure 209 — Dimensionless log-log rate-time "type curve" plot — Womack Hill We11 1639.

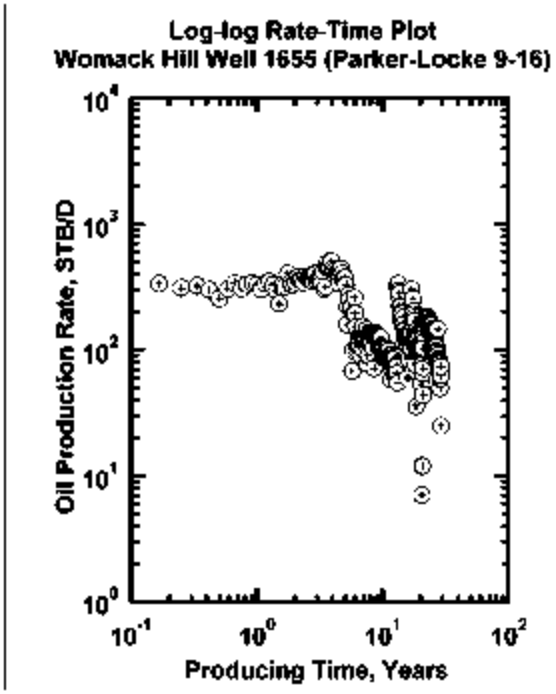

Figure 210 — Log-log rate-time plot — Womack Hill We11 1655.

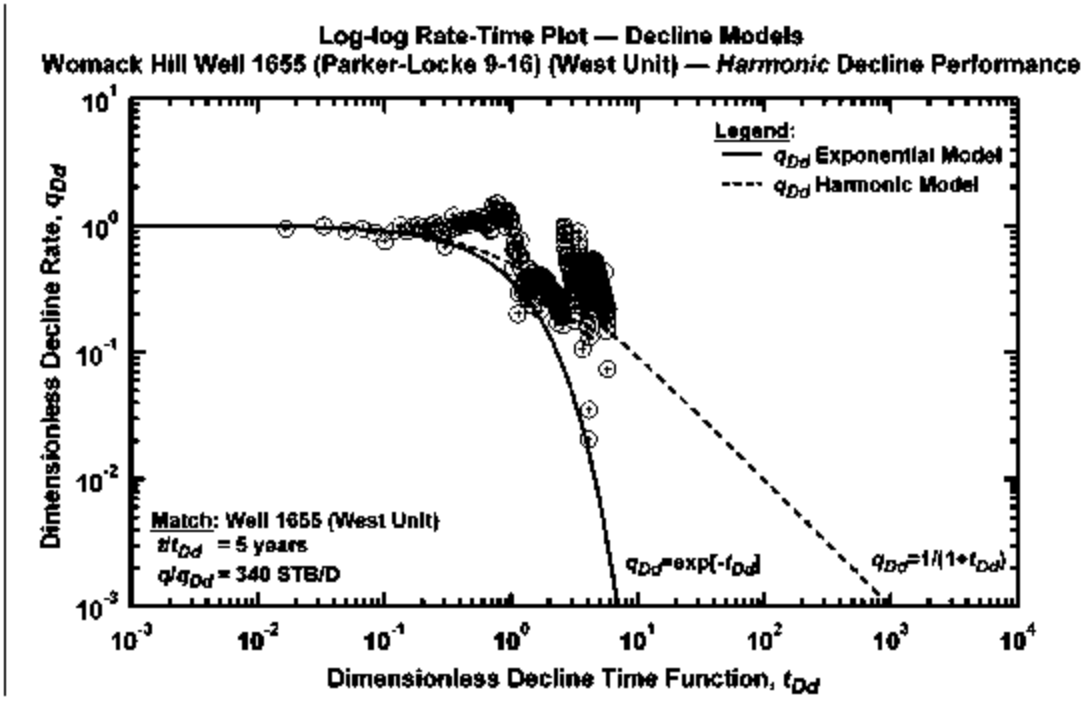

Figure 211 — Dimensionless log-log rate-time "type curve" plot — Womack Hill We11 1655.

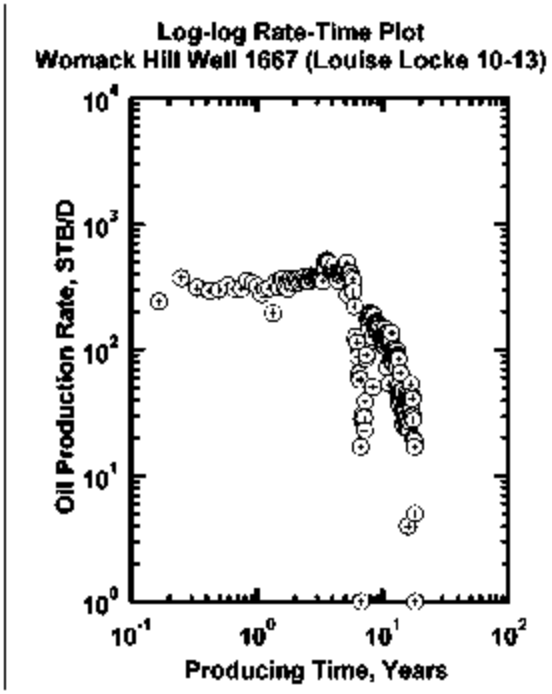

Figure 212 — Log-log rate-time plot — Womack Hill We11 1667.

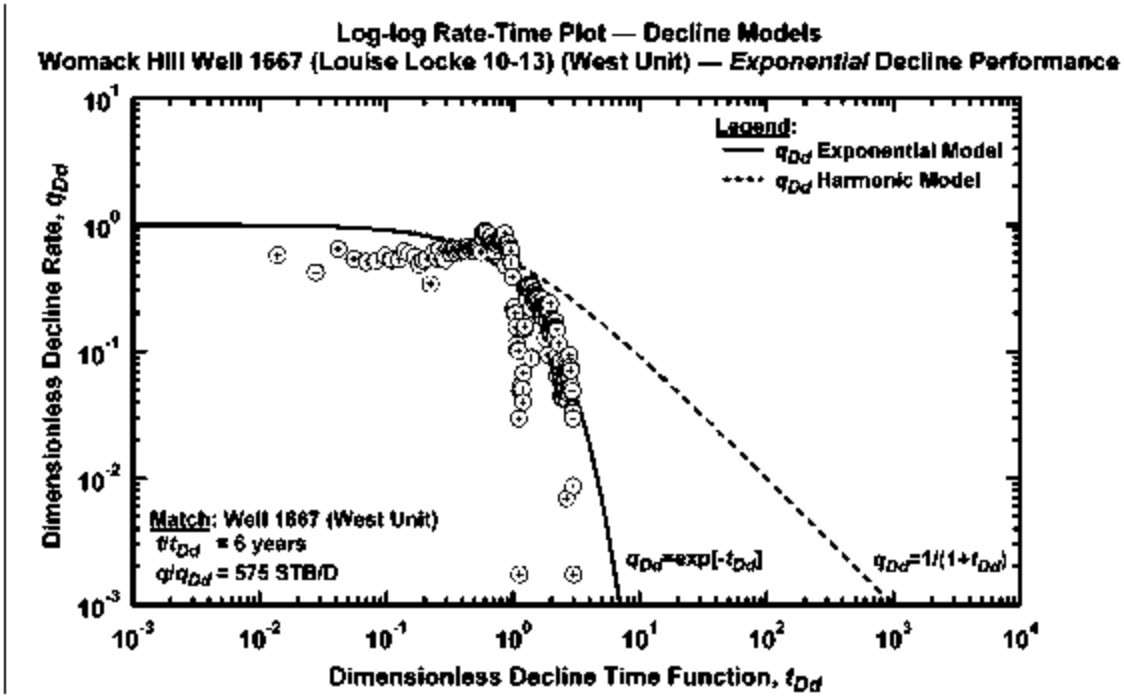

Figure 213 — Dimensionless log-log rate-time "type curve" plot — Womack Hill We11 1667.

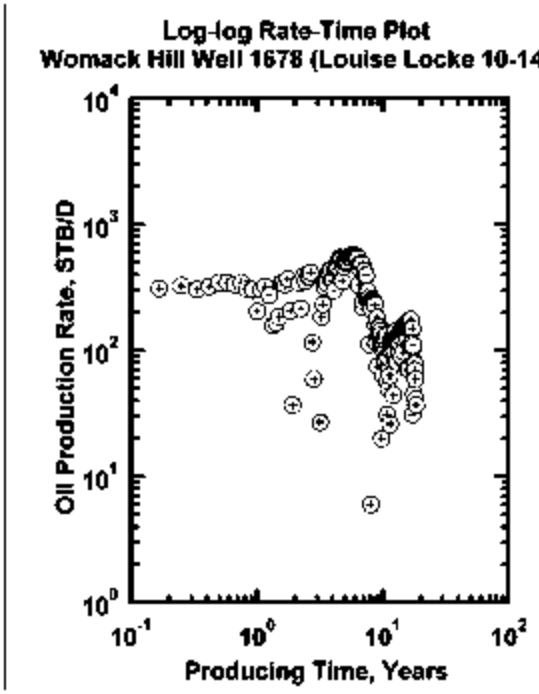

Figure 214 — Log-log rate-time plot — Womack Hill We11 1678.

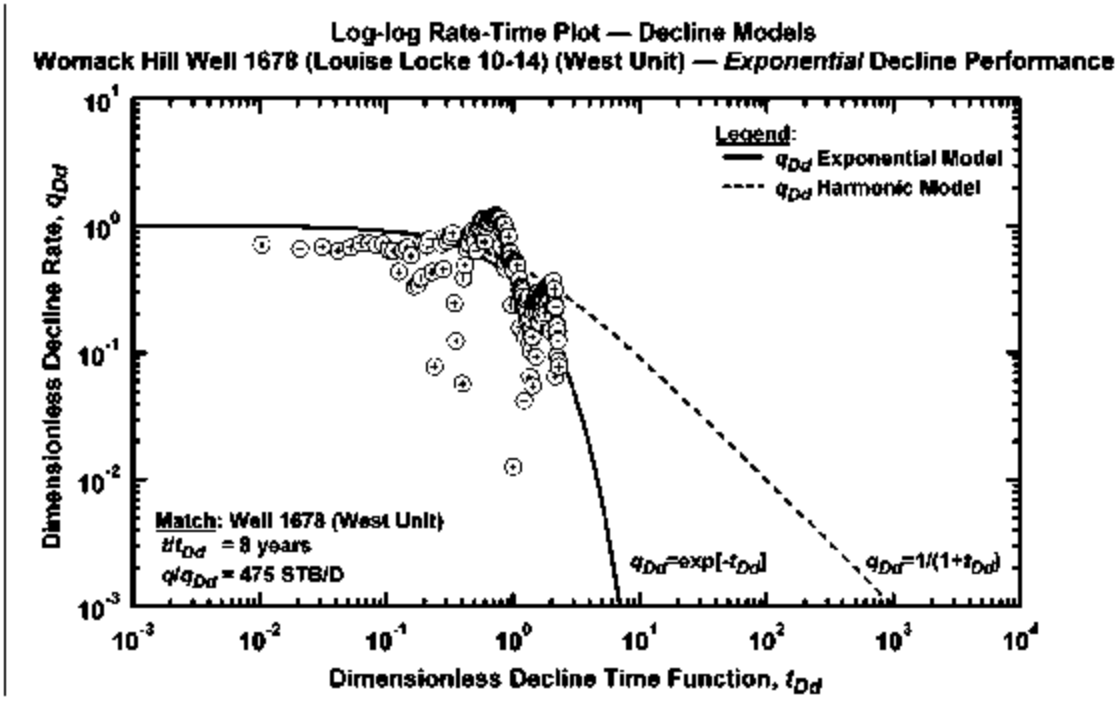

Figure 215 — Dimensionless log-log rate-time "type curve" plot — Womack Hill We11 1678.

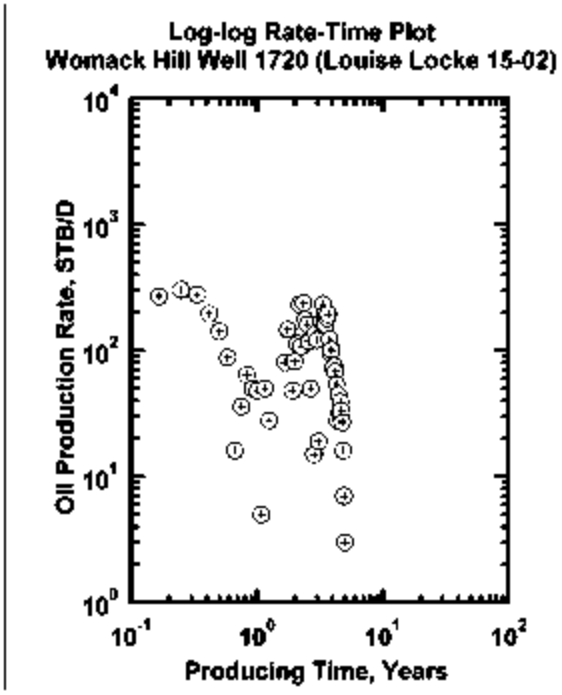

Figure 216 — Log-log rate-time plot — Womack Hill Well 1720.

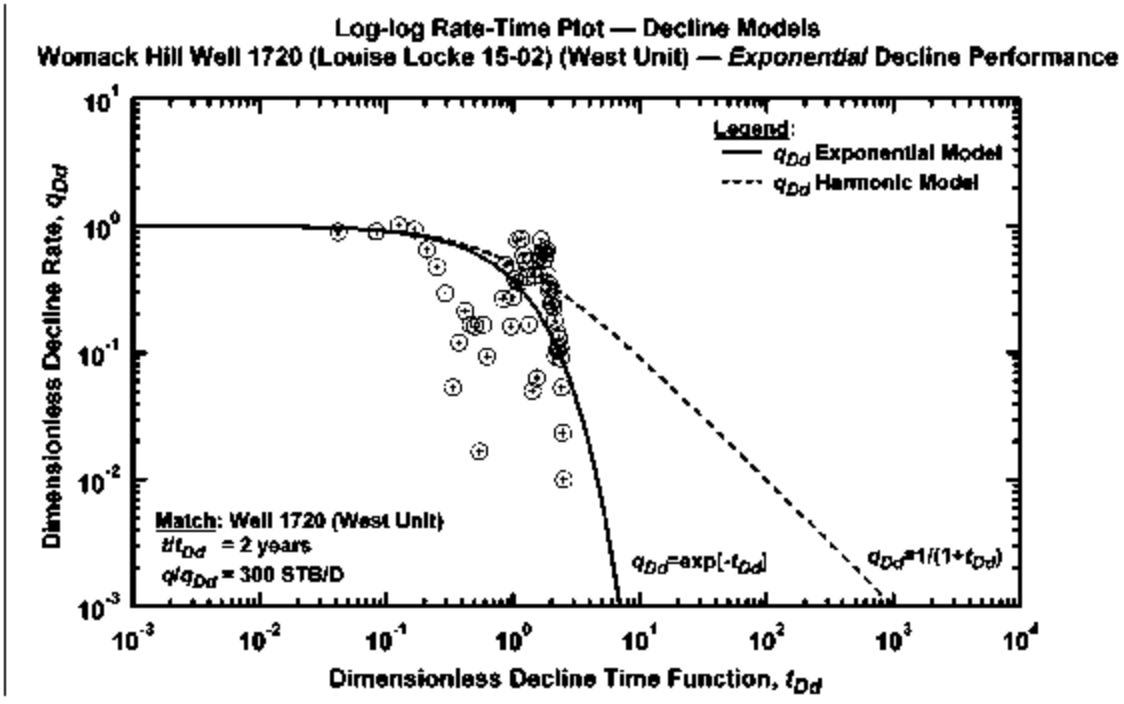

Figure 217 — Dimensionless log-log rate-time "type curve" plot — Womack Hill Well 1720.

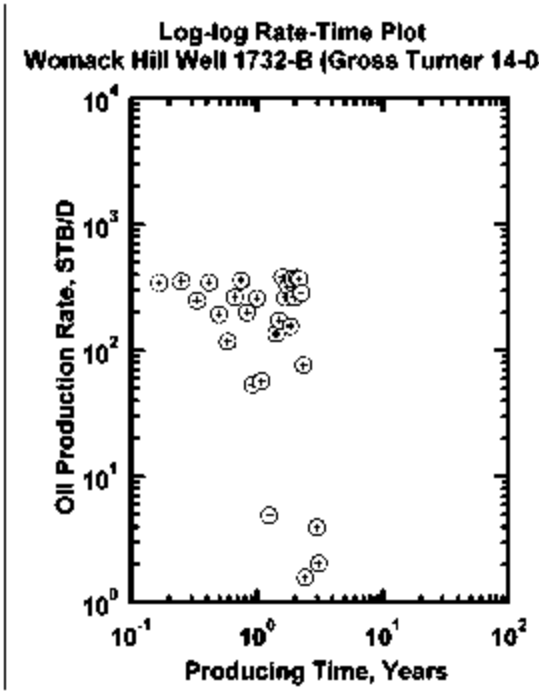

Figure 218 — Log-log rate-time plot — Womack Hill Well 1732.

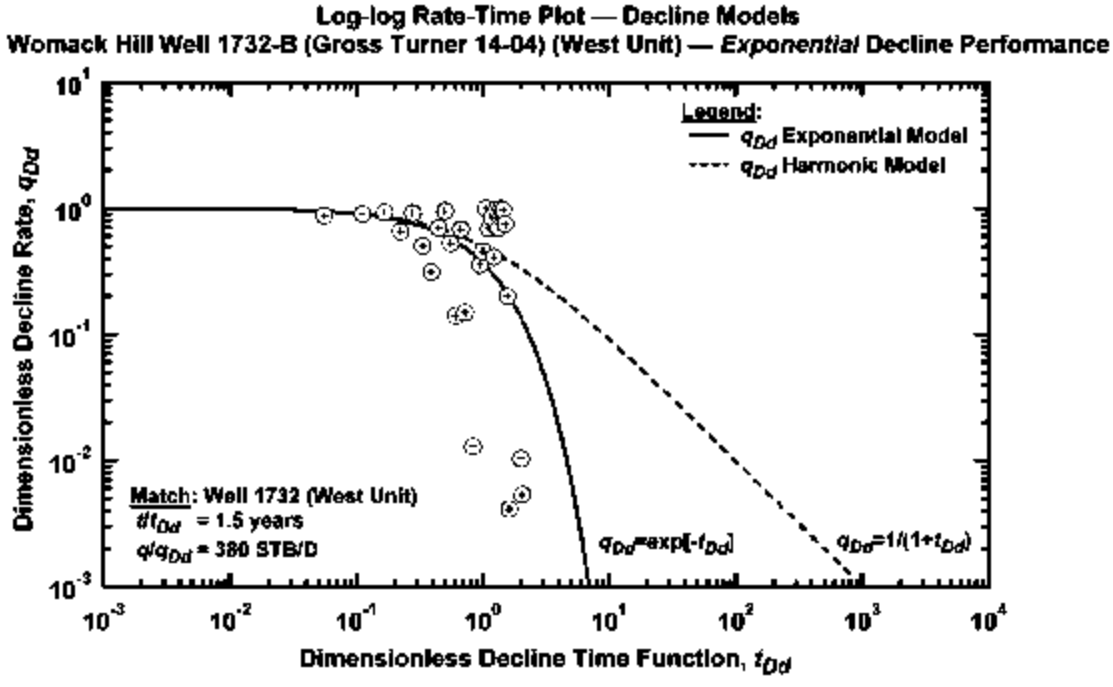

Figure 219 — Dimensionless log-log rate-time "type curve" plot — Womack Hill Well 1732.

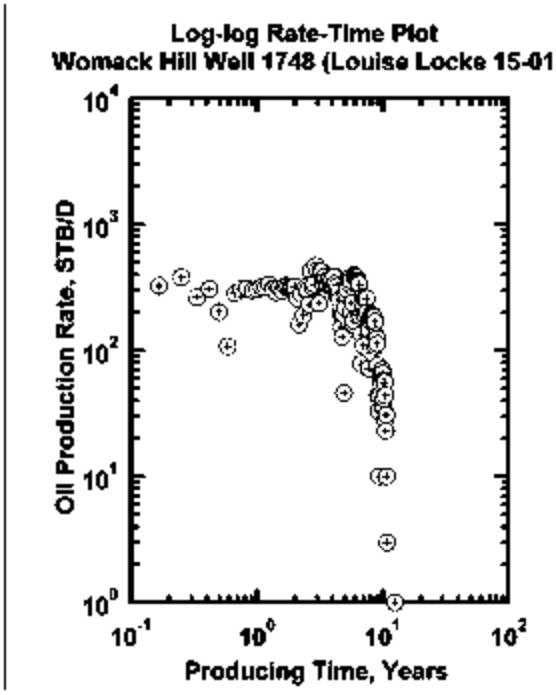

Figure 220 — Log-log rate-time plot — Womack Hill We11 1748.

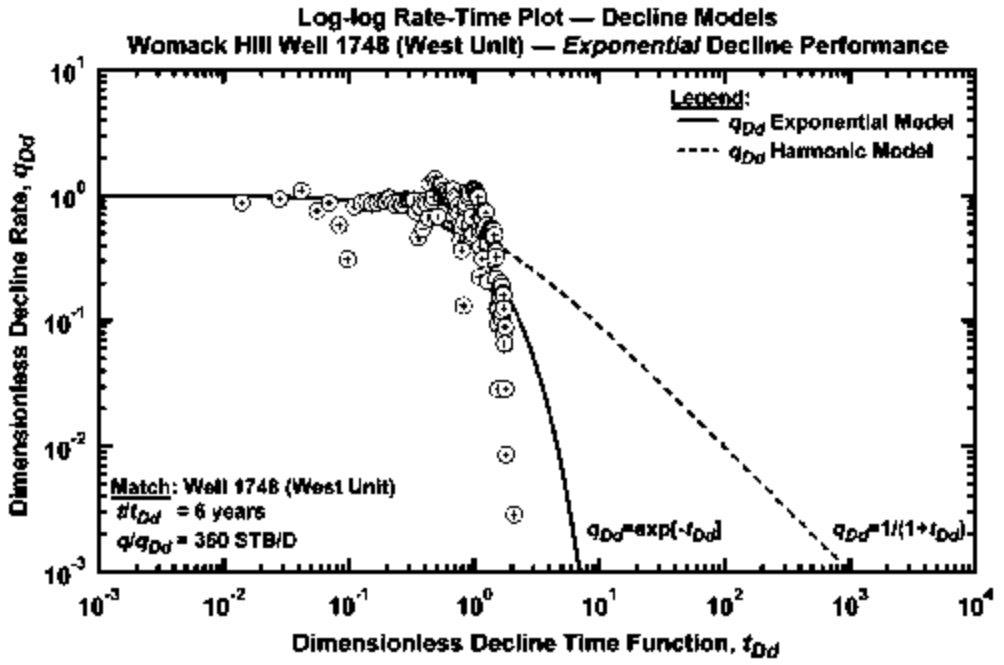

Figure 221 — Dimensionless log-log rate-time "type curve" plot — Womack Hill We11 1748.

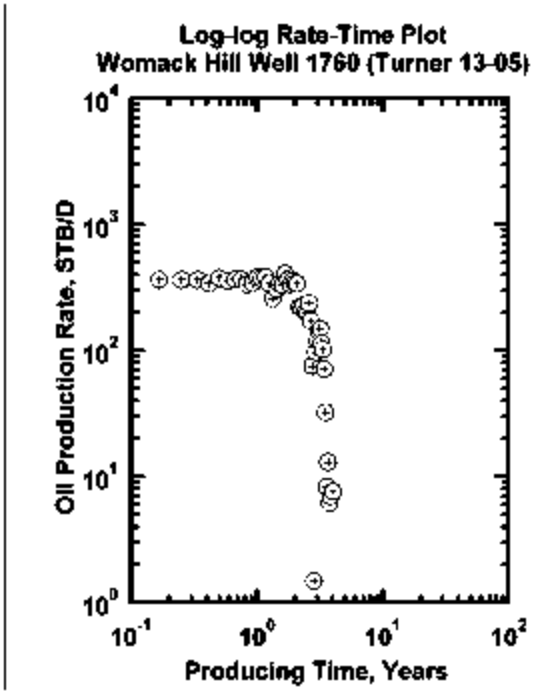

Figure 222 — Log-log rate-time plot — Womack Hill We11 1760.

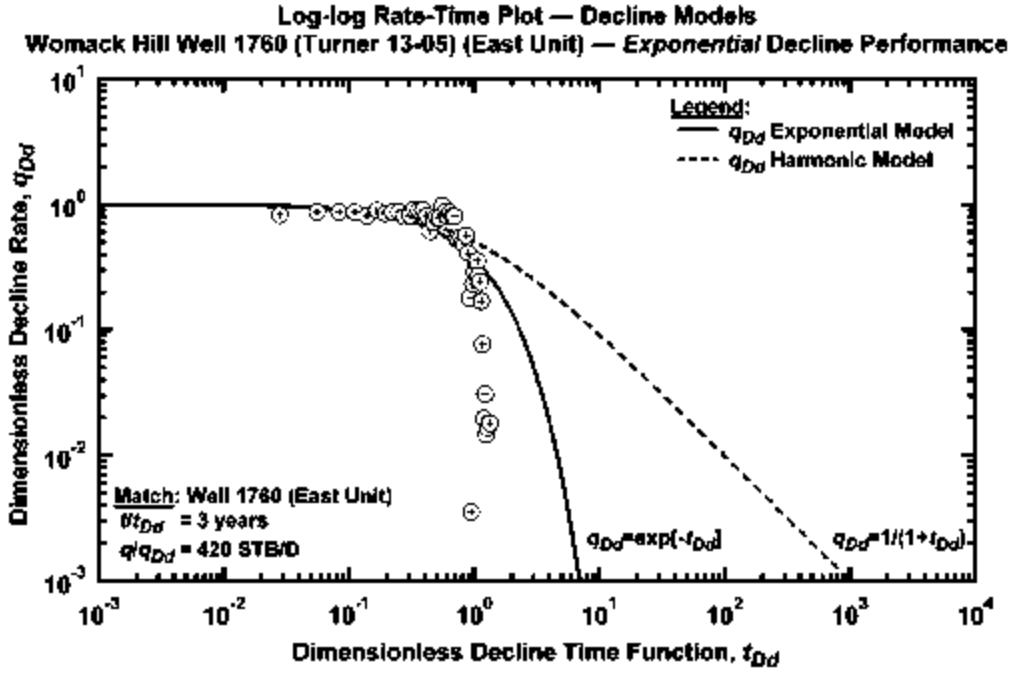

Figure 223 — Dimensionless log-log rate-time "type curve" plot — Womack Hill We11 1760.

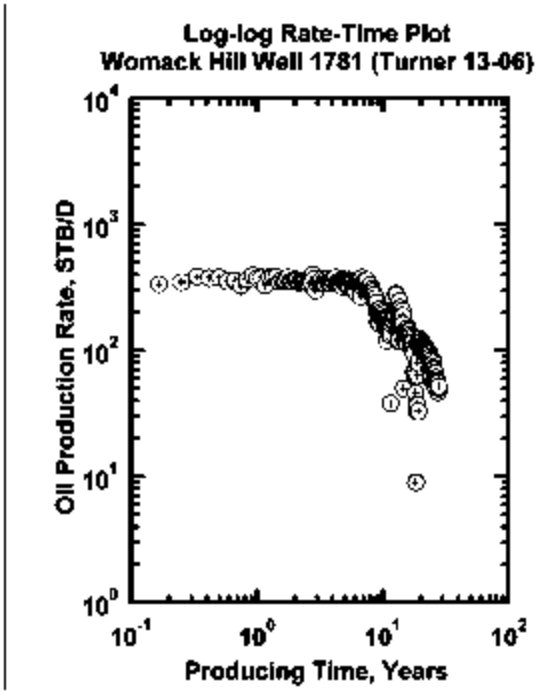

Figure 224 — Log-log rate-time plot — Womack Hill Well 1781.

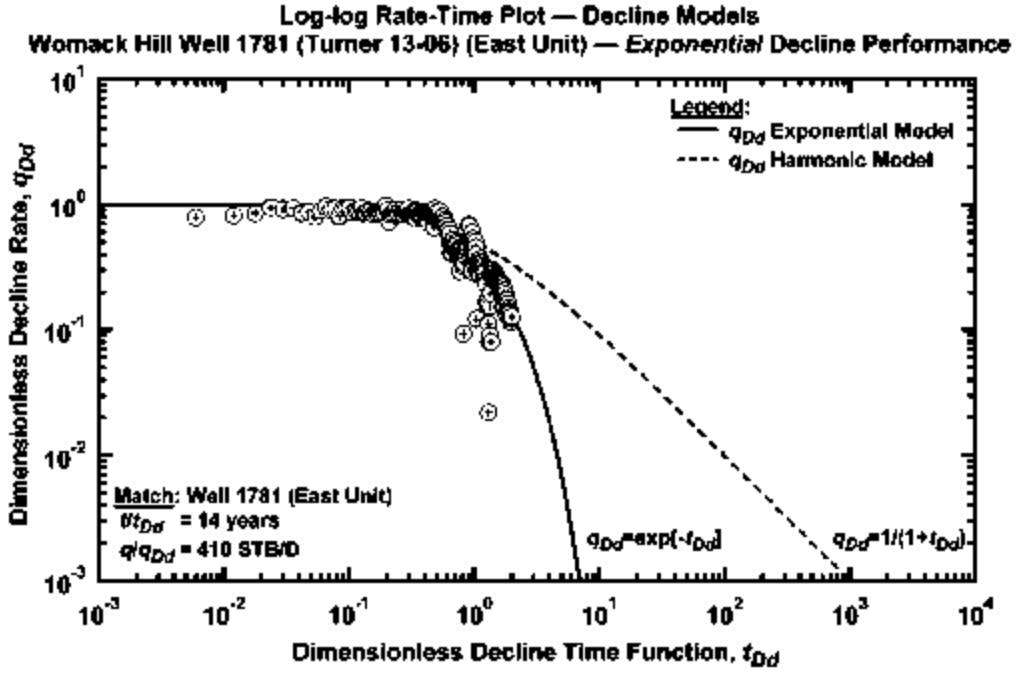

Figure 225 — Dimensionless log-log rate-time "type curve" plot — Womack Hill Well 1781.

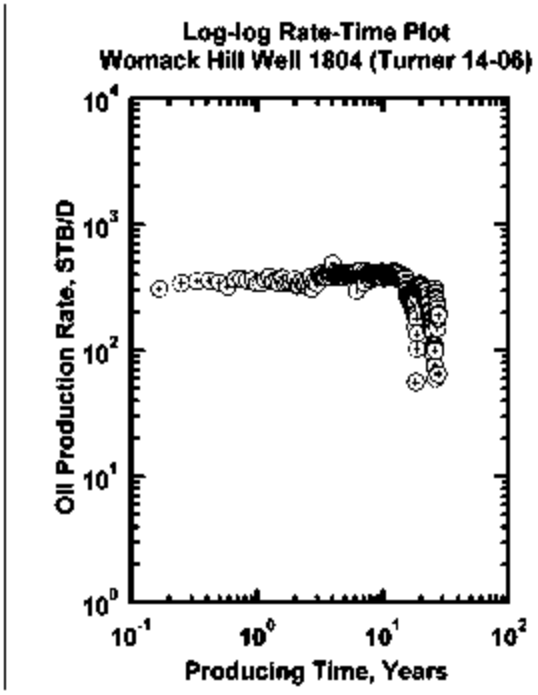

Figure 226 — Log-log rate-time plot — Womack Hill Well 1804.

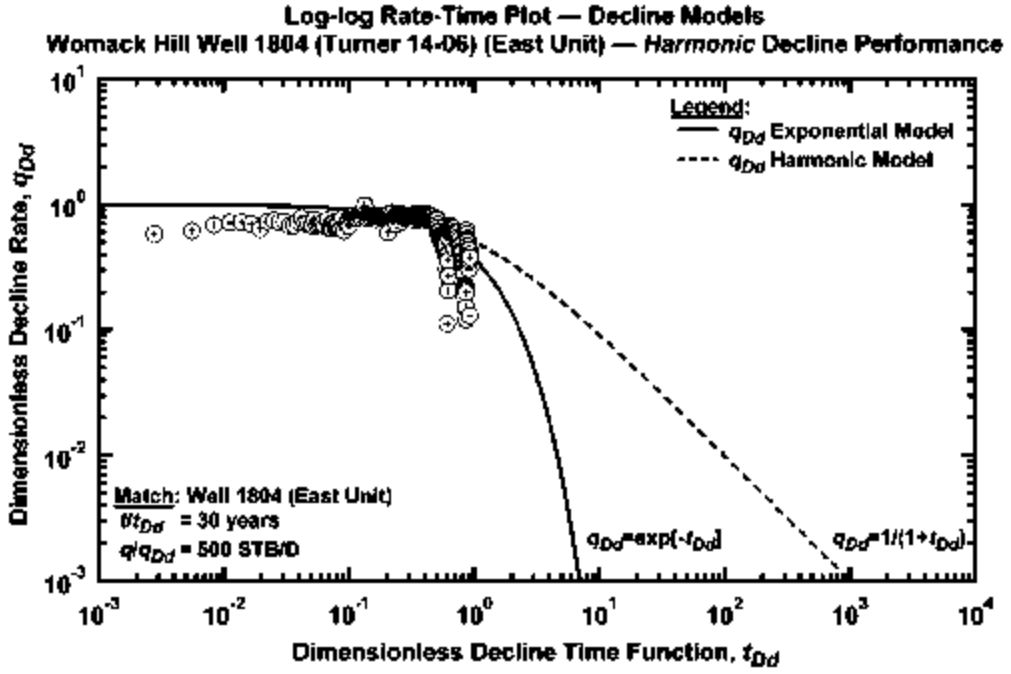

Figure 227 — Dimensionless log-log rate-time "type curve" plot — Womack Hill Well 1804.

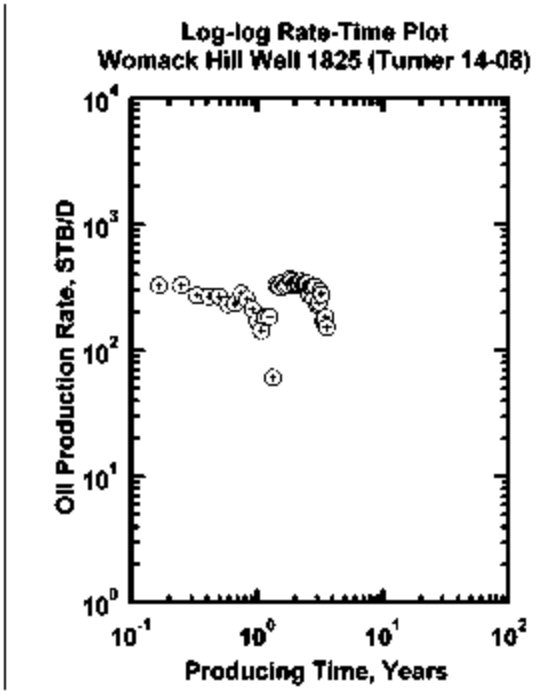

Figure 228 — Log-log rate-time plot — Womack Hill Well 1825.

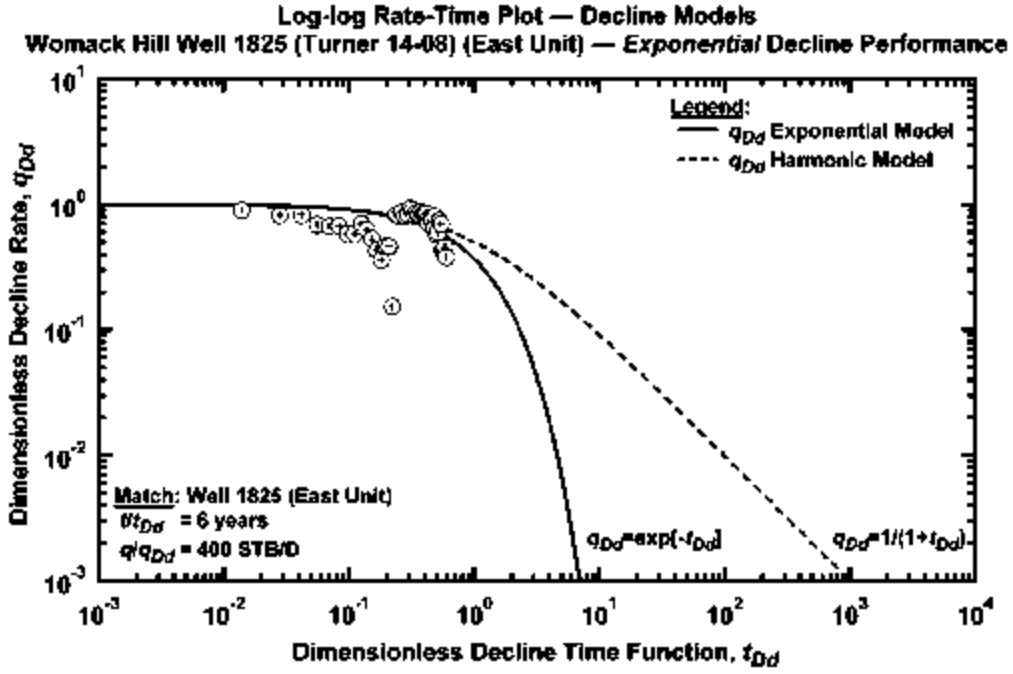

Figure 229 — Dimensionless log-log rate-time "type curve" plot — Womack Hill Well 1825.

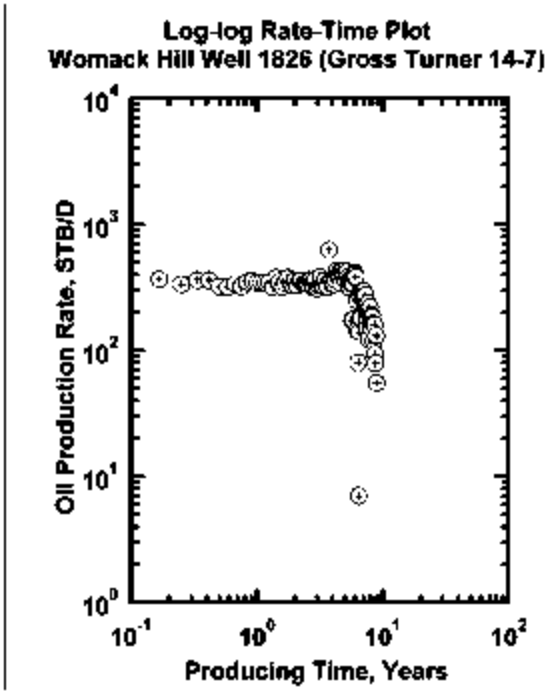

Figure 230 — Log-log rate-time plot — Womack Hill We11 1826.

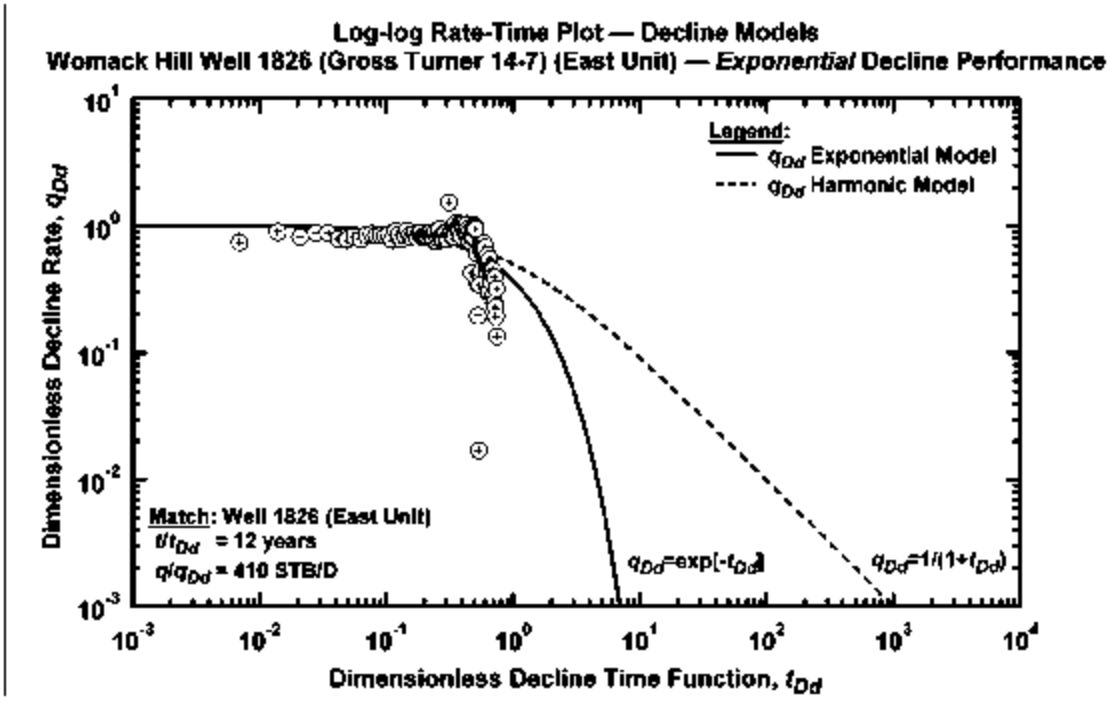

Figure 231 — Dimensionless log-log rate-time "type curve" plot — Womack Hill We11 1826.

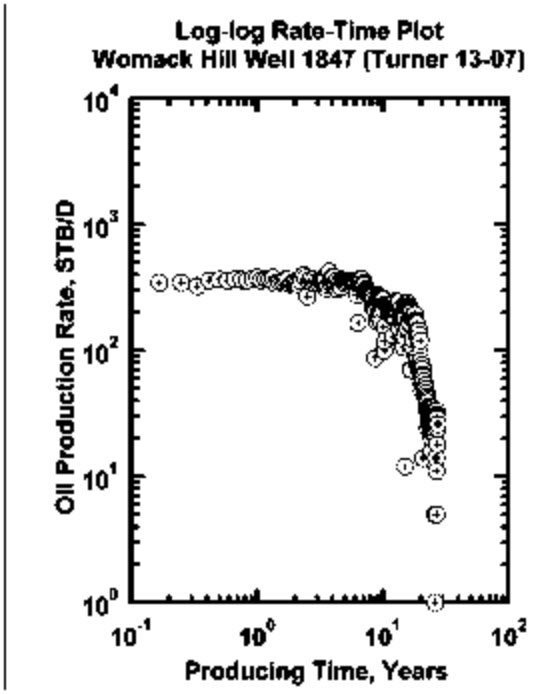

Figure 232 — Log-log rate-time plot — Womack Hill We11 1847.

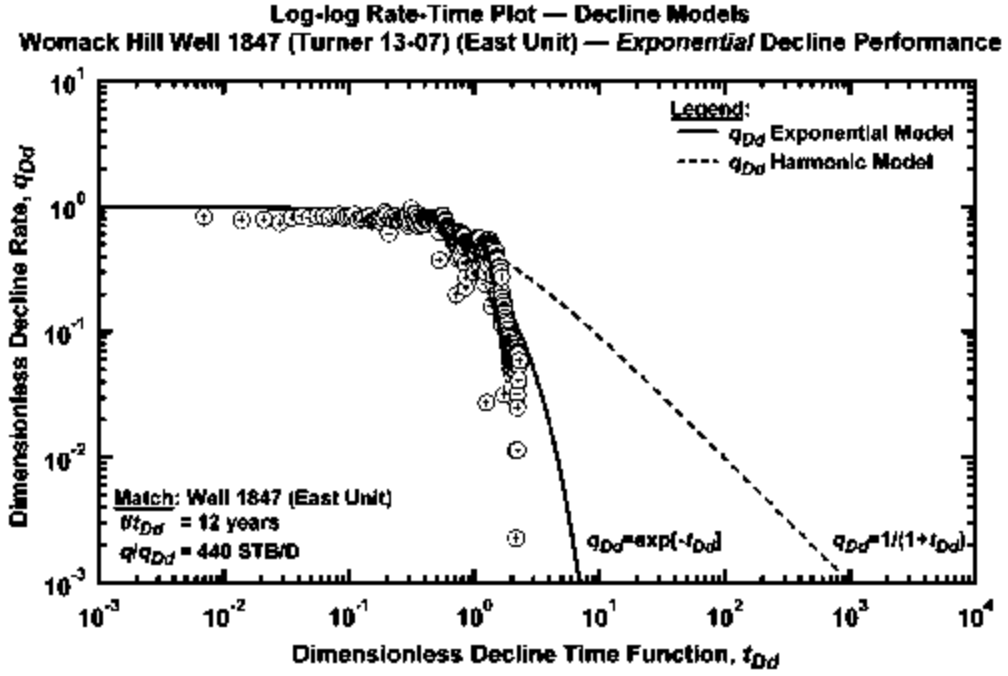

Figure 233 — Dimensionless log-log rate-time "type curve" plot — Womack Hill We11 1847.

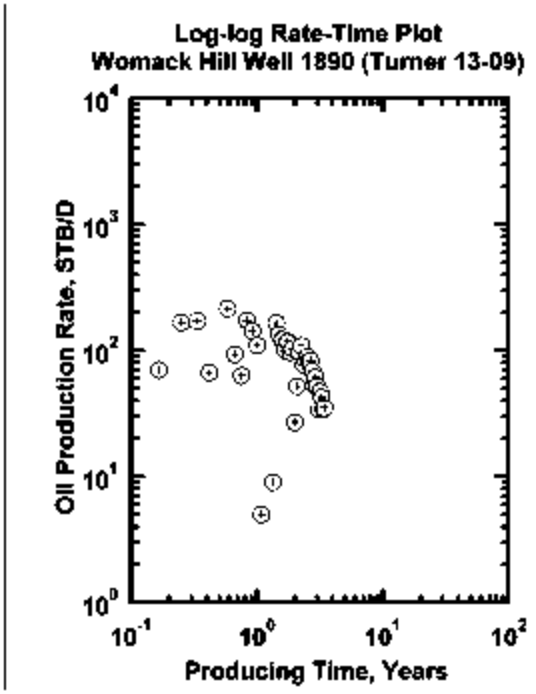

Figure 234 — Log-log rate-time plot — Womack Hill We11 1890.

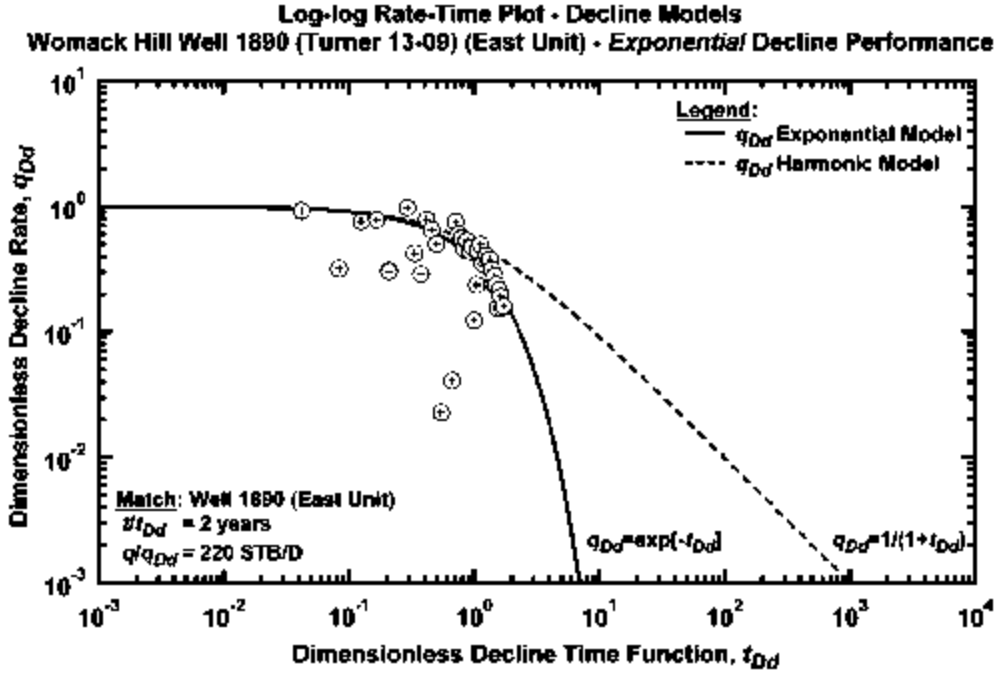

Figure 235 — Dimensionless log-log rate-time "type curve" plot — Womack Hill We11 1890.

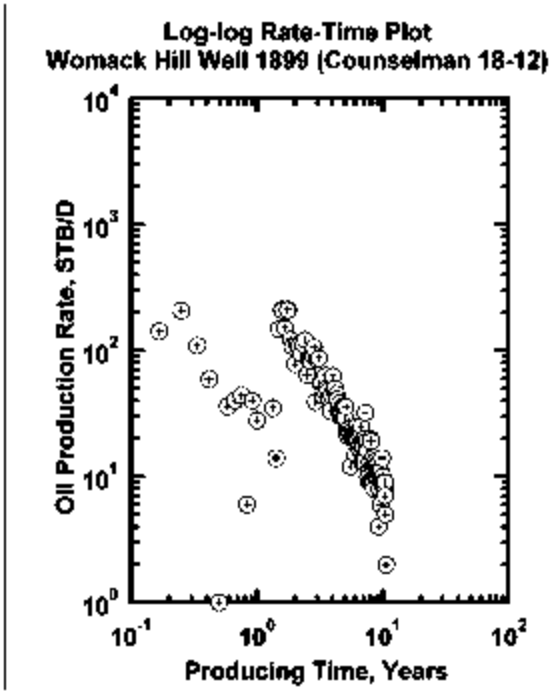

Figure 236 — Log-log rate-time plot — Womack Hill Well 1899.

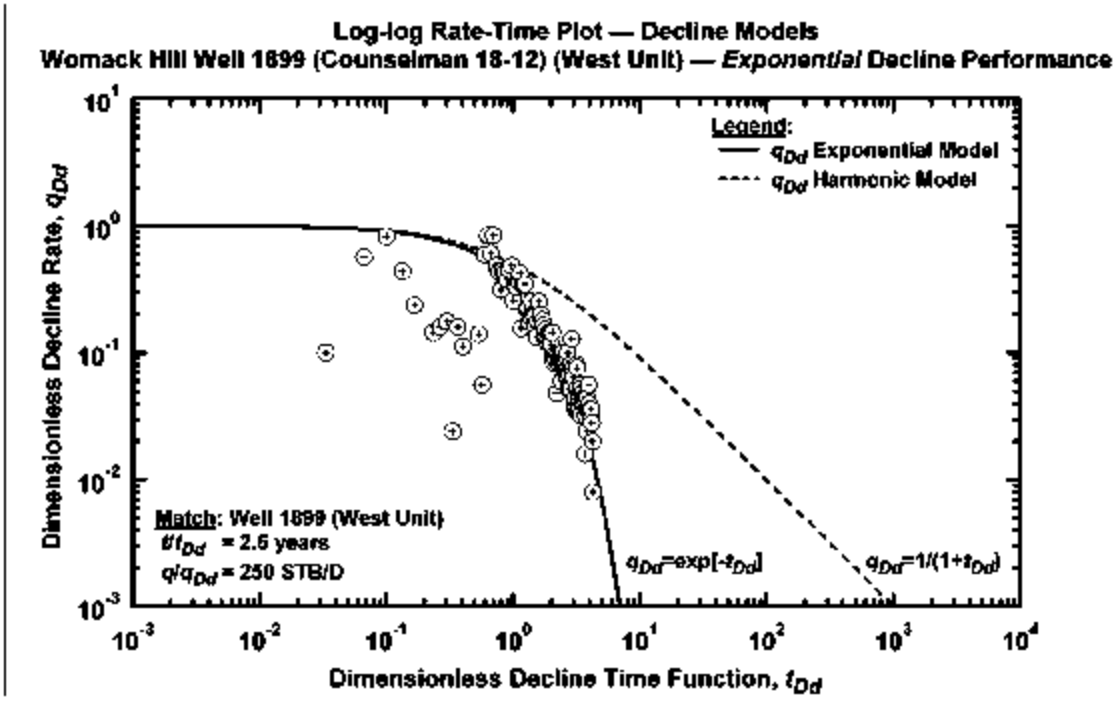

Figure 237 — Dimensionless log-log rate-time "type curve" plot — Womack Hill Well 1899.

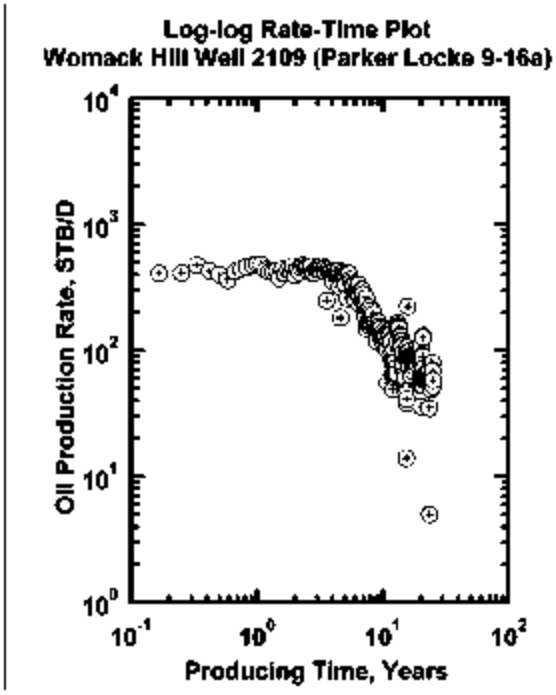

Figure 238 — Log-log rate-time plot — Womack Hill We11 2109.

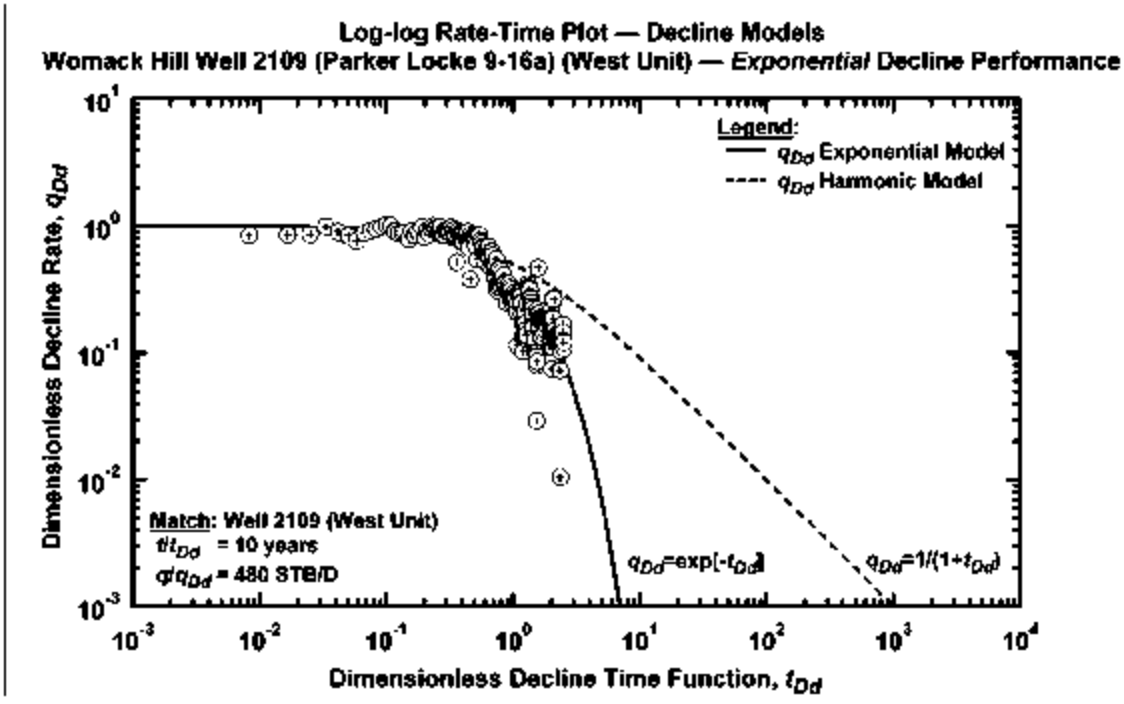

Figure 239 — Dimensionless log-log rate-time "type curve" plot — Womack Hill We11 2109.

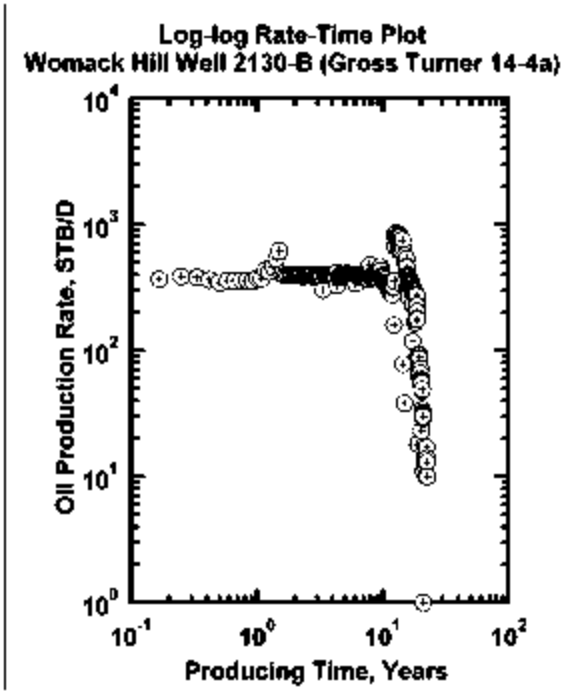

Figure 240 — Log-log rate-time plot — Womack Hill We11 2130.

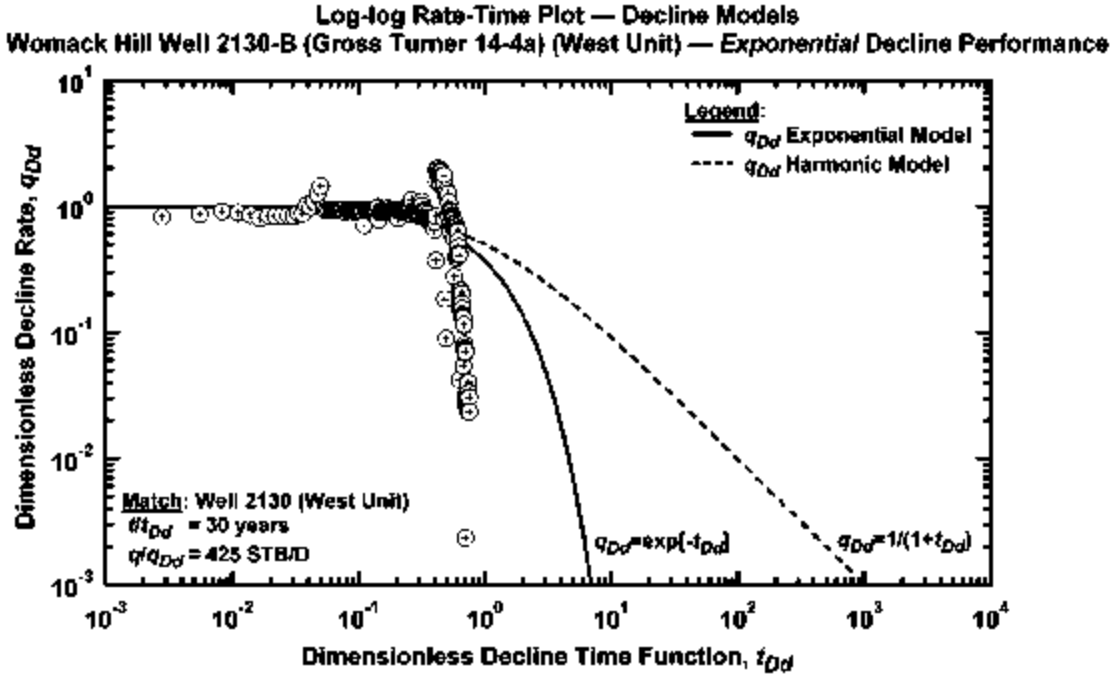

Figure 241 — Dimensionless log-log rate-time "type curve" plot — Womack Hill We11 2130.

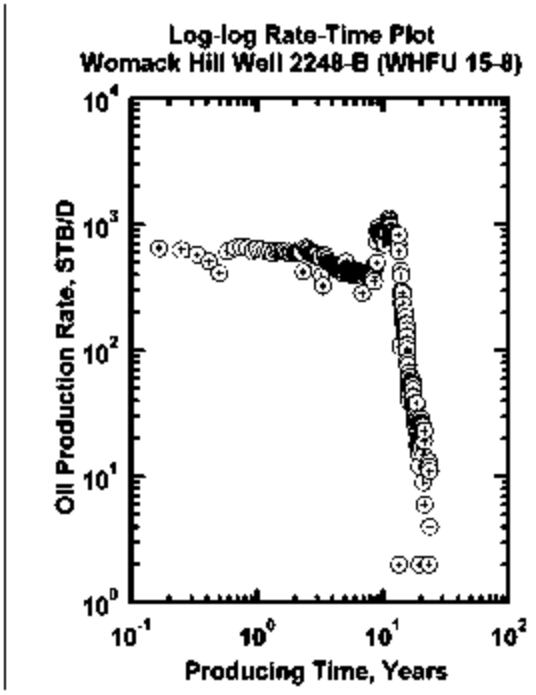

Figure 242 — Log-log rate-time plot — Womack Hill We11 2109.

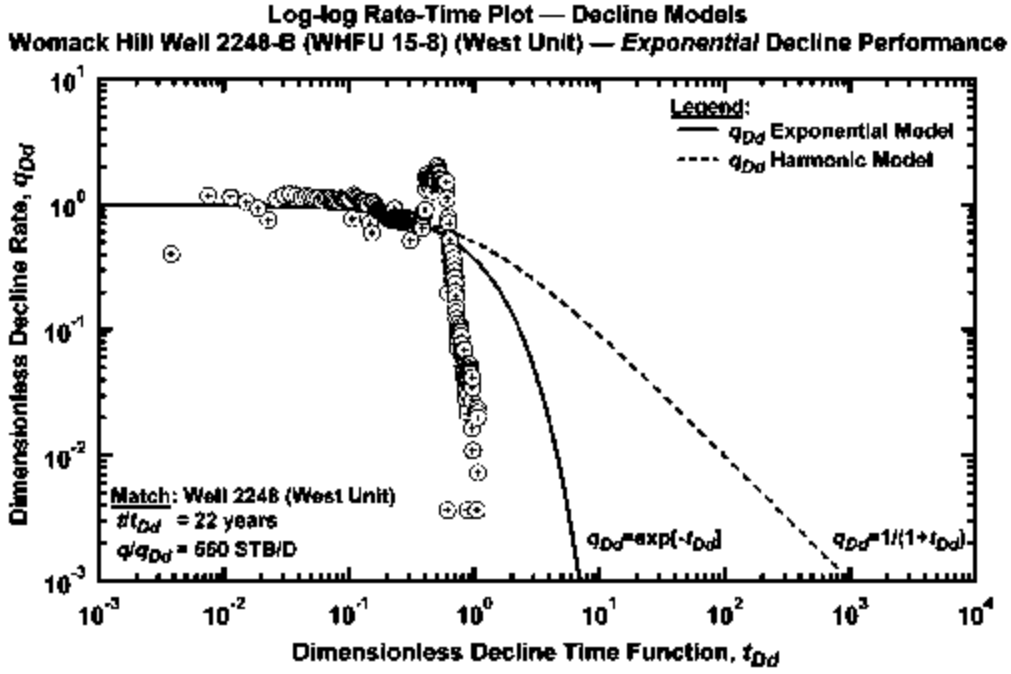

Figure 243 — Dimensionless log-log rate-time "type curve" plot — Womack Hill We11 2109.

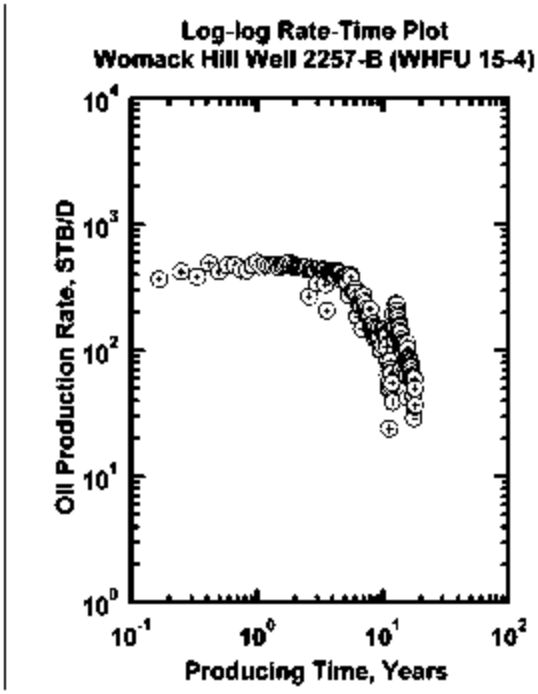

Figure 244 — Log-log rate-time plot — Womack Hill Well 2257.

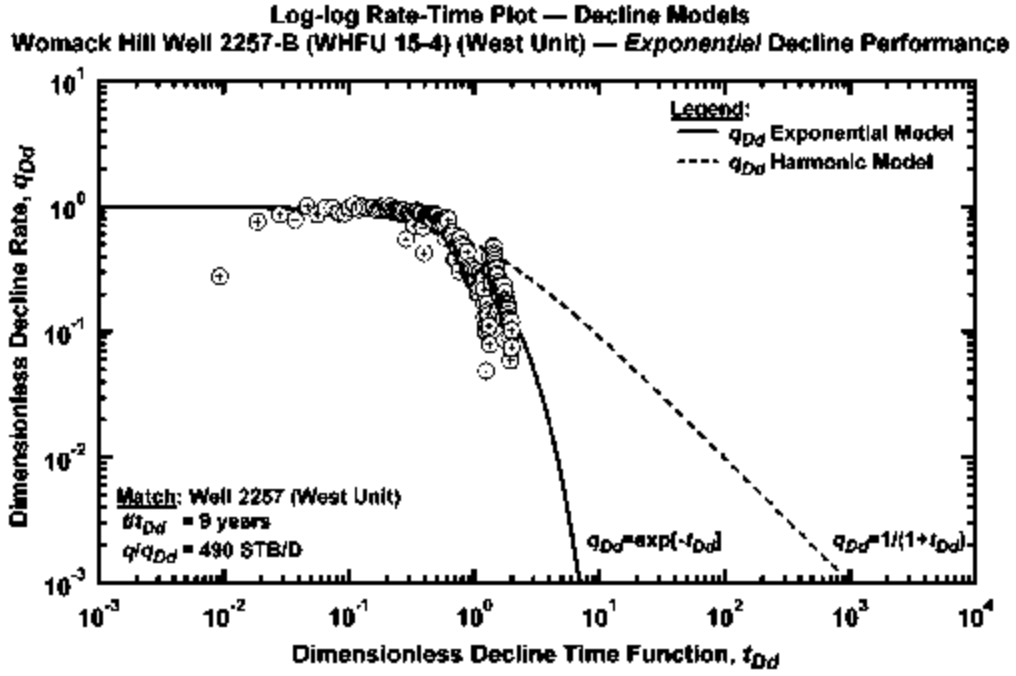

Figure 245 — Dimensionless log-log rate-time "type curve" plot — Womack Hill Well 2257.

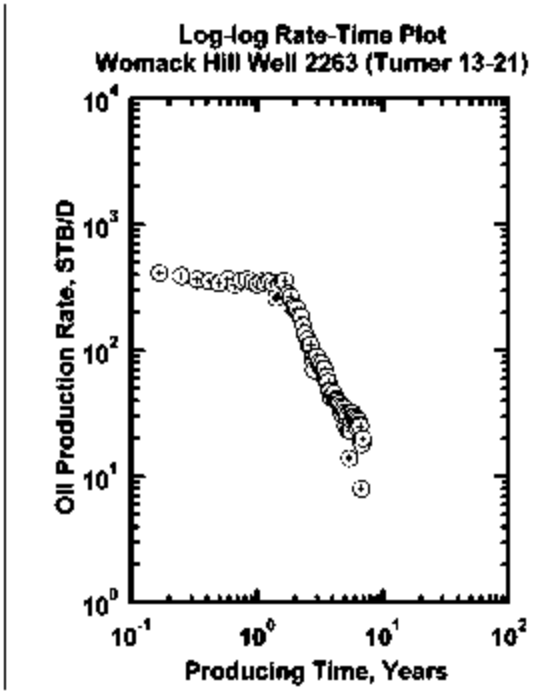

Figure 246 — Log-log rate-time plot — Womack Hill Well 2263.

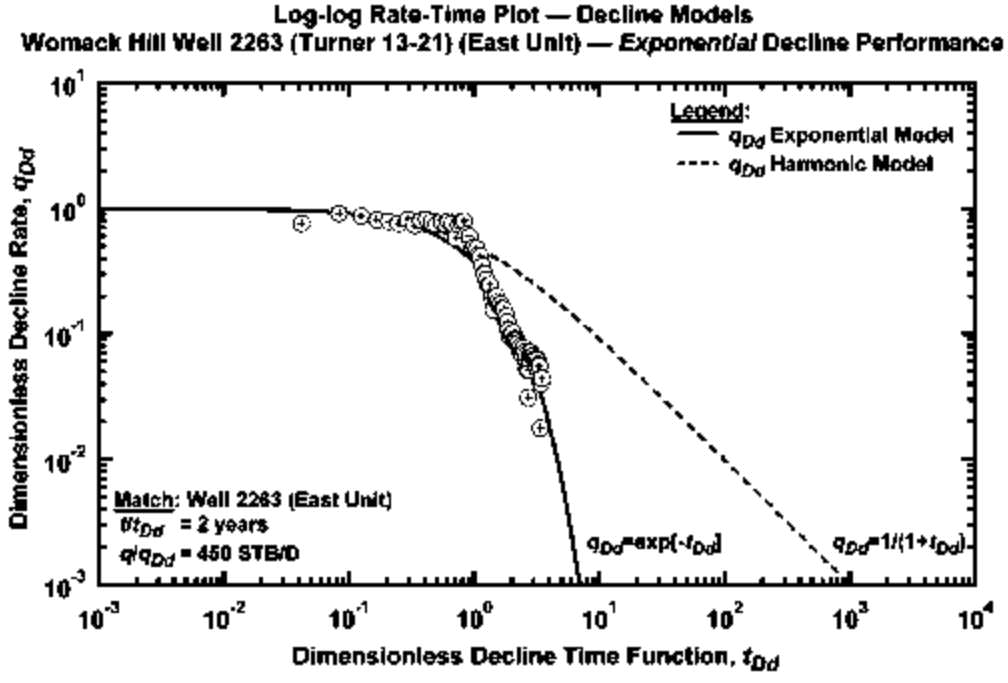

Figure 247 — Dimensionless log-log rate-time "type curve" plot — Womack Hill Well 2263.

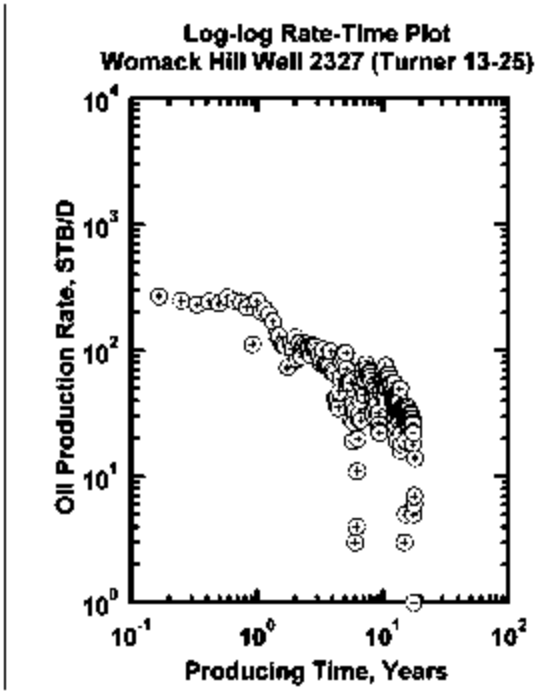

Figure 248 — Log-log rate-time plot — Womack Hill Well 2327.

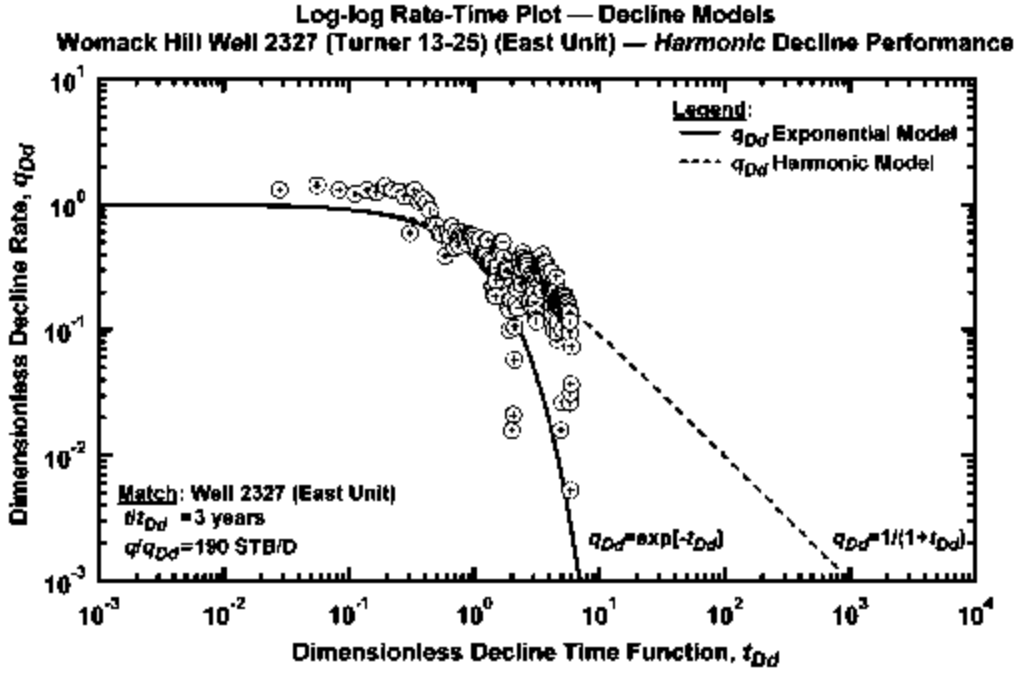

Figure 249 — Dimensionless log-log rate-time "type curve" plot — Womack Hill Well 2327.

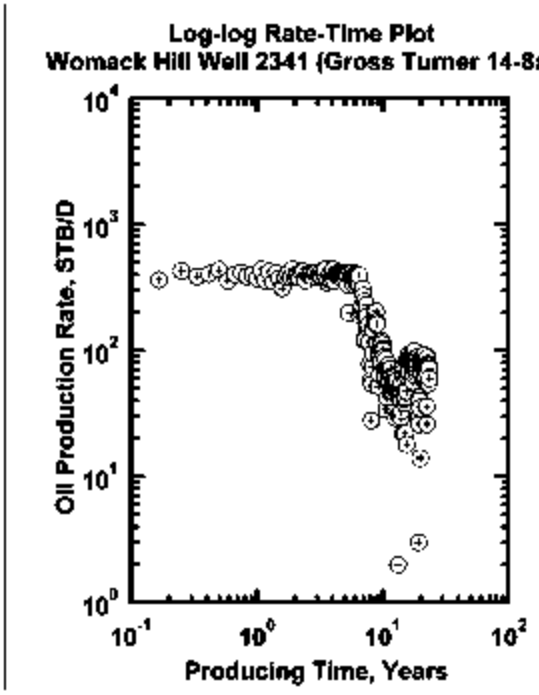

Figure 250 — Log-log rate-time plot — Womack Hill We11 2341.

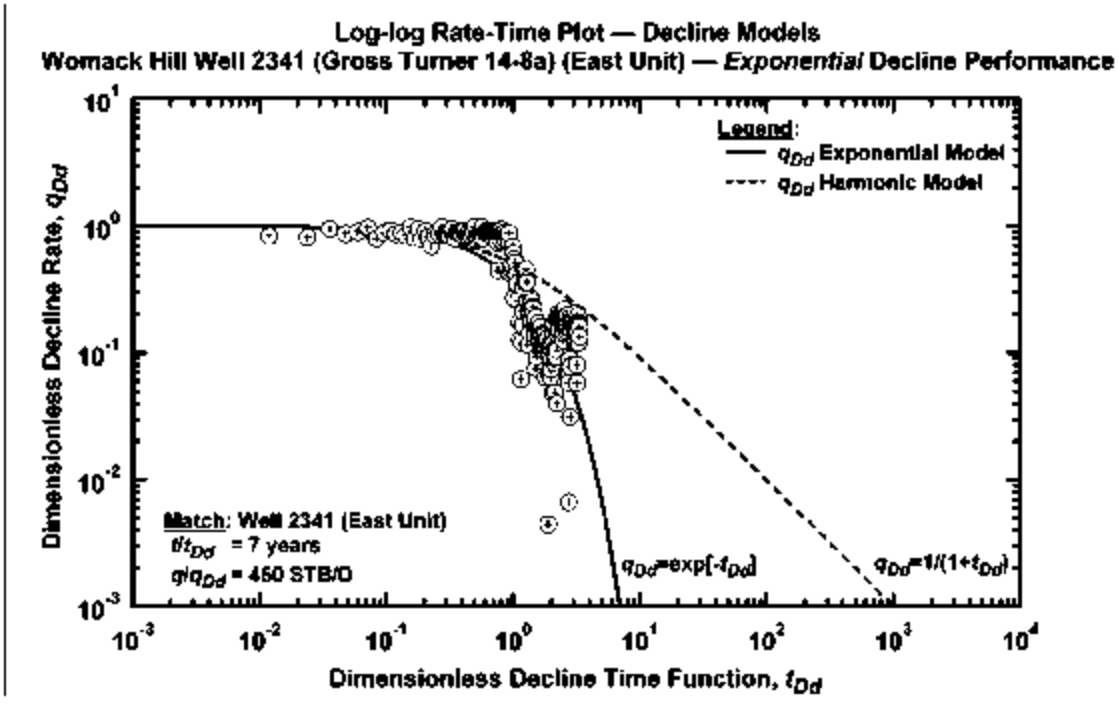

Figure 251 — Dimensionless log-log rate-time "type curve" plot — Womack Hill We11 2341.

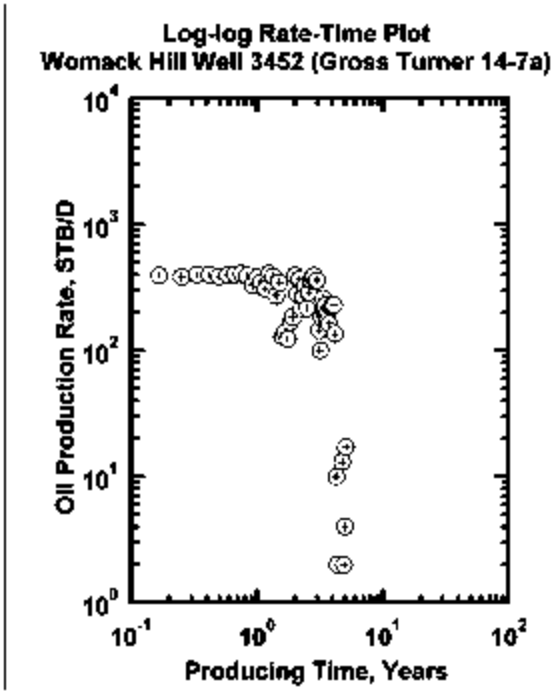

Figure 252 — Log-log rate-time plot — Womack Hill We11 3452.

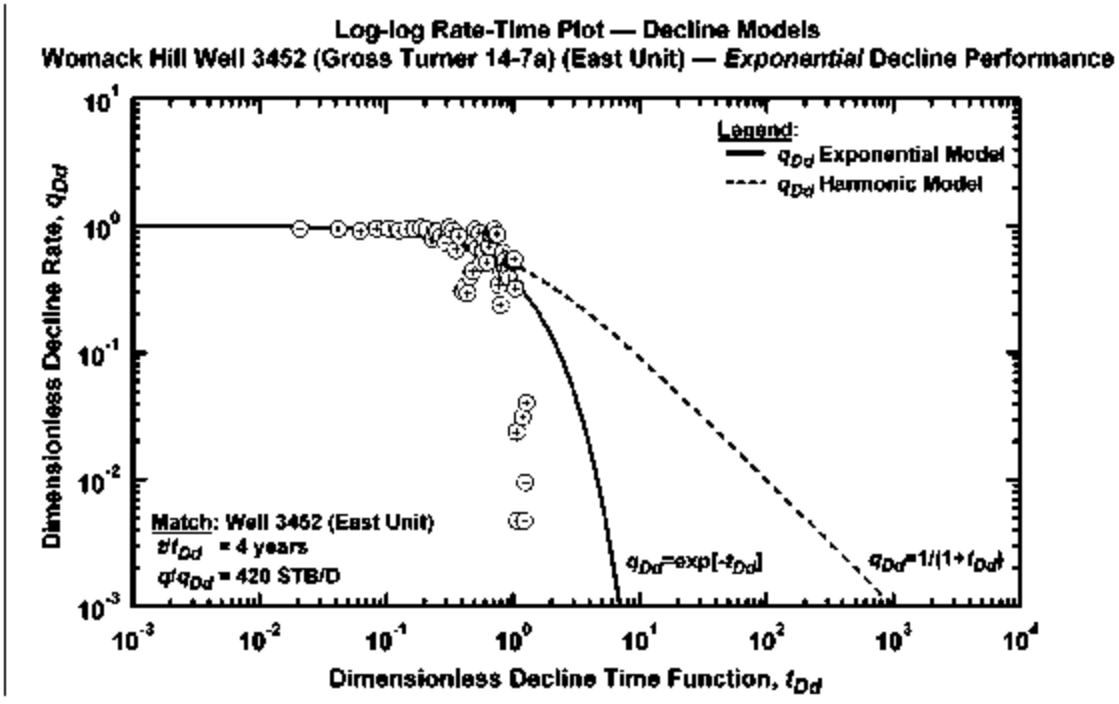

Figure 253 — Dimensionless log-log rate-time "type curve" plot — Womack Hill We11 3452.

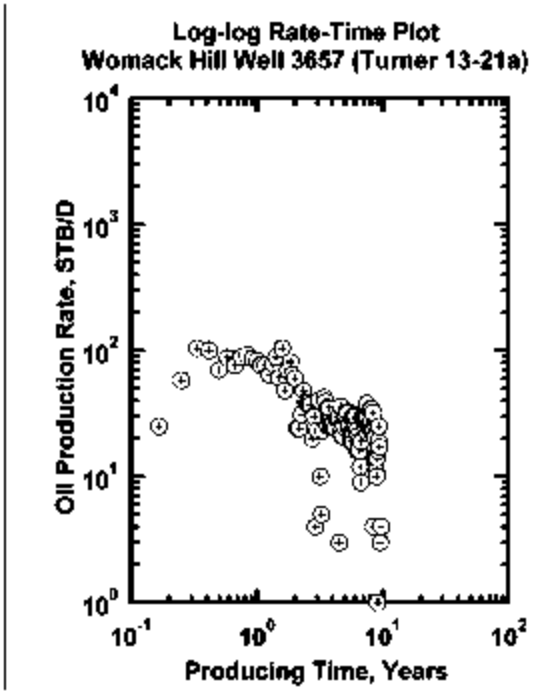

Figure 254 — Log-log rate-time plot — Womack Hill Well 3657.

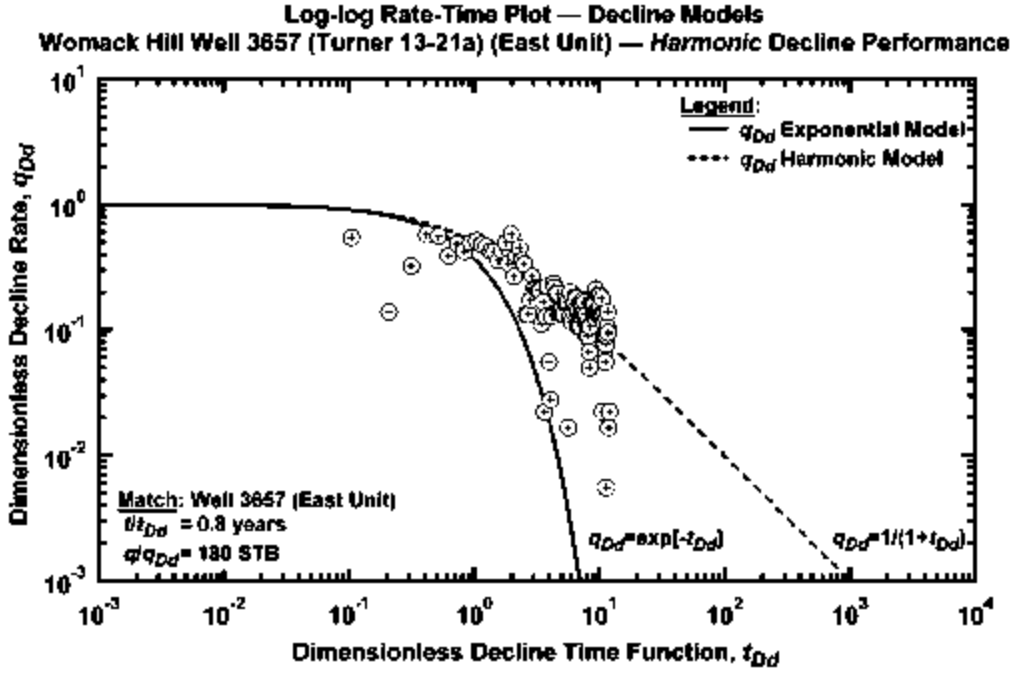

Figure 255 — Dimensionless log-log rate-time "type curve" plot — Womack Hill Well 3657.

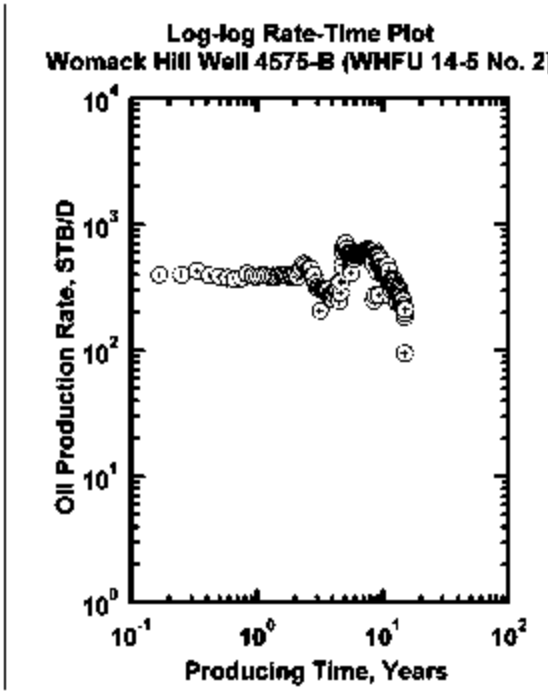

Figure 256 — Log-log rate-time plot — Womack Hill We11 4575.

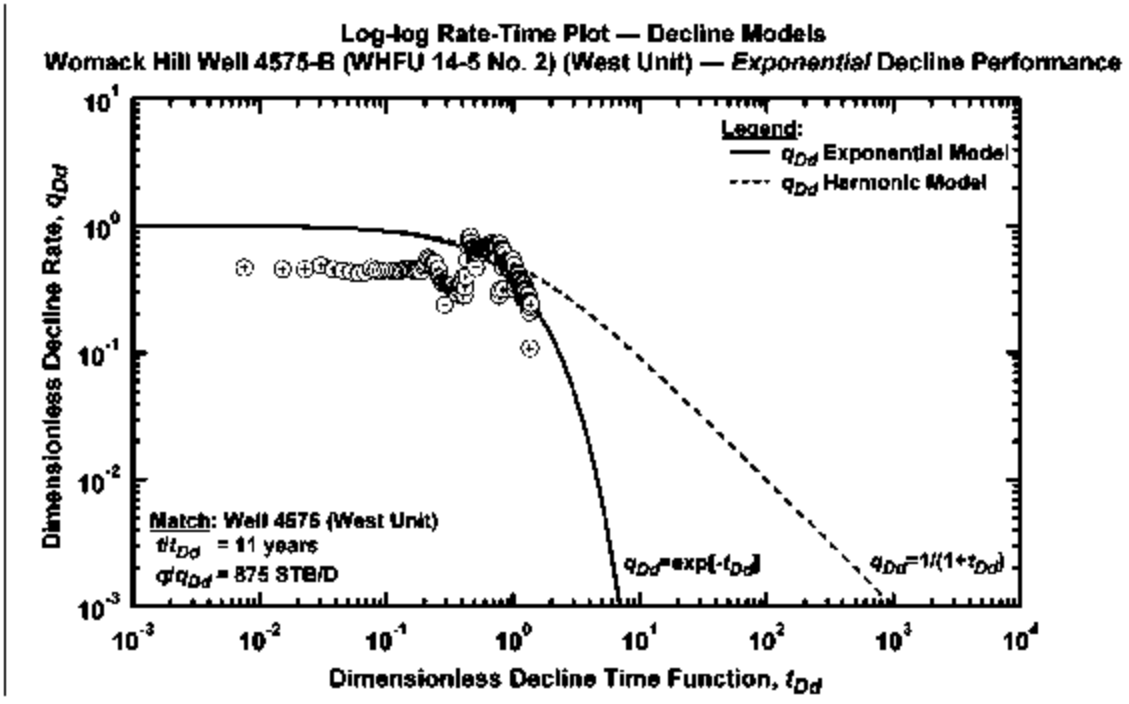

Figure 257 — Dimensionless log-log rate-time "type curve" plot — Womack Hill We11 4575.

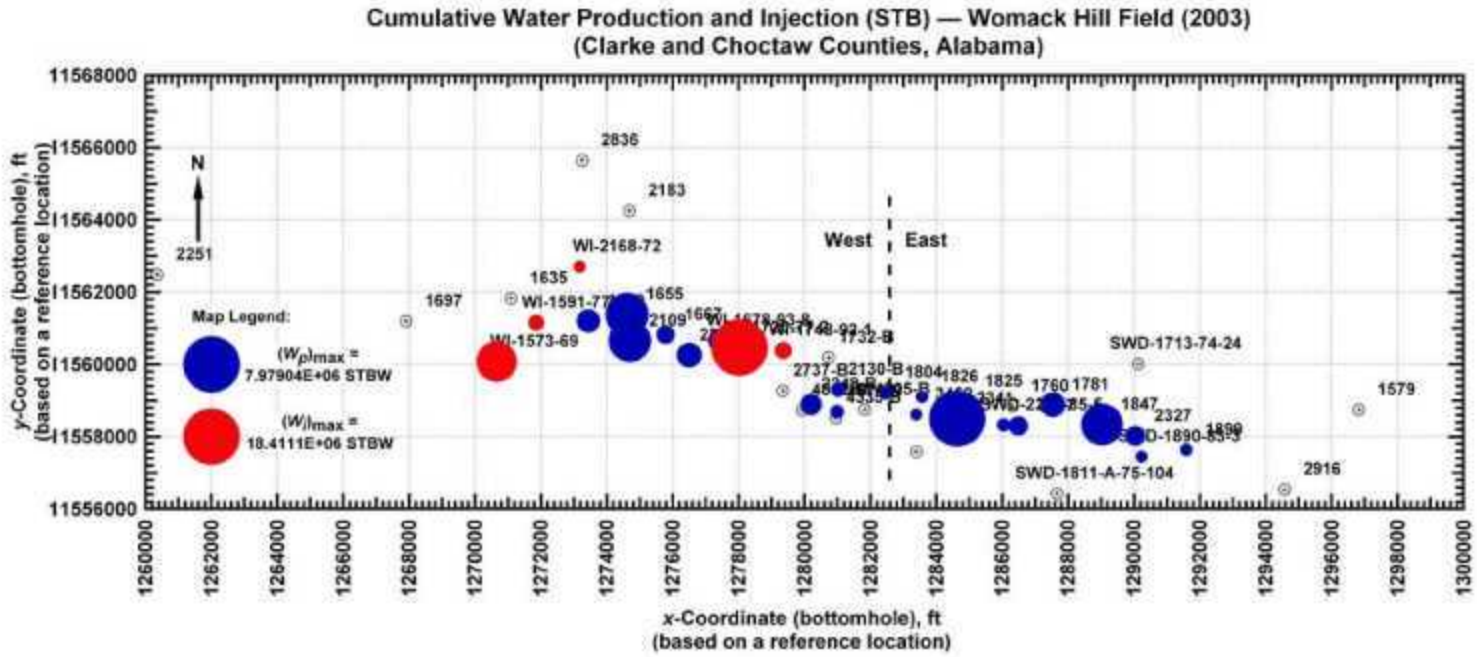

Figure 258 – Cumulative Water Production and Water Injection "Bubble Map" — Womack Hill Field.

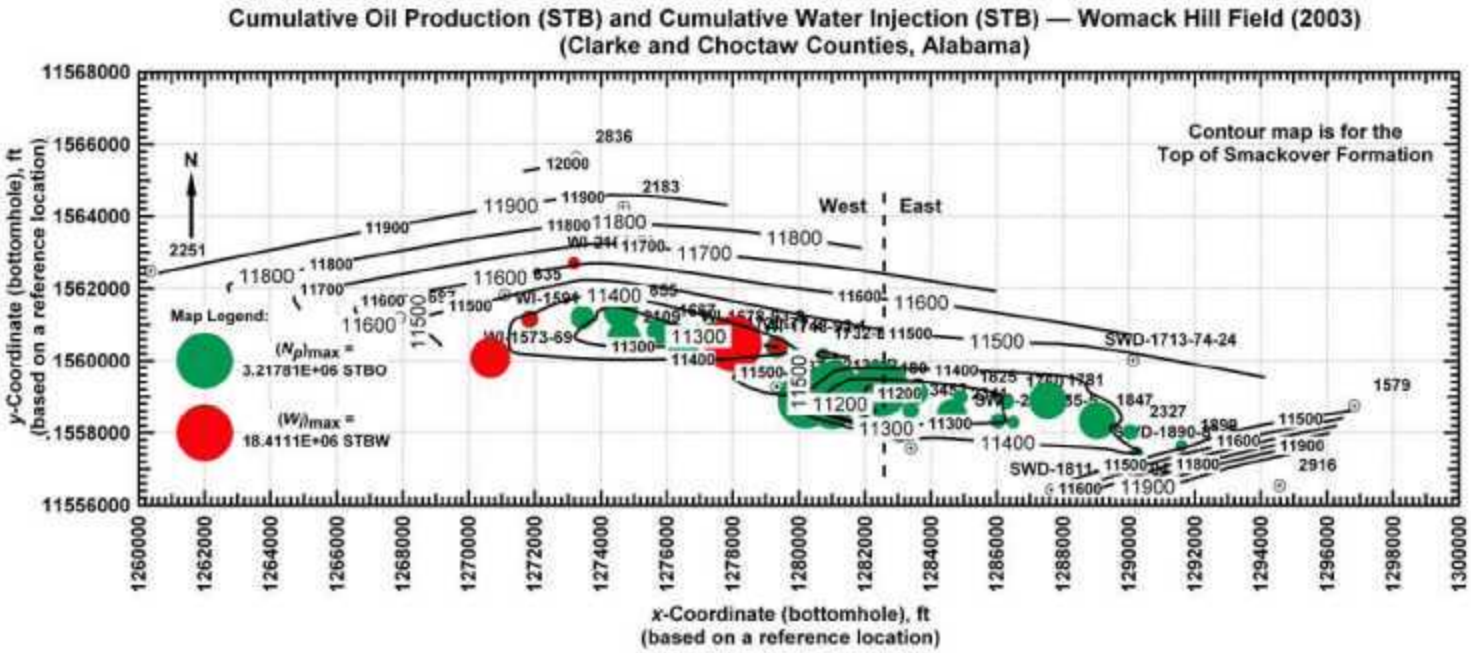

Figure 259 – Cumulative Oil Production and Cumulative Water Injection "Bubble Map," with "Top of Smackover" contour plot superimposed — Womack Hill Field.

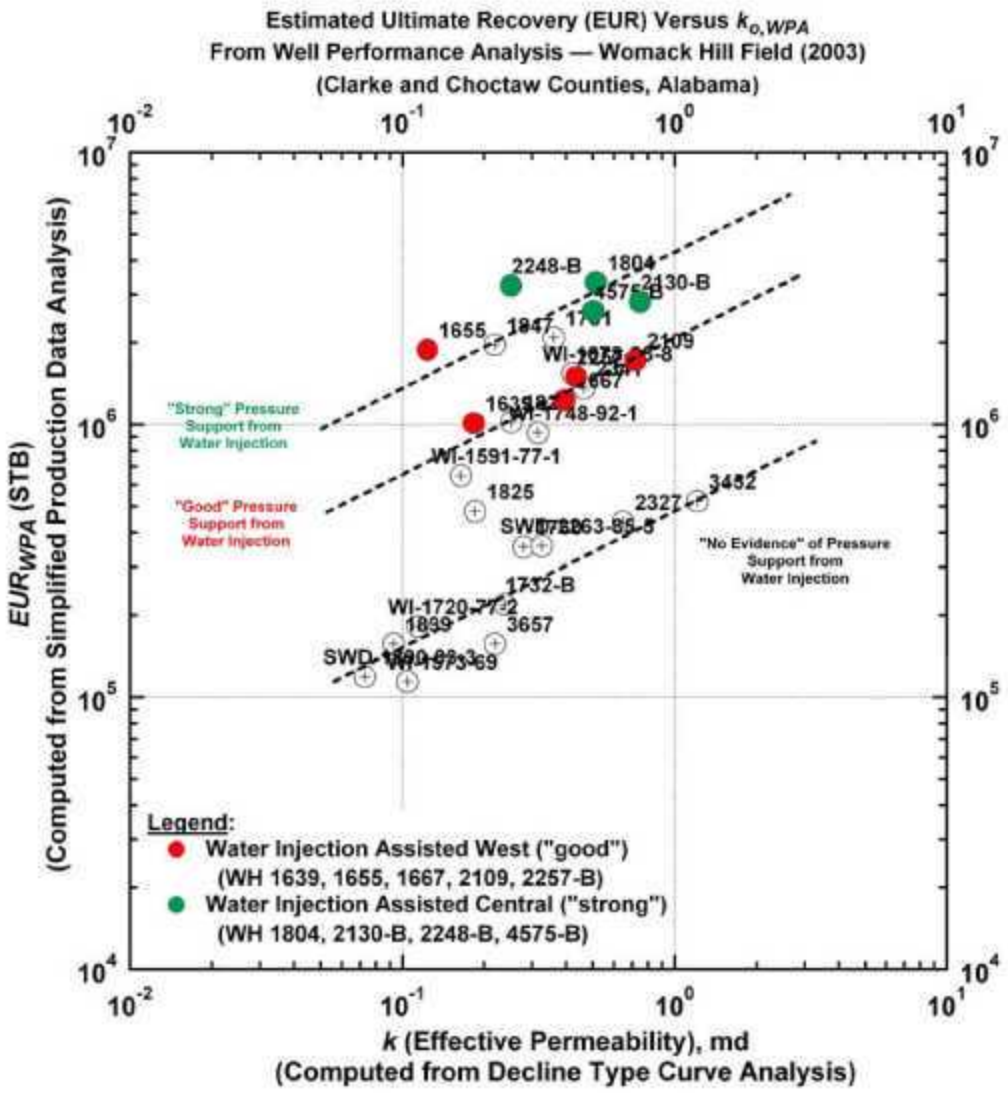

Figure 260 – Correlation of Estimated Ultimate Recovery (EUR) versus oil effective permeability (k_o) for Womack Hill Field. Note trends for "strong" and "good" water injection support.

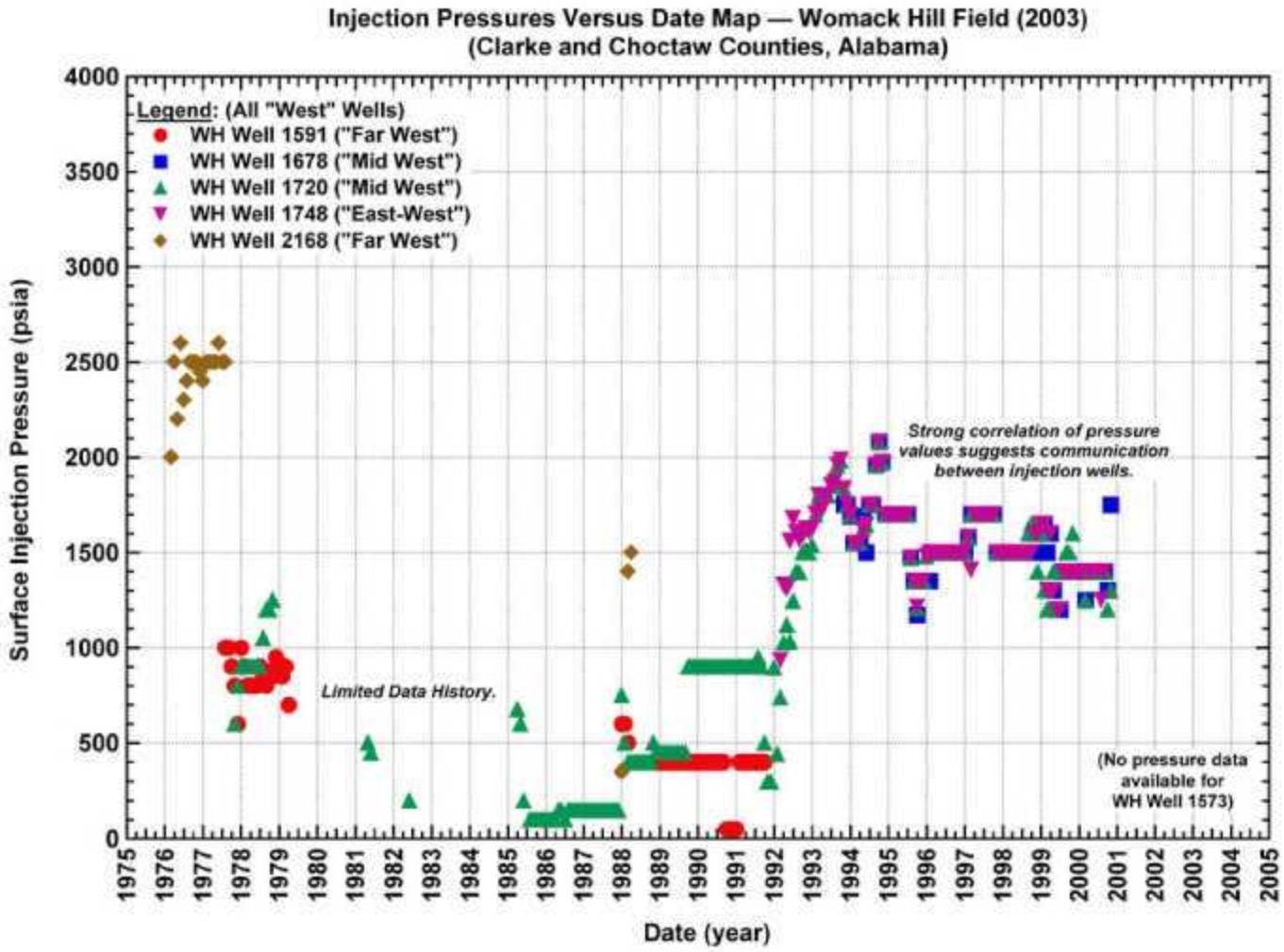

Figure 261 – Injection pressure history for Womack Hill Field.

A core plug testing system, operative at 90°C has been fabricated and is operational. Tests conducted at 90°C using dilute acetic acid illustrated the effectiveness of the acid in dissolving portions of cores from the Smackover Formation. Other tests conducted at ambient temperature suggest that a sodium nitrate concentration of 0.12% (w/v) and a sodium dihydrogen phosphate concentration of 0.03% (w/v) have been found to be satisfactory to stimulate the growth of indigenous bacteria. An ethanol concentration of 0.002% (v/v) appears to be effective for the production of acid by the bacteria. However, the results with limestone samples are more favorable than with dolostone samples. Results also suggest that supplemental sodium nitrate for cell maintenance will not be required for at least two months. Obviously, these results must be verified and/or modified using live cores from the Womack Oil Field reservoir.

Thus, although the implementation of an immobilized enzyme technology project at Womack Hill Field looks very promising, it is recommended that such a project not be initiated until a new well is drilled and cored in the field. The live core should then be used to confirm the microbial core experiments to date.

Technology Transfer

Technology Transfer Activities

Description of Work.--During this project, a technology workshop has been held in Jackson, Mississippi, to transfer the results of Phase I of this project. This workshop included results from the carbonate reservoir characterization, data integration, and carbonate reservoir and structural modeling tasks. Also, the results of this work have been presented at the annual meetings of GCAGS, SPE, and AAPG and have been published in the GCAGS Transactions and will be submitted to other journals for publication.

Rationale.--It is expected that the results of this work has application to other fields producing from the Smackover Formation in the Eastern Gulf Region and throughout the Gulf Coast from Florida to Texas. It is anticipated that the results of this work are applicable to other Class II Reservoirs throughout the U.S. As stated in the 1992 DOE report, geologically similar reservoirs, to some extent, have similar reservoir characteristics and production problems. Therefore, it is important to have the success and failures of this work in the hands of the producers as quickly as possible to support the goals of the 1998 Comprehensive National Energy Strategy.

Technology Transfer.--Technology transfer activities to date include:

1. Womack Hill Field Technology Workshop on Reservoir Characterization and Modeling (also included were Vocation, Appleton and North Blowhorn Creek Fields), August 14, 2002, Jackson, Mississippi (conducted by the Eastern Gulf Region of the Petroleum Technology Transfer Council).

2. **Technical Presentations (8)**

Hopkins, T.L., Determining reservoir quality by combined stratigraphic, petrographic and petrophysical methods as part of optimized recovery programs: Womack Hill Smackover Field, Clarke and Choctaw Counties, Alabama, AAPG Annual Meeting, Houston, Texas, March 11, 2002.

Mancini, E.A., Improved oil recovery from Upper Jurassic Smackover carbonates through application of advanced technologies at Womack Hill oil field, Choctaw and Clarke Counties, Alabama, eastern Gulf Coastal Plain, DOE Shallow Shelf Carbonate Project Review Meeting, Odessa, Texas, December 12, 2002.

Mancini, E.A., Reservoir characterization and modeling of Upper Jurassic Smackover carbonate shoal reservoirs, Womack Hill oil field, Choctaw and Clarke Counties, Alabama, GCAGS Annual Meeting, Austin, Texas, November 1, 2002.

Mancini, E.A., Reservoir characterization and modeling, Womack Hill Field, EGR-PTTC Technology Workshop, Jackson, Mississippi, August 14, 2002.

Mancini, E.A., DOE Class II Project-Improved oil recovery from Upper Jurassic Smackover carbonates, Womack Hill Field, Alabama, eastern Gulf of Mexico, AAPG Annual Meeting, Salt Lake City, Utah, May 13, 2002.

Tedesco, W.A., Stratigraphic and diagenetic controls on production from Smackover Formation reservoirs, Womack Hill Field, eastern Gulf Coastal Plain, AAPG Annual Meeting, Houston, Texas, March 13, 2002.

Avila, J.C., A petrophysics and reservoir performance-based reservoir characterization of the Womack Hill (Smackover) Field (Alabama), Annual SPE Technical Conference and Exhibition, San Antonio. Texas, September 30, 2002.

Blasingame, T.A., An integrated reservoir study of the Womack Hill (Smackover) Field (Alabama) reservoir engineering, Petrophysics and Upscaling: From Pore to Reservoir, SPWLA Spring Topical Conference, March 30, 2003.

Publications (14)

Hopkins, T.L., 2002, Integrated petrographic and petrophysical study of the Smackover Formation, Womack Hill Field, Clarke and Choctaw Counties, Alabama, M.S. thesis, Texas A&M University, 96 p.

Hopkins, T.L., and Ahr., W.M., 2002, Determining reservoir quality by combined stratigraphic, petrographic and petrophysical methods as part of optimized recovery programs: Womack

Hill Smackover Field, Clarke and Choctaw Counties, Alabama, Am. Assoc. Petroleum Geologists 2002 Abstract Volume, p. A80.

Avila, J.C., Archer, R.A., Mancini, E.A., and Blasingame, T.A., 2002, A petrophysics and reservoir performance-based reservoir characterization of the Womack Hill (Smackover) Field (Alabama), SPE 77758 Paper.

Mancini, E.A., Cate, D., Blasingame, T., Major, R.P., Brown, L., and Stafford, W., 2001, Improved oil recovery from Upper Jurassic Smackover carbonates through the application of advanced technologies at Womack Hill oil field, Choctaw and Clarke Counties, eastern Gulf Coastal Plain, U.S. Department of Energy, DE-FC26-00BC15129, 89 p.

Mancini, E.A., 2002, Improved oil recovery from Upper Jurassic Smackover carbonates through the application of advanced technologies at Womack Hill oil field, Choctaw and Clarke Counties, eastern Gulf Coastal Plain, DOE Shallow Shelf Carbonates Abstract Volume, p. 59-60.

Mancini, E.A., et al., 2002, Improved oil recovery from Upper Jurassic Smackover carbonates through the application of advanced technologies at Womack Hill oil field, Choctaw and Clarke Counties, eastern Gulf Coastal Plain, DOE Shallow Carbonate Class II Project Review Meeting, CD, p. 508-550.

Mancini, E.A., et al., 2002, Reservoir characterization and modeling, Smackover Formation, Womack Hill field, EGR-PTTC Technology Workshop on Reservoir Characterization and Modeling, 35 p.

Mancini, E.A., and Panetta, B.J., 2003, Reservoir characterization and modeling of Upper Jurassic Smackover carbonate shoal reservoirs, Womack Hill field, Choctaw and Clarke Counties, Alabama, GCAGS Transactions, v. 52, p. 707-716.

Mancini, E.A., and Panetta, B.J., 2002, Reservoir characterization and modeling of Upper Jurassic Smackover carbonate shoal reservoirs, Womack Hill field, Choctaw and Clarke Counties, Alabama, GCAGS Abstracts with Program, p. 93-94.

Mancini, E.A., et al., 2002, Improved oil recovery from Upper Jurassic Smackover carbonate through the application of advanced technologies at Womack Hill oil field, Choctaw and Clarke Counties, eastern Gulf Coastal Plain, DOE Topical Technical Report, Year 2, DE-FC26-00BC15129, 165 p.

Mancini, E.A., et al., 2003, Improved oil recovery from Upper Jurassic Smackover carbonates through the application of advanced technologies at Womack Hill oil field, Choctaw and Clarke Counties, eastern Gulf Coastal Plain, DOE Topical Technical Report, Year 3, DE-FC26-00BC15129, 97 p.

Mancini, E.A., and Panetta, B.J., 2003, DOE Class II Project-Improved oil recovery from Upper Jurassic Smackover carbonates, Womack Hill Field, Alabama, eastern Gulf of Mexico, AAPG 2003 Abstract Volume, p. A112.

Tedesco, W.A., 2002, Dolomitization and reservoir development of the Upper Jurassic Smackover Formation, Womack Hill Field, eastern Gulf Coastal Plain, Ph.D. dissertation, University of Mississippi, 251 p.

Tedesco, W.A., and Major, R.P., 2002, Stratigraphic and diagenetic controls on production from Smackover Formation reservoirs, Womack Hill Field, eastern Gulf Coastal Plain, Am. Assoc. Petroleum Geologists 2002 Abstract Volume, p. A174.

Demonstration Project

Decision to Implement Demonstration Project

Description of Work.--The project results, to date, will be evaluated by Pruet Production Co. and DOE to determine whether project continuation is justified.

Rationale.--This activity represents the decision process to determine whether it is feasible for Pruet Production Co. to implement the technologies addressed and evaluated in Phase I of this study. The decision may be to modify the pressure maintenance project, implement a strategic infill drilling program, and/or initiate an immobilized enzyme technology project at Womack Hill Field Unit. This activity also presents DOE with the opportunity to decide whether DOE will continue to support the project.

Pruet Decision.--Reproduced below is the contents of a letter received from Pruet Oil Company LLC on December 8, 2003, regarding initiating Phase II of the project.

> Please be advised that Pruet Production Co. does not plan to enter Phase Two of the referenced project. Neither post-stack DMO migration nor pre-stack time migration processing of the seismic data acquired during Phase One provided adequate quality to diminish our concerns and reduce the drilling risks associated with the problem of the large fault shadow prevalent in the entire area.
>
> We are currently pursuing the more complicated and time consuming pre-stack depth migration processing technique and we are hopeful it will clarify the data enough to provide a coherent interpretation and warrant a future well proposal. However, this will take an unknown amount of time and, because the technique is new to this general area, it is not certain that it will be successful. Thus, planning a well at this time is not feasible.

Pruet Production Co. learned a great deal about Womack Hill Field during the course of Phase One, which we consider a successful and worthwhile effort. We plan to utilize your geologic and engineering work in future unit operations but that will not require additional DOE funding. Should the PSDM processing technique prove successful, it could have exciting exploratory potential not only in Womack Hill Field but also for exploration elsewhere in the overall Smackover trend where the shadow effect has historically caused problems for prospect definition. If so, that will be directly attributable to the UA/DOE support.

RESULTS AND DISCUSSION

Reservoir Characterization

Geoscientific Reservoir Characterization

In the Womack Hill Field, the Smackover Formation ranges in thickness from 220 to 422 feet with an average thickness of 340 feet and overlies sandstone beds of the Norphlet Formation. The Norphlet Formation overlies the Jurassic Louann Salt, which in combination with faulting, is responsible for the petroleum trap at the field. The Smackover Formation is overlain by the Buckner Anhydrite Member of the Haynesville Formation. These anhydrite beds form the seal in the field. The Smackover Formation includes lower, middle and upper units in the Womack Hill Field. The Smackover lower member or unit typically is composed of peloidal packstone and wackestone (Benson, 1988), which has reservoir potential in the field area but generally is not the reservoir in the Womack Hill Field. The middle member or unit includes laminated carbonate mudstone and fossiliferous wackestone and mudstone. The upper member or unit ranges in thickness from 30 to 209 feet with an average thickness of 120 feet, and consists

of a series of three cycles, Cycle A, Cycle B, and Cycle C. Porosity is developed in the upper part of the middle Smackover in the central part of the field along the Tombigbee River on the Clarke County side of the river. Cycle A (carbonate shoal) is an upward shoaling cycle composed of lower energy, carbonate mudstone and peloidal wackestone at the base and is capped by higher energy, ooid grainstone. The carbonate mudstone and wackestone have been interpreted as restricted bay and lagoon sediments, and the grainstone has been described as beach shoreface and shoal deposits (McKee, 1990). Although Cycle A is present across the field, the reservoir quality in this cycle varies. The thickness of Cycle A ranges from 9 to 82 feet with an average thickness of 30 feet. The grainstone associated with Cycle A is dolomitized (upper dolomitized zone) in much of the field area, and is the main reservoir perforated in the field. Hydrocarbons have been produced from Cycle A in 21 of the 27 productive wells in the field. Six wells (Permit #1678, #1781, #1826, #2257B, #2327 and #3657) only have been perforated in Cycle A, and the cumulative oil production ranges from 127,000 to 2.0 million bbls for these wells. Porosity and permeability in the more productive wells (Permit #1678) average 16 percent and 11.5 md, respectively, and porosity and permeability in the less productive wells (Permit #2327) average 12 percent and 3 md, respectively. The mudstone/wackestone associated with this cycle has the potential to be a barrier to vertical flow in the field. Cycle B and Cycle C also occur across the field. Cycle B thickness ranges from 8 to 101 feet with an average thickness of 47 feet, and the thickness of Cycle C ranges from 11 to 86 feet with an average thickness of 40 feet. These cycles are part of shoal complexes which include lagoonal deposits. The reservoirs associated with these cycles are a result of depositional and diagenetic processes, particularly dolomitization. Dolomitization (lower dolomitized zone) can be pervasive in the shoal grainstone lithofacies and in the lagoon wackestone lithofacies in these cycles and the interval immediately

below Cycle C. Hydrocarbons have been produced from Cycle B in 18 wells, and oil and gas have been produced from Cycle C in 6 wells in the field. Three wells (Permit #1847, #2248B and #2263) only have been perforated in Cycle B, and the cumulative oil production is 350,000 to 3.2 million bbls for these wells, respectively. One well (Permit #2109) only has been perforated in Cycle C, and its cumulative oil production is 1.7 million bbls. Porosity and permeability in well Permit #1847 average 17.5 percent and 9 md, respectively. The large scatter of the porosity and permeability data for this well illustrates the heterogeneity in Cycle B. Production from the upper part of the middle Smackover interval immediately above Cycle C is from one well (Permit #4575B) perforated in this interval that is located in the central part of the field. Cumulative oil production for well Permit #4575B is 2.4 million bbls. Porosity and permeability in well Permit #4575B average 19 percent and 15 md, respectively. Permeability shows good correlation (0.87) with porosity in this interval probably due to dolomitization of these carbonates. The best producing well (Permit #1804) is perforated in Cycles A, B and C, and the well production is 3.4 million bbls of oil. Porosity and permeability in Cycle C in this well average 20 percent and 4 md, respectively. The variability of the porosity and permeability data for this well and wells (Permit #1732B and #4575B) illustrates the heterogeneity within and among Cycles A, B and C.

Although the primary control on reservoir architecture in Smackover reservoirs, including Womack Hill Field, is the fabric of the depositional lithofacies, diagenesis plays a significant role in modifying reservoir quality (Benson, 1985). Of the diagenetic events, the multiple dolomitization and dissolution events probably had the greatest influence on the quality in Smackover reservoirs. While the dolomitization created only minor amounts of intercrystalline porosity, it significantly enhanced permeability; it also stabilized the lithology which reduced the potential for later porosity loss due to compaction (Benson, 1985). The dissolution events

enlarged primary (interparticle) and early secondary (moldic and intercrystalline) pores (McKee, 1990). Although the dissolution did not create large amounts of new porosity, it did expand existing pore throats and enhanced permeability (Benson, 1985).

Porosity in the shoal grainstone reservoirs at Womack Hill Field is both primary and secondary. The main pore types in the Smackover reservoirs, including the Womack Hill Field area, are interparticle, intraparticle, solution-enlarged interparticle, grain moldic, intercrystalline dolomite, and vuggy. Primary interparticle porosity has been reduced in the field due to compaction and cementation. Solution-enlarged interparticle and grain moldic porosity is produced by early leaching in the vadose zone that dissolved aragonite in the Smackover carbonates (McKee, 1990). Moldic porosity is produced by early, fabric selective dissolution of aragonitic grains and is associated with areas of subaerial exposure (Benson, 1985). Several phases of dolomitization have been identified in the Smackover carbonates at Womack Hill Field. The upper zone of dolomitization is fabric-destructive and is a result of an early stage diagenetic event that involves downward-moving, evaporitically-concentrated brine, and the lower zone of dolomitization is, in part, fabric-destructive creating large amounts of intercrystalline porosity and permeability and is a result of mixing zone processes (Tedesco, 2002). Vuggy porosity of Choquette and Pray (1970), which is present in the field area, is the product of late, non-fabric selective dissolution of calcite or dolomite and is produced by solution enlargement of earlier formed interparticle or intercrystalline pores (Benson, 1985; Benson and Mancini, 1999). Reservoirs characterized by vuggy porosity have good porosity and permeability (Benson and Mancini, 1984).

Pore systems are the building blocks of reservoir architecture. Pore origin, geometry, and spatial distribution determine the amount and kind of reservoir heterogeneity. Pore systems

affect not only hydrocarbon storage and flow but also reservoir producibility and flow unit quality and comparative rank within a field. Hydrocarbon recovery efficiency and total recovery volume are determined by the 3-D shape and size of the pores and pore throats (Kopaska-Merkel and Hall, 1993; Ahr and Hammel, 1999). Therefore, the pore systems (pore topology and geometry and pore throat size distribution) of the Womack Hill Field reservoirs are extremely important. Pore throat size distribution is one of the important factors determining permeability because the smallest pore throats are the bottlenecks that determine the rate of which fluids pass through a rock. Permeability has been shown to be directly related to the inherent pore system and degree of heterogeneity in Smackover reservoirs (Carlson *et al.*, 1998; Mancini *et al.*, 2000). Generally, the more homogeneous (little variability in architecture and pore systems) the reservoir, the greater the hydrocarbon recovery from that reservoir. However, heterogeneity at one scale is not necessarily paralleled by heterogeneity at other scales. For example, the shoal grainstone reservoirs at Womack Hill Field can be dominated by a interparticle/solution-enlarged, moldic/intercrystalline or intercrystalline/vuggy pore system and have low mesoscopic-scale heterogeneity but low to high microscopic-scale heterogeneity, depending upon the pore system. The heterogeneity is a function of both depositional and diagenetic processes. The grainstones accumulated in linear shoal environments, which tend to have uniformity of paleoenvironmental condition within a given shoal, but these carbonates can be later subjected to dissolution and dolomitization, such as at Womack Hill Field, to produce dolograinstones and large crystalline dolostones. The moldic/intercrystalline pore system is characterized by multi-sized and more smaller-sized pores that are poorly connected by narrow pore throats. Pore size is dependent on the size of the carbonate grain that was leached. The intercrystalline/vuggy pore system is characterized by more larger-sized pores that are well-connected by larger and

more uniform pore throats. The size of the pores is dependent upon the dolomite crystal size. Interparticle porosity of Lucia (1999), which includes intergrain and intercrystal pore types in grainstones, dolograinstones and large crystalline dolostones, provides for high connectivity in carbonate reservoirs and results in high permeability (Lucia, 1999; Jennings and Lucia, 2001). In the Womack Hill Field, leached and dolomitized grainstone flow units dominated by moldic and intercrystalline porosity have lower reservoir potential than the grainstone flow units dominated by depositional interparticle and solution enlarged porosity because the leached grainstone pore system is characterized by a higher percent of smaller-sized pores poorly connected by narrow pore throats. Dolostone flow units dominated by intercrystalline and vuggy porosity have the highest reservoir potential due to a pore system characterized by a higher percent of large-sized pores well connected by larger pore throats.

Petrophysical and Engineering Characterization

Petrophysical and Engineering Characterization has involved extensive efforts to integrate and correlate the core and well log data for the field. Reservoir permeability has been correlated with core porosity, gamma ray well log response, and resistivity well log response. The petrophysical data have been segregated into flow units prescribed by the geological data, and for the data in these flow units a histogram of core porosity and the logarithm of core permeability. These histograms yield statistical measures, such as the mean and median values, which are used to develop spatial distributions and to provide data for the numerical simulation model. Evaluation of production, injection and shut-in bottomhole pressure data for the field have been interpreted and analyzed using appropriate mechanisms, such as decline type curve analysis and estimated ultimate recovery analysis. The volumetric results are relevant as virtually every well yielded an appropriate signature for decline type curve analysis. Utilizing estimated

ultimate recovery analysis, about 10% of the recoverable 34.6 million barrels of oil remains to be produced from Womack Hill Field. In utilizing cumulative oil and water production from the field, it is estimated that oil recovery for the field will be approximately 34.6 MMSTB. With production to date being 31.1 MMSTB, 3.5 MMSTB remain to be recovered. The remaining oil to be recovered is concentrated in the vicinity of the structural high in the eastern portion of the western part of the field (unitized area) and along an elongated west-east high in the eastern part of the field. A series of pressure transient tests were designed and implemented for the Womack Hill Field for evaluating current reservoir properties in the field. The well test data suggest compartmentalization in the Womack Hill Field reservoir. The new data support the interpretation that production from wells in the eastern part of the field is facilitated by a natural external influx of water from the bottom up. A study of the engineering properties of the fields producing from Smackover reservoirs in the vicinity of Womack Hill Field suggest that the presence of a large aquifer (Norphlet sandstone) underlying the Smackover Formation is providing energy (pressure support) to augment Smackover production. The test data indicate a fault bounding the field to the south.

Microbial Characterization

Microbial Characterization has involved initially taking water samples and core samples from wells in the Womack Hill Field yielded no micro-organisms capable of growing at 90 C. This result was due to a combination of factors, including the fact that the core samples were exposed to air for decades and the equipment necessary to maintain an anaerobic environment was inadequate. Well cuttings from the Smackover Formation acquired from a field near Womack Hill Field were analyzed for micro-organisms. Growth of micro-organisms was evident in the samples prepared from these well cuttings in association with oil from the Womack Hill

Field. These organisms consumed ethanol and are presumed to produce carbon dioxide or the gas was derived from organic acids produced from the oil reacting with carbonate. These findings suggest that micro-organisms capable of producing acetic acid from ethanol have a high probability of being present in Womack Hill Field and of being induced to grow and be metabolically active at the subsurface temperature in the reservoir.

Recovery Technology Analysis

3-D Geologic Modeling

The 3-D geologic model shows that the petroleum trap at Womack Hill Field is more complex than originally interpreted. The 2-D seismic data assists with the location of a major fault with significant stratal displacement to the south of the field. However, the seismic data are not adequate to determine if the petroleum trap is a fault trap (bounded on three sides by dip closure and on a fourth side by a fault) or a faulted anticline trap (four-way dip closure). The geologic modeling shows that the trap in the western part of the field is a fault trap with closure to the south against the fault, and that the trap in the central and eastern parts of the field is a faulted anticline trap with four-way dip closure. In addition, the fault salt anticline trap appears to consist of two distinct highs separated by a structural low in the central part of the field. The 2-D seismic data, which is along the northern margin of the field, shows a north-south trending fault in the vicinity of the Choctaw-Clarke County line. If the fault trace is projected south to intersect with the major west-east fault, the offset in the two structural highs along the southern margin of the field may be attributed to the effects of this north-south trending fault. Utilizing a correlation algorithm derived employing heuristic methods, a north-south trending fault is interpreted between well Permit #1748 (high) and well Permit #1732 (low). Also, the pressure difference between wells (well Permit #4575B) in the western and central parts of the field

(unitized area) and wells (well Permit #1804) in the eastern part of the field may be attributed to the flow barrier in the field due to this fault.

The 3-D geologic modeling also shows that the Smackover reservoirs at Womack Hill Field are heterogeneous. Four reservoir intervals are identified in the field area. These include Cycle A, Cycle B, Cycle C, and the interval immediately below Cycle C. Although the Cycle A reservoir is the most productive areally (has been productive in 21 wells), the production from this reservoir is highly variable with cumulative oil production ranging from 127,000 to 1.9 million bbls for wells only perforated in Cycle A. The thickness and lateral and vertical reservoir quality are also variable for the Cycle A reservoir interval. The Cycle B reservoir interval also is heterogeneous in thickness and lateral and vertical reservoir quality; however, the overall porosity as indicated by density log analysis is higher in this interval than the other reservoir intervals. The Cycle C reservoir interval also is heterogeneous in thickness and reservoir quality. Although the total oil production from this interval is not as high as the Cycle A and Cycle B reservoir intervals, production from well Permit #2109, the only well solely perforated in this interval and located in the western (unitized) part of the field has had a cumulative oil production of 1.7 million bbls. The reservoir interval immediately below Cycle C has only been perforated in one well (well Permit #4575B) in the central part (unitized) of the field. Reservoir quality is high and production is high. The geologic modeling indicates this reservoir interval has the potential for high reservoir quality in the western part (unitized) of the field in the vicinity of well Permit #2109. The high reservoir quality and productivity in this interval in well Permit #4575B is attributed to mixing zone dolomitization (fresh water lens development in structurally higher areas of the field). The area around well Permit #2109 is in a structurally higher area in the unitized part of the field. In the eastern or non-unitized part of the field, the structurally high

area north of well Permits #1804, #1826, #1825 and #1760 and the structurally high area around well Permits #1781 and #1847, and north of well Permit #1811, southwest of well Permit #1713, east of well Permit #1760 and west of well Permit #2327 have excellent potential for remaining oil to be recovered. Well Permits #1781 and #1847 continue to be high producing wells and well Permit #1804 is the best producing well in the field. The recent successful drilling of the producing well Permit #12762 immediately northwest of well Permit #1826 supports this interpretation.

A permeability barrier to flow, especially in the Cycle A reservoir interval, is present potentially between the western unitized area (well Permit #4575B) and eastern (well Permit #1804) area of the field. Communication in the field through the Cycle B reservoir interval appears likely, in comparing the porosity and permeability data between well Permit #1732B and well Permit #1804 and in comparing the field drainage area of well Permit #2130B with the area of well Permit #1804. The improved reservoir communication in the Cycle B interval is probably due to dolomitization. Porosity and permeability data are insufficient in the field to assess the potential of a permeability barrier to flow in the Cycle C reservoir interval and the reservoir interval immediately below Cycle C. Communication between the western (unitized) area of the field and the area of well Permit #1804 appears likely, but communication between the wells in the western (unitized) area and the other wells in the eastern area of the field probably is limited.

Reservoir Simulation

Reservoir simulation has produced a model for the Womack Hill Field reservoir based on the 3-D geologic model, and this simulation model has been used for history matching. The history match of the performance of the field is satisfactory and indicates that oil remains to be recovered in the eastern (non-unitized) part of the field in the area north of well Permits #1804

and #1826 and east of well Permit #1732. The western unitized area of the field appears to have little oil remaining to be recovered except in the vicinity of well Permits #4575B (cumulative production of 2.4 million barrels), #2130B (cumulative production of 2.8 million barrels), and #2248 (cumulative production of 3.2 million barrels). This area is in the structurally highest portion of the Unit area (central part of the field). Using the data resulting from the drilling and producing of well Permit #12762 in 2003, the simulation model was revised to assess the hydrocarbon potential of the area north of well Permit #1826. The revised simulation showed that a well capable of producing 664 to 825 MSTB could be drilled successfully in this portion of the eastern part of the field.

Microbial Core Experiments

A core plug testing system, operative at 90°C has been made and is operational. Tests conducted at 90°C using dilute acetic acid illustrated the effectiveness of the acid in dissolving portions of cores from the Smackover Formation. Other tests conducted at ambient temperature suggest that a sodium nitrate concentration of 0.12% (w/v) and a sodium dihydrogen phosphate concentration of 0.03% (w/v) have been found to be satisfactory to stimulate the growth of indigenous bacteria. An ethanol concentration of 0.002% (v/v) appears to be effective for the production of acetic acid by the bacteria. Results also suggest that supplemental sodium nitrate for cell maintenance will not be required for at least two months. The dissolution and flow tests with limestone (calcite) samples were more favorable than with dolostone (dolomite) samples. The solubility of dolomite is less than calcite suggesting that a longer exposure time to the acetic acid produced by microbes for dolomite may be required to provide the desired dissolution.

Recovery Technology Evaluation

Acquisition and Evaluation of New Seismic Data

Pruet Production Co. decided to acquire new high-quality 2-D seismic data, rather than 3-D seismic data, for a portion of the eastern part of Womack Hill Field. Their decision was based on the following. Their experience and the recent experiences of other operators have shown that the fault shadow associated with the major fault in Choctaw and Clarke Counties, Alabama (southern bounding fault at Womack Hill Field), causes imaging problems which could result in the drilling of a dry hole. Thus, the expense of acquiring 3-D seismic data was not justified. Pruet believes that high-quality, 2-D seismic data would be effective for determining whether they could drill a new productive well in the Womack Hill Field. They focused on the eastern part of the field because the engineering studies and reservoir simulation modeling from this study indicated there was little oil remaining to be recovered in the western unitized part of the field except in the area of the structural high in the vicinity of well Permit #4575B in the Unit area (south-central part of the field). In that this well is not perforated in the higher zones in the Smackover reservoir, Pruet believes they can recover much of this undrained oil by completing the well Permit #4575B in these higher zones without drilling another well. The same procedure is possible for well Permit #2109 which is located near the southern bounding fault to the west. With J. R. Pounds, Inc. drilling a successful well (well Permit #12762) north of well Permits #1804 and #1826, Pruet elected to focus on the area around well Permits #1781 and #1847 in the central part of Section 13.

Two high-quality 2-D seismic lines have been acquired, processed and evaluated. The new data have been described as better by far than previous data shot in the Womack Hill Field area. However, there is still a fault shadow effect from the major fault to the south. The effect of this

fault shadow increases the risk of drilling a successful well in this area. Pruet is now pursuing a pre-stack depth migration processing technique to minimize the effect of the fault shadow.

Evaluation of the Pressure Maintenance Project

Multiwell productivity analysis shows that the wells located in the western unitized part of the Womack Hill Field continue to receive stable water support through injection to maintain production and that the wells in the eastern part of the field (strong water drive) continue to experience natural water support to sustain production. Thus, the pressure maintenance project utilizing water injection continues to be effective, and the natural water influx in the western part of the field continues to facilitate production. Correlation of production performance shows that the average initial production rate for all wells in the field is on the order of 400 STB/D.

Evaluation of the Immobilized Enzyme Technology Project Concept

Bacteria that grow at 90°C have been found in well cuttings from an oil field near Womack Hill Field. These bacteria convert ethanol to an acid that reacts with carbonates. A core plug testing system, operative at 90°C has been constructed and is operational. Tests conducted at 90°C using dilute acetic acid illustrated the effectiveness of the acid in dissolving portions of the cores from the Smackover Formation. A sodium nitrate concentration and a sodium dihydrogen phosphate concentration have been found to be satisfactory to stimulate the growth of indigenous bacteria. An ethanol concentration appears to be effective for the production of acetic acid by the bacteria. Thus, although the implementation of the immobilized enzyme technology project at Womack Hill Field looks very promising, it is recommended that such a project not be initiated until live (freshly taken and properly preserved) core from the Smackover reservoir at Womack Hill Field is available to confirm the tests and experiments to date.

Decision to Implement Demonstration Project

Pruet Production Co. does not plan to drill a new well in the eastern part of Womack Hill Field at this time. Neither the post-stack DMO migration nor the pre-stack time migration processing of the new 2-D seismic data acquired provided the resolution required to alleviate Pruet's concerns about the drilling risks created by the fault shadow prevalent in the Womack Hill Field area. Pruet is currently pursuing a more complicated and time consuming pre-stack migration technique to see if this procedure will improve confidence in drilling a successful well in the eastern part of the Womack Hill Field. However, the pre-stack migration of the newly acquired data and the following seismic interpretation and well site selection requires additional time. Although Pruet is hopeful the pre-stack migration technique will be successful, they are not prepared to present a new well proposal to the other mineral interest owners in a proposed drilling and production unit. Thus, Pruet has concluded that the planning of such a well is not feasible at this time.

Pruet is integrating the information and results from the reservoir characterization, 3-D geologic modeling, reservoir performance and reservoir simulation studies that resulted from Phase I of this project into their field-scale reservoir management strategy to improve operations at Womack Hill Field. They will consider perforating well Permits #4575B and #2109 in higher zones in the Smackover reservoir in the western unitized area of the field at the appropriate time. The areas currently being drained by these wells were shown to have high potential for undrained (attic) oil through the 3-D geologic modeling and reservoir simulation studies performed as part of this project. Pruet also has used the new pressure transient test data acquired as a result of this project to assess the effectiveness of the pressure maintenance project involving water injection in the Unit area. The reservoir performance, multiwell productivity

analysis, and reservoir simulation studies indicate that water injection continues to provide stable support to maintain production from wells in the Unit area and that the strong water drive present in the eastern area of the field is adequate to sustain production in this part of the Womack Hill Field.

The successful drilling and testing of well Permit #12762 in 2003, by J. F. Pounds, Inc. in the eastern area of the field immediately northwest of well Permit #1826 demonstrates the remaining hydrocarbon potential of this area. This area was shown to have high potential for undrained oil through the 3-D geologic modeling and reservoir simulation studies performed as a part of this project.

Although the results from the microbial characterization and microbial core experiments are very promising, Pruet has elected not to implement an immobilized enzyme technology project in the Womack Hill Field Unit at this time. This project has shown that bacteria that grow at 90°C are present in the Smackover Formation, that these bacteria convert ethanol to acetic acid that reacts with carbonates, that a core plug testing system operative at 90°C has been constructed and is operational, that Smackover rock can be dissolved at 90°C by using dilute acetic acid, that a sodium nitrate concentration and a sodium dihydrogen phosphate concentration are satisfactory to stimulate the growth of Smackover indigenous bacteria, and that an ethanol concentration is effective for the production of acetic acid by the bacteria. However, to insure the success of an immobilized enzyme technology project, live (freshly taken and properly preserved) cores from the Smackover reservoir at Womack Hill Field need to be acquired to confirm the experiments to date. Such a core could be acquired as a result of the drilling and coring of the new well under consideration by Pruet.

CONCLUSIONS

Pruet Production Co. and the Center for Sedimentary Basin Studies at the University of Alabama, in cooperation with Texas A&M University, Mississippi State University, University of Mississippi, and Wayne Stafford and Associates proposed a three-phase, focused, comprehensive, integrated and multidisciplinary study of Upper Jurassic Smackover carbonates (Class II Reservoir), involving reservoir characterization and 3-D modeling (Phase I) and a field demonstration project (Phases II and III) at Womack Hill Oil Field Unit, Choctaw and Clarke Counties, Alabama, eastern Gulf Coastal Plain.

The principal problem at Womack Hill Field is productivity and profitability. With time, there has been a decrease in oil production from the field, while operating costs in the field continue to increase. In order to maintain pressure in the reservoir, increasing amounts of water must be injected annually. These problems are related to cost-effective, field-scale reservoir management, to reservoir connectivity due to carbonate rock architecture and heterogeneity, to pressure communication due to carbonate petrophysical and engineering properties, and to cost-effective operations associated with the oil recovery process.

Improved reservoir producibility will lead to an increase in productivity and profitability. To increase reservoir producibility, a field-scale reservoir management strategy based on a better understanding of reservoir architecture and heterogeneity, of reservoir communication and of the geological, geophysical, petrophysical and engineering properties of the reservoir is required. Also, an increased understanding of these reservoir properties should provide insight into operational problems, such as how the multiple pay zones in the field are vertically and laterally connected and the nature of the communication within a pay zone.

The objective of the project is to increase the producibility and profitability of the Womack Hill Field Unit, thereby extending the economic life of this Class II Reservoir. The specific objectives of Phase I of the project are to: demonstrate the significance and procedures for developing an integrated reservoir approach for making decisions regarding field operations, demonstrate the value of reservoir simulation to a pressure maintenance program, transfer the knowledge gained from the project to operators of fields with Class II Reservoirs, and contribute to knowledge about Class II Reservoirs.

Reservoir Characterization tasks of Phase I of the project included geoscientific reservoir characterization, petrophysical and engineering property characterization, microbial characterization, and integration of the characterization data.

Geoscientific Reservoir Characterization has shown the following. The upper part of the Smackover Formation is productive from carbonate shoal complex reservoirs that occur in vertically stacked heterogeneous porosity cycles (A, B, and C). The cycles typically consist of lime mudstone/wackestone at the base and ooid and oncoidal grainstone at the top. The lime mudstone/wackestone lithofacies has been interpreted as restricted bay and lagoon sediments, and the grainstone lithofacies has been described as beach shoreface and shoal deposits. Porosity has been enhanced through dissolution and dolomitization. The grainstone associated with Cycle A is dolomitized (upper dolomitized zone) in much of the field area. Although Cycle A is present across the field, its reservoir quality varies laterally. Dolomitization (lower dolomitized zone) can be pervasive in Cycle B, Cycle C and the interval immediately below Cycle C. Cycle B and Cycle C occur across the field, but they are heterogeneous in depositional texture and diagenetic fabric laterally. Porosity consists chiefly of depositional interparticle, intraparticle, solution-enlarged interparticle, grain moldic, dolomite intercrystalline and vuggy

pores. Dolostone pore systems and flow units dominated by intercrystalline and vuggy pores have the highest reservoir potential. Pore systems and flow units dominated by depositional interparticle and solution-enlarged pores have higher reservoir potential than pore systems and flow units dominated by intercrystalline and grain moldic pores. Dolostone flow units have a higher percentage of large-sized pores with larger pore throats, and dolomitized and leached grainstone flow units have a lower percentage of large-sized pores with narrow pore throats. Median pore throat aperture tends to increase with increasing porosity. Probe permeability strongly correlates with median pore throat aperture, and tortuosity increases with increasing median pore throat aperture. Larger tortuosity and median pore throat aperture values are associated with pore systems dominated by intercrystalline and vuggy pores.

Petrophysical and Engineering Characterization have shown the following. Reservoir permeability has been correlated with core porosity, gamma ray well log response, and resistivity well log response. The petrophysical data have been segregated into flow units prescribed by the geological data, and for the data in these flow units a histogram of core porosity and the logarithm of core permeability were prepared. These histograms yield statistical measures, such as the mean and median values, which were used to develop spatial distributions and to provide data for the numerical simulation model. Evaluation of production, injection and shut-in bottomhole pressure data for the field have been interpreted and analyzed using appropriate mechanisms, such as decline type curve analysis and estimated ultimate recovery analysis. The volumetric results are relevant as virtually every well yielded an appropriate signature for decline type curve analysis. Reservoir performance studies have shown that 10% of the recoverable 34.6 million barrels of oil remains to be produced from the field. The undrained oil is concentrated in the vicinity of the structural high in the south-central part of the field (unitized area) and along an

elongated west-east high in the eastern part of the field (non-unitized area). New pressure transient test data support the interpretations that the Womack Hill Field reservoir is compartmentalized and that a fault bounds the field reservoir to the south.

Microbial Characterization has shown the following. Initially water samples and core samples taken from wells in the Womack Hill Field yielded no micro-organisms capable of growing at 90 C. This result was due to a combination of factors, including the fact that the core samples were exposed to air for decades and the equipment necessary to maintain an anaerobic environment was inadequate. Well cuttings from the Smackover Formation acquired from a field near Womack Hill Field were analyzed for micro-organisms. Growth of micro-organisms was evident in the samples prepared from these well cuttings in association with oil from the Womack Hill Field. These organisms consumed ethanol and produced carbon dioxide. This gas is presumed to have come from the reaction of acetic acid with carbonate or from other organic acids produced directly from the oil reacting with carbonate. These findings suggest that micro-organisms capable of producing acetic acid from ethanol have a high probability of being present in Womack Hill Field and of being induced to grow and be metabolically active at the subsurface temperature in the reservoir.

Data for Womack Hill Field have been entered into a comprehensive digital database to facilitate integration into a field-scale reservoir management strategy to improve field operations.

Recovery Technology Analysis tasks included 3-D geologic modeling, reservoir simulation, and microbial core experiments.

A 3-D Geologic Model has been constructed for the Womack Hill Field structure and reservoirs. The 3-D geologic modeling shows that the petroleum trap is more complex than originally interpreted. The geologic modeling indicates that the trap in the western part of the

field is a fault trap with closure to the south against the fault, and that the trap in the central and eastern parts of the field is a faulted anticline trap with four-way dip closure. The pressure difference between wells in the western and central parts of the field and wells in the eastern part of the field may be attributed to a flow barrier due to the presence of a north-south trending fault in the field area. The presence of a north-south trending fault is indicated from old 2-D seismic data and by using a correlation algorithm employing heuristic methods for correlation of logs for wells located in the central part of the field. The geologic modeling shows that the Smackover reservoirs are heterogeneous. Four reservoir intervals are identified in the field area: Cycle A, Cycle B, Cycle C, and the interval immediately below Cycle C. A permeability barrier to flow is present potentially between the western and eastern parts of the field.

Reservoir Characterization and Geologic Modeling have shown that four areas in the Womack Hill Field have potential for the recovery of undrained/attic oil. Two areas are located in the western (unitized) part of the field. These include the northern part of the northeast quarter of Section 16, south of well Permit #2109 (only perforated in reservoir zone C), and the area around well Permit #4575B (only perforated below reservoir zone C) in the west-central part of Section 14. Two areas are located in the eastern (non-unitized) part of the field. These include the northern part of Section 14 and part of the northwest quarter of Section 13, north of well Permits #1804, #1826, #1825 and #1760, and the center of Section 13, around well Permits #1781 and #1847, and north of well Permit #1811, southwest of well Permit #1713, east of well Permit #1760, and west of well Permit #2327.

Reservoir Simulation has produced a model for the Womack Hill Field reservoir based on the 3-D geologic model, and this simulation model has been used for history matching. The history match of the performance of the field is satisfactory and indicates that oil remains to be

recovered in the eastern (non-unitized) part of the field. The simulation model showed that a well capable of producing 664 to 825 MSTB could be drilled successfully in the northwestern portion of the eastern part of the field. The western unitized part of the field appears to have little oil remaining to be recovered except in the south-central portion of the Unit area.

Microbial Core Experiments have resulted in the construction of a core plug testing system that is operative at 90°C. Tests conducted in the system with dilute acetic acid demonstrated the effectiveness of a weak acid concentration in dissolving portions of the Smackover core carbonate. Other tests conducted indicate that a sodium nitrate concentration and a sodium dihydrogen phosphate concentration appear to be satisfactory to stimulate the growth of indigenous bacteria. Test results suggest that an ethanol concentration appears to be effective for the production of acetic acid by the bacteria and that supplemental sodium nitrate for cell maintenance will not be required for at least two months. The dissolution and flow tests were more favorable for limestone samples than dolostone samples.

Recovery Technology Evaluation Tasks included acquiring and evaluating new 2-D seismic data, evaluating the existing pressure maintenance project in the Womack Hill Field Unit, and evaluating the concept of an immobilized enzyme technology project for the Womack Hill Field Unit.

Pruet Production Co. decided to acquire new 2-D seismic data, rather than 3-D seismic data, for the northeastern portion of the eastern part of Womack Hill Field. They focused on this part of the field because reservoir simulation indicated little oil remained to be recovered in the Unit area except in the south-central portion of the Unit area where Pruet believes they can recover the undrained oil in this area by perforating higher zones in the Smackover reservoir in a currently producing well. Also, in 2003 J. R. Pounds, Inc. drilled and tested a successful well in

the northwestern portion of the eastern part of the field proving that uncontacted oil remains in this part of the field to be recovered. Pruet's experience and the recent experiences of other operators have shown that the fault shadow associated with the major fault, with significant stratal displacement, bounding the southern border of the field causes seismic imaging problems which could result in increasing the risks of drilling a dry hole. The new 2-D seismic lines are of high quality, but the fault shadow effect from the major fault persists. Pruet is pursuing a pre-stack depth migration processing technique to minimize the effect of the fault shadow.

Multiwell Productivity Analysis has shown that the wells located in the unitized part of the Womack Hill Field continue to receive stable water support to maintain production and that the wells located in the eastern part of the field, where a strong bottom-up water drive exists, continue to experience natural water support to sustain production. This analysis indicates that the pressure maintenance project utilizing water injection continues to be effective in the Unit area and that the natural water influx in the western part of the field continues to facilitate production.

The Immobilized Enzyme Technology (IET) project concept appears very promising for implementation in the Womack Hill Field Unit area. Dissolution and flow tests and experiments utilizing carbonate core samples from other Smackover fields in southwest Alabama and other carbonate core samples have been effective. An IET project should not be implemented in the Unit area, however, until live (freshly taken and properly preserved) core is available to confirm the tests and experiments conducted on other Smackover carbonates. Water injection should be conducted down-dip and focused towards structurally low areas of the field.

Pruet Production Co. is integrating the information and results from Phase I of this project into their field-scale reservoir management strategy in order to improve operations at the

Womack Hill Field. They will consider perforating well Permits #4575B and #2109 in higher zones in the Smackover reservoir to recover undrained/attic oil in the Unit area at the appropriate time. Pruet is using the new pressure transient test data to assess the effectiveness of the pressure maintenance project involving water injection in the Unit area. Pruet continues to evaluate the cost-effectiveness and risks associated with instituting an infill drilling program to recover undrained oil in the eastern (non-unitized) area of the Womack Hill Field. They do not plan to drill a new well in Womack Hill Field at this time.

The results of Phase I of this project have contributed to the further understanding of the Class II Reservoirs, and these results have been and will continue to be transferred through technology workshops, technical presentations, and technical publications.

Pruet Production Co. has elected not to continue into Phase II of this project because they are not prepared to make a proposal to other mineral interest owners regarding the drilling of new wells as part of an infill drilling program in the Womack Hill Field at this time. This project, therefore, is concluded.

REFERENCES

Ahr, W.M., and Hammel, B., 1999, Identification and mapping flow units in carbonate reservoirs: an example from Spraberry (Permian) field, Garza County, Texas, USA: Energy Exploration and Exploitation, v. 17, p. 311-334.

Bebout, D.G., and Loucks, R.G., 1984, Handbook for logging carbonate rocks: Handbook 5, The University of Texas at Austin, Bureau of Economic Geology, Austin, Texas, 43 p.

Benson, D.J., 1985, Diagenetic controls on reservoir development and quality, Smackover Formation of southwest Alabama: Gulf Coast Association of Geological Societies Transactions, v. 35, p. 317-326.

Benson, D.J., 1988, Depositional history of the Smackover Formation in southwest Alabama: Gulf Coast Association of Geological Societies Transactions, v. 38, p. 197-205.

Benson, D.J., and Mancini, E.A., 1984, Porosity development and reservoir characteristics of the Smackover Formation in southwest Alabama, in Jurassic of the Gulf Rim, Proceedings GCS-SEPMF 3rd Research, p. 1-17.

Benson, D.J., and Mancini, E.A., 1999, Diagenetic influence on reservoir development and quality in the Smackover updip basement ridge play, southwest Alabama: Gulf Coast Association of Geological Society Transactions, v. 99, p. 95-101.

Blasingame, T.A. *et al.*, 1998, "Well Performance Analysis (*WPA*) (software) Vers. 1.8b, Texas A&M U., College Station, Texas (1998).

Breiman, L. and Friedman, J., 1985, Estimating Optimal Transformations for Multiple Regression and Correlation, Journal of the American Statistical Association (September 1985) 80, No. 391, 590.

Carlson, E.C., Benson, D.J., Groshong, R.H., and Mancini, E.A., 1998, Improved oil recovery from heterogeneous carbonate reservoirs associated with paleotopographic basement structures: Appleton Field, Alabama: SPE/DOE Eleventh Symposium on Improved Oil Recovery, p. 99-105.

Carozzi, A.V., 1958, Micro-mechanisms of sedimentation in the epicontinental environment: Journal of Sedimentary Petrology, v. 28, p. 133 – 150.

Choquette, P.W., and Pray, L.C., 1970, Geologic nomenclature and classification of porosity in sedimentary carbonates: American Association of Petroleum Geologists Bulletin, v. 54, p. 207-250.

Dake, L.P., 1977, Fundamentals of Reservoir Engineering, Elsevier, Amsterdam.

Doublet, L.E., and Blasingame, T.A., 1996, Evaluation of injection well performance using decline type curves: paper SPE 35205 presented at the 1996 SPE Permian Basin Oil and Gas Recovery Conference, Midland, TX, March 27-29.

Doublet, L.E., Pande, P.K., McCollum, T.J., and Blasingame, T.A., 1994, Decline curve analysis using type curves—analysis of oil well production data using material balance time: application to field cases: paper SPE 28688 presented at the 1994 Petroleum Conference and Exhibition of Mexico held in Veracrus, Mexico, October 10-13.

Erwin, C.R., Eby, D.E., and Whitesides Jr., V.S., 1979, Clasticity index: a key to correlating depositional and diagenetic environments of Smackover reservoirs, Oaks field, Claiborne Parish, Louisiana: Gulf Coast Association of Geological Societies Transactions, v. 29, p. 52–62.

Fetkovich, M.J., 1980, "Decline Curve Analysis Using Type Curves," JPT (June 1980) 1065.

Fratesi, S.E., and Lynch, F.L., 2001, Comparison of organic matter preservation techniques for SEM study of geologic samples: Geological Society of America annual meeting, abstracts with programs, p. A-296

Gregg, J.M., and Sibley, D.F., 1984, Epigenetic dolomitization and the origin of xenotopic dolomite texture: Journal of Sedimentary Petrology, v. 54, n. 3, p. 908–931.

Hopkins, T.L., 2002, Integrated petrographic and petrophysical study of the Smackover Formation, Womack Hill Field, Clarke and Choctaw Counties, Alabama: Texas A&M University, unpublished Masters thesis, 156 p.

Humphrey, J.D., Ransom, K.L., and Matthews, R.K., 1986, Early meteoric control of Upper Smackover production, Oaks field, Louisiana: American Association of Petroleum Geologists Bulletin, v. 70, n. 1, p. 70 – 85.

Jennings, J.W., and Lucia, F.J., 2001, Predicting permeability from well logs in carbonates with a link to geology for interwell permeability mapping: Society of Petroleum Engineers Paper 71336, p. 1-16.

Kerans, C., and Tinker, S.W., 1997, Sequence stratigraphy and characterization of carbonate reservoirs: SEPM Short Course No. 40, 13 p.

Kopaska-Merkel, D.C., and Hall, D.R., 1993, Reservoir characterization of the Smackover Formation in southwest Alabama: Geological Survey of Alabama Bulletin 153, 111 p.

Lucia, F.J., 1999, Carbonate reservoir characterization: Springer, New York, 226 p.

Mancini, E.A., Benson, D.J., Hart, B.S., Balch, R.S., Parcell, W.C., and Panetta, B.J., 2000, Appleton field case study (eastern Gulf Coastal Plain): field development model for Upper Jurassic microbial reef reservoirs associated with paleotopographic basement structures: American Association of Petroleum Geologists Bulletin, v. 84, p. 1699-1717.

McKee, D.A., 1990, Structural controls on lithofacies and petroleum geology of the Smackover Formation: eastern Mississippi Interior Salt Basin, Alabama: University of Alabama, unpublished master's thesis, 254 p.

Tedesco, W.A., 2002, Dolomitization and reservoir development of the Upper Jurassic Smackover Formation, Womack Hill Field, eastern Gulf Coastal Plain, Ph.D. dissertation, University of Mississippi, 251 p.

Temple, K.L., 1949, A new method for the preparation of silica gel plates: Journal of Bacteriology, v. 57, p. 383.

Valko, P.P., Doublet, T.A., and Blasingame, T.A., 2000, Development and application of the multiwell productivity index (MPI): Society of Petroleum Engineers Journal, v. 5, p. 1.